Supplementary Information (SI) for Chemical Science.
This journal is © The Royal Society of Chemistry 2024

SUPPORTING INFORMATION

Rapid, Potent, and Persistent Covalent Chemical Probes to Deconvolute PI3Kα Signaling

Lukas Bissegger[1†], Theodora A. Constantin[1†], Erhan Keles[1†], Luka Raguž[1], Isobel Barlow-Busch[3], Clara Orbegozo[1], Thorsten Schaefer[1], Valentina Borlandelli[1], Thomas Bohnacker[1], Rohitha Sriramaratnam[1], Alexander Schäfer[2], Matthias Gstaiger[2], John E. Burke[3,4], Chiara Borsari[1†‡], Matthias P. Wymann[1†*]

[1]Department of Biomedicine, University of Basel, Mattenstrasse 28, 4058 Basel, Switzerland

[2]Department of Biology, Institute of Molecular Systems Biology, ETH Zurich, Otto-Stern-Weg 3, 8093 Zürich, Switzerland

[3]Department of Biochemistry and Microbiology, University of Victoria, Victoria, British Columbia V8W 2Y2, Canada

[4]Department of Biochemistry and Molecular Biology, The University of British Columbia, Vancouver, British Columbia V6T 1Z3, Canada.

[†] Equal contribution

* Corresponding author: matthias.wymann@unibas.ch, Tel: +41 61 207 5046

Table of contents

Supporting Figures

Figure S1. X-ray crystal structures of p110α with compounds 1 and 2

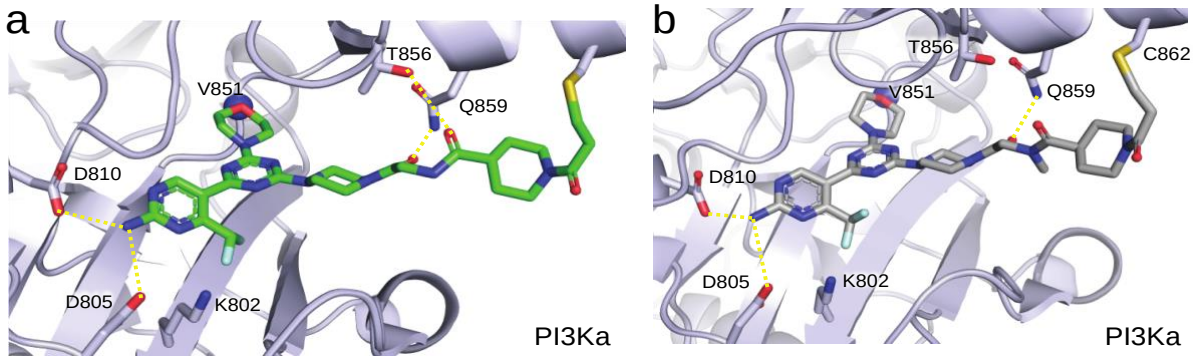

Figure S1. X-Ray cocrystal structure of **(a)** compound **1** and **(b)** compound **2** in p110α (PDB-ID: 7R9V and 7R9Y).[1] Hydrogen-bonds are depicted as dashed yellow lines.

Figure S2. Time-dependent IC_{50} shifts for compounds 1-9, 7r, 9r and CNX1351

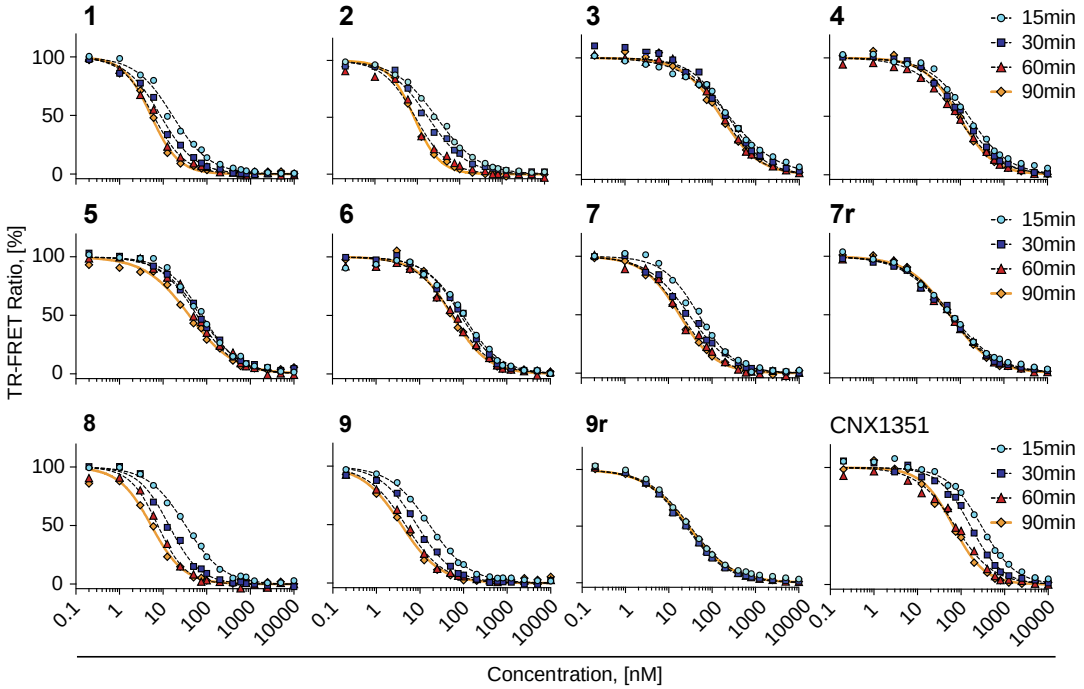

Figure S2. Time-dependent (15, 30, 60, 90 min) and time-resolved fluorescence resonance energy transfer (TR-FRET) IC_{50} shifts for compounds **1**-**9**, **7r**, **9r** and CNX1351 fitted to the "log(inhibitor) vs. normalized response – variable slope" function from raw data as exemplified in Figure S5. Data are presented as mean ± SEM (n = 3).

Figure S3. Mass spectrometry of p110α peptide adducts for 7 or 7r

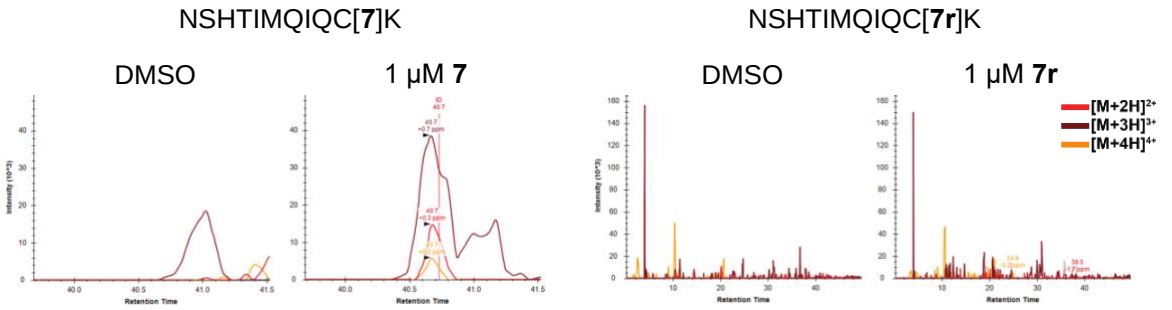

Figure S3. Recombinant PI3Kα protein (200 µg) was incubated with **7**, **7r** or DMSO at 1 µM for 2 h. Unbound compounds were removed by ultrafiltration and samples were analyzed by shotgun proteomics as detailed in the Methods section. MS1 XIC traces of the Cys862 containing peptide NSHTIMQIQCK covalently modified by **7** (left) and **7r** (right) are shown for the control (DMSO) sample and samples treated with the respective compounds. XIC traces for the charge states two, three and four are shown in red, brown and yellow, respectively and were extracted with 5ppm mass tolerance. "ID" flags indicate the presence of an MS/MS spectrum identifying the respective peptide-compound adduct.

Figure S4. Structural discussion of protein-ligand interactions

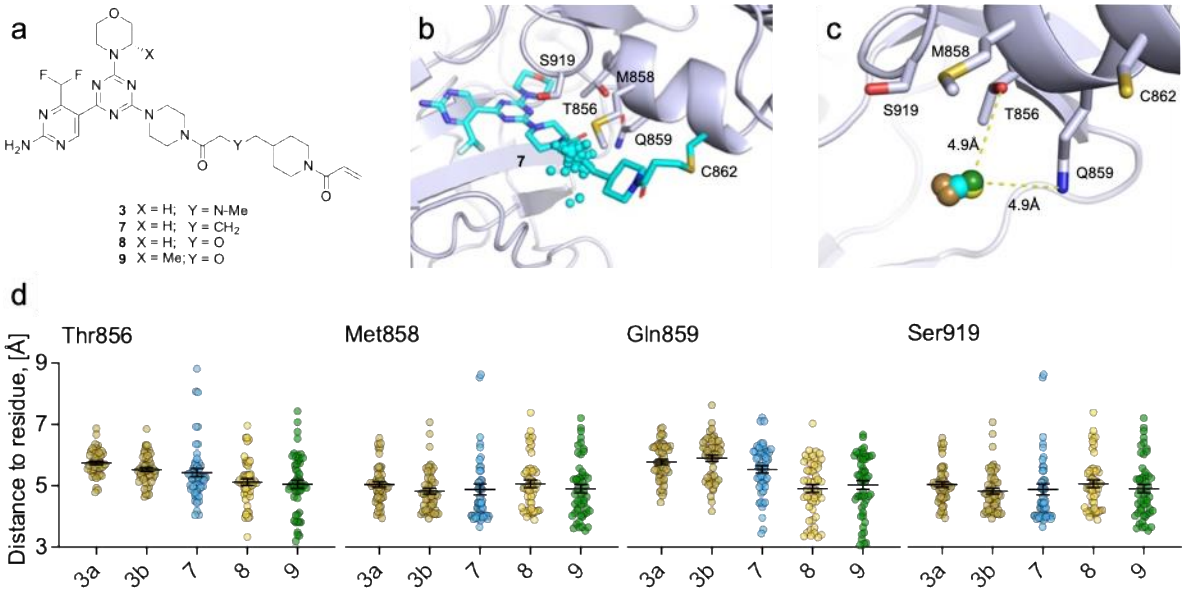

Figure S4. Efforts to rationalize substantial differences in target engagement. Compounds **3**, **7**, **8**, and **9 (a)** were covalently docked into the p110α X-ray co-crystal structure of compound **1** (PDB ID: 7R9V)[1] using CovDock (Maestro, Schrödinger Suite) with no constraints applied. In **(b)** the best 50 poses, represented by positions of the atom at position Y as cyan spheres are depicted, and in **(c)** the calculated centers of mass for the Y-atom positions across all 50 poses for each compound are shown. The spheres' color codes match the compound assignments in **(d)**, where individual distances between Y-atom positions and specific side-chain atoms of the nearest surface residues Thr856 (O-3), Met858 (S-4), Gln859 (N-4), and Ser919 (O-3) were analyzed. For compound **3**, 3a and 3b refer to the protonated enantiomers of the tertiary amine at position Y. For a short discussion, see the text below.

Based on the previously reported crystal structures of compounds **1** and **2** (Figure S1), it is likely that both carbonyl groups within the linker contribute to enhanced target engagement. This hypothesis is supported by the significantly reduced target engagement observed for

compounds **3** and **4**, which lack one of these carbonyl groups. However, compounds **7**, **8**, and **9**, despite also lacking one carbonyl group, appear to compensate for this structural deficit. Notably, compound **9** showed even enhanced target engagement. To rationalize this structure-activity relationship, we performed covalent docking of compounds **3**, **7**, and **9** using Maestro from Schrödinger without constraints, and analyzed the 50 best poses for each molecule (100 poses for compound **3**, due to the presence of two possible protonation isomers). We then measured the distances between the atoms at the Y position (Figure S4a) of the docked molecules in all 50 poses and the four closest amino acids within p110α (Thr856 (O-3), Met858 (S-4), Gln859 (N-4), and Ser919 (O-3), see Figure S4b). No consistent trend was observed in distances between Y atoms and Met858 or Ser919 across the tested compounds (Figure S4d). However, the mean distances from the Y atoms to Thr856 and Gln859 decreased with increasing k_{inact}/K_i values, suggesting a connection between target engagement and proximity of the linker region to the protein surface. To further visualize this observation, we calculated the center of mass for the Y atoms in each molecule's 50 poses and placed pseudoatoms at these positions (Figure S4c). This analysis showed a closer proximity of the Y position to Thr856 and Gln859 in compounds **9** (green) and **8** (yellow), as compared to **3** (brown) and **7** (cyan), but differences remained in the 1 Å range. One might therefore speculate that the observed structure-activity relationship is driven by a more restricted movement of **9** and **8** due to tighter surface association in the linker region, which reduces the degrees of freedom for warhead positioning and increases the likelihood of productive warhead orientation towards Cys862. This interpretation is in accordance with a well-defined electron density map of **9** in complex with p110α (Figure 3g; PDB-ID: 8TWY).

Figure S5. Time- and concentration-dependent TR-FRET ratio curves

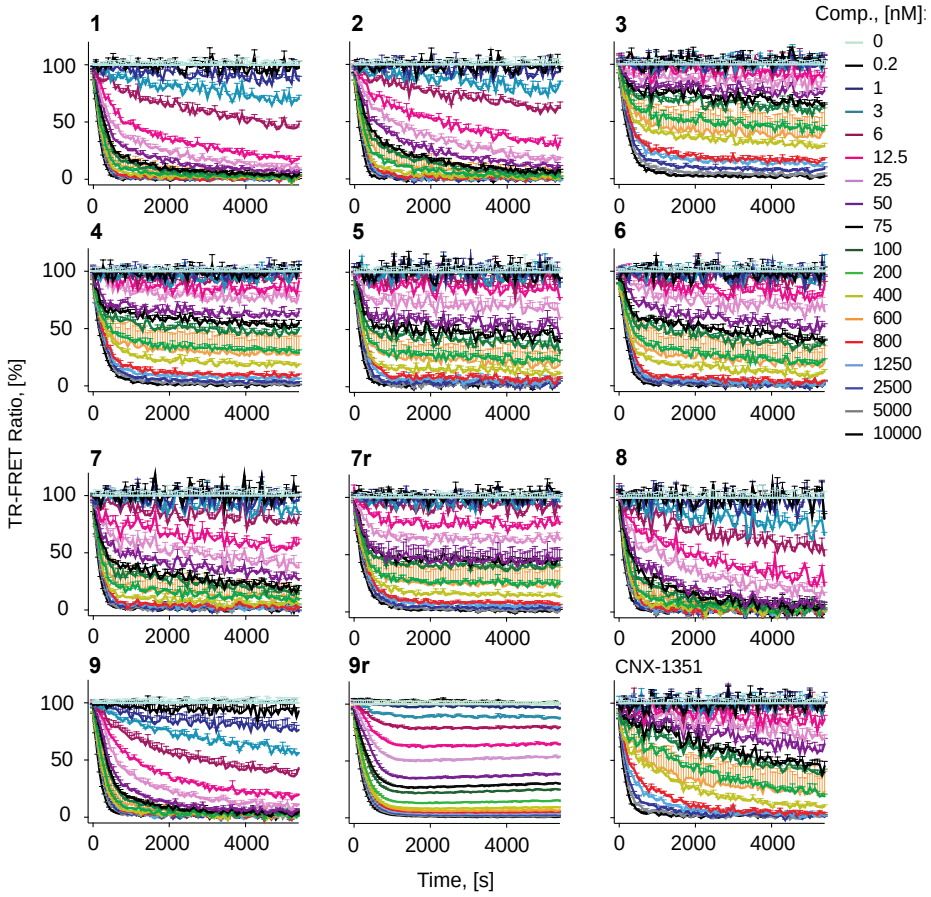

Figure S5. Time- and concentration-dependent TR-FRET ratio curves showing a time-dependent tracer displacement triggered by compound binding to recombinant PI3Kα protein. Data are presented as mean ± SEM (n = 3).

Figure S6. Solvent dependent conformers of 1, 7 and 9

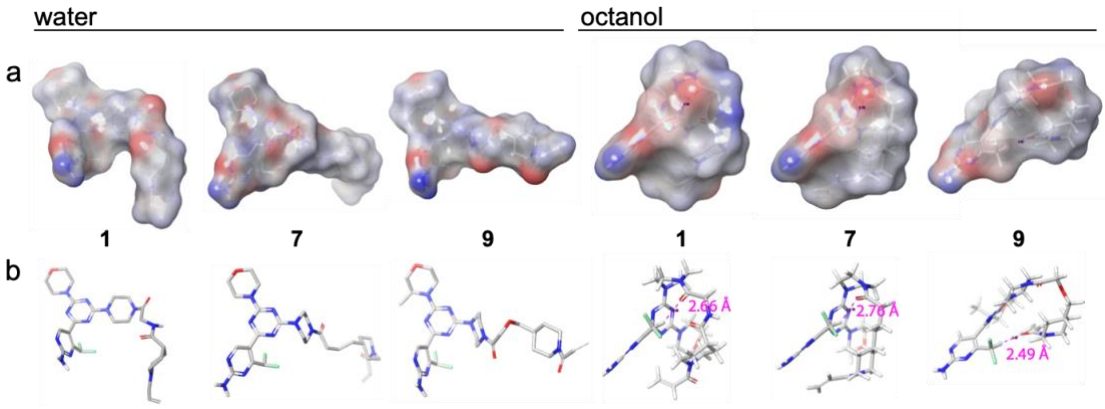

Figure S6. Representative conformers of **1**, **7**, and **9** observed during MacroModel conformational sampling in water or octanol. For each structure-solvent pair, the representative conformer is depicted as: **(a)** ligand surface, color coded according to its electrostatic potential, with color ramp in Red_White_Blue (min: -0.3; max 0.3); **(b)** thick tube representation via Maestro Schrödinger, with light grey atoms: C, red atoms: O, blue atoms: N, light green atoms: F. Intramolecular hydrogen bonds are depicted as a magenta dashed line. For TPSA and 3D PSA values see Table S6.

Figure S7. Cell cycle distribution and effect of loss of PTEN on growth rate

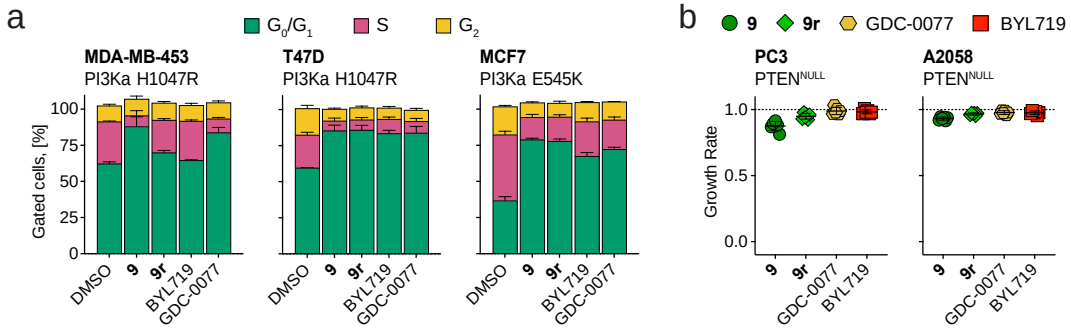

Figure S7. (a) Cell cycle distribution in cancer cell lines with mutated PI3Kα after 48 h exposure to 50 nM (MDA-MB-453) or 1 µM (T47D and MCF7) of the indicated inhibitors or DMSO. After DAPI staining, cell cycle profiles were determined by FACS (n=3, mean ± SEM). **(b)** Growth rate of cancer cell lines with loss of PTEN in response to intermittent exposure (4 h/day followed by washout for 4 days) to inhibitors (n = 2 with technical triplicates, mean ± SD). Experiments were carried out in complete growth medium containing 10% FCS.

Figure S8. IC_{50}s for pPKB and pS6; growth rate, and FOXO1 translocation

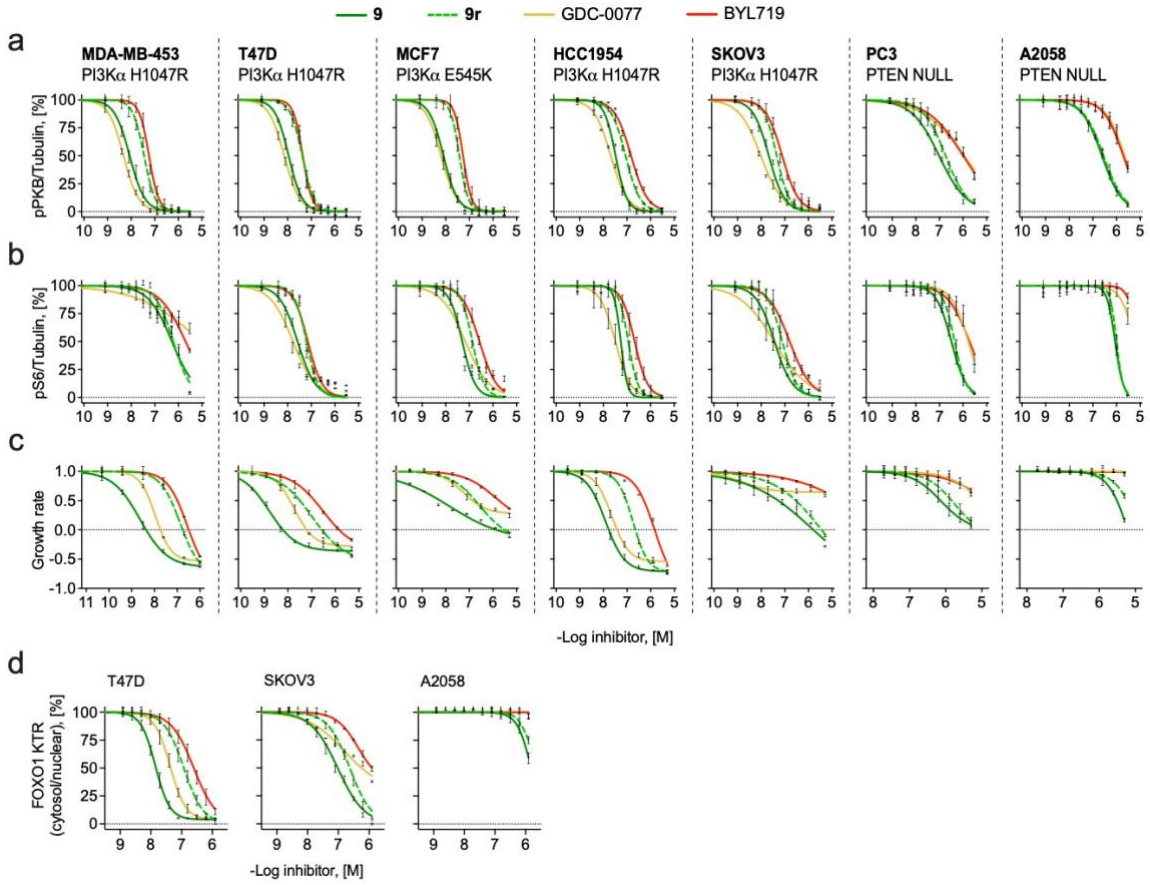

Figure S8. (a) Dose-response curves for pPKB (Ser473)/Tubulin determined by in-cell western (ICW) after 2 h incubation with indicated compounds. Data are shown as mean ± SEM. MDA-MB-453 and PC3 (n=4), T47D, MCF7, HCC1954, SKOV3 and A2058 (n=3). **(b)** Dose-response curves for pS6 (Ser235/Ser236)/Tubulin determined by ICW after 2 h incubation with compounds. Data are shown as mean ± SEM. MDA-MB-453, T47D, MCF7, HCC1954, SKOV3 and PC3 (n=3), A2058 (n=4). **(c)** Growth rate inhibition curves determined by resazurin assay after 72 h incubation with compounds. Data are shown as mean ± SEM. MDA-MB-453 and HCC1954 (n=3), T47D, MCF7, SKOV3, PC3, A2058 (n=4). **(d)** FOXO1 KTR translocation (cytosolic/nuclear ratio) determined by high-content microscopy after 2 h incubation with compounds. Data are shown as mean ± SEM (n = 3). Experiments were carried out in complete growth medium containing 10% FCS.

Figure S9. Western blots associated with Figure 5 and Figure S10

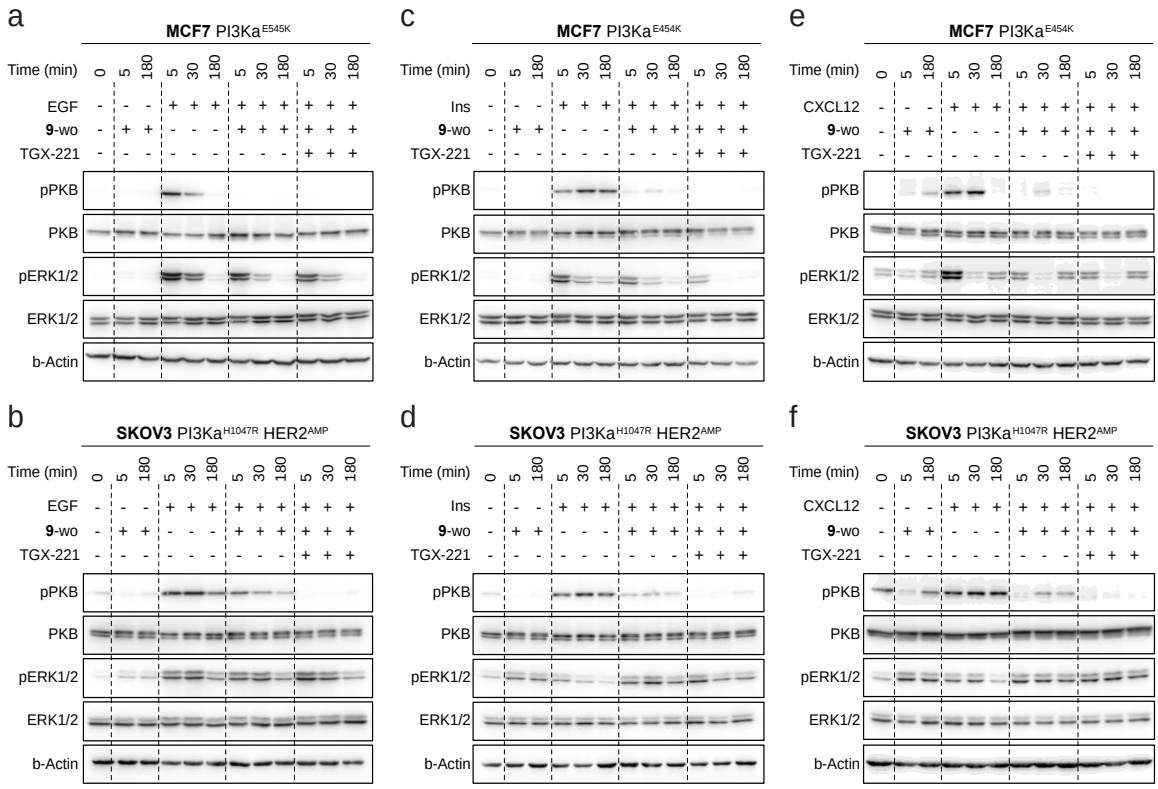

Figure S9. Representative western blots associated with data in Figure 5 and Figure S10. Serum-starved MCF7 or SKOV3 cells (24 h) were pre-incubated with **9** (1 μM) for 2 h followed by washout (labelled **9**-wo). Receptor ligands: **(a,b)** 10 ng/ml EGF, **(c,d)** 10 μg/ml insulin, and **(e,f)** 50 ng/ml CXCL12 were then added to the medium in the absence or presence of the PI3Kβ-selective inhibitor TGX221 (1 μM) for the indicated times (5, 30, 180 min) followed by lysis and measurement of phosphorylated and total Akt/PKB (Ser473) and ERK1/2 (Thr202/Tyr204) by western blot. β-Actin serves as loading control. Stimulations and washouts were carried out using medium without FCS.

Figure S10. MAPK pathway activation in cancer cell lines - washout assay

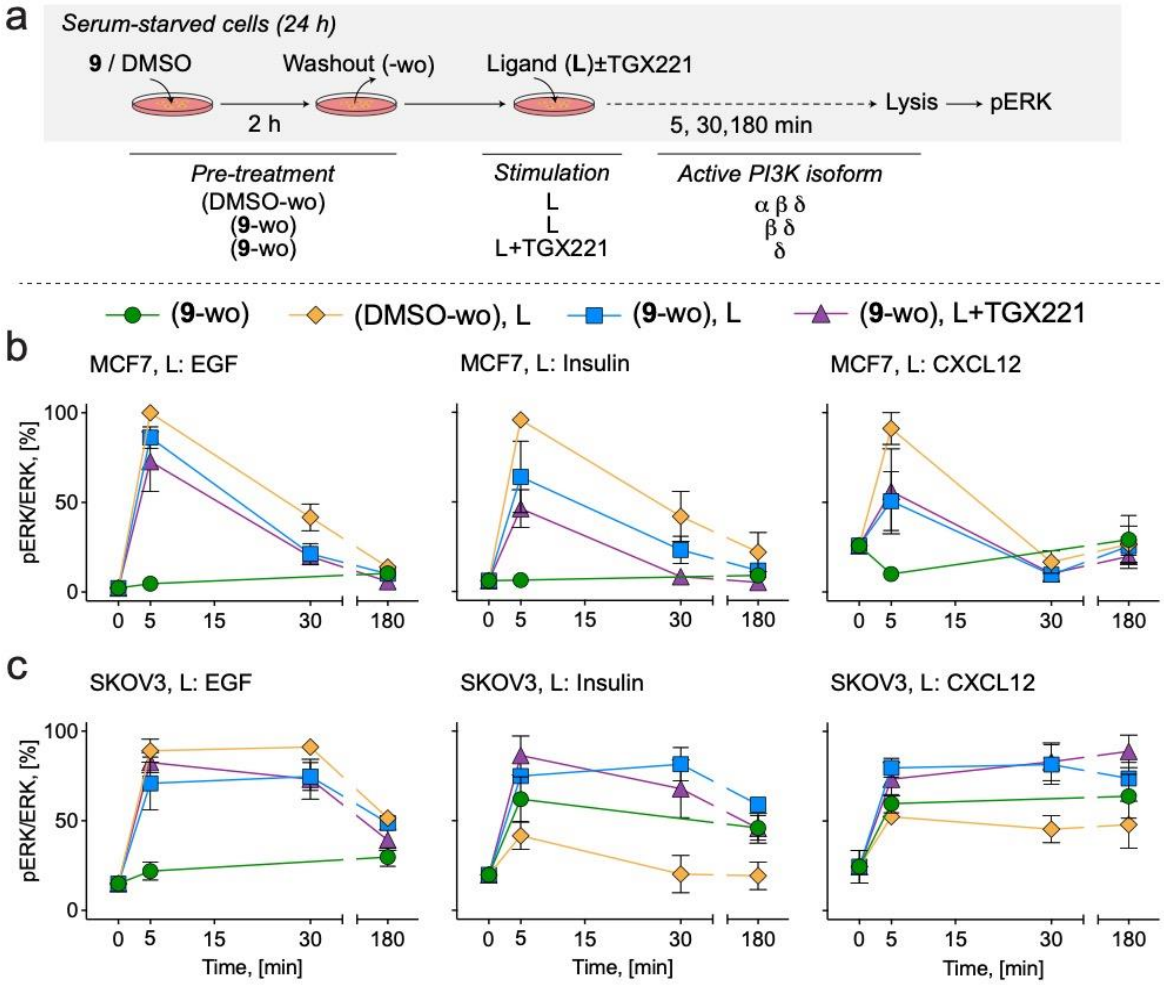

Figure S10. (a) Schematic diagram of MAPK pathway stimulation in cancer cell lines. Serum starved cells (24 h) were incubated with 1 µM **9** or DMSO for 2 h followed by washout (labelled **9**-wo or DMSO-wo). Receptor ligands (L) were then added to the medium in the absence or presence of the PI3Kβ-selective inhibitor TGX221 (1 µM) for the indicated times (5, 30, 180 min) prior to lysis. Total ERK1/2 and pERK1/2 (Thr202/Tyr204) levels were measured by western blot (Figure S9) as a readout of MAPK signaling. All treatments and media changes were carried out using serum-free medium. Depicted in the schematic are the PI3K isoforms remaining active after inhibitor treatments. **(b)** MAPK signaling in MCF7 cells treated with inhibitors and stimulated with 10 ng/ml EGF (left), 10 µg/ml insulin (center) or 50 ng/ml CXCL12 (right). **(c)** MAPK signaling in SKOV3 cells treated with inhibitors and stimulated with 10 ng/ml EGF (left), 10 µg/ml insulin (center) or 50 ng/ml CXCL12 (right). Stimulations and washouts were carried out using medium without FCS.

Figure S11. KinomeScan of 1, PQR514, PQR309, BYL719, GDC0980, and PKI-587

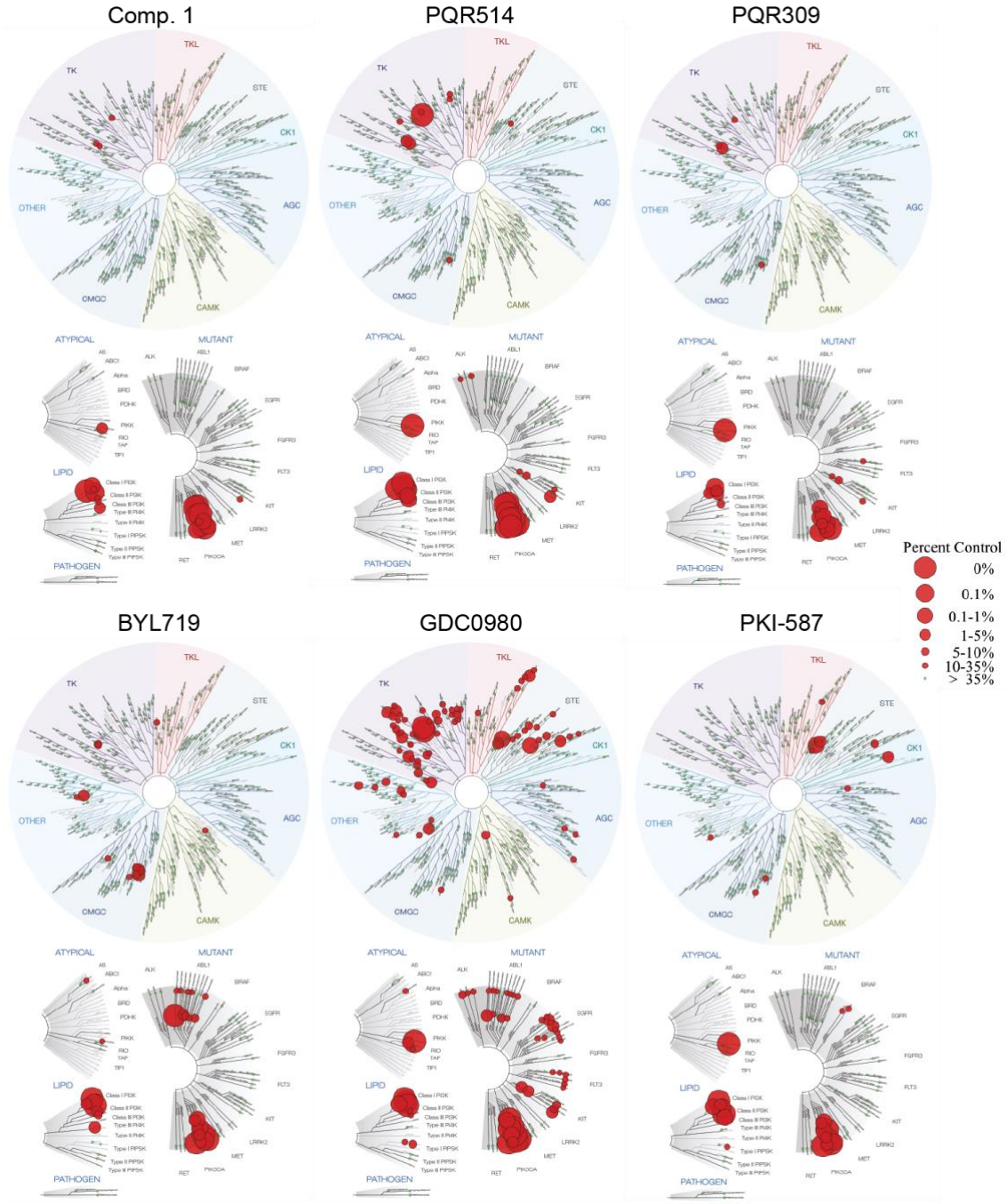

Figure S11. Kinome interactions of compound **1**, PQR514, PQR309, BYL719, GDC0980, PKI-587 as TREEspot Visualization. For data on **9** see Figure 6. Kinases that bind to compounds are marked by red circles (larger circles indicate higher-affinity; see free kinase as % of control). AGC: PKA, PKG and PKC kinases; CAMK: calcium-calmodulin-dependent protein kinases; CK1: casein kinase 1; CMGC: CDK, MAPK, GSK3, CLK family kinases; STE: Homologs of yeast Sterile 7, Sterile 11, Sterile 20 kinases; TK: Tyrosine kinases; TKL: Tyrosine kinase-like. Quantitative values for all compounds are in Table S11. Data for **1** and BYL719 (alpelisib) have been previously reported;[1] as well as PQR514;[2] PQR309, GDC0980 and PKI057.[3] Images were generated using TREEspot™ Software (KINOMEscan®, DiscoveRx). Selectivity scores are depicted in Table S12.

Supporting Tables

Table S1. Data for compounds 1-9, 7r, 9r, CNX1351, Ibrutinib, BYL719, GDC-0077

Compound	cLogP[a]	LogD		Solubility, [μM][b]		k_{chem} ·10^4, [M^{-1}s^{-1}][c,d]		k_{inact} ·10^4, [s^{-1}][d]		K_i, [nM][d]		k_{inact}/K_i·10^5, [nM^{-1}s^{-1}][d]		IC$_{50}$ pPKB, [nM][d,$]	
		Mean	SD	Mean	SD	Mean	SD	Mean	SD	Mean	SD	Mean	SD	Mean	SD
1	0.65	1.12	0.02	333	6.65	3.7	0.13	9.27	1.53	2.23	0.33	41.6	3.8	86	2.9
2	0.89	0.97	0.04	383	4.10	3.5	0.90	11.8	0.99	5.26	0.66	22.5	1.97	82	2.7
3	1.61	1.79	0.06	363	0.00	2.7	0.23	1.57	0.12	29.5	2.23	0.53	0.01	38	3.9
4	1.46	1.40	0.02	393	2.12	5.2[#]	0.43	1.13	0.15	13.7	1.42	0.82	0.08	69	15
5	3.85	3.32	0.01	7	0.28	3.2	0.27	0.85	0.05	8.4	1.01	1.03	0.15	54	5.6
6	3.85	2.66	0.03	46	0.14	2.9	0.47	2.14	0.15	11.6	1.18	1.85	0.07	41	7.0
7	2.68	2.67	0.04	243	0.42	2.5	0.01	3.09	0.31	5.00	0.91	6.24	0.53	22	2.4
7r	2.56	n.d.		n.d.		-	-	-	-	6.26	0.25	-	-	40	2.9
8	1.47	1.70	0.07	381	2.40	2.9	0.40	10.0	1.74	4.15	1.01	24.4	2.51	19	3.0
9	1.88	2.43	0.01	357	7.21	3.0	0.7	48.2	5.82	8.68	1.34	56.1	7.57	19	2.0
9r	1.76	n.d.		n.d.		-	-	-	-	2.9	0.12	-	-	48	3.6
CNX1351	4.68	3.96	0.17	10	0.00	2.22	0.61	7.79	0.77	43.3	6.93	1.82	0.19	172	27
Ibrutinib	3.57	4.08	0.03	10	0.42	10	1.02	-	-	-	-	-	-	-	-
BYL719	2.78	3.16	0.01	49	2.21	-	-	-	-	0.83	0.1	-	-	162	36
GDC-0077	1.12	1.10	0.02	357	2.55	-	-	-	-	0.50	0.04	-	-	10	1.5

[a]Calculated using MarvinSuite at pH 7.4; [b]Kinetic solubility measured by Bienta Enamine Biology Services at pH 7.4 (solubility in PBS). [c]Compound concentration was 1 mM and βME concentration was 600 mM. [d]Means and standard deviations (SD) were calculated from >= 3 independent measurements. [$]Phosphorylation of PKB/Akt on Ser473 was determined in SKOV3 cells by in-cell western assays after 1 h of compound exposure. [#]Approximation due to lack of baseline separation between starting material and adduct with βME; n.d., not determined.

Table S2. Summary of modified p110α peptides with

Peptide Probability	Treatment	Cys862 Modification	Modified Peptide Sequence	Protein	Neutral Mass	Charge	m/z	RT	ppm	mvh
0.999999	7	7	R.NSHTIM[147.04]QIQC[703.32]K.G	P42336	1917.9265	2	959.9705	2183.71	1.2449	20.72
0.999999	7	7	R.NSHTIMQIQC[703.32]K.G	P42336	1901.9316	2	951.9731	2443.76	2.561	18.14

Table S2. Peptide Probability: Trans Proteomic Pipeline derived probability; Cys862 Modification: Observed modification on Cys862; Modified Peptide Sequence,147.04 = oxidation, 703.32 = **7**; Protein, Protein Uniprot Accession; m/z, mass to change ratio; RT, retention time; ppm, ppm mass deviation precursor; mvh, mvh Myrimatch raw ion score.

Table S3. Data collection and refinement statistics (molecular replacement)

	PIK3CA-**9** (PDB: 8TWY)
Data collection	
Space group	P212121
Cell dimensions	
a, *b*, *c* (Å)	59.1 135.4 143.7
a, b, g (°)	90 90 90
Resolution (Å)	49.28 - 2.67 (2.73 - 2.67)*
R_{merge}	0.113 (3.7580)
$I / \sigma I$	15.7 (0.77)
CC1/2	0.999 (0.525)
Completeness (%)	99.68 (100.0)
Redundancy	13.5 (13.4)
Refinement	
Resolution (Å)	49.28 - 2.67
No. unique reflections	33570 (1573)
R_{work} / R_{free}	22.5/26.1
No. atoms	6631
Protein	6575
Ligand/ion	56
Water	0
B-factors	105.5
Protein	105.5
Ligand/ion	106.0
Water	
R.m.s. deviations	
Bond lengths (Å)	0.003
Bond angles (°)	0.57

*Values in parentheses are for highest-resolution shell.

Table S4. Lipophilic efficiency (LipE) calculations

Compound	LogD, pH 7.4	IC_{50} pPKB (S473) SKOV3, [nM]	pIC_{50}	LipE
1	1.12	81.7	7.09	5.97
2	0.97	85.7	7.07	6.10
3	1.79	38.3	7.42	5.63
4	1.40	68.4	7.17	5.77
5	3.32	54.1	7.27	3.95
6	2.66	41.0	7.39	4.73
7	2.67	21.5	7.67	5.00
8	1.7	19.3	7.71	6.01
9	2.43	19.2	7.71	5.29
CNX1351	3.96	172	6.76	2.80
BYL719	3.16	162	6.79	3.63

Table S4. LogD (pH7.4) were measured by Bienta Enamine Biology Services.

Lipophilic efficiency (LipE) calculations for compounds calculated to the following equation:

$$-\log(\mathrm{IC}_{50}) - \mathrm{LogD} = \mathrm{LipE}$$

Table S5. Relative diffusion coefficient calculations

Compound	$k_1\,[\mathbf{cm^3/s}]\cdot 10^4$		$D_{rel(BYL719)}\,[\mathbf{cm^2/s}]$	
	mean	SD	mean	SD
1	1.84	0.22	0.05	0.005
2	3.71	0.78	0.10	0.016
6	32.4	2.04	0.84	0.043
7	39.2	3.54	1.01	0.075
7r	39.5	6.44	1.02	0.136
8	88.3	7.99	2.28	0.168
9	108	2.7	2.78	0.057
9r	106	8.64	2.75	0.181
CNX1351	4.57	0.56	0.12	0.012
BYL719	38.8	4.23	1	0.089

Table S5. For detailed diffusion coefficient calculations see methods.

Table S6. TPSA and 3D PSA of representative conformers of 1, 7 and 9

Polar surface area	1	7	9
TPSA (Å^2)	175.9	146.8	156.0
3D PSA in water (Å^2)	165.1	137.0	141.1
3D PSA in octanol, (Å^2)	162.8	133.4	143.0

Table S6. For calculation of values see Computational Compound Conformation Searches.

Table S7. Growth rate inhibition (GR_{50}) for 9, 9r, GDC-0077 and BYL719

GR_{50}, [nM]														
Compound	T47D (n=4)		MCF7 (n=4)		MDA-MB-453 (n=3)		HCC1954 (n=3)		SKOV3 (n=4)		PC3 (n=4)		A2058 (n=4)	
	mean	SD	mean	SD	mean	SD	mean	SD	mean	SD	mean	SD	mean	SD
9	0.8	0.1	5.9	0.8	0.8	0.4	5.5	1.4	75.9	69	774	472	2693	266
9r	33.9	14.2	180	6.7	53.4	16.8	92.3	11.5	267	109	1576	809	>5000	-
GDC-0077	12.6	5.3	142	78.7	6.3	1.1	12.7	3.6	>5000	-	>5000	-	>5000	-
BYL719	67.2	15.9	1616	592	101	26.1	516	32.7	>5000	-	>5000	-	>5000	-

Table S8. pPKB (Ser473)/ Tubulin in-cell western IC_{50}s for 9, 9r, GDC-0077 and BYL719

pPKB/Akt, IC_{50}, [nM]														
Compound	T47D (n=3)		MCF7 (n=3)		MDA-MB-453 (n=4)		HCC1954 (n=3)		SKOV3 (n=3)		PC3 (n=4)		A2058 (n=3)	
	mean	SD	mean	SD	mean	SD	mean	SD	mean	SD	mean	SD	mean	SD
9	11.1	1.9	8.2	1.8	9.2	3.5	33.2	2.6	21.1	2.7	97.4	15.2	246	40.4
9r	43.4	11.8	38.1	7.0	35.6	7.5	87.8	13.3	45.9	4.4	183	16.3	287	49.2
GDC-0077	7.3	1.8	6.6	2.0	4.7	0.5	20.6	1.8	9.8	1.5	1212	479	2200	634
BYL719	43.8	6.7	54.6	8.8	57.4	11.8	149	17.7	76.5	14.3	1031	314	1940	604

Table S9. pS6/tubulin in-cell western: IC_{50}s for 9, 9r, GDC-0077 and BYL719.

pS6 IC_{50}, [nM]														
Compound	T47D (n=3)		MCF7 (n=3)		MDA-MB-453 (n=3)		HCC1954 (n=3)		SKOV3 (n=3)		PC3 (n=3)		A2058 (n=4)	
	mean	SD	mean	SD	mean	SD	mean	SD	mean	SD	mean	SD	mean	SD
9	26.4	3.7	50.3	8.8	549	189	56.4	12.2	36.7	9.2	325	76.5	876	110
9r	62.1	2.8	135	5.2	607	136	117	30.1	78.7	17.7	438	133	987	174
GDC-0077	17.1	4.1	68.3	10.3	>3000	-	33.1	15.8	36.3	16.9	1915	691	>3000	-
BYL719	70.2	6.4	267	67.9	2008	511	222	111	162	50.1	1648	626	>3000	-

Table S10. FOXO1 KTR translocation; IC_{50}s for 9, 9r, GDC-0077 and BYL719.

FOXO1 KTR, IC_{50}, [nM]						
Compound	T47D (n=3)		SKOV3 (n=3)		A2058 (n=3)	
	mean	SD	mean	SD	mean	SD
9	14.9	3.7	92.5	26.2	1547	225
9r	121	37.4	214	36.3	2384	449
GDC-0077	44.9	13.1	578	93.1	>3000	-
BYL719	249	114	1279	273	>3000	-

Table S11. Extended KINOMEscan data

↓ DiscoveRx Gene Symbol	% remaining; 1 μM for **9** and **1**; other compounds 10 μM						
Compound→	**9**	**1**	PQR514	PQR309	BYL719	GDC-0980	PKI-587
AAK1	100	100	62	83	17	50	99
ABL1(E255K)-phosphorylated	100	87	79	83	42	24	100
ABL1(F317I)-nonphosphorylated	76	100	84	100	2.8	100	100
ABL1(F317I)-phosphorylated	100	94	70	100	13	80	100
ABL1(F317L)-non-phosphorylated	50	90	81	100	8.8	88	79
ABL1(F317L)-phosphorylated	76	100	86	66	29	47	100
ABL1(H396P)-nonphosphorylated	99	94	60	92	0.05	2	100
ABL1(H396P)-phosphorylated	91	83	60	96	22	18	99
ABL1(M351T)-phosphorylated	78	99	68	100	32	20	100
ABL1(Q252H)-nonphosphorylated	96	94	70	89	32	7.5	100
ABL1(Q252H)-phosphorylated	72	100	47	88	85	13	94
ABL1(T315I)-nonphosphorylated	77	71	89	100	100	34	100
ABL1(T315I)-phosphorylated	95	82	64	80	100	16	100
ABL1(Y253F)-phosphorylated	76	90	63	100	81	21	97
ABL1-nonphosphorylated	100	80	70	62	9.4	25	100
ABL1-phosphorylated	97	93	61	86	30	23	99
ABL2	93	91	99	95	75	61	92
ACVR1	99	100	83	77	48	89	75
ACVR1B	100	82	94	99	77	100	100
ACVR2A	92	86	100	89	84	100	94
ACVR2B	88	91	100	76	96	86	83
ACVRL1	100	92	73	89	100	91	100
ADCK3	96	78	68	80	25	78	60
ADCK4	90	100	92	99	85	38	93
AKT1	100	94	94	75	44	96	93
AKT2	100	100	100	92	60	96	100
AKT3	100	100	59	97	55	100	95
ALK	72	71	26	94	87	17	80
ALK(C1156Y)	79	91	32	95	94	9.5	95
ALK(L1196M)	77	79	44	95	94	28	100
AMPK-alpha1	100	97	91	78	79	74	76
AMPK-alpha2	100	100	91	100	100	87	100
ANKK1	95	100	54	79	100	23	86
ARK5	100	99	94	97	92	72	82
ASK1	97	100	92	55	49	83	95
ASK2	96	100	76	100	100	72	100
AURKA	95	96	52	37	100	77	95
AURKB	100	56	91	81	100	100	100
AURKC	93	100	91	80	96	100	95
AXL	98	97	91	86	100	11	81
BIKE	90	94	91	87	36	78	80

↓ DiscoveRx Gene Symbol	% remaining; 1 μM for **9** and **1**; other compounds 10 μM						
Compound→	**9**	**1**	PQR514	PQR309	BYL719	GDC-0980	PKI-587
BLK	86	100	70	61	85	11	100
BMPR1A	100	80	93	100	74	73	72
BMPR1B	89	64	72	67	65	72	99
BMPR2	98	71	81	82	100	93	97
BMX	96	99	86	100	94	34	93
BRAF	90	92	36	75	61	78	20
BRAF(V600E)	81	89	42	65	67	77	14
BRK	97	100	97	100	83	57	84
BRSK1	100	100	91	98	83	80	78
BRSK2	100	100	92	61	74	95	97
BTK	100	66	26	83	85	4.5	93
BUB1	93	77	99	100	100	99	100
CAMK1	100	86	82	76	53	35	77
CAMK1B	97	100					
CAMK1D	100	100	100	83	72	78	91
CAMK1G	100	100	65	93	83	67	99
CAMK2A	100	96	64	88	68	80	70
CAMK2B	100	100	69	92	71	88	92
CAMK2D	100	100	66	100	88	93	94
CAMK2G	100	100	73	84	85	77	91
CAMK4	100	86	66	84	100	76	100
CAMKK1	98	96	70	100	83	73	93
CAMKK2	99	95	65	100	94	74	98
CASK	93	69	77	100	98	86	100
CDC2L1	100	100	95	100	100	100	91
CDC2L2	94	97	89	100	100	92	100
CDC2L5	96	95	95	80	94	100	96
CDK11	99	99	69	70	21	100	92
CDK2	100	100	100	93	96	93	88
CDK3	84	95	88	99	100	96	84
CDK4	100	92					
CDK4-cyclinD1	90	83	100	91	90	94	97
CDK4-cyclinD3	75	100	87	97	100	100	100
CDK5	100	100	100	85	100	73	98
CDK7	97	94	56	100	100	45	86
CDK8	96	100	100	100	52	87	84
CDK9	100	98	99	70	100	99	96
CDKL1	82	90	97	93	100	100	100
CDKL2	100	100	99	100	97	95	85
CDKL3	100	100	74	85	97	100	99
CDKL5	89	100	67	83	100	100	100
CHEK1	96	88	67	84	100	98	98
CHEK2	94	88	75	100	77	9.1	93
CIT	91	100	91	100	94	37	65

↓ DiscoveRx Gene Symbol	% remaining; 1 μM for **9** and **1**; other compounds 10 μM						
Compound→	**9**	**1**	PQR514	PQR309	BYL719	GDC-0980	PKI-587
CLK1	92	93	58	55	5.2	95	50
CLK2	79	91	41	84	3.4	60	90
CLK3	76	97	90	100	8.8	96	100
CLK4	100	100	30	32	4.2	87	29
CSF1R	86	77	14	7.4	68	12	98
CSF1R-autoinhibited	29	20	2.1	2.8	98	19	100
CSK	100	100	73	76	75	25	81
CSNK1A1	97	89	72	91	89	97	100
CSNK1A1L	97	100	74	95	79	100	99
CSNK1D	100	100	90	76	36	90	83
CSNK1E	90	87	38	78	62	83	3.2
CSNK1G1	100	99	79	100	86	80	75
CSNK1G2	99	100	85	82	100	73	56
CSNK1G3	100	100	95	100	93	85	81
CSNK2A1	92	75	79	59	97	97	91
CSNK2A2	88	100	69	100	100	89	95
CTK	100	78	100	91	100	57	97
DAPK1	91	96	94	86	85	82	89
DAPK2	100	95	76	94	59	75	81
DAPK3	100	89	80	94	64	78	78
DCAMKL1	100	59	86	84	84	70	73
DCAMKL2	92	98	86	100	100	100	100
DCAMKL3	100	96	73	85	100	100	100
DDR1	99	100	69	65	100	90	69
DDR2	100	83	57	100	100	66	73
DLK	72	97	91	81	86	15	87
DMPK	98	87	76	100	85	40	97
DMPK2	100	100	77	81	100	100	100
DRAK1	77	100	89	97	11	67	91
DRAK2	100	97	85	79	61	63	63
DYRK1A	85	94	48	100	30	96	90
DYRK1B	100	98	76	61	53	100	97
DYRK2	99	80	82	100	74	76	94
EGFR	89	100	56	73	90	11	78
EGFR(E746-A750del)	100	95	77	95	88	14	79
EGFR(G719C)	98	87	56	54	94	30	98
EGFR(G719S)	97	97	75	64	100	40	100
EGFR(L747-E749del, A750P)	93	100	63	85	100	17	98
EGFR(L747-S752del, P753S)	100	82	85	90	94	31	77
EGFR(L747-T751del,Sins)	100	98	77	84	97	25	100
EGFR(L858R)	89	100	40	90	100	18	100
EGFR(L858R,T790M)	98	97	74	78	90	3	85
EGFR(L861Q)	100	93	77	63	98	15	100
EGFR(S752-I759del)	100	92	88	73	93	22	100

↓ DiscoveRx Gene Symbol	% remaining; 1 μM for **9** and **1**; other compounds 10 μM						
Compound→	**9**	**1**	PQR514	PQR309	BYL719	GDC-0980	PKI-587
EGFR(T790M)	86	90	51	92	100	4.3	100
EIF2AK1	81	94	85	100	100	100	100
EPHA1	100	100	68	76	100	72	100
EPHA2	100	95	94	100	98	100	100
EPHA3	94	90	69	79	92	50	99
EPHA4	100	94	94	83	100	98	92
EPHA5	100	100	97	98	100	78	96
EPHA6	100	100	94	89	100	100	90
EPHA7	85	100	86	93	83	88	89
EPHA8	88	100	100	80	80	80	78
EPHB1	100	100	98	70	91	92	92
EPHB2	94	95	95	95	94	78	92
EPHB3	100	98	96	84	96	100	79
EPHB4	100	100	97	84	98	77	91
EPHB6	59	65	50	54	82	8.6	97
ERBB2	100	70	65	65	100	72	97
ERBB3	100	84	69	61	96	29	92
ERBB4	100	100	60	79	100	24	96
ERK1	100	100	89	77	100	98	100
ERK2	100	98	98	89	100	79	94
ERK3	100	96	88	78	100	100	100
ERK4	100	97	99	100	100	100	100
ERK5	100	100	97	86	100	99	82
ERK8	100	97	100	100	82	88	82
ERN1	100	100	80	73	100	73	100
FAK	100	100	100	79	99	83	99
FER	96	87	67	96	100	9.1	100
FES	100	100	91	76	100	94	84
FGFR1	100	100	94	100	63	100	94
FGFR2	100	89	90	93	100	100	100
FGFR3	100	96	88	100	100	91	98
FGFR3(G697C)	100	99	83	65	97	87	99
FGFR4	97	100	100	84	75	89	75
FGR	100	97	97	86	95	14	83
FLT1	96	99	91	98	99	62	82
FLT3	86	91	88	52	72	30	78
FLT3(D835H)	74	100	55	57	85	16	100
FLT3(D835V)	49	61					
FLT3(D835Y)	87	99	48	54	100	11	96
FLT3(ITD)	95	97	77	90	100	19	97
FLT3(ITD,D835V)	100	87					
FLT3(ITD,F691L)	44	95					
FLT3(K663Q)	61	100	48	69	83	18	89
FLT3(N841I)	95	100	46	35	75	34	100

↓ DiscoveRx Gene Symbol	% remaining; 1 μM for **9** and **1**; other compounds 10 μM						
Compound→	**9**	**1**	PQR514	PQR309	BYL719	GDC-0980	PKI-587
FLT3(R834Q)	77	84	95	87	88	60	100
FLT3-autoinhibited	92	99	50	78	100	58	100
FLT4	83	96	77	83	91	86	82
FRK	96	100	100	100	82	74	88
FYN	94	100	100	100	77	23	73
GAK	91	100	75	97	4.8	70	98
GCN2(Kin.Dom.2,S808G)	100	100	71	100	100	3.4	100
GRK1	100	67	86	100	100	96	100
GRK2	100	100					
GRK3	73	100					
GRK4	58	100	74	91	85	68	60
GRK7	100	87	67	100	100	89	100
GSK3A	93	92	91	61	100	98	88
GSK3B	99	74	74	92	100	100	100
HASPIN	71	75	71	70	78	98	44
HCK	100	86	77	95	98	1.6	100
HIPK1	96	97	69	76	53	44	82
HIPK2	75	83	59	100	71	19	34
HIPK3	100	100	56	78	98	57	89
HIPK4	100	100	100	86	7.5	91	86
HPK1	100	100	88	66	90	12	67
HUNK	79	79	78	100	100	91	64
ICK	75	95	72	100	100	100	100
IGF1R	92	100	78	67	100	31	100
IKK-alpha	76	71	39	100	100	94	64
IKK-beta	100	73	77	100	100	100	100
IKK-epsilon	84	71	99	100	95	51	85
INSR	94	99	50	86	100	7.3	100
INSRR	87	96	80	92	85	19	72
IRAK1	100	100	50	100	77	78	100
IRAK3	97	89	83	68	16	61	79
IRAK4	84	95	72	100	90	100	99
ITK	66	99	44	88	84	19	84
JAK1(JH1domain-catalytic)	91	100	90	80	100	96	100
JAK1(JH2domain-pseudokinase)	1.2	32	0.05	20	100	0	100
JAK2(JH1domain-catalytic)	90	88	65	88	100	7.4	100
JAK3(JH1domain-catalytic)	100	88	46	63	94	8.7	83
JNK1	93	93	86	74	55	47	100
JNK2	78	89	83	89	93	95	100
JNK3	80	100	90	83	59	93	100
KIT	96	93	20	29	100	2	81
KIT(A829P)	63	100	80	85	88	49	97
KIT(D816H)	57	100	89	81	86	57	94

↓ DiscoveRx Gene Symbol	% remaining; 1 μM for **9** and **1**; other compounds 10 μM						
Compound→	**9**	**1**	PQR514	PQR309	BYL719	GDC-0980	PKI-587
KIT(D816V)	90	79	58	94	86	40	84
KIT(L576P)	82	53	7.4	6.5	100	3	98
KIT(V559D)	95	78	18	21	100	1.1	94
KIT(V559D,T670I)	95	82	26	64	84	5.2	99
KIT(V559D,V654A)	98	100	43	45	98	7.6	87
KIT-autoinhibited	63	35	4.8	17	100	43	100
LATS1	96	100	82	96	100	59	39
LATS2	87	100	89	100	100	96	28
LCK	94	90	46	93	88	9.5	93
LIMK1	98	100	86	97	82	92	87
LIMK2	100	97	81	62	100	100	100
LKB1	77	100	91	92	82	100	79
LOK	100	95	64	72	85	28	76
LRRK2	89	63	97	91	96	98	100
LRRK2(G2019S)	92	79	91	80	92	82	93
LTK	91	100	26	86	87	10	76
LYN	90	100	95	85	100	43	97
LZK	78	100	100	97	87	20	95
MAK	100	100	100	79	86	91	93
MAP3K1	100	93	77	100	100	93	100
MAP3K15	97	100	61	100	100	96	100
MAP3K2	97	69	71	100	100	13	80
MAP3K3	100	99	72	79	100	10	100
MAP3K4	100	100	82	68	84	95	71
MAP4K2	81	100	78	90	98	9.8	90
MAP4K3	89	86	87	71	97	51	92
MAP4K4	85	80	100	99	86	78	83
MAP4K5	96	95	100	89	100	93	100
MAPKAPK2	90	100	85	80	100	96	85
MAPKAPK5	100	92	72	89	92	75	64
MARK1	100	100	88	75	67	67	97
MARK2	77	90	77	87	80	54	85
MARK3	100	65	100	78	91	67	97
MARK4	100	97	90	76	64	77	100
MAST1	97	100	90	100	83	69	94
MEK1	99	69	83	72	100	26	100
MEK2	99	59	77	98	100	7	100
MEK3	80	59	78	100	100	99	100
MEK4	93	100	96	100	100	100	100
MEK5	96	77	39	100	100	0.4	100
MEK6	100	100	92	70	100	68	60
MELK	100	100	82	64	64	73	76
MERTK	80	94	87	100	91	37	87
MET	94	75	63	60	100	63	95

↓ DiscoveRx Gene Symbol	% remaining; 1 μM for **9** and **1**; other compounds 10 μM						
Compound→	**9**	**1**	PQR514	PQR309	BYL719	GDC-0980	PKI-587
MET(M1250T)	97	95	100	93	100	83	98
MET(Y1235D)	100	98	92	100	94	68	74
MINK	100	99	66	86	100	24	64
MKK7	74	98	61	100	100	89	91
MKNK1	97	83	45	100	99	100	100
MKNK2	84	100	56	91	93	100	65
MLCK	99	92	84	94	98	74	62
MLK1	92	96	42	87	91	3.2	97
MLK2	100	99	53	59	43	41	100
MLK3	90	79	47	100	91	17	89
MRCKA	100	100	95	100	77	88	74
MRCKB	100	99	95	89	100	94	83
MST1	100	92	86	83	100	87	84
MST1R	100	100	96	69	92	81	91
MST2	100	97	95	72	100	92	91
MST3	100	98	91	92	97	93	96
MST4	100	100	91	56	100	97	100
MTOR	4.5	1.2	0	0	12	0.05	0
MUSK	100	79	92	100	80	90	74
MYLK	100	61	78	95	66	73	37
MYLK2	100	97	92	97	88	87	100
MYLK4	100	100	87	77	75	96	95
MYO3A	100	100	92	86	85	94	64
MYO3B	93	96	99	100	100	80	83
NDR1	92	88	66	71	100	26	54
NDR2	73	97	72	93	88	44	62
NEK1	90	96	99	76	70	85	62
NEK10	100	76	66	100	78	5	61
NEK11	65	69	89	100	87	50	82
NEK2	94	95	87	100	97	24	100
NEK3	96	51	78	100	98	100	100
NEK4	94	81	75	100	97	9.2	100
NEK5	100	100	92	100	60	100	100
NEK6	100	95	100	100	66	84	95
NEK7	89	100	70	100	39	87	100
NEK9	74	100	92	100	40	90	90
NIK	100	89	70	100	100	73	99
NIM1	85	100	68	92	100	100	98
NLK	100	94	88	99	83	75	68
OSR1	88	100	54	100	100	100	100
p38-alpha	100	100	82	98	88	92	98
p38-beta	100	89	98	95	97	79	92
p38-delta	100	99	95	55	74	72	73
p38-gamma	99	96	100	74	100	83	100

↓ DiscoveRx Gene Symbol	% remaining; 1 μM for **9** and **1**; other compounds 10 μM						
Compound→	**9**	**1**	PQR514	PQR309	BYL719	GDC-0980	PKI-587
PAK1	100	92	63	94	80	53	93
PAK2	97	100	58	88	98	65	100
PAK3	83	96	82	86	100	51	100
PAK4	88	99	58	93	84	3.9	100
PAK6	100	100	79	83	75	47	92
PAK7	84	79	52	86	92	0.65	87
PCTK1	90	100	90	100	100	100	100
PCTK2	100	89	100	98	100	95	76
PCTK3	91	95	82	100	100	98	100
PDGFRA	86	91	80	85	100	73	100
PDGFRB	100	100	69	97	100	8.9	75
PDPK1	100	93	83	53	100	96	80
PFCDPK1(P.falciparum)	100	81	57	100	87	67	84
PFPK5(P.falciparum)	92	65	64	78	100	99	100
PFTAIRE2	95	100	94	100	99	86	93
PFTK1	92	100	82	93	100	96	100
PHKG1	92	100	94	91	76	82	98
PHKG2	100	89	67	89	79	87	67
PIK3C2B	46	21	0.75	41	4	31	0
PIK3C2G	79	16	0.75	7	9.6	12	0.2
PIK3CA	0	0.4	0	0.1	0.05	0	0
PIK3CA(C420R)	0	0.6	0	0	0.05	0	0.15
PIK3CA(E542K)	1.2	0	0	0.2	0.1	0.05	0
PIK3CA(E545A)	0	0.5	0	0.1	0.05	0	0.15
PIK3CA(E545K)	0	0	0	0.2	0.2	0.05	0
PIK3CA(H1047L)	0	0.45	0	14	3.5	2	2.3
PIK3CA(H1047Y)	0.15	5.9	0	1.4	1	0.35	1.8
PIK3CA(I800L)	0.2	0	0.05	0.4	1.2	0.05	0.75
PIK3CA(M1043I)	11	0	0	13	1.5	0.65	3.5
PIK3CA(Q546K)	4.5	0	0	0.5	0.15	0.05	0.2
PIK3CB	0.55	0.05	0	2.6	2.9	0.3	0.25
PIK3CD	0.75	19	0	2.6	0.15	0	4.8
PIK3CG	0.55	0.1	0	1	0	0	0.1
PIK4CB	100	100	75	95	1.7	100	95
PIKFYVE	71	74					
PIM1	100	95	96	85	82	82	100
PIM2	100	82	92	86	79	87	66
PIM3	100	97	89	78	91	85	100
PIP5K1A	100	100	100	82	59	8.9	27
PIP5K1C	95	85	100	100	100	27	80
PIP5K2B	86	99	100	94	100	84	99
PIP5K2C	90	95	84	96	100	96	83
PKAC-alpha	92	100	85	67	100	70	84
PKAC-beta	93	90	61	83	95	72	94

↓ DiscoveRx Gene Symbol	% remaining; 1 μM for **9** and **1**; other compounds 10 μM						
Compound→	**9**	**1**	PQR514	PQR309	BYL719	GDC-0980	PKI-587
PKMYT1	92	92	98	66	100	98	87
PKN1	100	83	49	73	87	71	93
PKN2	94	84	100	100	87	93	100
PKNB(M.tuberculosis)	91	67	66	100	100	100	66
PLK1	100	99	66	49	100	100	95
PLK2	100	95	73	65	88	67	89
PLK3	100	58	83	96	97	69	97
PLK4	87	89	69	81	100	57	100
PRKCD	100	100	97	100	65	62	76
PRKCE	85	79	96	42	100	26	73
PRKCH	100	100	91	100	100	45	86
PRKCI	100	95	95	92	100	100	100
PRKCQ	99	83	37	100	100	63	97
PRKD1	100	90	80	100	100	100	100
PRKD2	94	100	99	90	99	100	89
PRKD3	100	93	67	85	100	98	84
PRKG1	96	87	79	100	77	85	68
PRKG2	100	69	90	92	99	91	89
PRKR	100	100	91	72	96	20	98
PRKX	99	100	90	75	74	59	73
PRP4	84	100	100	79	99	75	84
PYK2	95	100	70	100	98	58	100
QSK	98	76	72	84	100	94	100
RAF1	100	93	98	92	100	100	100
RET	91	94	100	80	81	68	76
RET(M918T)	79	97	78	84	87	62	99
RET(V804L)	82	100	88	86	90	63	92
RET(V804M)	98	100	73	86	90	57	87
RIOK1	71	98	82	97	43	24	63
RIOK2	100	83	51	90	100	2.1	67
RIOK3	100	100	98	84	81	79	61
RIPK1	100	100	91	84	100	100	100
RIPK2	95	100	100	100	60	76	72
RIPK4	100	76	82	100	100	99	53
RIPK5	100	72	79	98	94	53	78
ROCK1	100	100	99	100	93	76	65
ROCK2	96	90	100	100	86	75	58
ROS1	88	87	54	65	88	26	96
RPS6KA4(Kin.Dom.1-N-terminal)	93	82	82	86	100	89	96
RPS6KA4(Kin.Dom.2-C-terminal)	100	100	63	88	92	92	91
RPS6KA5(Kin.Dom.1-N-terminal)	100	100	88	92	99	91	93

↓ DiscoveRx Gene Symbol	% remaining; 1 μM for **9** and **1**; other compounds 10 μM						
Compound→	**9**	**1**	PQR514	PQR309	BYL719	GDC-0980	PKI-587
RPS6KA5(Kin.Dom.2-C-terminal)	100	100	88	95	80	83	91
RSK1(Kin.Dom.1-N-terminal)	93	100	75	74	68	25	100
RSK1(Kin.Dom.2-C-terminal)	96	100	88	86	85	92	91
RSK2(Kin.Dom.1-N-terminal)	100	85	59	96	100	14	84
RSK2(Kin.Dom.2-C-terminal)	82	63	84	96	100	100	100
RSK3(Kin.Dom.1-N-terminal)	100	82	44	100	100	51	100
RSK3(Kin.Dom.2-C-terminal)	90	93	95	100	90	88	95
RSK4(Kin.Dom.1-N-terminal)	84	100	48	100	100	66	77
RSK4(Kin.Dom.2-C-terminal)	84	95	94	100	94	99	99
S6K1	100	56	76	100	89	73	91
SBK1	100	100	60	100	98	75	89
SGK	91	85	77	93	100	100	100
SgK110	91	87	85	76	100	57	100
SGK2	100	86	84	96	100	100	100
SGK3	99	100	44	89	100	69	85
SIK	100	89	100	91	97	49	94
SIK2	91	96	97	97	100	98	70
SLK	82	80	24	96	95	14	86
SNARK	100	100	50	100	100	52	97
SNRK	87	99	81	100	92	89	85
SRC	94	91	57	77	92	1.6	100
SRMS	89	72	88	94	100	27	97
SRPK1	100	75	82	78	91	66	93
SRPK2	88	100	100	58	92	80	58
SRPK3	95	99	77	77	100	64	64
STK16	100	92	56	78	66	22	73
STK33	98	100	94	66	43	61	93
STK35	94	93	55	85	98	12	87
STK36	98	95	99	86	88	92	84
STK39	100	76	70	100	82	71	100
SYK	96	86	61	100	69	1.8	71
TAK1	98	100	91	100	81	35	91
TAOK1	93	80	60	86	96	100	2
TAOK2	90	72	92	100	88	75	0.6
TAOK3	100	77	70	87	100	100	12
TBK1	100	91	95	76	91	71	90
TEC	94	99	58	80	94	8.4	67
TESK1	100	100	72	83	93	86	87
TGFBR1	100	100	100	100	100	100	89
TGFBR2	100	88	69	90	78	89	100
TIE1	100	100	84	100	80	80	64
TIE2	100	97	99	100	93	86	100
TLK1	89	99	92	93	100	97	94

↓ DiscoveRx Gene Symbol	% remaining; 1 μM for **9** and **1**; other compounds 10 μM						
Compound→	**9**	**1**	PQR514	PQR309	BYL719	GDC-0980	PKI-587
TLK2	100	100	100	74	91	88	88
TNIK	92	87	82	75	81	27	73
TNK1	94	83	83	90	80	92	100
TNK2	98	100	85	75	71	81	87
TNNI3K	97	100	100	100	78	62	72
TRKA	59	81	78	88	91	32	88
TRKB	95	89	74	84	87	30	100
TRKC	36	86	87	92	100	51	96
TRPM6	65	71	59	85	72	32	66
TSSK1B	100	95	100	90	65	49	75
TSSK3	100	100					
TTK	100	92	84	80	65	56	80
TXK	100	100	56	74	89	30	94
TYK2(JH1domain-catalytic)	81	92	56	91	100	56	98
TYK2(JH2domain-pseudokinase)	65	56	15	100	97	0.05	92
TYRO3	100	100	81	68	66	56	95
ULK1	68	85	57	100	100	100	100
ULK2	100	96	72	91	100	100	100
ULK3	96	81	60	100	100	6.6	100
VEGFR2	94	81	41	100	100	30	100
VPS34	29	4.5					
VRK2	71	93	64	100	100	97	97
WEE1	98	89	100	84	100	100	100
WEE2	97	100	82	100	96	88	100
WNK1	100	99	57	100	58	46	38
WNK2	69	92					
WNK3	93	96	56	100	52	24	31
WNK4	46	92					
YANK1	87	91	94	100	100	100	100
YANK2	100	93	90	76	100	79	89
YANK3	100	99	100	79	81	64	94
YES	84	97	80	76	83	15	100
YSK1	100	96	93	69	98	95	70
YSK4	63	42	41	100	83	1.8	6.7
ZAK	100	100	80	83	59	96	99
ZAP70	98	100	94	87	97	35	100

Data for **1** and BYL719 (Alpelisib) have been reported previously;[1] PQR514 data are from Ref. 2; PQR309, GDC0980 and PKI057 are from Ref. 3.

Table S12. Selectivity profile based on KinomeScan data.

S-Score[a]	S35 (# of hits)	S10 (# of hits)	S1(# of hits)	# of Kinases	Drug [μM]
9	0.020 (8)	0.015 (6)	0.010 (4)	403	1
1	0.025 (10)	0.012 (5)	0.007 (3)	403	1
PQR514	0.041 (16)	0.025 (10)	0.02 (8)	395	10
PQR309	0.025 (10)	0.018 (7)	0.005 (2)	395	10
BYL719	0.053 (21)	0.035 (14)	0.008 (3)	395	10
GDC0980	0.215 (85)	0.086 (34)	0.023 (9)	395	10
PKI-587	0.046 (18)	0.028 (11)	0.018 (7)	395	10

[a]Selectivity Score (S-score) is a quantitative measure of compound selectivity, and is calculated with the formula:

S = Number of hits / Number of tested kinases (excluding mutant variants).

S35, S10, S1 were calculated using % of control as a potency threshold (35, 10, 1%), e.g. S(35) = (number of non-mutant kinases with % of control <35)/(number of non-mutant kinases tested).

Extended Materials and Methods

Determination of Covalent PI3Kα Modification by Mass Spectrometry

Determination of covalent PI3Kα modification by mass spectrometry was carried out as described earlier:[1] 200 ng bovine serum albumin, (BSA, Thermo Scientific) and 200 ng PI3Kα (Life Technologies) were diluted in 100 µL reaction buffer (50 mM HEPES, 10 mM $MgCl_2$, 1 mM EGTA, pH 7.5). Compound **7** and **7r** or DMSO were added to a final concentration of 1 µM and incubated at 25 °C for 2 h with gentle agitation. Microcon Ym-10 ultrafiltration filters (Merck) were washed with 200 µL urea buffer (8 M urea, 100 mM Tris, pH 8). All centrifugation steps were performed at 14000 g at room temperature for 30 min. Samples were applied to the Ym-10 filters followed by centrifugation. The retentates were dissolved in 250 µL urea buffer supplemented with 5 mM DTT (Sigma) and incubated at 37 °C for 30 min. The filters were centrifuged and 250 µL urea buffer supplemented with 10 mM iodoacetamide (Sigma) was added. Samples were incubated in the dark for 30 min and centrifuged again. The retentates were washed twice in 250 µL 100 mM Tris (pH 8) followed by another centrifugation step. Finally, samples were diluted in 200 µL of 100 mM Tris (pH 8) and digested with 100 ng Lys-C (Wako) for 1 h followed by 200 ng Trypsin (Promega) overnight at 37 °C. Peptides were harvested in clean Eppendorf tubes by centrifugation, addition of 200 µL of 100 mM Tris pH 8 and subsequent centrifugation. Peptides were concentrated by SPE in UltraMicro spin columns (Nest Group) according to manufacturer instructions and dried in a Speedvac. Dried peptides were reconstituted in 8 µL of 2% acetonitrile (ACN), 0.5% trifluoroacetic acid (TFA) and subjected to LC-MS/MS analysis.

LC-MS/MS data was acquired in data-dependent mode on a system consisting of a Proxeon Ultra easy LC and an Orbitrap Elite (Thermo Scientific). Peptides were separated on a PepMap100 column (C18, 0.075 x 150 mm, 2 µm, 100A) with solvent A: 5% ACN, 0.1% formic acid (FA) in water and solvent B: 98% ACN, 0.1% FA. Gradient settings were: 0 – 60 min: 5%B-30%B at 300 nL/min. The Orbitrap Elite was run in data-dependent mode with parallel MS1/MS2 acquisition. Survey full scan MS1 spectra (from m/z 350 to 1600) were acquired in the Orbitrap with resolution R= 120000 at m/z 400. Up to 15 ions with charge state ≥ +2 were selected for fragmentation per cycle with a dynamic exclusion window of 30 s.

Peptides were identified using the Trans-Proteomic-Pipeline (TPP) version 5.1 with the search engine Myrimatch and the parameters: precursor tolerance: 10 ppm; fragment tolerance: 0.5 Da; dynamic modifications: iodoacetamide (C), oxidation (M); **7** (C) and **7r** (C); enzyme: Trypsin; missed cleavages: 2. Peptide probabilities were assigned with PeptideProphet and iProphet and the dataset was filtered with a peptide probability (iprobability) of 0.9. MS1 XIC traces of the C862 containing peptides with different covalent modifications were extracted using Skyline version 4.2.

The conversion rate of PI3Kα C862 through the compounds was quantified using LC-SRM. 40 ng and 40 ng BSA were incubated with the compounds under study or DMSO at 1 µM and digested as detailed above. All analyses were performed in triplicates. The resulting peptides were analyzed on a TSQ Vantage (Thermo Scientific) coupled to a nanoLC Ultra1D+ (Eksigent). Peptides were separated on a column (0.075 x 100 mm, C18 ProntoSIL 200 3 µM, 200 A) packed into a PicoTip Emitter (New Objective). Peptides were separated along a linear gradient of B (98% ACN, 0.1% FA) in A (2% ACN, 0.1% FA), running from 2% – 35% B in 20 min. The TSQ was run in SRM mode, monitoring the NSHTIMQIQCK peptide with or without oxidized methionine as well as three, four and five peptides derived from p110α, p85α and BSA respectively. Samples were injected in randomized order. SRM data was processed in Skyline version 4.2 and exported to R version 3.5.1. NSHTIMQIQCK SRM intensity was normalized to the intensity of all other peptides.

Determination of Distribution Coefficient (LogD, pH 7.4)

Determination of distribution coefficient (LogD) was performed according to the Enamine's distribution coefficient SOP. Incubations were carried out in Eppendorf-type polypropylene microtubes in triplicates. Briefly, 5 µL aliquot of 10 mM test compound stock (in 100% DMSO) was added into the previously mutually saturated mixture containing 500 µL of phosphate-buffered saline (PBS, pH 7.4) and 500 µL of octanol. The solution was allowed to mix in a rotator for 1 h at 30 rpm. Phase separation was assured by centrifugation for 2 min at 6000 rpm. The octanol phase was diluted 100-fold with 40% acetonitrile, and the aqueous phase (PBS buffer) was diluted 10-fold; for the compound CNX1351 the aqueous phase was analyzed without dilution. The samples (both phases) were analyzed using HPLC system coupled with tandem mass spectrometer. Mebendazole was used as a reference compound. Calculations of the partition ratios were carried out using the equation:

$$\mathrm{D} = \frac{d_o * S_o}{d_p * S_p}, \qquad \text{eq. 1}$$

where S_o is peak area of the analyte in octanol phase, S_p is peak area of the analyte in PBS buffer, d_o is dilution coefficient for octanol phase, and d_p is dilution coefficient for aqueous phase.

Analysis of Aqueous Solubility (Kinetic Solubility)

Kinetic solubility assay was performed according to the Enamine's aqueous solubility SOP. Briefly, using a 20 mM compound stock solution (in 100% DMSO) dilutions were prepared to a theoretical concentration of 400 µM in duplicates in PBS pH 7.4 with 2% final DMSO. The experimental compound dilutions in PBS were further allowed to equilibrate at 25 °C on a thermostatic shaker for 2 h and then filtered through HTS filter plates using a vacuum manifold.

The filtrates of test compounds were diluted 2-fold with acetonitrile with 2% DMSO before measuring. In parallel, compound dilutions in 50% acetonitrile/PBS were prepared to theoretical concentrations of 0 µM (blank), 10 µM, 25 µM, 50 µM, 100 µM, and 200 µM with 2% final DMSO to generate calibration curves. Ondansetron was used as reference compound to control proper assay performance. 200 µL of each sample was transferred to 96-well plate and measured in 200-550 nm range with 5 nm step. Absorbance wavelengths for calculations were selected for each compound manually based on absorbance maximums (the minimum and maximum concentration points within a 0-3 OD range in absolute absorbance units). The effective range of this assay is within approximately 2-400 µM and the compounds returning values close to the upper limit of the range may have higher actual solubility (for example 5'-deoxy-5-fluorouridine).

Intrinsic Warhead Reactivity (k_{chem}) assay

The assay was carried out as outlined earlier[1] with minor modifications: compound stock solutions of 2 mM in pure DMSO were prepared. Subsequently, the following solutions were mixed in a HPLC vial (volume = 1.5 mL): (i) 750 µL of 2 mM test compound stock solution; (ii) 375 µL pure DMSO and (iii) 285 µl phosphate-buffered saline (PBS). The solutions were maintained at 37°C and analyzed using an Ultimate 3000SD System from ThermoFisher with LPG-3400SD pump system, ACC-3000 autosampler and column oven, and DAD- 3000 diode array detector. An Acclaim-120 C18 reversed-phase column from ThermoFisher was used as stationary phase.

Gradient elution (5:95 for 0.2 min, 5:95 → 100:0 over 10 min, 100:0 for 3 min) of the mobile phase consisting of ACN / MeOH:H_2O (10:90) was used at a flow rate of 0.5 mL / min at 40°C. Following the first injection (time zero), 90 µL of 10 M β-mercaptoethanol (βME) in PBS were added, to yield a final concentration of 600 mM βME. The loss of inhibitor and the formation of inhibitor + βME adduct was monitored every 20 min for the first 3 h and every 1 h thereafter for up to 8 h. The inhibitor + βME adduct was identified by MALDI-ToF mass spectra obtained on a Voyager-DeTM Pro measured in m/z (see supplementary data set). The percent of inhibitor + βME adduct in each sample was determined by measuring the area under the curve in HPLC chromatograms. Moles of inhibitors were plotted versus time (in seconds) using GraphPad Prism to determine *k'* for the reaction (unit of *k'* = s^{-1}). Dividing *k'* for the concentration of βME used in the assay, pseudo-first order reactions were converted into second-order reaction and k_{chem} (in units of $M^{-1} \cdot s^{-1}$) was determined. Experiments were performed in triplicates and results are given in means ± SD.

Determination of Kinetic Constants of Inhibitor/PI3K Interaction

The inhibitory constant (K_i) and the covalent reaction rate k_{inact} of compounds and p110α were determined using LanthaScreen Technology (Life Technologies) as described earlier[1] with some modifications. An *N*-terminally His_6-tagged p110α recombinant protein (5 nM, PV4789) was combined with a biotinylated anti-His_6-tag antibody (2 nM, PV6089), an Europium-labeled Streptavidin complex (2 nM, PV5899) and an AlexaFluor647-labelled kinase Tracer (Tracer 314, 20 nM, PV6087, K_D of 2.26 nM for p110α) in TR-FRET assay buffer (50 mM N-(2-hydroxyethyl)piperazine-N′-ethanesulfonic acid (HEPES) pH 7.5, 10 mM $MgCl_2$, 1 mM ethylene glycol-bis(β-aminoethyl ether)-N,N,N′,N′-tetraacetic acid (EGTA), and 0.01% (v/v) Brij-35). The prepared kinase-antibody-tracer (KAT) complex was dispensed into a 384-well plate (14 µL per well). The plate was then centrifuged (700 g for 5 min) and incubated in the dark at room temperature for 45 min. Subsequently, compounds were diluted in TR-FRET assay buffer and then dispensed to the KAT solution (in triplicate) at a final concentration range between 10 µM and 0.2 nM using an I.DOT One dispenser (Dispendix). Immediately after addition of the compounds, TR-FRET was measured for 90 min using a Synergy Neo2 plate reader. (BioTek instruments; excitation at 330/80 nm using a Xenon flash lamp (except for **9r**, there, a TRF laser at 337 nM was used); Emission filters: 665/8 nm and 620/10 nm; 100 µs delay, 200 µs data collection; 37 °C; dichroic mirror 400 nm). The emission ratio of 665/620 nm was normalized and subsequently, the data was fitted to a model using KinTek Global Kinetic Explorer modelling software (Version 10.0.200717). The reaction model depicted below was used to calculate K_i and k_{inact} values. T is the Tracer, E~T is the reversible enzyme-tracer complex, I is the inhibitor, E~I is the reversible enzyme-inhibitor complex and EI is the covalent enzyme-inhibitor complex.

$$E{\sim}T \underset{}{\overset{K_D}{\rightleftharpoons}} E + I \overset{K_i}{\rightleftharpoons} E{\sim}I \xrightarrow{k_{inact}} EI$$

Cellular, covalent target engagement using NanoBRET (Inhibitor displacement)

NanoBRET assays were carried out as described before[1] with some modifications. Expression vectors encoding a Nanoluciferase (NanoLuc) *N*-terminally fused to various class IA PI3K catalytic subunit isoforms and one mutant were purchased from Promega (PI3Kα wild type, #NV3901; PI3Kα C862S; custom vector; PI3Kβ, #NV4011; and PI3Kδ, #NV4021). For transient transfections, $2x10^6$ HEK293 cells were co-transfected with a total of 10 µg of plasmid DNA for NanoLuc-PI3K and the regulatory subunit p85α (Promega, #NV4031) at a mass ratio of 1:10 (catalytic subunit:regulatory subunit) using jetPEI transfection reagent (Polyplus transfection, #101B-010N) according to the manufacturers protocol, followed by incubation for

20 h (37 °C, 5% CO_2). Cells were then reseeded into white opaque, flat-bottom 96-well plates (Falcon, #353296) at a density of 2 x 10^5 cells per mL in Opti-MEM without phenol red (Gibco, #11058021) and incubated for 4 h (37 °C, 5% CO_2). Inhibitors were diluted in PBS (pH 7.4) and dispensed to a final concentration of 3 µM using an I.DOT dispenser (Dispendix). Cells were then incubated for 2 h (37 °C, 5% CO_2). After incubation, medium containing inhibitors was gently aspirated and cells were washed twice with inhibitor-free Opti-MEM. The energy transfer probe Tracer K-3 (200 nM, Promega, #N2602), NanoGlo substrate (Promega, #N157C) together with Extracellular NanoLuc Inhibitor (10 µM, Promega, #N235B) were dispensed using an I.DOT dispenser (Dispendix). Immediately after dispensing, filtered luminescence was measured sequentially on a Berthold Mithras^2 LB 943 Plate Reader luminometer at 25 °C equipped with 460 nm BP filter (donor) and 600 nm LP filter (acceptor), using 0.5 s integration time.

Drug-Target Engagement Kinetics in HEK293 Cells; NanoBRET diffusion assay

For kinetic measurement of drug-target engagement in living cells, HEK293 cells were transiently co-transfected with vectors expressing *N*-terminal NanoLuc fused to p110α wildtype (Promega #NV3901) and regulatory subunit p85α (Promega #NV4031) as described in the previous section. Tracer K-3 (200 nM), NanoBRET NanoGlo Substrate and Extracellular NanoLuc Inhibitor (10 µM) were dispensed using an I.DOT One dispenser (Dispendix) with subsequent incubation for 20 min (37 °C, 5% CO_2). Immediately after addition of the test compounds at the concentration range between 5000 nM and 78 nM (2-fold dilution steps) using an I.DOT One dispenser (Dispendix), BRET measurements were performed at 25 °C for 4 h on a Berthold Mithras^2 LB 943 Plate Reader luminometer equipped with 460 nm BP filter (donor) and 600 nm LP filter (acceptor), using 0.5 s integration time.

Computational Compound Conformation Searches

Computational conformational searches were carried out via MacroModel (version 10.0) in Maestro Schrödinger version 13.3.121 (2022-3 release). The structures of **1**, **7**, and **9** were prepared via LigPrep software, and ionized according to Epik at pH 7. The conformational search was set up via MacroModel software, for both water and octanol as explicit solvents. All simulations for each molecule-solvent pair were performed by searching for viable conformations within an energy window of 21.0 kJ/mol (i.e., 5.02 kcal/mol) using the OPLS4 force field. All simulations were submitted with the default parameters for a maximum number of 500 conformers – when accessible within the selected energy window – to be generated for each structure-solvent combination, using the default mixed torsional/low-mode sampling method for MacroModel conformational search. Redundant conformers were eliminated using a maximum atom deviation cutoff of 0.5 Å.

For each structure-solvent combination, all conformers were screened for conformational similarity and intramolecular hydrogen bonds. For each structure-solvent pair, the representative conformers *xyz* coordinates were exported to Pymol software. 3D PSA values were computed using a Pymol script.[4] For the representative conformers in octanol intramolecular hydrogen bonds (IMHBs) were detected (see Figure S6).

KinTek Modelling to Estimate On/Off Target Covalent Modification

On-target and off-target covalent binding for each inhibitor were modelled using KinTek Global Kinetic Explorer modelling software.[5,6] Numerical integration to the enzymatic reaction model was carried out as given below:

$$E + I \leftrightharpoons E\sim I \mapsto EI \text{ (covalent on-target reaction)}$$

$$S+I \mapsto SI \text{ (covalent off-target reaction)}$$

E denotes enzyme concentration; I denotes inhibitor concentration; E~I is the reversible inhibitor-enzyme complex, whose equilibrium is defined by experimentally determined K_i; and EI is the covalent enzyme-inhibitor complex whose formation rate is defined by experimentally determined k_{inact}. S denotes thiol concentration and SI denotes the covalent thiol-inhibitor adduct which forms with an experimentally determined rate, k_{chem}.

The reaction parameters [K_i and k_{inact}] and the intrinsic warhead reactivity [k_{chem}] were determined experimentally (see "Determination of Inhibitor Dissociation and Kinetic Constants" and "Determination of Intrinsic Warhead Reactivity (k_{chem}) Using β-Mercaptoethanol"). The on-target reaction with 10 nM cellular PI3Kα enzyme and off-target reaction with 7 mM thiol[7] were modelled for the indicated inhibitors at a concentration of 100 nM.

Cellular Diffusion Coefficients

Using the results obtained by drug-target engagement tracer displacement in HEK293 cells (see section "Measurement of Drug-Target Engagement Kinetics in Living HEK293 Cells Using NanoBRET (Tracer Displacement)"), modeling to calculate kinetic parameters was carried out through global fitting for numerical integration using KinTek Global Kinetic Explorer modelling software.<<Johnson, 2009 19897109; Johnson, 2009 19154726>> Specifically, the recorded NanoBRET assay tracer displacement data were fitted with the KinTek Global Kinetic Explorer modelling software to a process/enzymatic reaction model as given below:

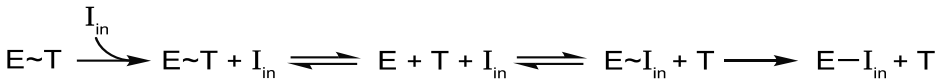

where I_{in} is the intracellular inhibitor concentration. E~T is the reversible enzyme (E) ~ tracer (T) complex, E~I_{in} is the initial reversible inhibitor-enzyme complex, and E-I is the covalent enzyme-inhibitor complex.

The traversing of an inhibitor across the plasma membrane ($I_{out} \leftrightharpoons I_{in}$) can be formulated as a reversible process ($Y \leftrightharpoons Z$). As the extracellular compartment volume (V_{ex}) is much larger than the intracellular volume (V_{in}), the extracellular concentration I_{out} can be assumed to remain constant ($I_{out} = I_0$). This process can then be described by the following differential equation (*eq. 2*).

$$\frac{dI_{in}}{dt} = [I_0] * k_1 - [I_{in}] * k_{-1} \qquad \textit{eq. 2}$$

Small molecule inhibitors are assumed to traverse the plasma membrane by simple passive diffusion, therefore $k_1 = k_{-1}$ and equation *eq. 2* yields:

$$\frac{dI_{in}}{dt} = (I_0 - [I_{in}]) * k_1 \qquad \textit{eq.3}$$

Based on Fick's first law, the diffusion of a small molecule across a membrane can be described by the following equation (*eq. 4)*:[8]

$$J' = -\frac{dI}{dt} = D * A * \frac{dI}{dx} \qquad \textit{eq. 4}$$

where J' or $-\frac{dI}{dt}$ is the mean molecular diffusion rate of the inhibitor in $[{cm^3}/{s}]$, D the diffusion coefficient in $[{cm^2}/{s}]$, A is the surface area of the cell plasma membrane in $[cm^2]$, and $\frac{dI}{dx}$ is the concentration gradient of the inhibitor over the plasma membrane in $[{mol}/{cm^4}]$. The gradient $\frac{dI}{dx}$ can be approximated by a stepwise gradient $([I_0] - [I_{in}])/\Delta x$, where Δx is the thickness of the cell plasma membrane in $[cm]$, yielding:

$$\frac{dI_{in}}{dt} = D * A * \frac{[I_0]-[I_{in}]}{\Delta x} = \frac{D*A}{\Delta x} * ([I_0] - [I_{in}]) \qquad \textit{eq. 5}$$

setting *eq. 3* equal to *eq. 5* one yields *eq. 6*

$$\frac{dI_{in}}{dt} = \frac{D*A}{\Delta x} * ([I_0] - [I_{in}]) = (I_0 - [I_{in}]) * k_1 \qquad \textit{eq. 6}$$

which defines k_1 as

$$k_1 = \frac{D*A}{\Delta x} \qquad \textit{eq. 7}$$

where $k_1$is the diffusion kinetic rate constant $[{cm^3}/{s}]$, determined by fitting the experimental NanoBRET intensity curves (see Fig. 3) to the process/enzymatic reaction model using KinTek Global Kinetic Explorer modelling software, with restriction that $I_{out} = I_0$ during the diffusion process.

With k_1 obtained by modelling and *eq. 7*, the diffusion coefficient D in $[{cm^2}/{s}]$ could be calculated with A and Δx:

$$D = \frac{k_1 * \Delta x}{A} \qquad \textit{eq. 8}$$

although values for the thickness of the plasma membrane ($\Delta x = 8$ nm[9]), and the surface area of HEK293 cells[10] (A) have been reported, the NanoBRET assay is influenced by transfection efficiency and fusion protein expression in individual cells. We therefore present a standardized diffusion coefficient ($D_{rel\ of\ ac}$) for the assessed compounds (ac) ($D_{of\ ac}$). This relative value is expressed in relation to the diffusion coefficient of BYL719 ($D_{of\ BYL719}$) where

$$D_{rel\ of\ ac} = \frac{D_{of\ ac}}{D_{of\ BYL719}} = \frac{k_{1\ of\ ac}}{k_{1\ of\ BYL719}} \qquad \textit{eq. 9}$$

The available area (A) for an inhibitor to diffuse into per well was approximated with the following considerations. The surface area of one HEK293 cell for an inhibitor to diffuse into can be approximated using the following formula:[10]

$$A \approx \frac{4\pi(\frac{(ab)^{1.6}(ac)^{1.6}(bc)^{1.6}}{3})^{1/1.6}}{2} \qquad \textit{eq. 10}$$

The values for a = b = 10 µm, c = 5 µm have been published earlier,[10] yielding a total available surface area of a model HEK293 cell of 434 µm^2. The total available surface area was calculated by multiplying the surface area of one HEK293 cell by the number of transfected cells per well, which yields a total surface area for the inhibitor to diffuse into of 0.0651 cm^2.

Cell Line Maintenance

HEK293, T47D, MCF7, SKOV3, A2058, and PC3 cell lines were obtained from the ATCC as frozen stocks. HCC1954 and MDA-MB-453 were a gift from Prof. Mohamed Bentires-Alj

(University of Basel). Cell lines were cultured according to ATCC recommendations. DMEM (Sigma, #D5671) was used to culture HEK293, SKOV3, and MDA-MB-453 cell lines. Low glucose DMEM (Sigma, #D6046) was used to culture T47D and MCF7 cell lines. RPMI-1641 (Sigma, #R0883) was used to culture A2058, PC3 and HCC1954 cell lines. Complete growth media were obtained by supplementing with 10% fetal calf serum (FCS, Sigma, #F7524, Batch BCBV4855), 2 mM L-glutamine (Sigma, #G7513), 100 U/mL penicillin and 100 µg/mL streptomycin (Gibco, #15140122), (medium with all supplements dubbed below as complete growth medium) in humidified incubators maintained at 37 °C and 5% CO_2. Cell lines were maintained in culture ~15 passages from the point of cryopreservation before being replaced with new frozen aliquots. Cell lines in culture were routinely screened for Mycoplasma infection using the MycoAlert Detection Kit (Lonza #LT07-418).

Cellular PKB/Akt and S6 Ribosomal Protein Phosphorylation

Phosphorylation of PKB/Akt and ribosomal protein S6 were measured using in-cell western (ICW) assays as described earlier,[1] with modifications. Cells were seeded into 96-well CellCarrier black plates with optically clear bottom (PerkinElmer) in complete growth medium and allowed to adhere overnight (37 °C, 5% CO_2). Inhibitor stock solutions prepared in DMSO (2 mM) were added using an I.DOT One dispenser (Dispendix) to generate a concentration range in 0.05% DMSO. Cells were incubated for 2 h (37 °C, 5% CO_2) unless otherwise stated, fixed with 4% paraformaldehyde (PFA) in PBS for 30 min at room temperature, permeabilized with 1% BSA, 0.1% Triton X-100 in PBS for 30 min at room temperature, blocked with 5% goat serum, 1% BSA, 0.1% Triton X-100 in PBS for 30 min at room temperature, and stained with rabbit monoclonal anti-phospho-Ser473 PKB/Akt (Cell Signaling Technology, #4058, 1:500) or anti-phospho-Ser235/236 S6 ribosomal protein (Cell Signaling Technology, #4856, 1:500) and mouse monoclonal anti-α-tubulin (Sigma, #T9026, 1:2000) antibodies overnight at 4 °C. Primary antibodies were removed and cells were washes 3 times with PBS before secondary antibodies (IRDye680-conjugated goat anti-mouse [LICOR, #926-68070, 1:500] and IRDye800-conjugated goat anti-rabbit [LICOR, #926-32211, 1:500]) were added and incubated for 90 min with shaking in the dark at room temperature. After removal of secondary antibodies and 3 washes with PBS, fluorescence was recorded on an Odyssey CLx infrared imaging scanner (LICOR) set on “In Cell Western” mode, offset 4.0 µm, automatic exposure. Background signal (wells without primary antibody) was first subtracted from test wells in both channels. Phosphorylated protein signal was corrected for cellular protein as determined by α-tubulin signal. Corrected values were normalized to DMSO, representing 100% signal. The calculated percentages of remaining phospho-PKB/S6 signals were plotted as a function of inhibitor concentration (log scale) and dose-response curves were fit in GraphPad Prism (v9.3.1) using the formula:

$$Y = \frac{100}{1+10^{(\mathrm{LogIC_{50}}-\mathrm{LogX})*\mathrm{HillSlope}}} \qquad \textit{eq. 11}$$

where X is the inhibitor concentration. IC_{50} values of inhibitors were determined by interpolating the concentration X where Y = 50%.

FOXO1 KTR Translocation Assay

Cell lines (A2058, SKOV3, T47D) stably expressing a FOXO1 Clover fusion protein were prepared using lentiviral transduction with the pLenti-FoxO1-Clover[11] plasmid (www.addgene.org) and 3rd generation lentiviral packaging plasmids according to the laboratory protocol for lentivirus production of the Broad Institute The RNAi Consortium (TRC). As a transfection reagent, jetPEI was used as an alternative to FuGENE. Cells were then selected by incubation with puromycin and sorted by fluorescence intensity using a FACS BD FACSAria IIIu cell sorter.

Stably transfected cells were seeded in 95 µL complete DMEM into 96-well plates (Cell Carrier, Perkin Elmer) the day before inhibitor treatment. To generate inhibitor dose-response curves, cells were exposed to inhibitors for 1 h unless otherwise stated, and fixed with 4% PFA for 30 min at room temperature. Cells were permeabilized and stained with Hoechst33324 (10 µg/mL) diluted in 1% BSA, 0.1% Triton-X in PBS for 30 min at room temperature in the dark. Fluorescent microscopy images were acquired on an Operetta high content analysis system (Perkin Elmer). At least 35 fields of view/well were acquired as wide field images (20xWD objective, N.A. 0.45). Nuclei (and nuclear DNA content) were imaged using the Hoechst filter set and FOXO1 localization was imaged using the YFP filter set. Images were batch analyzed using Cell Profiler version 4.2.4[12] (Broad Institute, www.cellprofiler.org). Nuclei were identified using primary object identification using the nuclear stain fluorescence and cells were identified by extending the nuclear segmentation to create a ring around the nucleus a specified number of pixels based on the FOXO1 Clover reporter fluorescence (secondary object). Subsequently, the nuclear region was subtracted from the cellular region to give a cytosolic ring (“cytoring”). The average ratio of the median fluorescence intensity of the cytoring/nucleus was calculated for each inhibitor concentration or DMSO control well and used to quantify FOXO1 localization (i.e. low values indicate nuclear translocation while high values indicate cytosol translocation). Data were expressed as percentage of DMSO control (representing 100% response), with the lowest cytoring/nuclear ratio subtracted as background (representing 0% response after subtraction). Dose-response curves were fit in GraphPad Prism version 9.3.1 using the formula:

$$Y = \text{Bottom} + \frac{(\text{Top}-\text{Bottom})}{1+10^{(\text{LogIC}_{50}-\text{LogX})*\text{HillSlope}}} \quad \textit{eq. 12}$$

where X is inhibitor concentration, Top = 100 and Bottom must be a value between 0 and 100. IC_{50} values of inhibitors were determined by interpolating the concentration X where Y = 50%. Live cell imaging studies were performed in phenol red-free medium with 2% FCS and nuclei were stained with SiR Hoechst (spirochrome.com) for 1 h prior to imaging using a Leica DMi8 microscope (Leica) with a stage top incubator maintained at 37 °C, and in 95% air, 5% CO_2. Cells were exposed to vehicle or inhibitors (3 µM) for 2 h followed by washout of inhibitors (media was removed and replaced twice) and imaging was continued for a further 10 h. Cells were imaged every min until 1 h following washout and at later time points every 30 min using a 20x HC Plan-Apo objective (N.A. 0.8), and a GFP filter cube (excitation band, 470/40 nm; emission band, 525/50 nm) and a Cy5 filter cube (excitation band, 620/60 nm; emission band, 700/72 nm). Image analysis was performed as described above.

Resazurin Assay to Measure Cellular Viability

Cells were seeded into 96-well CellCarrier black plates (PerkinElmer) in complete growth medium and allowed to adhere overnight (37 °C, 5% CO_2). Inhibitors were serially diluted in medium and added to the wells (max. 0.25% DMSO). Relative live cells numbers were measured using the resazurin assay at the beginning (t = 0 h) and at the end of the incubation period (t = 72 h for generation of concentration-response curves and t = 96 h for intermittent exposure experiments). A 11X resazurin solution (0.3 mg/ml diluted in Dulbecco's PBS, filter sterilized) was added to the wells containing cells alongside at least one well per plate containing medium only (background signal) and incubated for 4 h at 37 °C, 5% CO_2. Fluorescence was recorded on a Synergy 4 plate reader (BioTek) using a 565/590 nm excitation/emission filter set (top read, 4 mm offset). Background fluorescence values were subtracted from raw test values and growth rates at concentration c ($GR_{(c)}$) were calculated using the equation:

$$\text{GR}_{(c)} = 2^{\frac{\log_2 \frac{x_{(c)}}{x_{(0)}}}{\log_2 \frac{x_{(DMSO)}}{x_{(0)}}}} - 1 \quad \textit{eq. 13}$$

where $x_{(0)}$ represents the initial fluorescence read, $x_{(c)}$ represents the final fluorescence read at inhibitor concentration c, and $x_{(DMSO)}$ represents the final fluorescence read in the vehicle control.

To generate dose-response curves, the calculated GR values were fitted in GraphPad Prism (version 9.3.1) using the equation:

$$Y = \text{Bottom} + \frac{(\text{Top}-\text{Bottom})}{1+10^{(\text{LogIC}_{50}-\text{LogX})*\text{HillSlope}}} \quad \textit{eq. 14}$$

where X is the inhibitor concentration, Top = 1, and Bottom ≥ -1. Finally, GR_{50} values were determined by interpolating the concentration X[13] where Y = 0.5.

Cell Lysis

Cells seeded in 6-well plates in complete growth medium were allowed to adhere overnight at 37 °C and 5% CO_2. For determination of p110α levels, inhibitors (1 µM) were added to the medium and incubated for 48 h. For experiments using serum-starved cells, plating medium was removed and replaced with medium containing no FCS for 24 h. Compound **9** and TGX221 were used at a final concentration of 1 µM, and receptor ligands were added at the following final concentrations: 10 ng/mL epidermal growth factor (EGF, Sigma #E9644), 10 µg/mL insulin (Sigma #I9278), 50 ng/mL CXCL12 (Peprotech #250-20A). After incubation at 37 °C and 5% CO_2 for the indicated times, medium was removed and cells were washed twice with cold PBS. Adherent cells were detached and lysed using 1x cell lysis buffer (Cell Signaling Technology #9803) supplemented immediately before use with either Halt™ Protease and Phosphatase Inhibitor Single-Use Cocktail (100X; Thermo Scientific, #78442) or cOmplete™ EDTA-free protease inhibitor cocktail (Roche), PhosSTOP™ phosphatase inhibitor cocktail (Roche) and 1 mM PMSF, for 30 min on ice. Cell extracts were cleared in a cooled centrifuge (4 °C, 10 min, 16'000 g) and supernatants were transferred to cooled Eppendorf tubes and used for SDS-PAGE immediately or stored frozen at -20 °C until further processing.

SDS-PAGE

Total protein content of cell lysates was determined using a Pierce™ BCA protein assay kit (Thermo Scientific). Equal amounts of protein were denatured in SDS-PAGE sample buffer and heated at 95 °C for 10 min. Denatured protein samples were subjected to SDS-PAGE and transferred to precut 0.2 µm nitrocellulose membranes using the Trans-Blot Turbo Transfer System (Bio-Rad).

Western Blotting

Membranes were blocked in TBS buffer containing 0.1% Tween-20 (TBST) with either 1% BSA or 5% (w/v) non-fat dry milk powder (Cell Signaling Technologies, #9999). Primary antibodies against pSer473-PKB/Akt (#4058, 1:1000), pThr308-PKB/Akt (#9275, 1:1000), pan-PKB/Akt (#2920, 1:1000), p44/42 MAPK (Erk1/2, 1:1000) (#4695) and pThr202/Tyr204-p44/42 MAPK (Erk1/2, 1:1000) (#4370) were from Cell Signaling Technology and primary antibody against β-actin (A5441, 1:10000) was from Sigma. Primary antibody against p110α U3A (diluted 1:2000) has been described previously.[14] Membranes were incubated with primary antibodies overnight followed by extensive washing using TBST and subsequent probing using HRP-conjugated secondary antibodies (goat anti-mouse IgG peroxidase

conjugate, Sigma #A4416, 1:5000 and goat anti-rabbit IgG peroxidase conjugate, Sigma #A6154, 1:5000). Chemiluminescent signals were visualized using Immobilon western HRP substrate (Millipore) on a Fusion FX (Vilber Lourmat) imaging system. Levels of phosphorylated and total protein signals were quantified using ImageJ. Phospho-protein levels in each sample were normalized to total protein signals.

Cell Cycle Distribution Analysis

Cells seeded in 6-well plates in complete growth medium were allowed to adhere overnight at 37 °C and 5% CO_2. Inhibitors or DMSO control were added at the indicated final concentrations for 48 h. Subsequently, cells were detached, fixed in 70% cold ethanol and stained with 1 µg/mL DAPI diluted in PBS with 0.1% Triton X-100 for 30 min in the dark. Cell cycle profiles were acquired by flow cytometry (CytoFlex LX, Beckman Coulter) and analyzed with FlowJo (Treestar) software.

Kinome Profiling

Compound binding affinity and selectivity were determined as previously described[1] using the KINOMEscan™ scanMAX platform of DiscoverX. Experiments were performed at DiscoverX, San Diego using its automated and standardized *in vitro* assay and data analysis and TreeSpot™ visualization tools.

Chemical Structures

Final Compounds

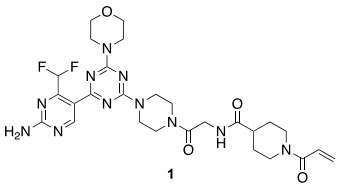

1

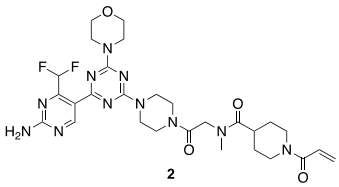

2

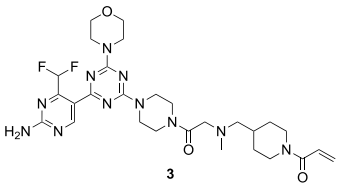

3

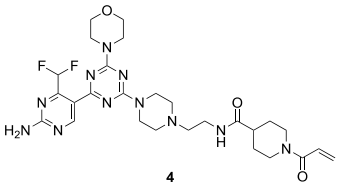

4

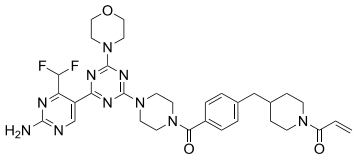

5

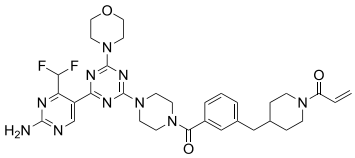

6

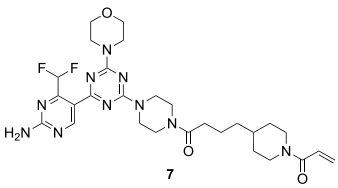

7

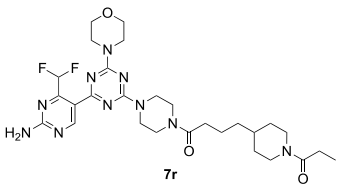

7r

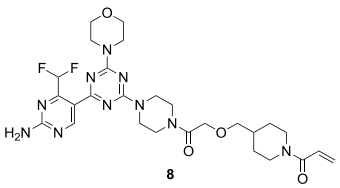

8

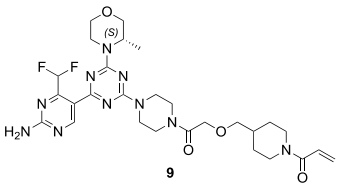

9

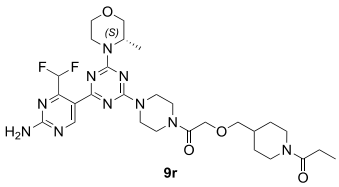

9r

Reference Compounds

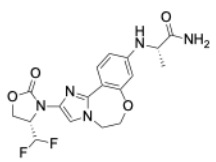

GDC0077

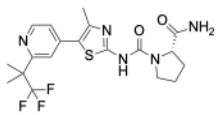

BYL719

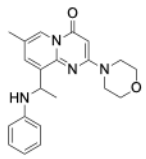

TGX221

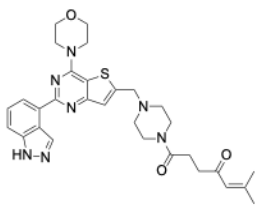

CNX1351

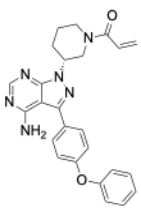

Ibrutinib

Intermediates

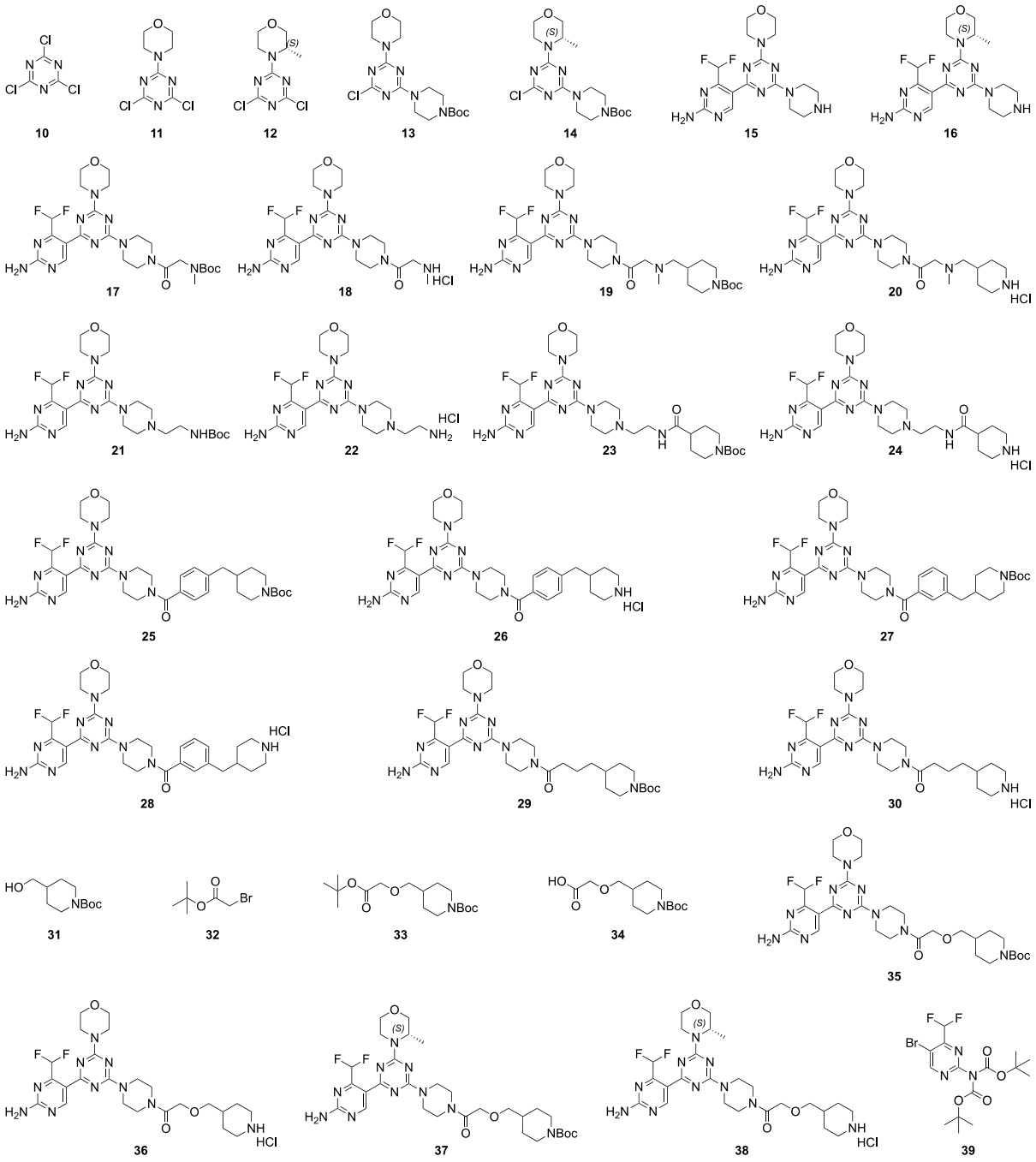

Synthesis and Characterization

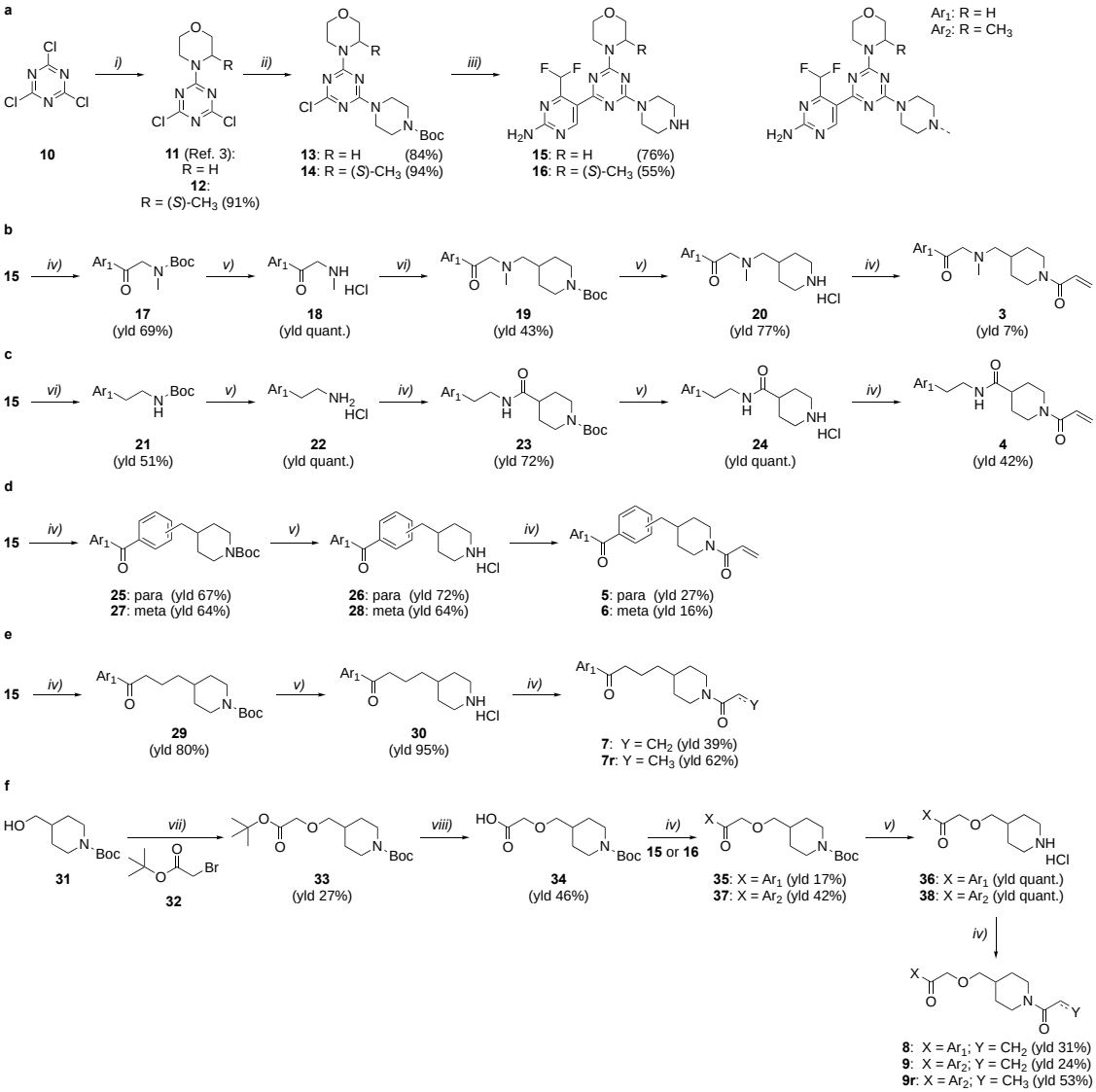

General Information, Chemistry

Reagents were purchased at the highest commercial quality from Acros Organics, Sigma-Aldrich, Apollo Scientific or Fluorochem and used without further purification. Solvents were purchased from Acros Organics in AcroSeal® bottles over molecular sieves. Grignard reactions, cross-coupling reactions and peptide-coupling reactions were carried out under nitrogen atmosphere in anhydrous solvents, and glassware was oven dried prior to use. Thin layer chromatography (TLC) plates were purchased from Merck KGaA (Polygram SIL / UV254, 0.2 mm silica with fluorescence indicator) and UV light (254 nm) was used to visualize the compounds. Flash chromatography was performed with Isco CombiFlash Companion systems using prepacked silica gel columns (40 - 60 µm particle size RediSep). ^{1}H, ^{19}F and ^{13}C NMR spectra were recorded on a Bruker Avance 400 spectrometer. NMR spectra were obtained in deuterated solvents, namely $CDCl_3$ or $(CD_3)_2SO$. The chemical shift (δ values) are reported in ppm and corrected to the signal of the deuterated solvents (7.26 ppm (^{1}H NMR) and 77.16 ppm (^{13}C NMR) for $CDCl_3$; and 2.50 ppm (^{1}H NMR) and 39.52 ppm (^{13}C NMR) for $(CD_3)_2SO$. ^{19}F NMR spectra are calibrated relative to $CFCl_3$ (δ = 0 ppm) as external standard. When peak multiplicities are reported, the following abbreviations are used: s (singlet), d (doublet), dd (doublet of doublets), t (triplet), td (triplet of doublets), q (quartet), doublet of quartets (dq), m (multiplet), br (broadened signal). Coupling constants are reported in Hertz (Hz). High resolution mass spectra (HRMS) were recorded on a Thermo Fisher Scientific LTQ Orbitrap XL (nanoESI-MS) spectrometer. MALDI-ToF mass spectra were obtained on a Voyager-De™ Pro measured in *m/z*. The chromatographic purity of final compounds was determined by high performance liquid chromatography (HPLC) analyses on an Ultimate 3000SD System from ThermoFisher with LPG-3400SD pump system, ACC-3000 autosampler and column oven, and DAD-3000 diode array detector. An Acclaim-120 C18 reversed-phase column from ThermoFisher was used as stationary phase. Gradient elution (5:95 for 0.2 min, 5:95 → 100:0 over 10 min, 100:0 for 3 min) of the mobile phase consisting of CH_3CN / MeOH:H_2O (10:90) was used at a flow rate of 0.5 mL / min at 40 °C. The purity of all final compounds was higher than 95% (except for **9r:** 92.9%).

Chemical Procedures

General procedure 1 (GP1). To a solution of the respective carboxylic acid (1.0-1.5 equiv) in anhydrous *N,N*-dimethylformamide (DMF, approx. 1 mL / 0.18 mmol), O-(1*H*-6-chlorobenzotriazole-1-yl)-1,1,3,3-tetramethyluronium hexafluorophosphate (HCTU, 1.1 equiv) and *N,N*-diisopropylethylamine (3.2 equiv) were added at 0 °C under nitrogen atmosphere. The resulting mixture was stirred for 5 min at 0 °C, then **15** or the respective HCl salt (1.0 equiv) was added and the reaction was stirred at room temperature for 4-16 h. After completion of the reaction, DMF was removed under high vacuum. The crude was dissolved in DCM and the organic layer was washed with deionized H_2O (2 x) and an aqueous saturated Na_2CO_3-solution (3 x). The organic layer was dried over Na_2SO_4, filtered and concentrated under reduced pressure. The crude product was purified by column chromatography on silica gel and then recrystallized from DCM / pentane.

General procedure 2 (GP2). To a solution of the respective Boc-protected amine (1.0 equiv.) in THF (approx. 1 mL / 0.10 mmol), a 4 M solution of HCl in dioxane (17 equiv.) was added dropwise. The mixture was stirred at room temperature for 3-16 h. The mixture was reduced to dryness under reduced pressure. The product was precipitated from ACN, filtered and washed with cold ACN. The HCl salt of the product was used for the next step without further purification.

General procedure 3 (GP3). Compound **15** (1 equiv.), the respective bromo derivative (1 equiv.) and K_2CO_3 (4 equiv.) were charged in a flask under nitrogen atmosphere. Dry DMF (approx. 1 mL / 0.33 mmol) was added and the reaction was stirred at 80 °C overnight. After completion of the reaction monitored by TLC, the solvent was removed under reduced pressure. The crude was dissolved in DCM and washed with water (2x). The organic layer was dried over anhydrous Na_2SO_4, filtered and concentrated under reduced pressure. The crude product was purified by column chromatography on silica gel.

1-acryloyl-*N*-(2-(4-(4-(2-amino-4-(difluoromethyl)pyrimidin-5-yl)-6-morpholino-1,3,5-triazin-2-yl)piperazin-1-yl)-2-oxoethyl)piperidine-4-carboxamide (**1**)

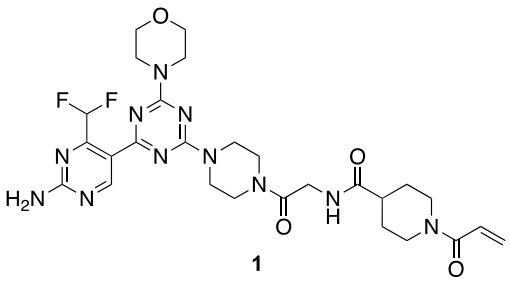

1

Compound **1** was prepared according to the literature.[1]

1-acryloyl-*N*-(2-(4-(4-(2-amino-4-(difluoromethyl)pyrimidin-5-yl)-6-morpholino-1,3,5-triazin-2-yl)piperazin-1-yl)-2-oxoethyl)-N-methylpiperidine-4-carboxamide (**2**)

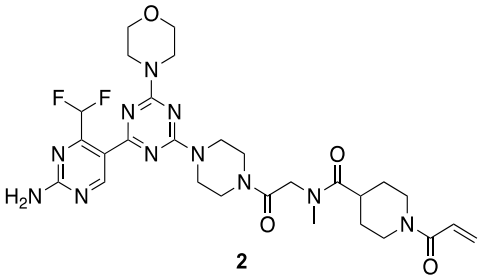

2

Compound **2** was prepared according to the literature.[1]

1-(4-(((2-(4-(4-(2-amino-4-(difluoromethyl)pyrimidin-5-yl)-6-morpholino-1,3,5-triazin-2-yl)piperazin-1-yl)-2-oxoethyl)(methyl)amino)methyl)piperidin-1-yl)prop-2-en-1-one (**3**)

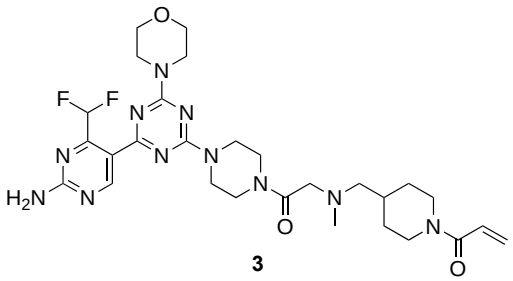

3

Compound **3** was prepared according to **GP1** from intermediate **20** (191 mg, 0.32 mmol, 1.0 equiv). Purification by column chromatography on silica gel (DCM / methanol / ammonia: 100:0:0 → 97:3:0.03) gave compound **3** as a colorless solid (14 mg, 0.023 mmol, 7%). **^{1}H NMR** (400 MHz, $CDCl_3$): δ 9.23 (s, 1 H), 7.61 (t, J = 54.4 Hz, 1 H), 6.58 (dd, J = 16.8, 10.6 Hz, 1 H), 6.25 (d, J = 16.8 Hz, 1 H), 5.79 (br s, 2 H), 5.67 (d, J =10.6 Hz, 1 H), 4.70-4.60 (m, 1 H), 4.05-3.96 (m, 1 H), 3.94-3.80 (m, 6 H), 3.81-3.72 (m, 4 H), 3.73-3.60 (m, 4 H), 3.49 (s, 1 H), 3.22 (s, 2 H), 3.11-2.99 (m, 1 H), 2.70-2.60 (m, 1 H), 2.28 (s, 3 H), 1.90-1.70 (m, 4 H), 1.17-1.02 (m, 2 H), 0.93-0.79 (m, 2 H) ppm. **^{19}F{^{1}H} NMR** (376 MHz, $CDCl_3$): δ -121.62 (s, 2 F) ppm. **^{13}C{^{1}H} NMR** (101 MHz, $CDCl_3$): δ 169.02 (s, 1 C), 167.74 (s, 1 C), 165.41 (s, 1 C),

164.54 (s, 2 C), 163.33 (s, 1 C), 162.46 (s,1 C), 159.51 (s, 1 C), 127.89 (s, 1 C), 127.47 (s, 1 C), 119.82 (s, 1 C), 109.49 (t, *J* = 240.7 Hz, 1 C), 66.74 (s, 2 C), 63.39 (s, 1 C), 62.53 (s, 1 C), 45.96 (br s, 1 C), 45.43 (br s, 1 C), 43.69-42.92 (m, 4 C), 42.17 (br s, 1 C), 41.75 (br s, 1 C), 34.21 (s, 1 C), 31.35 (s, 1 C), 30.25 (s, 1 C), 29.27 (s, 1 C) ppm. **HRMS** (*m/z*): $[M + H]^+$ calc. for $C_{28}H_{40}F_2N_{11}O_3$, 616.3278; found: 616.3283; $[M + Na]^+$ calc. for $C_{28}H_{39}F_2N_{11}NaO_3$, 638.3098; found: 638.3102. **HPLC** (ACN with 0.1% TFA): t_R = 5.32 min (96.6% purity).

1-acryloyl-*N*-(2-(4-(4-(2-amino-4-(difluoromethyl)pyrimidin-5-yl)-6-morpholino-1,3,5-triazin-2-yl)piperazin-1-yl)ethyl)piperidine-4-carboxamide (**4**)

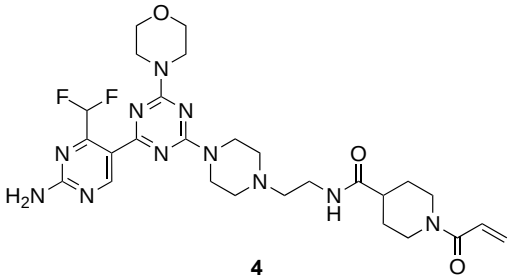

4

Compound **4** was prepared according to **GP1** from intermediate **24** (263 mg, 0.45 mmol, 1.0 equiv). Purification by column chromatography on silica gel (DCM / methanol / ammonia: 100:0:0 → 97:3:0.03) gave compound **4** as a colorless solid (114 mg, 0.19 mmol, 42%). **^{1}H NMR** (400 MHz, $CDCl_3$): *δ* 9.23 (s, 1 H), 7.62 (t, *J* = 54.4 Hz, 1 H), 6.58 (dd, *J* = 16.8 Hz, $^3J_{H,H}$ = 10.6 Hz, 1 H), 6.27 (dd, *J* = 16.8 Hz, *J* = 1.9 Hz, 1 H), 6.06 (br s, 1 H), 5.69 (dd, *J* = 10.6 Hz, *J* = 1.9 Hz, 1 H), 5.53 (br s, 2 H), 4.71-4.60 (m, 1 H), 4.10-3.99 (m, 1 H), 3.95-3.79 (m, 8 H), 3.78-3.69 (m, 4 H), 3.40 (q, *J* = 5.6 Hz, 2 H), 3.18-3.08 (m, 1 H), 2.83-2.72 (m, 1 H), 2.57-2.45 (m, 6 H), 2.44-2.35 (m, 1 H), 1.97-1.87 (m, 2 H), 1.77-1.64 (m, 2 H) ppm. **^{19}F{^{1}H} NMR** (376 MHz, $CDCl_3$): *δ* -121.70 (s, 2 F) ppm. **^{13}C{^{1}H} NMR** (101 MHz, $CDCl_3$): *δ* 173.95 (s, 1 C), 167.63 (s, 1 C), 165.49 (s, 1 C), 164.55 (s, 1 C), 164.31 (s, 1 C), 163.44 (s, 1 C), 162.48 (s, 1 C), 159.43(t, *J* = 21.4 Hz, 1 C), 127.74 (s, 1 C), 127.68 (s, 1 C), 119.70 (t, *J* = 3.7 Hz, 1 C), 109.51 (t, *J* = 240.7 Hz, 1 C), 66.73 (s, 2 C), 56.67 (s, 1 C), 52.69 (s, 1 C), 45.36 (s, 1 C), 43.64 (br s, 1 C), 43.30-42.95 (m, 2 C), 43.01 (s, 1 C), 41.52 (s, 1 C), 35.83 (s, 1 C), 30.94 (s, 1 C), 29.16 (s, 1 C), 29.11 (s, 1 C), 28.54 (s, 1 C) ppm. **HRMS** (*m/z*): $[M + H]^+$ calc. for $C_{27}H_{38}F_2N_{11}O_3$, 602.3122; found: 602.3126; $[M + Na]^+$ calc. for $C_{27}H_{37}F_2N_{11}NaO_3$, 624.2941; found: 624.2942. **HPLC** (ACN with 0.1% TFA): t_R = 4.90 min (97.0% purity).

1-(4-(4-(4-(4-(2-amino-4-(difluoromethyl)pyrimidin-5-yl)-6-morpholino-1,3,5-triazin-2-yl)piperazine-1-carbonyl)benzyl)piperidin-1-yl)prop-2-en-1-one (**5**)

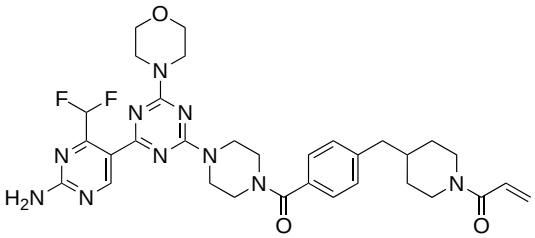

5

Compound **5** was prepared according to **GP1** from intermediate **26** (150 mg, 0.24 mmol, 1.0 equiv). Purification by column chromatography on silica gel (DCM / methanol / ammonia: 100:0:0 → 96:4:0.04) gave compound **5** as a colorless solid (42.6 mg, 0.066 mmol, 27%). **^{1}H NMR** (400 MHz, $CDCl_3$): δ 9.22 (s, 1 H), 7.59 (t, J = 54.4 Hz, 1 H), 7.38 (d, J = 8.1 Hz, 2 H), 7.20 (d, J = 8.0 Hz, 2 H), 6.57 (dd, J = 16.8, 10.6 Hz, 1 H), 6.26 (dd, J = 16.8, 1.9 Hz, 1 H), 5.66 (dd, J = 10.6, 1.9 Hz, 1 H), 5.59 (s, 2 H), 4.66 (d, J = 14.8 Hz, 1 H), 4.05-3.47 (m, 17 H), 3.00 (t, J = 13.5 Hz, 1 H), 2.63-2.53 (m, 3 H), 1.86-1.67 (m, 2 H), 1.30-0.98 (m, 3 H) ppm. **^{19}F{^{1}H} NMR** (376 MHz, $CDCl_3$): δ -121.68 (s, 2 F) ppm. **^{13}C{^{1}H} NMR** (101 MHz, $CDCl_3$): δ 170.75 (s, 1 C), 167.85 (s, 1 C), 165.42 (s, 1 C), 164.62 (s, 1 C), 164.58 (s, 1 C), 163.48 (s, 1 C), 162.54 (s, 1 C), 159.56 (t, J = 20.8 Hz, 1 C), 142.26 (s, 1 C), 133.25 (s, 1 C), 129.36 (s, 2 C), 128.00 (s, 1 C), 127.43 (s, 1 C), 127.36 (s, 2 C), 119.64 (t, J = 3.8 Hz, 1 C), 109.56 (t, J = 240.9 Hz, 1 C), 66.77 (s, 2 C), 46.15 (s, 1 C), 43.73 (s, 4 C), 42.80 (s, 2 C), 42.38 (s, 2 C), 38.21 (s, 1 C), 32.67 (s, 1 C), 31.74 (s, 1 C) ppm. **HRMS** (*m/z*): $[M + H]^+$ calc. for $C_{32}H_{39}F_2N_{10}O_3$, 649.3169; found: 649.3162; $[M + Na]^+$ calc. for $C_{32}H_{38}F_2N_{10}NaO_3$, 671.2989; found: 671.2989. **HPLC** t_R = 7.82 min (98.9% purity).

1-(4-(3-(4-(4-(2-amino-4-(difluoromethyl)pyrimidin-5-yl)-6-morpholino-1,3,5-triazin-2-yl)piperazine-1-carbonyl)benzyl)piperidin-1-yl)prop-2-en-1-one (**6**)

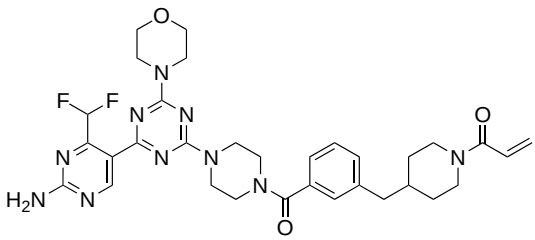

6

Compound **6** was prepared according to **GP1** from intermediate **28** (130 mg, 0.21 mmol, 1.0 equiv). Purification by column chromatography on silica gel (DCM / methanol / ammonia: 100:0:0 → 96:4:0.04) gave compound **6** as a light-yellow solid (28.3 mg, 0.044 mmol, 16%). **^{1}H NMR** (400 MHz, $CDCl_3$): δ 9.22 (s, 1 H), 7.58 (t, J = 54.3 Hz, 1 H), 7.36 (t, J = 7.8 Hz, 1 H), 7.28 (s, 1 H), 7.24-7.20 (m, 2 H), 6.56 (dd, J = 16.8, 10.6 Hz, 1 H), 6.25 (dd, J = 16.8, 1.9 Hz,

1 H), 5.66 (dd, *J* = 10.6, 1.9 Hz, 1 H), 5.58 (s, 2 H), 4.65 (d, *J* = 13.3 Hz, 1 H), 3.99-3.61 (m, 16 H), 3.51 (br s, 1 H), 2.99 (t, *J* = 12.6 Hz, 1 H), 2.68-2.52 (m, 3 H), 1.89-1.76 (m, 1 H), 1.71 (d, *J* = 9.5 Hz, 2 H), 1.26-1.15 (m, 2 H) ppm. **^{19}F{^{1}H} NMR** (376 MHz, $CDCl_3$): *δ* -121.68 (s, 2 F) ppm. **^{13}C{^{1}H} NMR** (101 MHz, $CDCl_3$): *δ* 170.85 (s, 1 C), 167.90 (s, 1 C), 165.50 (s, 1 C), 164.69 (s, 1 C), 164.64 (s, 1 C), 163.47 (s, 1 C), 162.58 (s, 1 C), 159.65 (s, 1 C), 140.76 (s, 1 C), 135.64 (s, 1 C), 130.87 (s, 1 C), 128.70 (s, 1 C), 128.03 (s, 1 C), 127.82 (s, 1 C), 127.51 (s, 1 C), 124.90 (s, 1 C), 119.82 (s, 1 C), 109.60 (t, *J* = 241.0 Hz, 1 C), 66.83 (s, 2 C), 46.20 (s, 1 C), 43.79 (s, 2 C), 42.91 (s, 1 C), 42.43 (s, 1 C), 38.23 (s, 1 C), 35.54 (s, 1 C), 32.74 (s, 1 C), 31.83 (s, 1 C), 26.55 (s, 1 C) 26.44 (s, 1 C), 22.81 (s, 1 C) ppm. **HRMS** (*m/z*): $[M + H]^+$ calc. for $C_{32}H_{39}F_2N_{10}O_3$, 649.3169; found: 649.3170; $[M + Na]^+$ calc. for $C_{32}H_{38}F_2N_{10}NaO_3$, 671.2989; found: 671.2991. **HPLC**: t_R = 7.83 min (96.9% purity).

4-(1-acryloylpiperidin-4-yl)-1-(4-(4-(2-amino-4-(difluoromethyl)pyrimidin-5-yl)-6-morpholino-1,3,5-triazin-2-yl)piperazin-1-yl)butan-1-one (**7**)

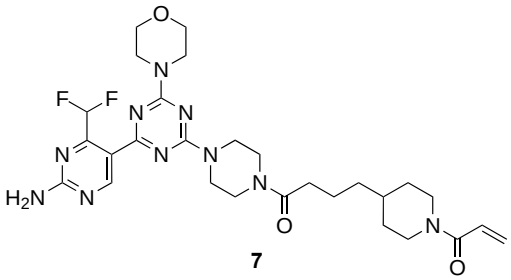

7

Compound **7** was prepared according to **GP1** from intermediate **30** (250 mg, 0.60 mmol, 1.0 equiv). Purification by column chromatography on silica gel (DCM / methanol / ammonia: 100:0:0 → 97:3:0.03) gave compound **7** as a colorless solid (141 mg, 0.23 mmol, 39%). **^{1}H NMR** (400 MHz, $CDCl_3$): *δ* 9.23 (s, 1 H), 7.60 (t, *J* = 54.4 Hz, 1 H), 6.58 (dd, *J* = 16.8, 10.6 Hz, 1 H), 6.25 (dd, *J* = 16.8, 2.0 Hz, 1 H), 5.65 (dd, *J* = 10.5, 2.0 Hz, 1 H), 5.63 (br s, 2 H), 4.67-4.61 (m, 1 H), 4.01-3.95 (m, 1 H), 3.93-3.80 (m, 8 H), 3.78-3.73 (m, 4 H), 3.72-3.67 (m, 2 H), 3.57-3.52 (m, 2 H), 3.03 (t, *J* = 12.6 Hz, 1 H), 2.62 (t, *J* = 12.7 Hz, 1 H), 2.37 (t, *J* = 7.5 Hz, 2 H), 1.82-1.63 (m, 4 H), 1.59-1.49 (m, 1 H), 1.35-1.27 (m, 2 H), 1.20-1.09 (m, 2 H) ppm. **^{19}F{^{1}H} NMR** (376 MHz, $CDCl_3$): *δ* -121.63 (s, 2 F) ppm. **^{13}C{^{1}H} NMR** (101 MHz, $CDCl_3$): *δ* 171.52 (s, 1 C), 167.77 (s, 1 C), 165.33 (s, 1 C), 164.53 (s, 1 C), 164.52 (s, 1 C), 163.39 (s, 1 C), 162.47 (s, 1 C), 159.54 (t, *J* = 21.5 Hz, 1 C), 128.03 (s, 1 C), 127.20 (s, 1 C), 119.69 (s, 1 C), 109.50 (t, *J* = 240.9 Hz, 1 C), 66.72 (s, 2 C), 46.18 (s, 1 C), 45.27 (br s, 1 C), 43.69-42.86 (m, 4 C), 42.39 (s, 1 C), 41.28 (br s, 1 C), 36.14 (s, 1 C), 36.13 (s, 1 C), 33.38 (s, 1 C), 32.84 (s, 1 C), 31.87 (s, 1 C), 22.30 (s, 1 C) ppm. **HRMS** (*m/z*): $[M + H]^+$ calc. for $C_{28}H_{39}F_2N_{10}O_3$, 601.3169; found: 601.3169; [M + Na]+ calc. for $C_{28}H_{38}F_2N_{10}NaO_3$, 623.2989; found: 623.2984. **HPLC**: t_R = 7.22 min (99.0% purity).

1-(4-(4-(2-amino-4-(difluoromethyl)pyrimidin-5-yl)-6-morpholino-1,3,5-triazin-2-yl)piperazin-1-yl)-4-(1-propionylpiperidin-4-yl)butan-1-one (**7r**)

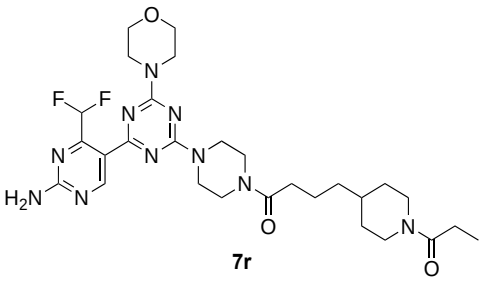

7r

Compound **7r** was prepared according to **GP1** from intermediate **30** (300 mg, 0.51 mmol, 1.0 equiv). Purification by column chromatography on silica gel (DCM / methanol / ammonia: 100:0:0 → 96:4:0.04) gave compound **7r** as a colorless solid (190 mg, 0.32 mmol, 62%). **^{1}H NMR** (400 MHz, $CDCl_3$): δ 9.21 (s, 1 H), 7.59 (t, J = 54.4 Hz, 1 H), 6.01 (s, 2 H), 4.63 – 4.54 (m, 1 H), 3.93-3.77 (m, 10 H), 3.77-3.72 (m, 4 H), 3.68 (t, J = 5.1 Hz, 2 H), 3.52 (t, J = 5.3 Hz, 2 H), 2.95 (td, J = 12.9, 2.7 Hz, 1 H), 2.50 (td, J = 12.9, 2.8 Hz, 1 H), 2.38- 2.27 (m, 4 H), 1.79-1.63 (m, 4 H), 1.54- 1.43 (m, 1 H), 1.34-1.24 (m, 2 H), 1.12 (t, J = 7.5 Hz, 4 H) ppm. **^{19}F{^{1}H} NMR** (376 MHz, $CDCl_3$): δ -121.63 (s, 2 F) ppm. **^{13}C{^{1}H} NMR** (101 MHz, $CDCl_3$): δ 172.16 (s, 1 C), 171.61 (s, 1 C), 167.82 (s, 1 C), 164.58 (s, 1 C), 164.57 (s, 1 C), 163.50 (s, 1 C), 162.54 (s, 1 C), 159.46 (t, J = 21.4 Hz, 1 C), 119.67 (s, 1 C), 109.57 (t, J = 241.3 Hz, 1 C), 66.78 (s, 2 C), 45.81 (s, 1 C), 45.33 (s, 1 C), 43.75 (s, 2 C), 43.40 (br s, 2 C), 42.03 (s, 1 C), 41.35 (s, 1 C), 36.24 (s, 1 C), 36.20 (s, 1 C), 33.45 (s, 1 C), 32.81 (s, 1 C), 32.01 (s, 1 C), 26.66 (s, 1 C), 22.37 (s, 1 C), 9.70 (s, 1 C) ppm. **HRMS** (*m/z*): $[M + Na]^+$ calc. for $C_{28}H_{40}F_2N_{11}NaO_3$, 625.3145; found: 625.3142. **HPLC** t_R = 7.41 min (> 99.9% purity).

1-(4-((2-(4-(4-(2-amino-4-(difluoromethyl)pyrimidin-5-yl)-6-morpholino-1,3,5-triazin-2-yl)piperazin-1-yl)-2-oxoethoxy)methyl)piperidin-1-yl)prop-2-en-1-one (**8**)

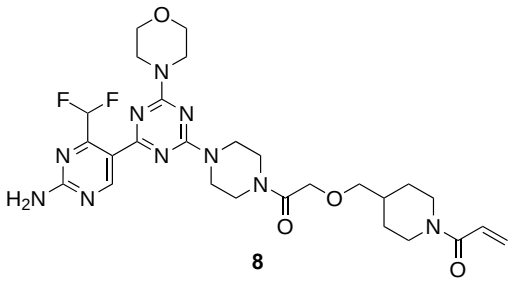

8

Compound **8** was prepared according to **GP1** from intermediate **36** (653 mg, 0.99 mmol, 1.0 equiv). Purification by column chromatography on silica gel (DCM / methanol / ammonia: 100:0:0 → 92:8:0.08) gave compound **8** as a colorless solid (183 mg, 0.30 mmol, 31%). **^{1}H NMR** (400 MHz, $CDCl_3$): δ 9.23 (s, 1 H), 7.59 (t, J = 54.4 Hz, 1 H), 6.57 (dd, J = 16.8, 10.6 Hz, 1 H), 6.25 (dd, J = 16.8, 2.0 Hz, 1 H), 5.66 (dd, J = 10.6, 2.0 Hz, 1 H), 5.61 (br s, 2 H), 4.72-4.63 (m, 1 H), 4.19 (s, 2 H), 4.06-3.98 (m, 1 H), 3.95-3.79 (m, 8 H), 3.79-3.73 (m, 4 H),

3.72-3.65 (m, 2 H), 3.62-3.55 (m, 2 H), 3.39 (d, *J* = 6.2 Hz, 2 H), 3.06 (t, *J* = 13.1 Hz, 1 H), 2.65 (t, *J* = 12.6 Hz, 1 H), 1.96-1.87 (m, 1 H), 1.88-1.75 (m, 2 H), 1.29-1.17 (m, 2 H) ppm. **^{19}F{^{1}H} NMR** (376 MHz, $CDCl_3$): *δ* -121.64 (s, 2 F) ppm. **^{13}C{^{1}H} NMR** (101 MHz, $CDCl_3$): *δ* 167.95 (s, 1 C), 167.80 (s, 1 C), 165.41 (s, 1 C), 164.53 (s, 2 C), 163.42 (s, 1 C), 162.49 (s, 1 C), 159.52 (t, *J* = 21.5 Hz, 1 C), 127.90 (s, 1 C), 127.44 (s, 1 C), 119.65 (s, 1 C), 109.51 (t, *J* = 240.9 Hz, 1 C), 75.86 (s, 1 C), 70.83 (s, 1 C), 66.72 (s, 2 C), 45.78 (s, 1 C), 44.94 (s, 1 C), 43.68-42.91 (m, 4 C), 41.96 (s, 1 C), 41.60 (s, 1 C), 36.59 (s, 1 C), 29.78 (s, 1 C), 28.61 (s, 1 C) ppm. **HRMS** (*m/z*): $[M + H]^+$ calc. for $C_{27}H_{37}F_2N_{10}O_4$, 603.2962; found: 603.2961; $[M + Na]^+$ calc. for $C_{27}H_{36}F_2N_{10}NaO_4$, 625.2781; found: 625.2783. **HPLC**: t_R = 6.62 min (98.9% purity).

(S)-1-(4-((2-(4-(4-(2-amino-4-(difluoromethyl)pyrimidin-5-yl)-6-(3-methylmorpholino)-1,3,5-triazin-2-yl)piperazin-1-yl)-2-oxoethoxy)methyl)piperidin-1-yl)prop-2-en-1-one (**9**)

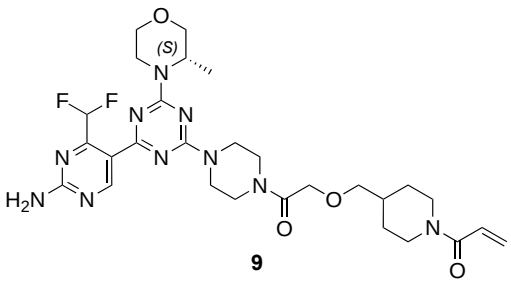

9

Compound **9** was prepared according to **GP1** from intermediate **38** (370 mg, 0.62 mmol, 1.0 equiv). Purification by column chromatography on silica gel (DCM / methanol / ammonia: 100:0:0 → 95:5:0.05) gave compound **9** as a light-yellow solid (92.7 mg, 0.15 mmol, 24%). **^{1}H NMR** (400 MHz, $CDCl_3$): *δ* 9.24 (s, 1 H), 7.61 (t, *J* = 54.4 Hz, 1 H), 6.57 (dd, *J* = 16.8, 10.6 Hz, 1 H), 6.25 (dd, *J* = 16.8, 2.0 Hz, 1 H), 5.66 (dd, *J* = 10.6, 2.0 Hz, 1 H), 5.58 (s, 2 H), 4.79-4.62 (m, 1 H), 4.48-4.33 (m, 1 H), 4.18 (s, 2 H), 3.99 (dd, *J* = 11.4, 3.8 Hz, 2 H), 3.95-3.75 (m, 4 H), 3.73-3.64 (m, 3 H), 3.62-3.47 (m, 3 H), 3.39 (d, *J* = 6.2 Hz, 2 H), 3.29 (t, *J* = 12.7 Hz, 1 H), 3.06 (t, *J* = 12.8 Hz, 1 H), 2.64 (t, *J* = 12.6 Hz, 1 H), 1.99-1.73 (m, 2 H), 1.33 (d, *J* = 6.8 Hz, 3 H), 1.32-1.17 (m, 5 H) ppm. **^{19}F{^{1}H} NMR** (376 MHz, $CDCl_3$): *δ* -121.75 (s, 2 F) ppm. **^{13}C{^{1}H} NMR** (101 MHz, $CDCl_3$): *δ* 168.03 (s, 1 C), 167.82 (s, 1 C), 165.49 (s, 1 C), 164.65 (s, 1 C), 164.28 (s, 1 C), 163.43 (s, 1 C), 162.54 (s, 1 C), 159.63 (s, 1 C), 127.98 (s, 1 C), 127.52 (s, 1 C), 119.80 (s, 1 C), 109.60 (t, *J* = 241.0 Hz, 1 C), 75.93 (s, 1 C), 71.06 (s, 1 C), 70.90 (s, 1 C), 67.00 (s, 2 C), 46.64 (s, 1 C), 45.86 (s, 1 C), 45.01 (s, 1 C), 42.04 (s, 1 C), 41.68 (s, 1 C), 38.74 (s, 1 C), 36.67 (s, 1 C), 29.86 (s, 1 C), 29.78 (s, 1 C), 28.69 (s, 1 C) ppm. **HRMS** (*m/z*): $[M + Na]^+$ calc. for $C_{28}H_{38}F_2N_{10}NaO_4$, 639.2938; found: 639.2941. **HPLC**: t_R = 7.05 min (96.6% purity).

(*S*)-1-(4-((2-(4-(4-(2-amino-4-(difluoromethyl)pyrimidin-5-yl)-6-(3-methylmorpholino)-1,3,5-triazin-2-yl)piperazin-1-yl)-2-oxoethoxy)methyl)piperidin-1-yl)propan-1-one (**9r**)

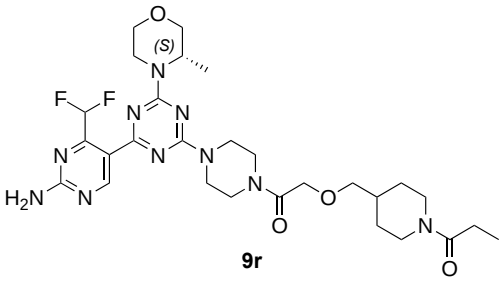

9r

Compound **9r** was prepared according to **GP1** from intermediate **38** (301 mg, 0.50 mmol, 1.0 equiv). Purification by column chromatography on silica gel (DCM / methanol / ammonia: 100:0:0 → 95:5:0.05) followed by preparative TLC (DCM / methanol / ammonia: 94:6:0.06) gave compound **9r** as a light-yellow solid (164 mg, 0.27 mmol, 53%). **^{1}H NMR** (400 MHz, $CDCl_3$): *δ* 9.22 (s, 1H), 7.60 (t, *J* = 54.4 Hz, 1H), 6.00 (s, 2H), 4.72 (br s, 1H), 4.64-4.61 (m, 1H), 4.38 (d, *J* = 14.0 Hz, 1H), 4.17 (s, 2H), 3.98 (dd, *J* = 11.3, 3.5 Hz, 1H), 3.93-3.80 (m, 5H), 3.80-3.75 (m, 1H), 3.72-3.62 (m, 3H), 3.61-3.53 (m, 2H), 3.52-3.46 (m, 1H), 3.37 (d, *J* = 5.6 Hz, 2H), 3.33-3.22 (m, 1H), 3.05-2.93 (m, 1H), 2.59-2.48 (m, 1H), 2.32 (q, *J* = 7.5 Hz, 2H), 1.93-1.77 (m, 2H), 1.77-1.68 (m, 1H), 1.32 (d, *J* = 6.8 Hz, 3H), 1.26-1.15 (m, 2H), 1.12 (t, *J* = 7.5 Hz, 3H) ppm. **^{19}F{^{1}H} NMR** (376 MHz, $CDCl_3$): *δ* -121.68 (s, 2 F) ppm. **^{13}C{^{1}H} NMR** (101 MHz, $CDCl_3$): *δ* 172.29 (s, 1 C), 168.08 (s, 1 C), 167.85 (s, 1 C), 164.66 (s, 1 C), 164.29 (s, 1 C), 163.51 (s, 1 C), 162.58 (s, 1 C), 159.62 (t, *J* = 21.7 Hz, 1 C), 119.73 (s, 1 C), 109.62 (t, *J* = 241.2 Hz, 1 C), 76.04 (s, 1 C), 71.07 (s, 1 C), 70.92 (s, 1 C), 67.01 (s, 1 C), 46.64 (s, 1 C), 45.43 (s, 1 C), 45.03 (s, 1 C), 43.47 (s, 1 C), 42.95 (s, 1 C), 41.71 (s, 1 C), 41.63 (s, 1 C), 38.75 (s, 1 C), 36.69 (s, 1 C), 29.78 (s, 1 C), 28.77 (s, 1 C), 26.68 (s, 1 C), 14.45 (s, 1 C), 9.69 (s, 1 C) ppm. **HRMS** (*m/z*): $[M + Na]^+$ calc. for $C_{28}H_{38}F_2N_{10}NaO_4$, 641.3094; found: 641.3107. **HPLC**: t_R = 7.17 min (92.9% purity).

2,4-Dichloro-6-(morpholin-4-yl)-1,3,5-triazine (**11**)

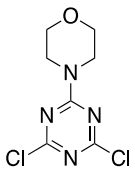

11

Compound **11** was prepared according to the literature.[15]

(*S*)-4-(4,6-dichloro-1,3,5-triazin-2-yl)-3-methylmorpholine (**12**)

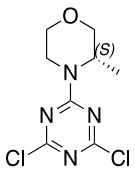

12

Compound **12** was prepared according to the literature.[16]

tert-butyl 4-(4-chloro-6-morpholino-1,3,5-triazin-2-yl)piperazine-1-carboxylate (**13**)

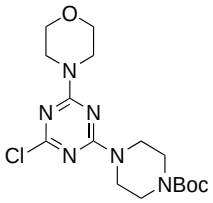

13

To a solution of 2,4-dichloro-6-(morpholin-4-yl)-1,3,5-triazine (**11**) (20.7 g, 87.9 mmol, 0.9 equiv) in ethanol, DIPEA (16.2 g, 21.4 mL, 125.6 mmol, 1.3 equiv) and 1-Boc-piperazine (18.0 g, 96.6 mmol, 1.0 equiv) were added at 0 °C. The reaction mixture was stirred at room temperature for 5 h. The solvent was removed under reduced pressure. DCM (300 mL) was added and the resulting organic layer was washed with an aqueous saturated $NaHSO_4$-solution (4 x 200 mL). The organic layer was dried over anhydrous Na_2SO_4, filtered and concentrated under reduced pressure. The product was recrystallized from DCM / heptane to obtain compound **13** as a colorless solid (22.7 g, 58.9 mmol, 80%). **^{1}H NMR** (400 MHz, $CDCl_3$): *δ* 3.85-3.69 (m, 12 H), 3.50-3.43 (m, 4 H), 1.48 (s, 9 H) ppm. **^{13}C{^{1}H} NMR** (101 MHz, $CDCl_3$): *δ* 169.68 (s, 1 C), 164.47 (s, 2 C), 154.62 (s, 1 C), 80.24 (s, 1 C), 66.69 (s, 2 C), 66.54 (s, 2 C), 43.86 (s, 2 C), 43.28 (s, 2 C), 28.39 (s, 3 C) ppm. **MALDI-MS**: *m/z* = 385.643 $[M + H]^+$. **HPLC**: t_R = 6.53 min (100.0 % purity).

tert-butyl (*S*)-4-(4-chloro-6-(3-methylmorpholino)-1,3,5-triazin-2-yl)piperazine-1-carboxylate (**14**)

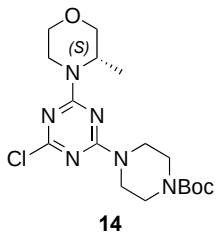

14

To a solution of (*S*)-4-(4,6-dichloro-1,3,5-triazin-2-yl)-3-methylmorpholine (**12**) (30.3 g, 122 mmol, 1.0 equiv) in ethanol, DIPEA (23.7 g, 32.1 mL, 184 mmol, 1.5 equiv) and 1-Boc-piperazine (27.3 g, 146 mmol, 1.2 equiv) were added at 0 °C. The reaction mixture was stirred

at room temperature for 3 h. The solvent was removed under reduced pressure. DCM (300 mL) was added and the resulting organic layer was washed with an aqueous saturated $NaHSO_4$-solution (4 x 200 mL). The organic layer was dried over anhydrous Na_2SO_4, filtered and concentrated under reduced pressure. The product was recrystallized from DCM / heptane to obtain compound **14** as a colorless solid (51.2 g, 128 mmol, quantitative yield). **^{1}H NMR** (400 MHz, $CDCl_3$): *δ* 4.66 (s, 1 H), 4.33 (t, *J* = 7.1 Hz, 1 H), 3.94 (dd, *J* = 11.5, 3.7 Hz, 1 H), 3.84-3.69 (m, 5 H), 3.63 (dd, *J* = 11.5, 3.3 Hz, 1 H), 3.47 (m, 5 H), 3.25 (ddd, *J* = 13.7, 12.3, 3.8 Hz, 1 H), 1.48 (s, 9 H), 1.30 (d, *J* = 6.9 Hz, 3 H) ppm. **^{13}C{^{1}H} NMR** (101 MHz, $CDCl_3$): *δ* 169.70 (s, 1 C), 164.55 (s, 1 C), 164.23 (s, 1 C), 154.67 (s, 1 C), 80.25 (s, 1 C), 79.88 (s, 1 C), 70.86 (s, 1 C), 66.84 (s, 1 C), 46.70 (s, 2 C), 43.28 (s, 2 C), 38.86 (s, 1 C), 28.40 (s, 3 C), 14.12 (s, 1 C) ppm. **MALDI-MS**: *m/z* = 399.661 $[M + H]^+$.

4-(difluoromethyl)-5-(4-morpholino-6-(piperazin-1-yl)-1,3,5-triazin-2-yl)pyrimidin-2-amine (**15**).

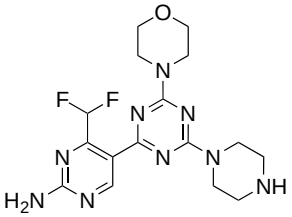

15

Step 1. The bromo derivative **39** (7.00 g, 16.5 mmol, 1.0 equiv), bis(pinacolato)diboron (6.29 g, 24.75 mmol, 1.5 equiv), potassium acetate (5.02 g, 51.2 mmol, 3.1 equiv), [1,1′-bis(diphenylphosphino)ferrocene]dichloropalladium(II) ($Pd(dppf)Cl_2$, 1.21 g, 1.65 mmol, 0.1 equiv) were charged in flask under nitrogen atmosphere. Absolute 1,4-dioxane (40 mL) was added and the mixture was stirred at 95 °C for 1.5 h. After completion of the reaction, the mixture was allowed to cool down to room temperature. *Step 2.* Monochloro-triazine **13** (6.99 g, 18.2 mmol, 1.1 equiv), chloro(2-dicyclohexylphosphino-2′,4′,6′-triisopropyl-1,1′-biphenyl)[2-(2′-amino-1,1′-biphenyl)]palladium(II) (XPhos Pd G2, 0.519 g, 0.66 mmol, 0.04 equiv), potassium phosphate tribasic (10.5 g, 49.5 mmol, 3.0 equiv) and deionized H_2O (10 mL) were added. The resulting mixture was stirred at 100 °C overnight. After completion of the reaction, the mixture was allowed to cool down to room temperature and the crude was filtered on celite. To the solution, deionized H_2O (300 mL) and ethyl acetate (300 mL) were added. The layers were separated and the organic layer was washed with deionized H_2O and brine (2x). The aqueous layer was extracted with DCM (2x). The combined organic layers were concentrated under reduced pressure. *Step 3.* The above residue was dissolved in 1,4-dioxane (40 mL) and an aqueous solution of HCl (3 M, 40 mL) was added. The reaction mixture was stirred at 80 °C overnight. After completion of the reaction, the mixture was cool down to room temperature.

Ethyl acetate (200 mL) and deionized H_2O (200 mL) were added and the two layers were separated. The aqueous layer was washed with ethyl acetate (3x). The aqueous layer was basified to pH = 10. The solid formed was filtered and washed with acetonitrile to obtain compound **15** as a beige solid (4.91 g, 12.5 mmol, 76%). **^{1}H NMR** (400 MHz, DMSO-d_6): δ 9.09 (s, 1 H), 7.63 (t, J = 54.1 Hz, 1 H), 7.57 (br s, 2 H), 3.86-3.56 (m, 12 H), 2.82-2.63 (s, 4 H) ppm. **^{19}F{^{1}H} NMR** (376 MHz, DMSO-d_6): δ -120.60 (s, 2 F) ppm. **^{13}C{^{1}H} NMR** (101 MHz, DMSO-d_6): δ 167.22 (s, 1 C), 163.99 (s, 1 C), 163.73 (s, 1 C), 163.72 (s, 1 C), 161.64 (s, 1 C), 158.82 (t, J = 21.2 Hz, 1 C), 117.68 (s, 1 C), 109.80 (t, J = 239.2 Hz, 1 C), 65.91 (s, 2 C), 45.43 (s, 2 C), 44.08 (s, 2 C), 43.20 (s, 2 C) ppm. **MALDI-MS**: m/z = 394.205 $[M + H]^+$.

(*S*)-4-(difluoromethyl)-5-(4-(3-methylmorpholino)-6-(piperazin-1-yl)-1,3,5-triazin-2-yl)pyrimidin-2-amine (**16**)

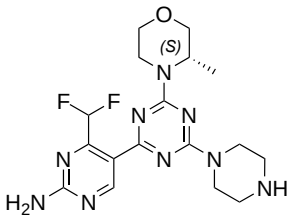

16

Step 1. The bromo derivative **39** (14.5 g, 34.2 mmol, 1.0 equiv), bis(pinacolato)diboron (13.0 g, 51.3 mmol, 1.5 equiv), potassium acetate (10.4 g, 106.2 mmol, 3.1 equiv), [1,1′-bis(diphenylphosphino)ferrocene]dichloropalladium(II) (Pd(dppf)Cl_2, 1.26 g, 1.72 mmol, 0.05 equiv) were charged in a flask under nitrogen atmosphere. Absolute 1,4-dioxane (65 mL) was added and the mixture was stirred at 95 °C for 3 h. After completion of the reaction, the mixture was allowed to cool down to room temperature. *Step 2.* Monochloro-triazine **14** (15.0 g, 37.6 mmol, 1.1 equiv), chloro(2-dicyclohexylphosphino-2′,4′,6′-triisopropyl-1,1′-biphenyl)[2-(2′-amino-1,1′-biphenyl)]palladium(II) (XPhos Pd G2, 812 mg, 1.03 mmol, 0.03 equiv), potassium phosphate tribasic (23.6 g, 102.5 mmol, 3.0 equiv) and deionized H_2O (22 mL) were added. The resulting mixture was stirred at 100 °C overnight. After completion of the reaction, the mixture was allowed to cool down to room temperature and the crude was filtered on celite. To the solution, deionized H_2O (300 mL) and ethyl acetate (300 mL) were added. The layers were separated and the organic layer was washed with deionized H_2O and brine (2x). The aqueous layer was extracted with DCM (2x). The combined organic layers were concentrated under reduced pressure. *Step 3.* The above residue was dissolved in 1,4-dioxane (65 mL) and an aqueous solution of HCl (3 M, 150 mL) was added. The reaction mixture was stirred at 80 °C overnight. After completion of the reaction, the mixture was cool down to room temperature. DCM (200 mL) were added to the reaction mixture, the aqueous phase was collected and basified to pH 11 with NaOH pellets. The formed precipitate was filtered and

washed with acetonitrile to obtain compound **16** as a beige solid (7.70 g, 18.9 mmol, 55%). **^{1}H NMR** (400 MHz, $CDCl_3$): *δ* 9.24 (s, 1 H), 7.66 (t, *J* = 54.5 Hz, 1 H), 5.57 (s, 2 H), 4.73 (d, *J* = 7.8 Hz, 1 H), 4.40 (d, *J* = 13.6 Hz, 1 H), 3.98 (dd, *J* = 11.4, 3.7 Hz, 1 H), 3.89-3.74 (m, 5 H), 3.73-3.64 (m, 1 H), 3.52 (td, *J* = 11.9, 3.0 Hz, 1 H), 3.27 (td, *J* = 12.8, 3.7 Hz, 1 H), 2.92 (t, *J* = 5.1 Hz, 4 H), 1.32 (d, *J* = 6.8 Hz, 3 H) ppm. **^{19}F{^{1}H} NMR** (376 MHz, $CDCl_3$): *δ* -121.74 (s, 2 F) ppm. **^{13}C{^{1}H} NMR** (101 MHz, $CDCl_3$): *δ* 167.64 (s, 1 C), 164.50 (s, 1 C), 164.34 (s, 1 C), 163.46 (s, 1 C), 162.62 (s, 1 C), 159.53 (t, *J* = 21.4 Hz, 1 C), 120.07 (t, *J* = 3.8 Hz, 1 C), 109.61 (t, *J* = 240.8 Hz, 1 C), 71.13 (s, 1 C), 67.07 (s, 1 C), 46.51 (s, 1 C), 46.07 (s, 2 C), 44.49 (s, 2 C), 38.66 (s, 1 C), 14.36 (s, 1 C) ppm. **MALDI-MS**: *m/z* = 408.532 $[M + H]^+$.

tert-butyl (2-(4-(4-(2-amino-4-(difluoromethyl)pyrimidin-5-yl)-6-morpholino-1,3,5-triazin-2-yl)piperazin-1-yl)-2-oxoethyl)(methyl)carbamate (**17**)

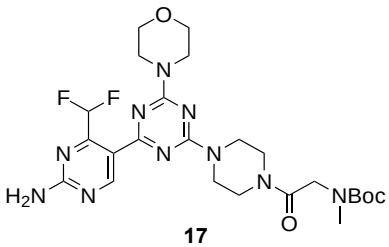

17

Compound **17** was prepared according to **GP1** from **15** (1.40 g, 3.57 mmol, 1.0 eq.) and *N*-(*tert*-butoxycarbonyl)-*N*-methylglycine (1.01 g, 5.35 mmol, 1.5 eq.). Compound **17** was obtained as a colorless solid (1.40 g, 2.48 mmol, 69%). **^{1}H NMR** (400 MHz, $CDCl_3$): *δ* 9.22 (s, 1 H), 7.59 (t, *J* = 54.4 Hz, 1 H), 5.60 (br s, 2 H), 4.15-4.09 (m, 2 H), 4.03-3.80 (m, 8 H), 3.78-3.73 (m, 4 H), 3.73-3.66 (m, 2 H), 3.56-3.48 (m, 2 H), 2.05 (s, 3 H), 1.48 (s, 9 H) ppm. **^{19}F{^{1}H} NMR** (376 MHz, $CDCl_3$): *δ* -121.68 (s, 2 F) ppm. **^{13}C{^{1}H} NMR** (101 MHz, $CDCl_3$): *δ* 167.78 (s, 1 C), 167.48 (s, 1 C), 164.53 (s, 1 C), 164.51 (s, 1 C), 163.43 (s, 1 C), 162.47 (s, 1 C), 159.53 (t, *J* = 21.6 Hz, 1 C), 156.19 (s, 1 C), 119.60 (s, 1 C), 109.50 (t, *J* = 240.9 Hz, 1 C), 80.19 (s, 1 C), 66.72 (s, 2 C), 60.40 (s, 1 C), 44.58 (br s, 1 C), 43.69-42.87 (m, 4 C), 41.67 (br s, 1 C), 35.54 (s, 1 C), 28.37 (s, 3 C) ppm. **MALDI-MS**: *m/z* = 565.111 $[M + H]^+$.

2-(4-(4-(2-amino-4-(difluoromethyl)pyrimidin-5-yl)-6-morpholino-1,3,5-triazin-2-yl)piperazin-1-yl)-*N*-methyl-2-oxoethan-1-aminium chloride (**18**)

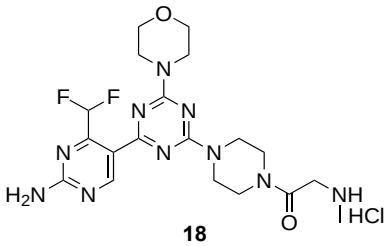

18

Compound **18** was prepared according to **GP2** from intermediate **17** (1.15 g, 2.04 mmol, 1.0 equiv). Compound **18** was obtained as a colorless solid (1.02 g, 2.04 mmol, quantitative yield). **^{1}H NMR** (400 MHz, DMSO-d_6): δ 9.12 (s, 1 H), 9.07 (br s, 2 H), 7.64 (br s, 2 H), 7.63 (t, J = 54.0 Hz, 1 H), 4.10 (t, J = 5.9 Hz, 2 H), 3.90-3.74 (m, 8 H), 3.68-3.64 (m, 4 H), 3.62-3.58 (m, 2 H), 3.50-3.45 (m, 2 H), 2.58-2.55 (m, 3 H) ppm. **^{19}F{^{1}H} NMR** (376 MHz, DMSO-d_6): δ -120.67 (s, 2 F) ppm. **MALDI-MS**: *m/z* = 465.437 $[M + H]^+$.

tert-butyl 4-(((2-(4-(4-(2-amino-4-(difluoromethyl)pyrimidin-5-yl)-6-morpholino-1,3,5-triazin-2-yl)piperazin-1-yl)-2-oxoethyl)(methyl)amino)methyl)piperidine-1-carboxylate (**19**)

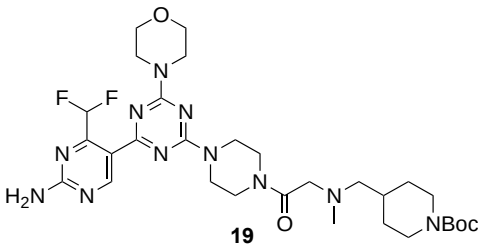

19

Compound **19** was prepared according to **GP3** from intermediate **18** (651 g, 1.30 mmol, 1 equiv.) and 1-boc-4-bromomethylpiperidine (362 mg, 1.30 mmol, 1 equiv.). Purification by column chromatography on silica gel (DCM / methanol / ammonia: 100:0:0 → 93:7:0.07) gave compound **19** as a colorless solid (370 mg, 0.56 mmol, 43%). **^{1}H NMR** (400 MHz, $CDCl_3$): δ 9.23 (s, 1 H), 7.61 (t, J = 54.4 Hz, 1 H), 5.98 (br s, 2 H), 4.18-4.03 (m, 3 H), 3.94-3.80 (m, 8 H), 3.79-3.73 (m, 4 H), 3.72-3.65 (m, 3 H), 3.56-3.44 (m, 1 H), 2.76-2.63 (m, 2 H), 2.70 (s, 3 H), 1.96-1.60 (m, 5 H), 1.45 (s, 9 H), 1.31-0.99 (m, 3 H) ppm. **^{19}F{^{1}H} NMR** (376 MHz, $CDCl_3$): δ -121.65 (s, 2 F) ppm. **^{13}C{^{1}H} NMR** (101 MHz, $CDCl_3$): δ 169.13 (s, 1 C), 167.78 (s, 1 C), 167.07 (s. 1 C), 164.53 (s, 1 C), 163.41 (s, 1 C), 162.47 (s, 1 C), 159.51 (s, 1 C), 154.86 (s, 1 C), 119.70 (s, 1 C), 109.50 (t, J = 240.9 Hz, 1 C), 79.41 (s, 1 C), 66.73 (s, 2 C), 63.66 (s, 1 C), 62.88 (br s, 1 C), 45.43 (br s, 2 C), 43.68-43.05 (m, 4 C), 41.62 (br s, 2 C), 35.91 (s, 1 C), 34.10 (s, 1 C), 30.57 (s, 1 C), 28.65 (br s, 1 C), 28.47 (s, 3 C) ppm. **MALDI-MS**: *m/z* = 662.218 $[M + H]^+$.

4-(((2-(4-(4-(2-amino-4-(difluoromethyl)pyrimidin-5-yl)-6-morpholino-1,3,5-triazin-2-yl)piperazin-1-yl)-2-oxoethyl)(methyl)amino)methyl)piperidin-1-ium chloride (**20**)

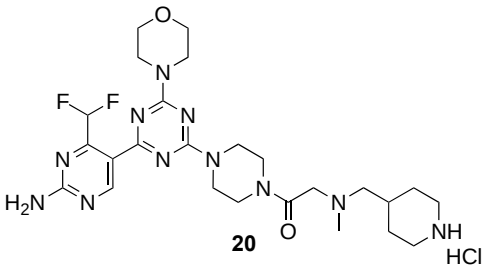

20

Compound **20** was prepared according to **GP2** from intermediate **19** (331 mg, 0.50 mmol, 1.0 equiv). Compound **20** was obtained as a colorless solid (229 mg, 0.38 mmol, 77%). **^{1}H NMR** (400 MHz, DMSO-d_6): δ 9.55 (br s, 1 H), 9.21 (s, 1 H), 9.15-8.87 (m, 2 H), 7.72 (t, J = 54.0 Hz, 1 H), 7.71 (br s, 1 H), 4.50-4.44 (m, 1 H), 4.24 (d, J = 7.0 Hz, 1 H), 4.02-3.47 (m, 14 H), 3.39-3.05 (m, 4 H), 3.01-2.87 (m, 4 H), 2.16 (s, 3 H), 1.94-1.77 (m, 2 H), 1.59-1.44 (m, 3 H) ppm. **^{19}F{^{1}H} NMR** (376 MHz, DMSO-d_6): δ -120.66 (s, 2 F) ppm.

tert-butyl (2-(4-(4-(2-amino-4-(difluoromethyl)pyrimidin-5-yl)-6-morpholino-1,3,5-triazin-2-yl)piperazin-1-yl)ethyl)carbamate (**21**)

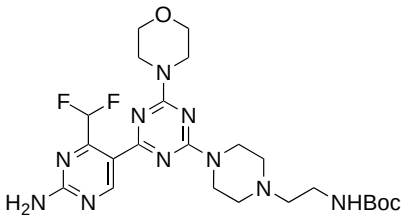

21

Compound **21** was prepared according to **GP3** from intermediate **15** (1.18 g, 3.00 mmol, 1 equiv.) and 2-(boc-amino)ethyl bromide (672 mg, 3.00 mmol, 1 equiv.). Purification by column chromatography on silica gel (DCM / methanol / ammonia: 100:0:0 → 97:3:0.03) gave compound **21** as a colorless solid (826 mg, 1.54 mmol, 51%).**^{1}H NMR** (400 MHz, DMSO-d_6): δ 9.10 (s, 1 H), 7.63 (t, J = 54.1 Hz, 1 H), 7.55 (br s, 2 H), 6.68 (t, J = 5.7 Hz, 1 H), 3.82-3.70 (m, 8 H), 3.67-3.59 (m, 4 H), 3.08 (q, J= 6.4 Hz, 2 H), 2.46-2.40 (m, 4 H), 2.37 (t, J = 6.8 Hz, 2 H), 1.38 (s, 9 H) ppm. **^{19}F{^{1}H} NMR** (376 MHz, DMSO-d_6): δ -121.70 (s, 2 F) ppm. **^{13}C{^{1}H} NMR** (101 MHz, DMSO-d_6): δ 167.81 (s, 1 C), 164.50 (s, 1 C), 164.26 (s, 1 C), 164.24 (s, 1 C), 162.17 (s, 1 C), 159.36 (t, J = 21.2 Hz, 1 C), 156.04 (s, 1 C), 118.10 (s, 1 C), 110.32 (t, J = 239.3 Hz, 1 C), 78.00 (s, 1 C), 66.41 (s, 2 C), 57.75 (s, 1 C), 52.90 (s, 2 C), 43.74-43.08 (m, 4 C), 37.79 (s, 1 C), 28.72 (s, 3 C) ppm. **MALDI-MS**: *m/z* = 481.542 [M – tert-butyl + H]$^+$.

2-(4-(4-(2-amino-4-(difluoromethyl)pyrimidin-5-yl)-6-morpholino-1,3,5-triazin-2-yl)piperazin-1-yl)ethan-1-aminium chloride (**22**)

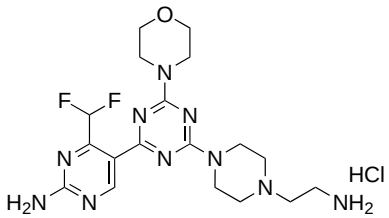

22

Compound **22** was prepared according to **GP2** from intermediate **21** (800 mg, 1.49 mmol, 1.0 equiv). Compound **22** was obtained as a colorless solid (705 mg, 1.49 mmol, quantitative yield). **^{1}H NMR** (400 MHz, DMSO-d_6): δ 9.14 (s, 1 H), 8.38 (br s, 3 H), 7.62 (t, J = 53.9 Hz, 1 H), 4.79 (br s, 1 H), 3.84-3.75 (m, 5 H), 3.70-3.61 (m, 7 H), 3.51-3.43 (m, 2 H), 3.39-3.31 (m, 4 H), 3.20-3.08 (s, 2 H) ppm. **^{19}F{^{1}H} NMR** (376 MHz, DMSO-d_6): δ -120.68 (s, 2 F) ppm. **MALDI-MS**: m/z = 437.676 $[M + H]^+$.

tert-butyl 4-((2-(4-(4-(2-amino-4-(difluoromethyl)pyrimidin-5-yl)-6-morpholino-1,3,5-triazin-2-yl)piperazin-1-yl)ethyl)carbamoyl)piperidine-1-carboxylate (**23**)

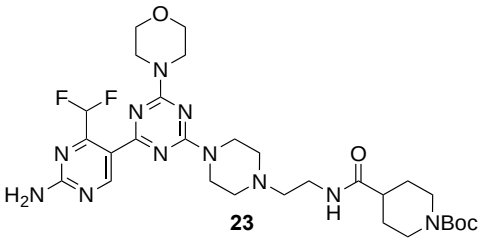

23

Compound **23** was prepared according to **GP1** from **22** (368 g, 0.78 mmol, 1.0 equiv). Purification by column chromatography on silica gel (DCM / methanol / ammonia: 100:0:0 → 96:4:0.04) gave compound **23** as a colorless solid (366 mg, 0.56 mmol, 72%). **^{1}H NMR** (400 MHz, $CDCl_3$): δ 9.23 (s, 1 H), 7.62 (t, J = 54.4 Hz, 1 H), 6.05 (br s, 1 H), 5.57 (br s, 2 H), 4.23-4.10 (m, 2 H), 3.95-3.79 (m, 8 H), 3.78-3.73 (m, 4 H), 3.40 (q, J = 5.6 Hz, 2 H), 2.76 (t, J = 12.7 Hz, 2 H), 2.57-2.47 (m, 6 H), 2.26 (tt, J = 11.6, 3.7 Hz, 1 H), 1.86-1.79 (m, 2 H), 1.70-1.57 (m, 2 H), 1.46 (s, 9 H) ppm. **^{19}F{^{1}H} NMR** (376 MHz, $CDCl_3$): δ -121.70 (s, 2 F) ppm. **^{13}C{^{1}H} NMR** (101 MHz, $CDCl_3$): δ 174.44 (s, 1 C), 167.65 (s, 1 C), 164.57 (s, 1 C), 164.33 (s, 1 C), 163.36 (s, 1 C), 162.47 (s, 1 C), 159.49 (t, J = 21.5 Hz, 1 C), 154.70 (s, 1 C), 119.88 (t, J = 3.8 Hz, 1 C), 109.48 (t, J = 240.8 Hz, 1 C), 79.65 (s, 1 C), 66.75 (s, 2 C), 56.66 (s, 1 C), 52.68 (s, 2 C), 43.66 (br s, 2 C), 43.30-42.84 (m, 4 C), 43.29 (s, 1 C), 35.78 (s, 1 C), 28.67 (s, 2 C), 28.44 (s, 3 C) ppm.

4-((2-(4-(4-(2-amino-4-(difluoromethyl)pyrimidin-5-yl)-6-morpholino-1,3,5-triazin-2-yl)piperazin-1-yl)ethyl)carbamoyl)piperidin-1-ium chloride (**24**).

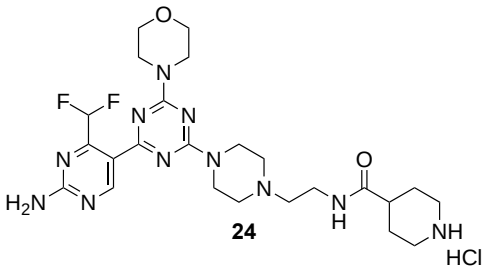

24

Compound **24** was prepared according to **GP2** from intermediate **23** (336 g, 0.52 mmol, 1.0 equiv). Compound **24** was obtained as a colorless solid (302 mg, 0.52 mmol, quantitative yield). **^{1}H NMR** (400 MHz, DMSO-d_6): δ 11.19 (br s, 1 H), 9.14 (s, 1 H), 8.90 (br s, 1 H), 8.66 (br s, 1 H), 8.39 (t, J = 5.7 Hz, 1 H), 7.62 (t, J = 53.9 Hz, 1 H), 7.61 (br s, 1 H), 4.81-4.69 (m, 2 H), 3.85-3.74 (m, 4 H), 3.70-3.58 (m, 5 H), 3.55-3.44 (m, 4 H), 3.30-3.23 (m, 2 H), 3.21-3.15 (m, 2 H), 3.13-3.02 (m, 2 H), 2.88 (q, J = 11.6 Hz, 2 H), 2.52-2.42 (m, 2 H), 1.95-1.87 (m, 2 H), 1.81-1.69 (m, 2 H) ppm. **^{19}F{^{1}H} NMR** (376 MHz, DMSO-d_6): δ -120.68 (s, 2 F) ppm. **MALDI-MS**: m/z = 548.421 $[M + H]^+$.

tert-butyl 4-(4-(4-(4-(2-amino-4-(difluoromethyl)pyrimidin-5-yl)-6-morpholino-1,3,5-triazin-2-yl)piperazine-1-carbonyl)benzyl)piperidine-1-carboxylate (**25**)

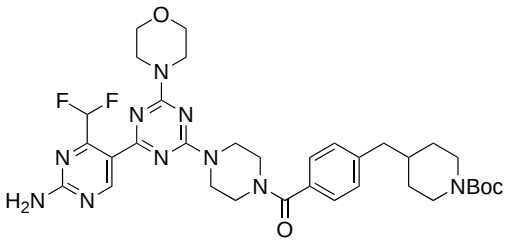

25

Compound **25** was prepared according to **GP1** from intermediate **15** (279 mg, 0.71 mmol, 1.0 equiv.) and 4-((1-(tert-butoxycarbonyl)piperidin-4-yl)methyl)benzoic acid (249 mg, 0.78 mmol, 1.1 equiv.). Purification by column chromatography on silica gel (DCM / methanol / ammonia: 100:0:0 → 97:3:0.03) gave compound **25** as a yellow solid (331 mg, 0.48 mmol, 67%). **^{1}H NMR** (400 MHz, $CDCl_3$): δ 9.22 (s, 1 H), 7.59 (t, J = 54.4 Hz, 1 H), 7.37 (d, J = 8.1 Hz, 2 H), 7.20 (d, J = 7.9 Hz, 2 H), 5.61 (s, 2 H), 4.18-4.01 (m, 2 H), 3.98-3.46 (m, 14 H), 2.64 (t, J = 12.8 Hz, 2 H), 2.58 (d, J = 7.0 Hz, 2 H), 1.74-1.55 (m, 5 H), 1.45 (s, 9 H), 1.23-1.10 (m, 2 H) ppm. **^{19}F{^{1}H} NMR** (376 MHz, $CDCl_3$): δ -121.68 (s, 2 F) ppm. **^{13}C{^{1}H} NMR** (101 MHz, $CDCl_3$) δ 170.75 (s, 1 C), 167.78 (s, 1 C), 164.56 (s, 1 C), 164.51 (s, 1 C), 163.41 (s, 1 C), 162.48 (s, 1 C), 159.50 (t, J = 21.4 Hz, 1 C), 154.84 (s, 1 C), 142.54 (s, 1 C), 133.03 (s, 1 C), 129.32 (s, 2 C), 127.23 (s, 2 C), 119.63 (t, J = 3.8 Hz, 1 C), 109.49 (t, J = 240.9 Hz, 1 C), 79.31 (s, 1 C),

66.71 (s, 2 C), 44.34-43.02 (s, 6 C), 42.95 (s, 2 C), 38.05 (s, 2 C), 31.91 (s, 2 C), 28.47 (s, 3 C) ppm. **MALDI-MS**: *m/z* = 639.769 [M – *tert*-butyl + H]$^+$.

4-(4-(4-(4-(2-amino-4-(difluoromethyl)pyrimidin-5-yl)-6-morpholino-1,3,5-triazin-2-yl)piperazine-1-carbonyl)benzyl)piperidin-1-ium chloride (**26**)

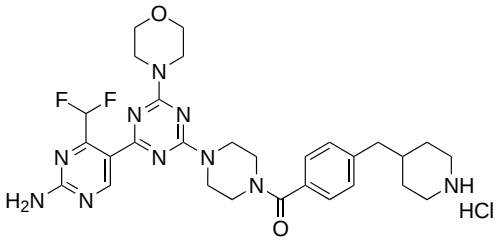

26

Compound **26** was prepared according to **GP2** from intermediate **25** (283 mg, 0.41 mmol, 1.0 equiv). Compound **26** was obtained as a colorless solid (185 mg, 0.29 mmol, 72%). **^{1}H NMR** (400 MHz, DMSO-d_6): δ 9.11 (s, 1 H), 8.85 (br s, 1 H), 8.57 (br s, 1 H), 7.62 (t, *J* = 54.0 Hz, 1 H), 7.41-7.34 (m, 2 H), 7.32-7.22 (m, 2 H), 3.94-3.75 (m, 8 H), 3.72-3.56 (m, 6 H), 3.41 (t, *J* = 6.4 Hz, 1 H), 3.22 (d, *J* = 12.5 Hz, 2 H), 2.79 (q, *J* = 11.5 Hz, 2 H), 2.59 (d, *J* = 7.1 Hz, 2 H), 1.89-1.78 (m, 1 H), 1.71 (d, *J* = 14.1 Hz, 3 H), 1.36 (q, *J* = 12.1 Hz, 2 H) ppm. **^{19}F{^{1}H} NMR** (376 MHz, DMSO-d_6): δ -120.67 (s, 2 F) ppm. **MALDI-MS**: *m/z* = 595.621 [M + H]$^+$.

tert-butyl 3-(3-(4-(4-(2-amino-4-(difluoromethyl)pyrimidin-5-yl)-6-morpholino-1,3,5-triazin-2-yl)piperazine-1-carbonyl)benzyl)piperidine-1-carboxylate (**27**)

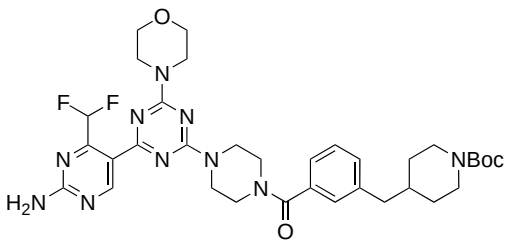

27

Compound **27** was prepared according to **GP1** from intermediate **15** (279 mg, 0.71 mmol, 1.0 equiv.) and 3-((1-(tert-butoxycarbonyl)piperidin-4-yl)methyl)benzoic acid (249 mg, 0.78 mmol, 1.1 equiv.). Purification by column chromatography on silica gel (DCM / methanol / ammonia: 100:0:0 → 97:3:0.03) gave compound **27** as a light-yellow solid (318 mg, 0.46 mmol, 64%). **^{1}H NMR** (400 MHz, $CDCl_3$): δ 9.20 (s, 1 H), 7.58 (t, *J* = 54.1 Hz, 1 H), 7.36-7.30 (m, 1 H), 7.25-7.17 (m, 3 H), 5.98 (br s, 2 H), 4.16-3.98 (m, 2 H), 3.98-3.78 (m, 10 H), 3.78-3.71 (m, 4 H), 3.61-3.38 (m, 2 H), 2.71-2.50 (m, 4 H), 1.73-1.56 (m, 3 H), 1.43 (s, 9 H), 1.20-1.07 (m, 2 H) ppm. **^{19}F{^{1}H} NMR** (376 MHz, $CDCl_3$): δ -121.60 (s, 2 F) ppm. **^{13}C{^{1}H} NMR** (101 MHz, $CDCl_3$): δ 170.86 (s, 1 C), 167.87 (s, 1 C), 164.64 (s, 1 C), 164.59 (s, 1 C), 163.49 (s, 1 C), 162.55 (s,

1 C), 159.58 (t, *J* = 21.7 Hz, 1 C), 154.91 (s, 1 C), 141.01 (s, 1 C), 135.51 (s, 1 C), 130.85 (s, 1 C), 128.57 (s, 1 C), 127.80 (s, 1 C), 124.74 (s, 1 C), 119.66 (d, *J* = 3.8 Hz, 1 C), 109.57 (t, *J* = 241.0 Hz, 1 C), 79.38 (s, 1 C), 66.79 (s, 2 C), 44.36-43.00 (m, 6 C), 43.07 (s, 2 C), 38.08 (s, 2 C), 32.01 (s, 2 C), 28.53 (s, 3 C) ppm. **MALDI-MS**: *m/z* = 639.698 $[M - tert\text{-butyl} + H]^+$.

4-(3-(4-(4-(2-amino-4-(difluoromethyl)pyrimidin-5-yl)-6-morpholino-1,3,5-triazin-2-yl)piperazine-1-carbonyl)benzyl)piperidin-1-ium chloride (**28**)

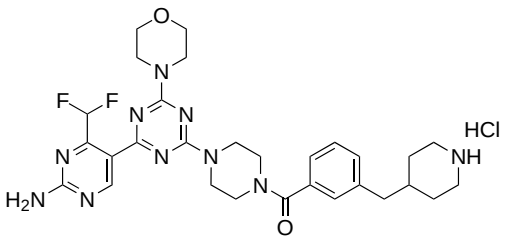

28

Compound **28** was prepared according to **GP2** from intermediate **27** (272 mg, 0.39 mmol, 1.0 equiv). Compound **28** was obtained as a light-yellow solid (156 mg, 0.25 mmol, 64%). **^{1}H NMR** (400 MHz, DMSO-d_6): δ 9.11 (s, 1 H), 8.93 (s, 1 H), 8.64 (s, 1 H), 7.62 (t, *J* = 54.2 Hz, 1 H), 7.43-7.35 (m, 1 H), 7.34-7.19 (m, 3 H), 3.97-3.54 (m, 13 H), 3.50-3.31 (m, 2 H), 3.28-3.14 (m, 2 H), 2.78 (q, *J* = 11.7 Hz, 2 H), 2.59 (d, *J* = 6.9 Hz, 2 H), 1.89-1.76 (m, 1 H), 1.75-1.64 (m, 2 H), 1.45-1.25 (m, 2 H) ppm. **^{19}F{^{1}H} NMR** (376 MHz, DMSO-d_6): δ -120.69 (s, 2 F) ppm. **MALDI-MS**: *m/z* = 595.644 $[M + H]^+$.

tert-butyl 4-(4-(4-(4-(2-amino-4-(difluoromethyl)pyrimidin-5-yl)-6-morpholino-1,3,5-triazin-2-yl)piperazin-1-yl)-4-oxobutyl)piperidine-1-carboxylate (**29**)

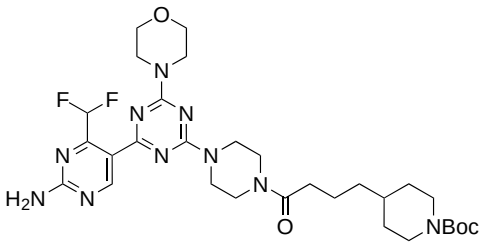

29

Compound **29** was prepared according to **GP1** from intermediate **15** (400 mg, 1.00 mmol, 1 equiv.) and 4-(1-(*tert*-butoxycarbonyl)piperidin-4-yl)butanoic acid (276 mg, 1.00 mmol, 1 equiv.). Purification by column chromatography on silica gel (DCM / methanol / ammonia: 100:0:0 → 97:3:0.03) gave compound **29** as a colorless solid (498 mg, 0.77 mmol, 77%). **^{1}H NMR** (400 MHz, $CDCl_3$): δ 9.22 (s, 1 H), 7.59 (t, *J* = 54.4 Hz, 1 H), 5.94-5.78 (m, 2 H), 4.06 (s, 2 H), 3.90-3.79 (m, 8 H), 3.78-3.72 (m, 4 H), 3.71-3.61 (m, 2 H), 3.56-3.44 (m, 2 H), 2.66 (t, *J* = 12.8 Hz, 2 H), 2.35 (t, *J* = 7.5 Hz, 2 H), 1.84-1.74 (m, 1 H), 1.72-1.61 (m, 4 H), 1.44 (s, 9 H), 1.30 (dd, *J* = 10.1, 6.0 Hz, 2 H), 1.08 (qd, *J* = 12.1, 4.1 Hz, 2 H) ppm.**^{19}F{^{1}H} NMR** (376 MHz, DMSO-d_6): δ -121.59 (s, 2 F) ppm. **^{13}C{^{1}H} NMR** (101 MHz, $CDCl_3$): δ 171.64 (s, 1 C), 171.57 (s, 1 C), 167.75 (s, 1

C), 164.52 (s, 1 C), 164.51 (s, 1 C), 163.43 (s, 1 C), 162.49 (s, 1 C), 159.50 (s, 1 C), 154.89 (s, 1 C), 119.63 (s, 1 C), 109.51 (t, *J* = 239.5 Hz, 1 C), 79.20 (s, 1 C), 66.72 (s, 2 C), 45.29 (s, 1 C), 43.68 (s, 1 C), 41.27 (s, 1 C), 36.32 (s, 2 C), 35.98 (s, 2 C), 33.47 (s, 2 C), 32.12 (s, 2 C), 28.48 (s, 3 C), 22.34 (s, 2 C) ppm. **MALDI-MS**: *m/z* 591.531 [M – *tert*-butyl + H]$^+$.

4-(4-(4-(4-(2-amino-4-(difluoromethyl)pyrimidin-5-yl)-6-morpholino-1,3,5-triazin-2-yl)piperazin-1-yl)-4-oxobutyl)piperidin-1-ium chloride (**30**)

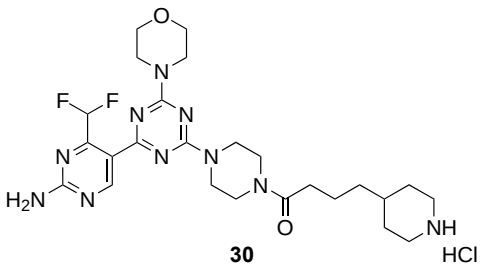

30

Compound **30** was prepared according to **GP2** from intermediate **29** (450 mg, 0.70 mmol, 1.0 equiv). Compound **30** was obtained as a colorless solid (390 mg, 0.67 mmol, 95%). **^{1}H NMR** (400 MHz, DMSO-d_6): δ 9.10 (s, 1 H), 9.03 (d, *J* = 10.9 Hz, 1 H), 8.79 (m, 1 H), 7.63 (t, *J* = 54.0 Hz, 1 H), 3.76 (m, 8 H), 3.66-3.63 (m, 4 H), 3.54-3.46 (m, 4 H), 3.20 (d, *J* = 12.5 Hz, 2 H), 2.79 (q, *J* = 11.9 Hz, 2 H), 2.34 (t, *J* = 7.3 Hz, 2 H), 1.78-1.74 (m, 2 H), 1.53-1.49 (m, 3 H), 1.39-1.19 (m, 4 H) ppm. **^{19}F{^{1}H} NMR** (376 MHz, DMSO-d_6): δ -120.65 (d, *J* = 19.5 Hz, 2 F) ppm. **MALDI-MS**: *m/z* = 547.516 [M + H]$^+$.

tert-butyl 4-((2-(tert-butoxy)-2-oxoethoxy)methyl)piperidine-1-carboxylate (**33**)

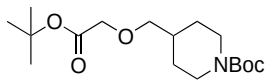

33

To a cold solution (0 °C) of *N*-boc-4-hydroxymethylpiperidine (**31**) (244 mg, 1.13 mmol, 1 equiv.) in dry DMF (3.5 mL) under inert atmosphere, NaH (60% dispersion in mineral oil, 95 mg, 2.38 mmol, 2.1 equiv.) was added portionwise. The resulting mixture was stirred for. Then *tert*-butyl bromoacetate (**32**) (449 mg, 2.30 mmol, 0.34 mL, 2 equiv.) was added and the mixture was stirred at 0 °C for 15 min. After reaction completion monitored by TLC, distilled H_2O was added to quench the reaction and the product was extracted with EtOAc. The organic layer was washed with brine (2x), dried over Na_2SO_4 and concentrated under reduced pressure. Purification by column chromatography on silica gel (cyclohexane / ethyl acetate: 100:0 → 80:20) gave compound **33** as a colorless oil (99 mg, 0.30 mmol, 27%). **^{1}H NMR** (400 MHz, $CDCl_3$): δ 4.17-4.01 (m, 2 H), 3.93 (s, 2 H), 3.35 (d, *J* = 6.2 Hz, 2 H), 2.69 (t, *J* = 12.2 Hz, 2 H), 1.85-1.68 (m, 3 H), 1.47 (s, 9 H), 1.44 (s, 9 H), 1.15 (td, *J* = 12.1, 4.4 Hz, 2 H) ppm.

2-((1-(*tert*-butoxycarbonyl)piperidin-4-yl)methoxy)acetic acid (**34**).

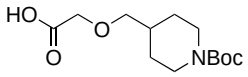

34

To a cold solution (0 °C) of **33** (1.26 g, 3.84 mmol, 1.0 equiv.) in THF (20 mL), a LiOH aqueous solution (5M, 20 mL, 25 equiv.) was added. The resulting mixture was stirred for 5 h at 60ºC. After reaction completion monitored by TLC, the solvent was removed under pressure and the aqueous phase was washed with EtOAc. The aqueous phase was collected and acidified to pH 1 with HCl 1 M and extracted with EtOAc (3x). The organic layer was washed with brine (2x), dried over Na_2SO_4 and concentrated under reduced pressure, giving compound **34** as a colorless solid (478 mg, 1.75 mmol, 46%). **^{1}H NMR** (400 MHz, $CDCl_3$): *δ* 4.11 (s, 4 H), 3.41 (d, *J* = 6.4 Hz, 2 H), 2.71 (t, *J* = 12.8 Hz, 2 H), 1.86-1.77 (m, 1 H), 1.77-1.70 (m, 2 H), 1.45 (s, 9 H), 1.17 (qd, *J* = 12.5, 4.4 Hz, 2 H) ppm.

tert-butyl 4-((2-(4-(4-(2-amino-4-(difluoromethyl)pyrimidin-5-yl)-6-morpholino-1,3,5-triazin-2-yl)piperazin-1-yl)-2-oxoethoxy)methyl)piperidine-1-carboxylate (**35**)

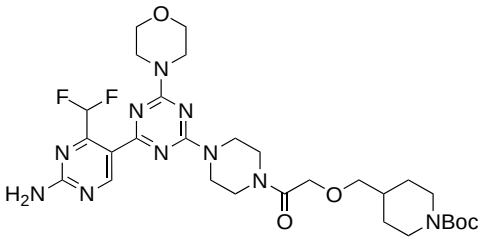

35

Compound **35** was prepared according to **GP1** from intermediate **15** (310 mg, 0.80 mmol, 1.0 equiv.) and **34** (234 mg, 0.14 mmol, 1.1 equiv.). Purification by column chromatography on silica gel (DCM / methanol / ammonia: 100:0:0 → 97:3:0.03) gave compound **35** as a light-yellow solid (89 mg, 0.48 mmol, 17%). **^{1}H NMR** (400 MHz, $CDCl_3$): *δ* 9.21 (s, 1 H), 7.59 (t, *J* = 54.4 Hz, 1 H), 5.96 (s, 2 H), 4.17 (s, 2 H), 4.14-4.02 (m, 2 H), 3.94-3.80 (m, 8 H), 3.78-3.71 (m, 4 H), 3.70-3.64 (m, 2 H), 3.63-3.56 (m, 2 H), 3.36 (d, *J* = 6.4 Hz, 2 H), 2.69 (t, *J* = 12.1 Hz, 2 H), 1.82-1.75 (m, 1 H), 1.74-1.65 (m, 2 H), 1.43 (s, 9 H), 1.15 (td, *J* = 12.2, 4.0 Hz, 2 H) ppm. **^{19}F{^{1}H} NMR** (376 MHz, $CDCl_3$): *δ* -121.65 (s, 2 F) ppm. **^{13}C{^{1}H} NMR** (101 MHz, $CDCl_3$): *δ* 181.89 (s, 1C), 168.13 (s, 1 C), 167.87 (s, 1 C), 164.61 (s, 1 C), 164.60 (s, 1 C), 163.50 (s, 1 C), 162.56 (s, 1 C), 154.91 (s, 1 C), 119.72 (s , 1 C), 109.69 (t, *J* = 241.3 Hz, 1 C), 79.45 (s, 1 C), 71.03 (s, 1 C), 66.80 (s, 2 C), 45.07 (s, 2 C), 43.89-42.94 (m, 4 C), 41.69 (m, 2 C), 36.56 (s, 2 C), 29.03 (s, 2 C), 28.53 (s, 3 C) ppm. **MALDI-MS**: *m/z* = 549.981 $[M - Boc + H]^+$.

4-((2-(4-(4-(2-amino-4-(difluoromethyl)pyrimidin-5-yl)-6-morpholino-1,3,5-triazin-2-yl)piperazin-1-yl)-2-oxoethoxy)methyl)piperidin-1-ium chloride (**36**)

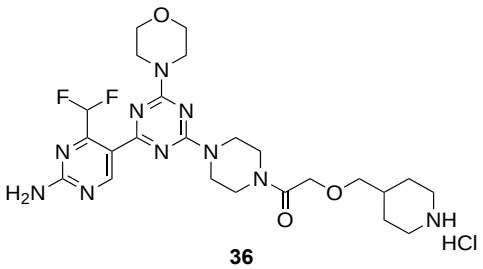

36

Compound **36** was prepared according to **GP2** from intermediate **35** (641 mg, 0.99 mmol, 1.0 equiv). Compound **36** was obtained as a colorless solid (653 mg, 1.12 mmol, quantitative yield). **^{1}H NMR** (400 MHz, DMSO-d_6): δ 9.11 (s, 1 H), 8.81 (br s, 1 H), 8.50 (br s, 1 H), 7.63 (t, J = 54.0 Hz, 1 H), 4.19 (s, 2 H), 3.87-3.72 (m, 8 H), 3.69-3.61 (m, 4 H), 3.54-3.45 (m, 4 H), 3.41 (t, J = 6.4 Hz, 1 H), 3.32 (d, J = 5.9 Hz, 2 H), 3.24 (d, J = 12.5 Hz, 2 H), 2.84 (q, J = 11.8 Hz, 2 H), 1.84-1.77 (m, 3 H), 1.45-1.32 (m, 2 H) ppm. **^{19}F{^{1}H} NMR** (376 MHz, DMSO-d_6): δ -120.62 (s, 2 F) ppm. **MALDI-MS**: m/z = 549.739 $[M + H]^+$.

tert-butyl (*S*)-4-((2-(4-(4-(2-amino-4-(difluoromethyl)pyrimidin-5-yl)-6-(3-methylmorpholino)-1,3,5-triazin-2-yl)piperazin-1-yl)-2-oxoethoxy)methyl)piperidine-1-carboxylate (**37**)

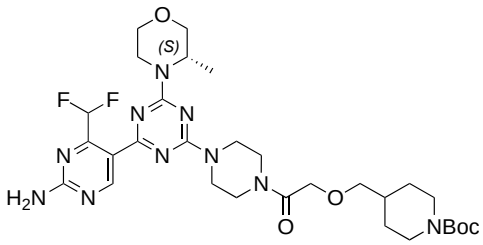

37

Compound **37** was prepared according to **GP1** from intermediate **16** (599 mg, 1.47 mmol, 1 equiv.) and **34** (444 mg, 1.62 mmol, 1 equiv.). Purification by column chromatography on silica gel (DCM / methanol / ammonia: 100:0:0 → 97:3:0.03) gave compound **37** as a colorless solid (413 mg, 0.62 mmol, 42%).**^{1}H NMR** (400 MHz, $CDCl_3$): δ 9.24 (s, 1 H), 7.61 (t, J = 54.4 Hz, 1 H), 5.58 (s, 2 H), 4.74 (s, 1 H), 4.40 (d, J = 13.6 Hz, 1 H), 4.18 (br s, 2 H), 4.12 (br s, 1 H), 3.99 (dd, J = 11.5, 3.7 Hz, 1 H), 3.94-3.76 (m, 5 H), 3.68 (dd, J = 11.3, 3.4 Hz, 3 H), 3.64-3.47 (m, 4 H), 3.37 (d, J = 6.3 Hz, 2 H), 3.29 (t, J = 12.8 Hz, 1 H), 2.70 (t, J = 13.0 Hz, 2 H), 1.84-1.75 (m, 1 H), 1.71 (d, J = 13.4 Hz, 2 H), 1.45 (s, 9 H), 1.33 (d, J = 6.8 Hz, 3 H), 1.16 (qd, J = 12.5, 4.2 Hz, 2 H) ppm. **^{19}F{^{1}H} NMR** (376 MHz, $CDCl_3$): δ -121.74 (s, 2 F) ppm. **^{13}C{^{1}H} NMR** (101 MHz, $CDCl_3$): δ 168.27 (s, 1 C), 167.98 (s, 1 C), 164.78 (s, 1 C), 164.41 (s, 1 C), 163.61 (s, 1 C), 162.73 (s, 1 C), 160.32-159.34 (m, 1 C), 155.05 (s, 1 C), 119.92 (s, 1 C), 109.74 (t, J = 241.0 Hz, 1 C), 79.59 (s, 1 C), 76.41 (s, 1 C), 71.20 (s, 2 C), 67.14 (s, 1 C), 46.75 (s, 1 C), 45.20 (s, 1 C), 43.68 (s, 3 C), 41.83 (s, 1 C), 38.86 (s, 1 C), 36.70 (s, 1 C),

29.91 (s, 1 C), 29.17 (s, 2 C), 28.67 (s, 3 C), 14.56 (s, 1 C) ppm. **MALDI-MS**: *m/z* = 663.613 $[M + H]^+$.

(*S*)-4-((2-(4-(4-(2-amino-4-(difluoromethyl)pyrimidin-5-yl)-6-(3-methylmorpholino)-1,3,5-triazin-2-yl)piperazin-1-yl)-2-oxoethoxy)methyl)piperidin-1-ium chloride (**38**)

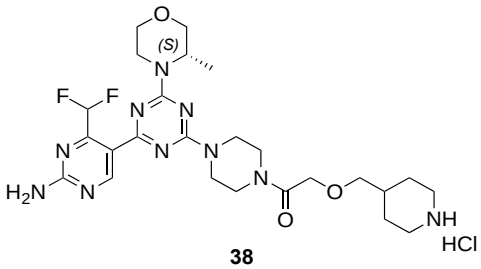

38

Compound **38** was prepared according to **GP2** from intermediate **37** (373 mg, 0.56 mmol, 1.0 equiv). Compound **38** was obtained as a light-yellow solid (404 mg, 0.67 mmol, quantitative yield). **^{1}H NMR** (400 MHz, DMSO-d_6): δ 9.11 (s, 1 H), 8.91 (s, 1 H), 8.60 (s, 1 H), 7.64 (t, *J* = 54.1 Hz, 1 H), 4.33 (d, *J* = 13.6 Hz, 1 H), 4.18 (s, 2 H), 3.97-3.89 (m, 1 H), 3.87-3.69 (m, 5 H), 3.65 (td, *J* = 6.7, 6.3, 5.2 Hz, 1 H), 3.53 (d, *J* = 9.6 Hz, 4 H), 3.41 (t, *J* = 6.4 Hz, 1 H), 3.32 (d, *J* = 6.0 Hz, 2 H), 3.26-3.14 (m, 3 H), 2.83 (q, *J* = 11.9 Hz, 2 H), 1.88-1.72 (m, 4 H), 1.39 (q, *J* = 11.9, 11.4 Hz, 2 H), 1.23 (d, *J* = 6.8 Hz, 3 H) ppm.**^{19}F{^{1}H} NMR** (376 MHz, DMSO-d*6*): δ -120.65 (s, 2 F) ppm. **MALDI-MS**: *m/z* = 563.709 $[M + H]^+$.

tert-Butyl *N*-[5-bromo-4-(difluoromethyl)pyrimidin-2-yl]-*N*-[(*tert*-butoxy)carbonyl]carbamate (**39**).

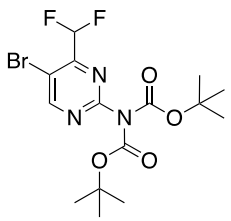

39

Compound **39** was prepared according to the literature.[16]

References

(1) Borsari, C., Keles, E., McPhail, J. A., Schaefer, A., Sriramaratnam, R., Goch, W., Schaefer, T., De Pascale, M., Bal, W., Gstaiger, M., Burke, J. E., Wymann, M. P. Covalent Proximity Scanning of a Distal Cysteine to Target PI3Kα. *J Am Chem Soc* **2022**, *144*, 6326-6342. https://DOI.org/10.1021/jacs.1c13568

(2) Borsari, C., Rageot, D., Beaufils, F., Bohnacker, T., Keles, E., Buslov, I., Melone, A., Sele, A. M., Hebeisen, P., Fabbro, D., Hillmann, P., Wymann, M. P. Preclinical Development of PQR514, a Highly Potent PI3K Inhibitor Bearing a Difluoromethyl-Pyrimidine Moiety. *ACS Med Chem Lett* **2019**, *10*, 1473-1479. https://DOI.org/10.1021/acsmedchemlett.9b00333

(3) Beaufils, F., Cmiljanovic, N., Cmiljanovic, V., Bohnacker, T., Melone, A., Marone, R., Jackson, E., Zhang, X., Sele, A., Borsari, C., Mestan, J., Hebeisen, P., Hillmann, P., Giese, B., Zvelebil, M., Fabbro, D., Williams, R. L., Rageot, D., Wymann, M. P. 5-(4,6-Dimorpholino-1,3,5-triazin-2-yl)-4-(trifluoromethyl)pyridin-2-amine (PQR309), a Potent, Brain-Penetrant, Orally Bioavailable, Pan-Class I PI3K/mTOR Inhibitor as Clinical Candidate in Oncology. *J Med Chem* **2017**, *60*, 7524-7538. https://DOI.org/10.1021/acs.jmedchem.7b00930

(4) Rossi Sebastiano, M., Doak, B. C., Backlund, M., Poongavanam, V., Over, B., Ermondi, G., Caron, G., Matsson, P., Kihlberg, J. Impact of Dynamically Exposed Polarity on Permeability and Solubility of Chameleonic Drugs Beyond the Rule of 5. *Journal of Medicinal Chemistry* **2018**, *61*, 4189-4202. https://DOI.org/10.1021/acs.jmedchem.8b00347

(5) Johnson, K. A. Fitting enzyme kinetic data with KinTek Global Kinetic Explorer. *Methods Enzymol* **2009**, *467*, 601-626. https://DOI.org/10.1016/S0076-6879(09)67023-3

(6) Johnson, K. A., Simpson, Z. B., Blom, T. Global kinetic explorer: a new computer program for dynamic simulation and fitting of kinetic data. *Anal Biochem* **2009**, *387*, 20-29. https://DOI.org/10.1016/j.ab.2008.12.024

(7) Montero, D., Tachibana, C., Rahr Winther, J., Appenzeller-Herzog, C. Intracellular glutathione pools are heterogeneously concentrated. *Redox Biol* **2013**, *1*, 508-513. https://DOI.org/10.1016/j.redox.2013.10.005

(8) Geremia, S., Campagnolo, M., Demitri, N., Johnson, L. N. Simulation of diffusion time of small molecules in protein crystals. *Structure* **2006**, *14*, 393-400. https://DOI.org/10.1016/j.str.2005.12.007

(9) Zhao, W., Tian, Y., Cai, M., Wang, F., Wu, J., Gao, J., Liu, S., Jiang, J., Jiang, S., Wang, H. Studying the nucleated mammalian cell membrane by single molecule approaches. *PLoS One* **2014**, *9*, e91595. https://DOI.org/10.1371/journal.pone.0091595

(10) Shen, T., Shirinzadeh, B., Zhong, Y., Smith, J., Pinskier, J., Ghafarian, M. Sensing and Modelling Mechanical Response in Large Deformation Indentation of Adherent Cell Using Atomic Force Microscopy. *Sensors (Basel)* **2020**, *20*, 1764. https://DOI.org/10.3390/s20061764

(11) Gross, S. M., Rotwein, P. Akt signaling dynamics in individual cells. *J Cell Sci* **2015**, *128*, 2509-2519. https://DOI.org/10.1242/jcs.168773

(12) McQuin, C., Goodman, A., Chernyshev, V., Kamentsky, L., Cimini, B. A., Karhohs, K. W., Doan, M., Ding, L., Rafelski, S. M., Thirstrup, D., Wiegraebe, W., Singh, S., Becker, T., Caicedo, J. C.,

Carpenter, A. E. CellProfiler 3.0: Next-generation image processing for biology. *PLoS Biol* **2018**, *16*, e2005970. https://DOI.org/10.1371/journal.pbio.2005970

(13) Hafner, M., Niepel, M., Chung, M., Sorger, P. K. Growth rate inhibition metrics correct for confounders in measuring sensitivity to cancer drugs. *Nat Methods* **2016**, *13*, 521-527. https://DOI.org/10.1038/nmeth.3853

(14) Klippel, A., Escobedo, J. A., Hirano, M., Williams, L. T. The interaction of small domains between the subunits of phosphatidylinositol 3-kinase determines enzyme activity. *Mol Cell Biol* **1994**, *14*, 2675-2685. https://DOI.org/10.1128/mcb.14.4.2675

(15) Bohnacker, T., Prota, A. E., Beaufils, F., Burke, J. E., Melone, A., Inglis, A. J., Rageot, D., Sele, A. M., Cmiljanovic, V., Cmiljanovic, N., Bargsten, K., Aher, A., Akhmanova, A., Díaz, J. F., Fabbro, D., Zvelebil, M., Williams, R. L., Steinmetz, M. O., Wymann, M. P. Deconvolution of Buparlisib's mechanism of action defines specific PI3K and tubulin inhibitors for therapeutic intervention. *Nat Commun* **2017**, *8*, 14683. https://DOI.org/10.1038/ncomms14683

(16) Rageot, D., Bohnacker, T., Keles, E., McPhail, J. A., Hoffmann, R. M., Melone, A., Borsari, C., Sriramaratnam, R., Sele, A. M., Beaufils, F., Hebeisen, P., Fabbro, D., Hillmann, P., Burke, J. E., Wymann, M. P. (S)-4-(Difluoromethyl)-5-(4-(3-methylmorpholino)-6-morpholino-1,3,5-triazin-2-yl)pyridin-2-amine (PQR530), a Potent, Orally Bioavailable, and Brain-Penetrable Dual Inhibitor of Class I PI3K and mTOR Kinase. *J Med Chem* **2019**, *62*, 6241-6261. https://DOI.org/10.1021/acs.jmedchem.9b00525

Synthetic Schemes and Spectroscopic/Analytic Data, Table of Contents

Spectra by Type

Figures of Spectra

^{1}H-NMR spectra

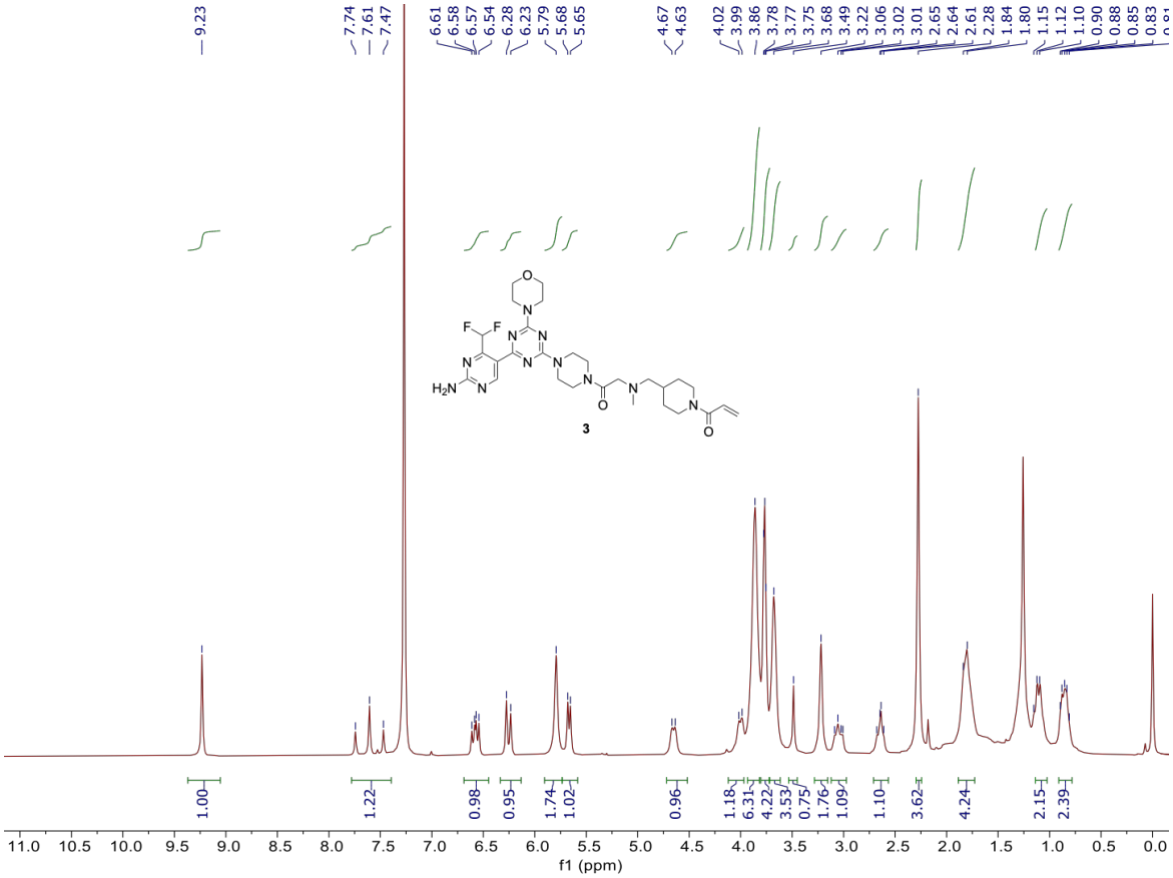

Figure S12. ^{1}H-NMR of compound **3** (400 MHz) in $CDCl_3$.

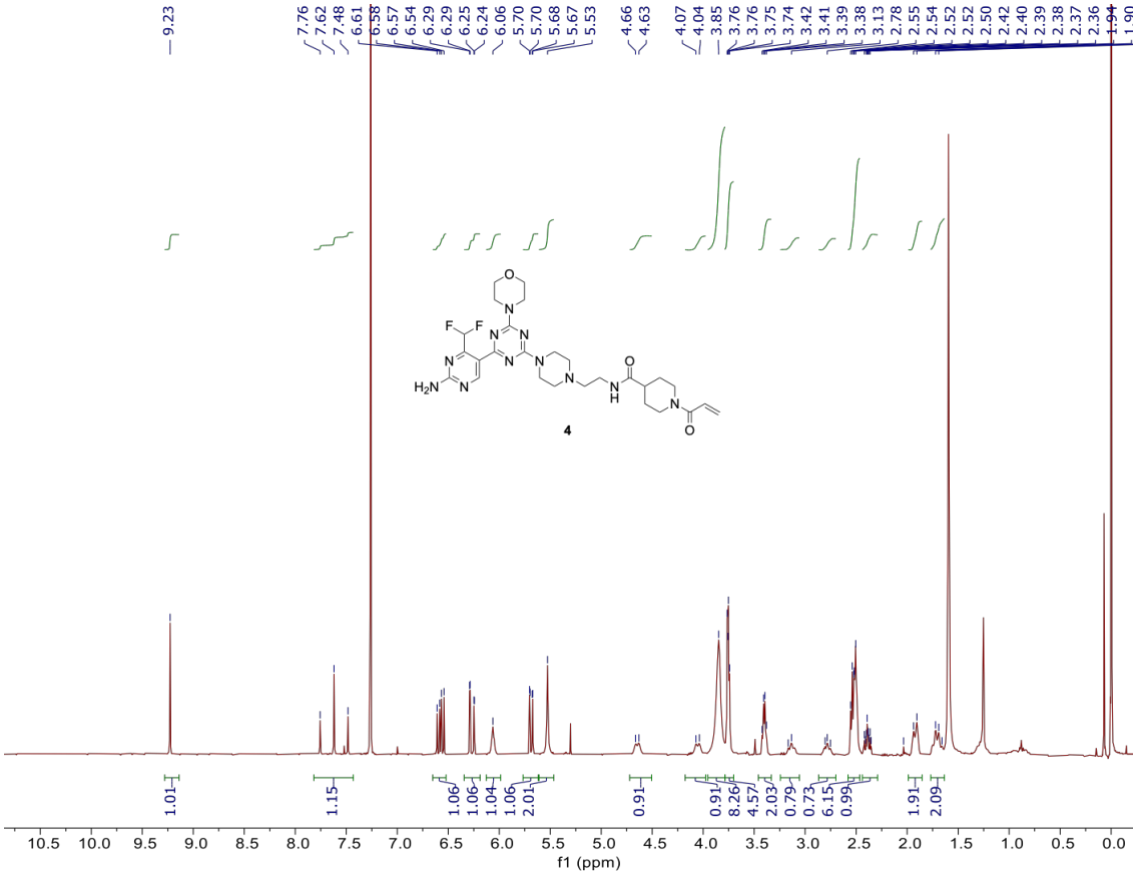

Figure S13. ^{1}H-NMR of compound **4** (400 MHz) in $CDCl_3$.

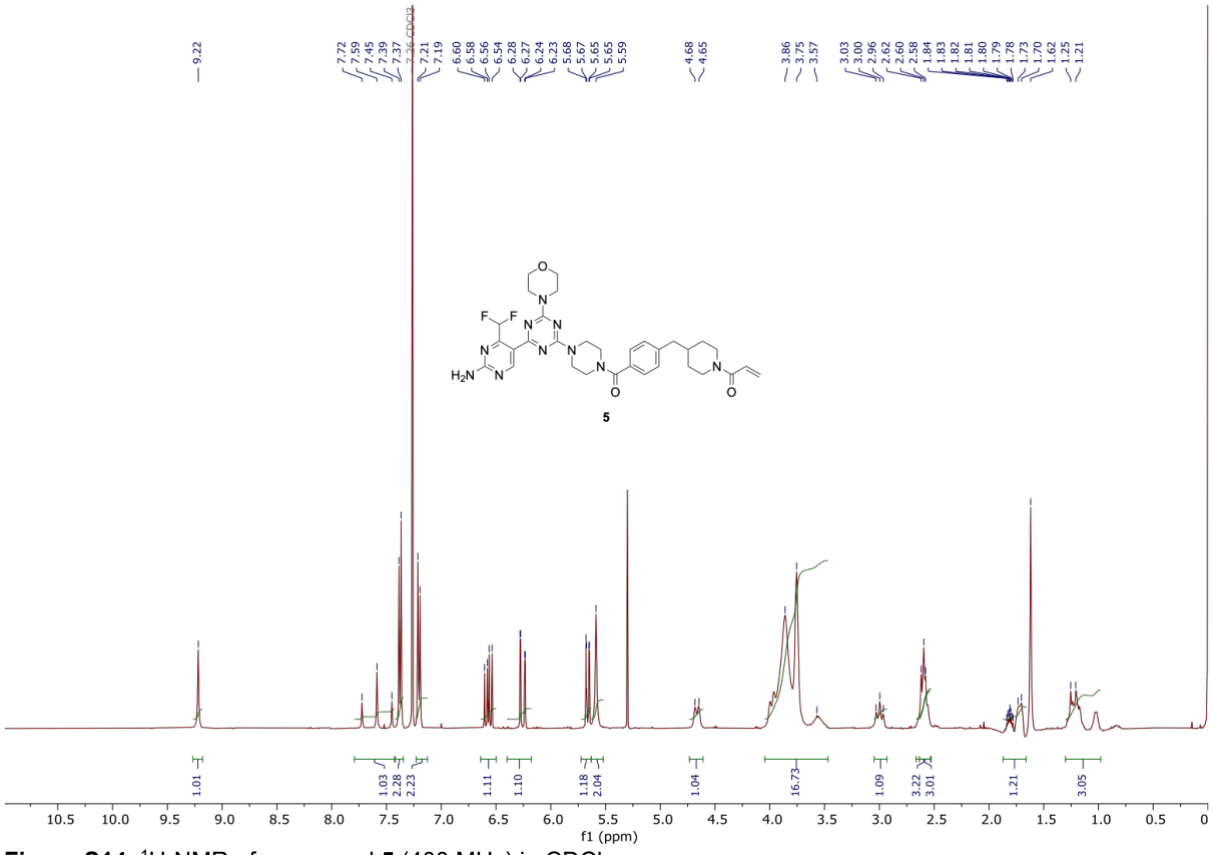

Figure S14. ^{1}H-NMR of compound **5** (400 MHz) in $CDCl_3$.

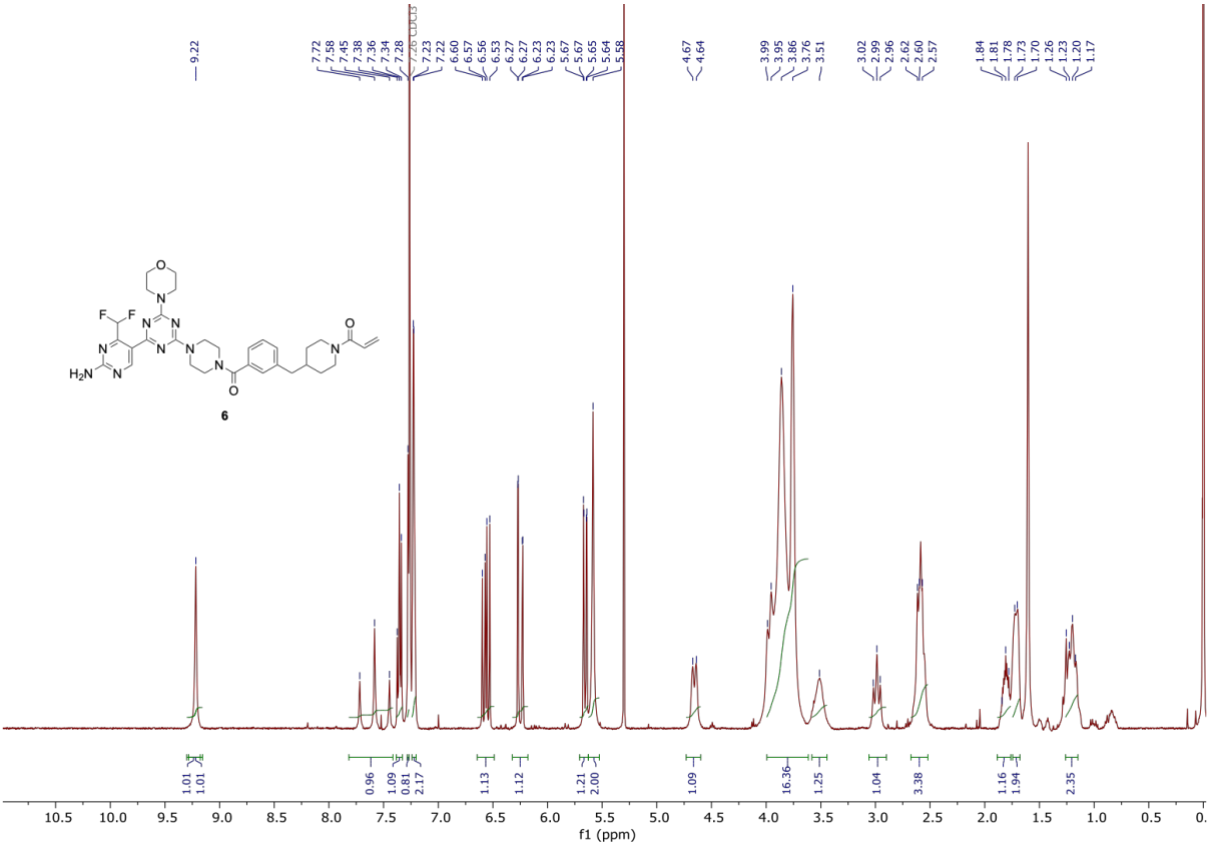

6

Figure S15. ^{1}H-NMR of compound **6** (400 MHz) in $CDCl_3$.

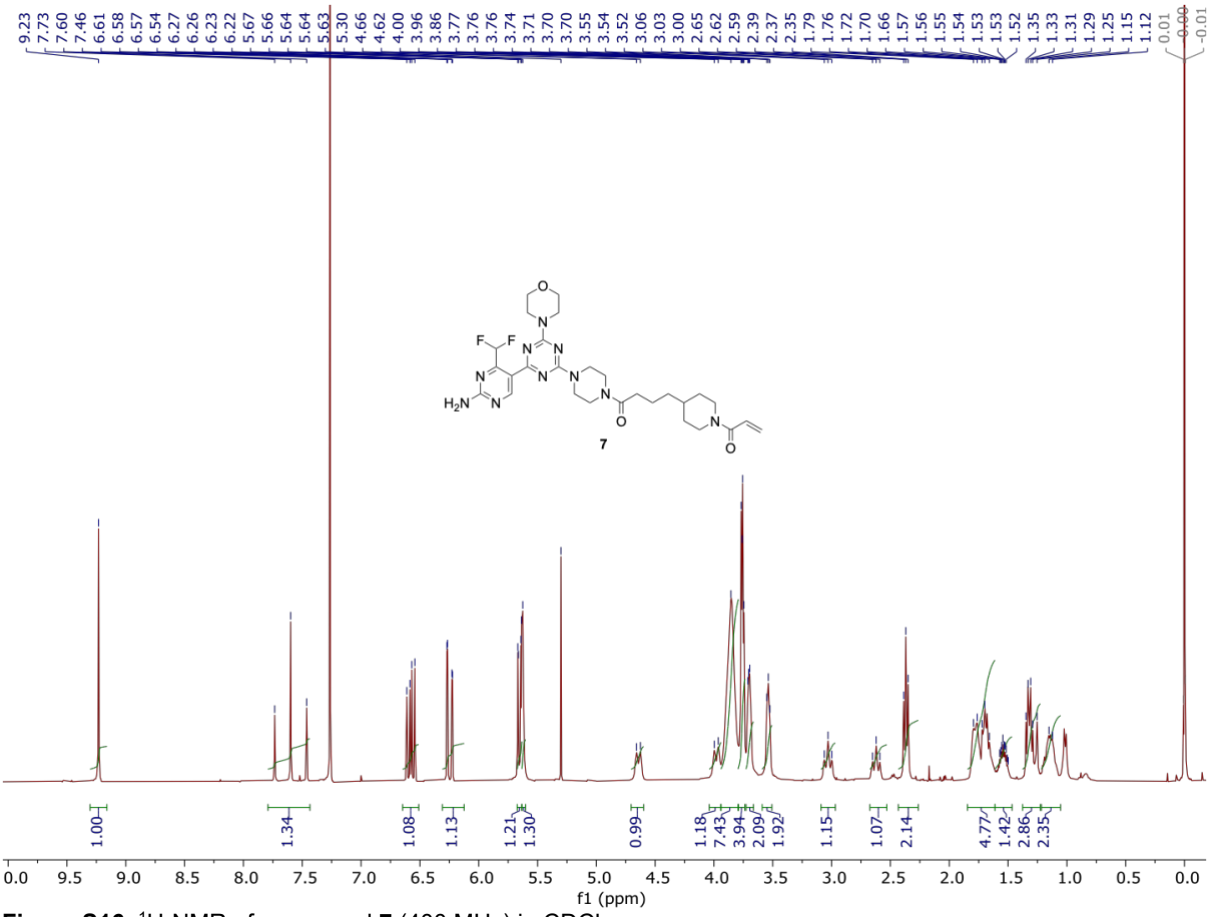

Figure S16. ^{1}H-NMR of compound **7** (400 MHz) in $CDCl_3$.

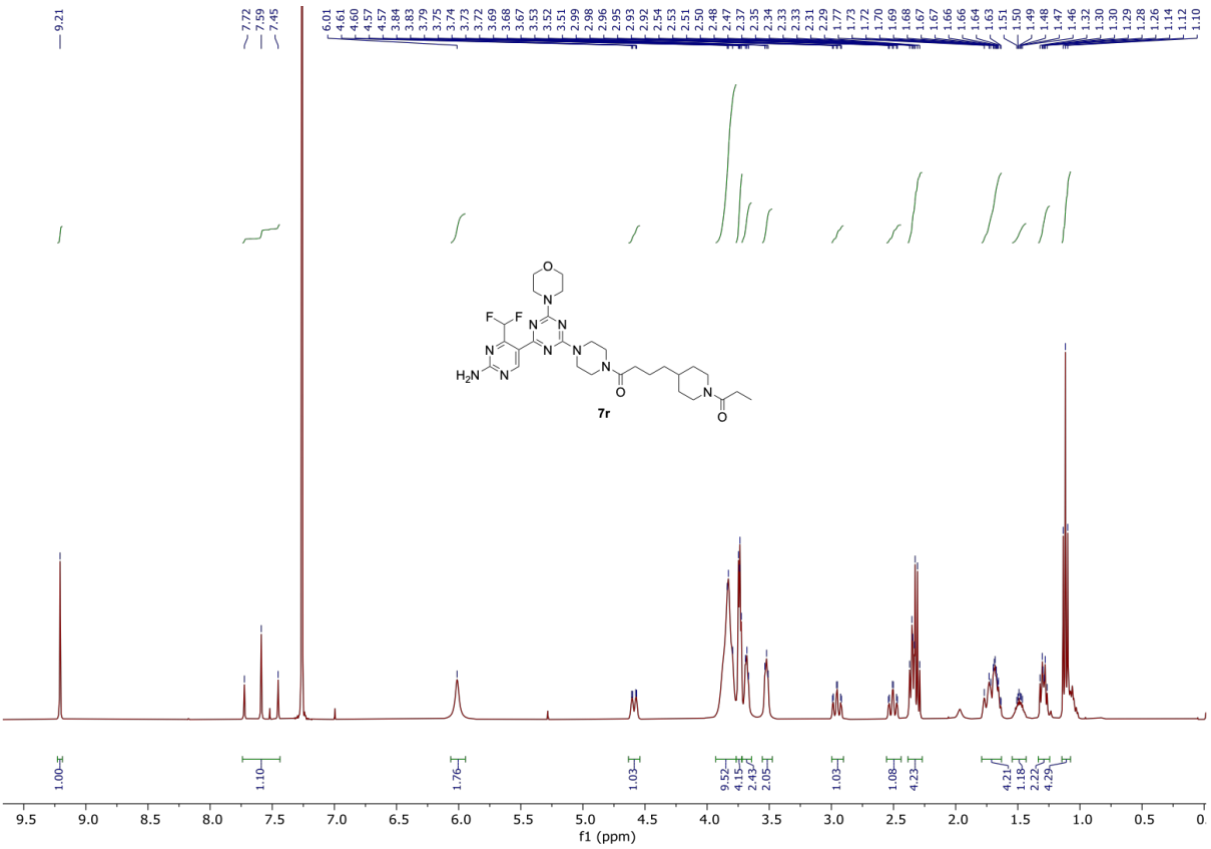

Figure S17. ^{1}H-NMR of compound **7r** (400 MHz) in $CDCl_3$.

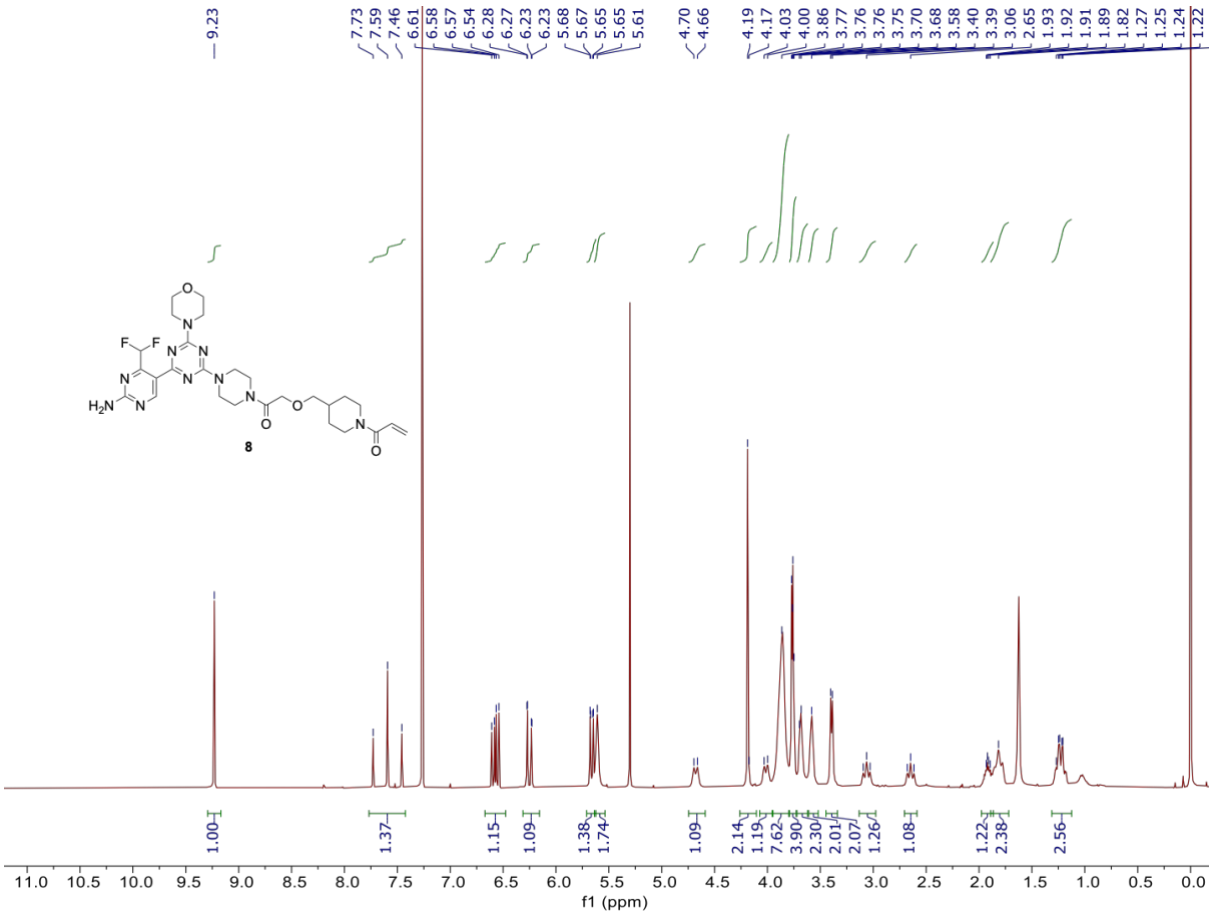

Figure S18. ^{1}H-NMR of compound **8** (400 MHz) in $CDCl_3$.

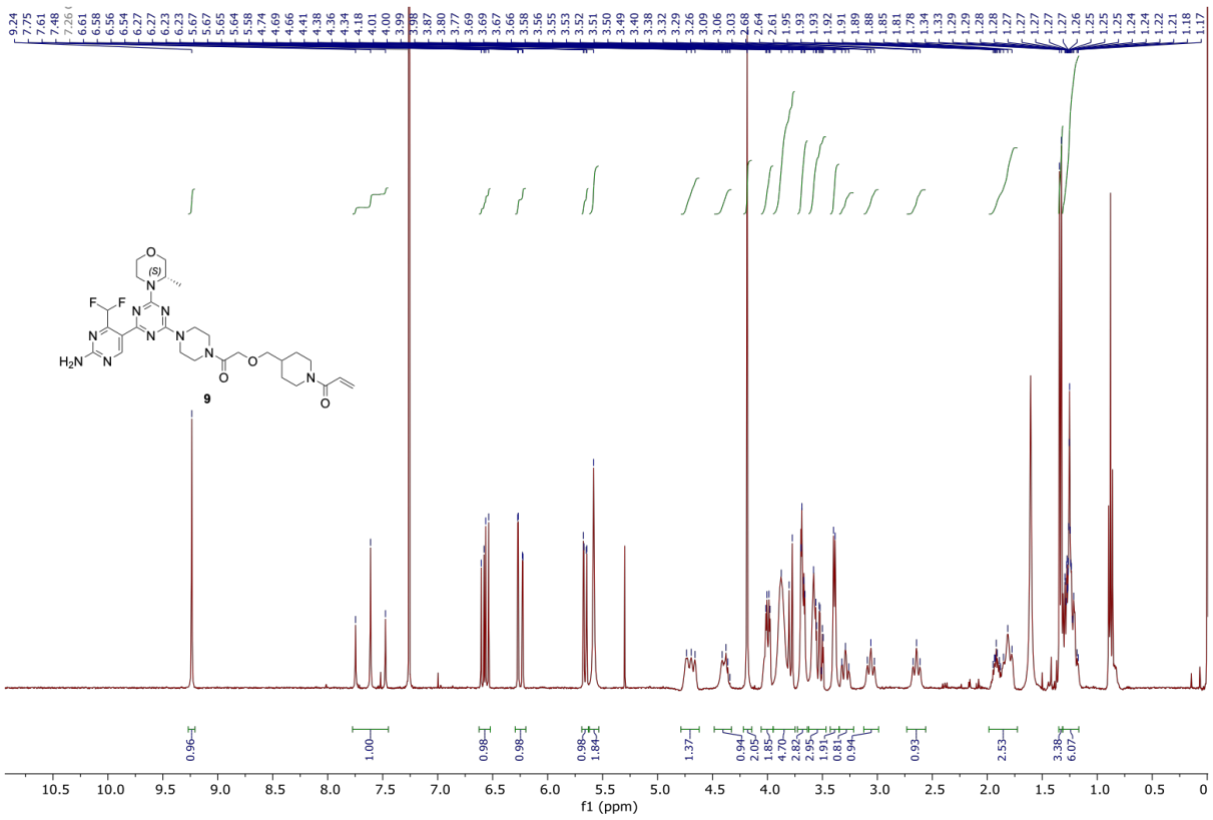

Figure S19. ^{1}H-NMR of compound **9** (400 MHz) in $CDCl_3$.

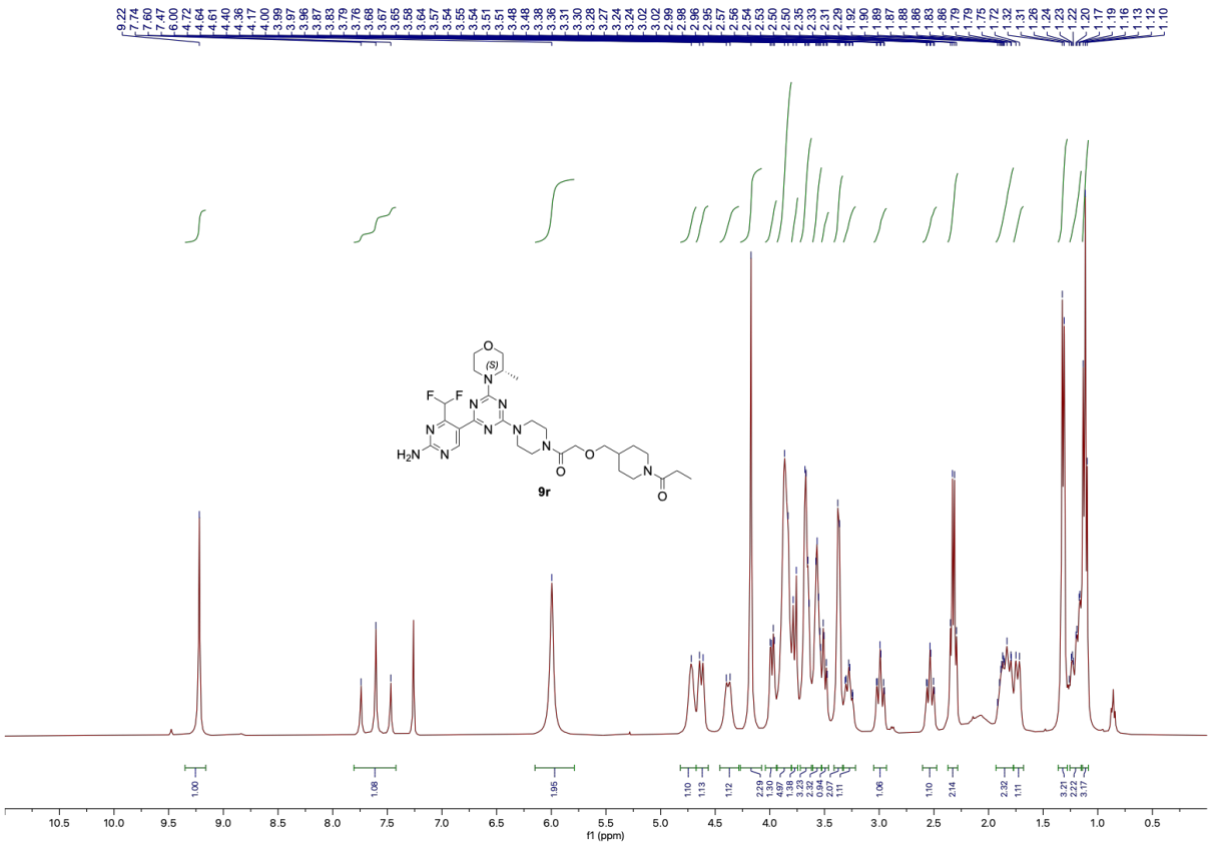

Figure S20. ^{1}H-NMR of compound **9r** (400 MHz) in $CDCl_3$.

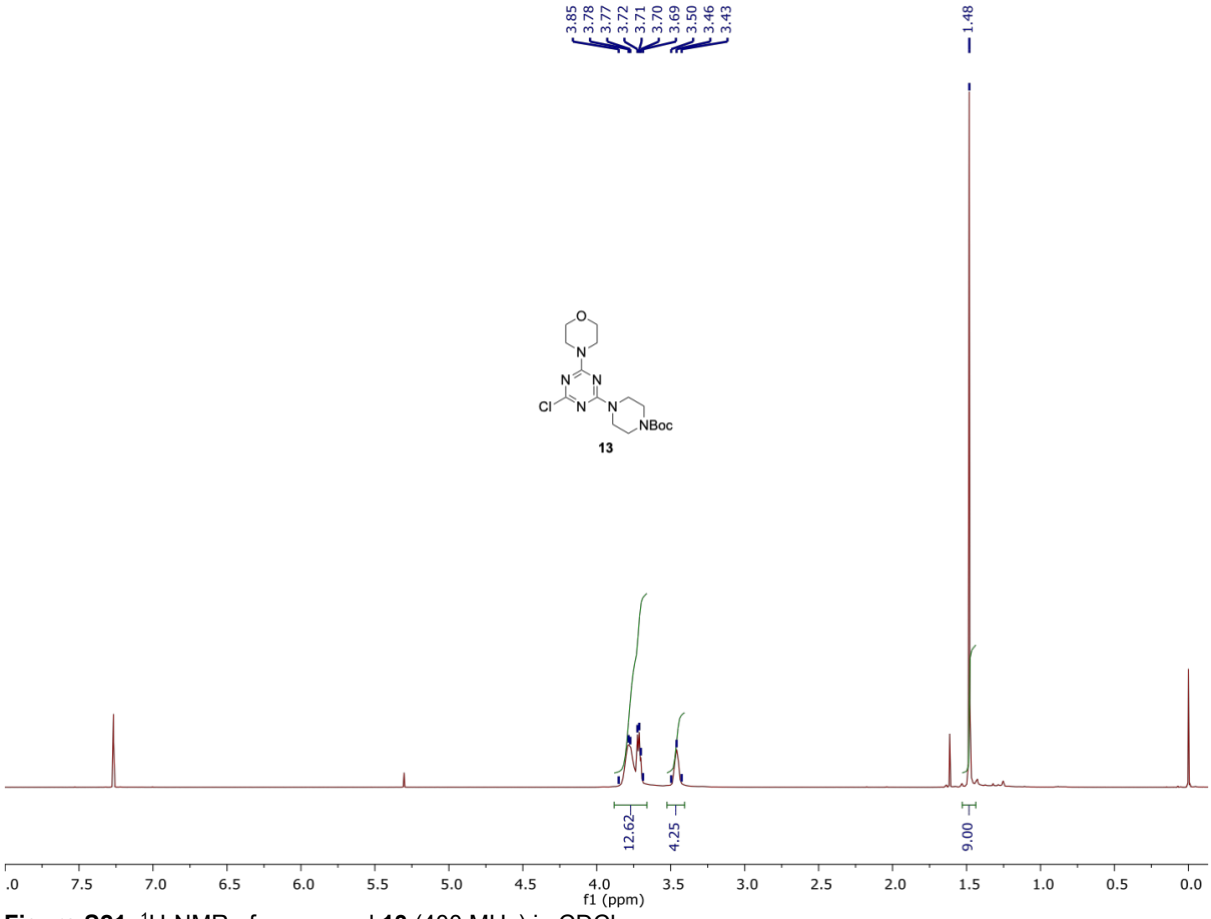

Figure S21. ^{1}H-NMR of compound **13** (400 MHz) in $CDCl_3$.

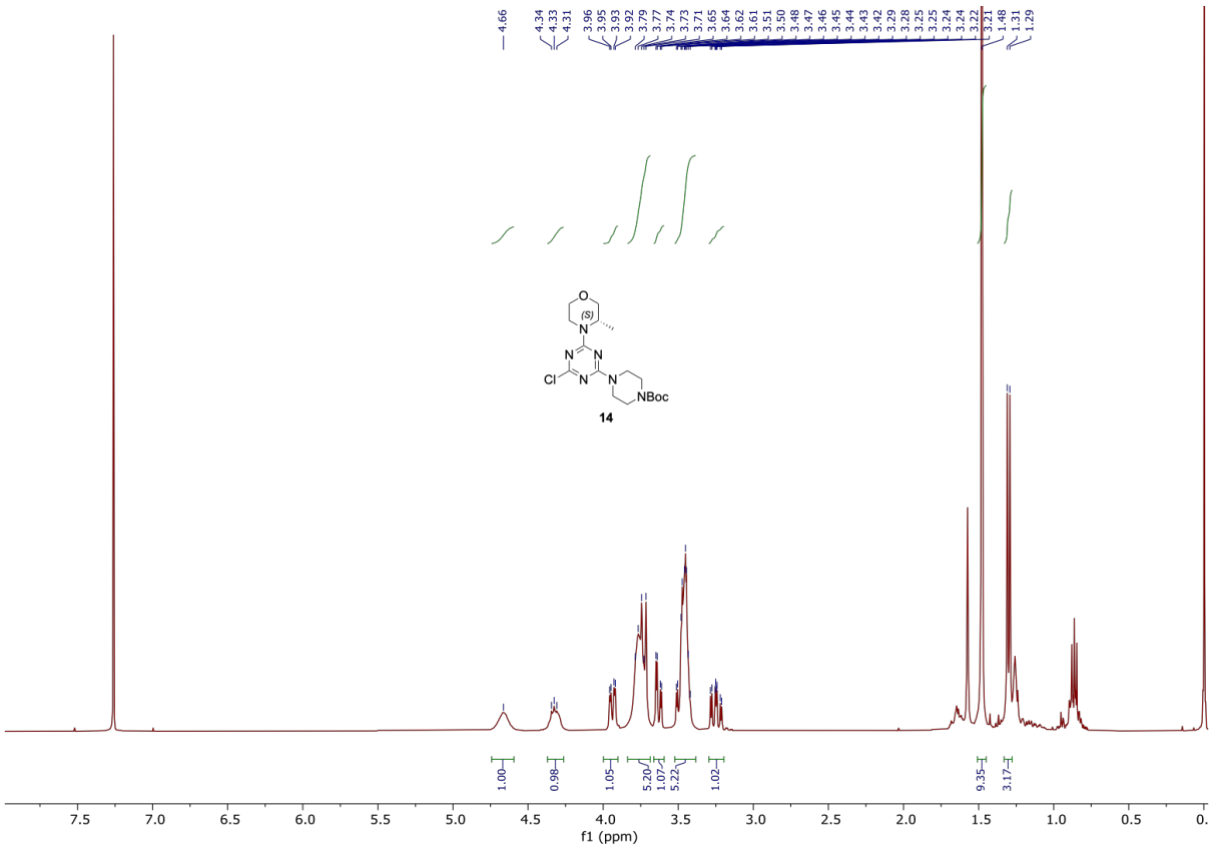

Figure S22. ^{1}H-NMR of compound **14** (400 MHz) in $CDCl_3$.

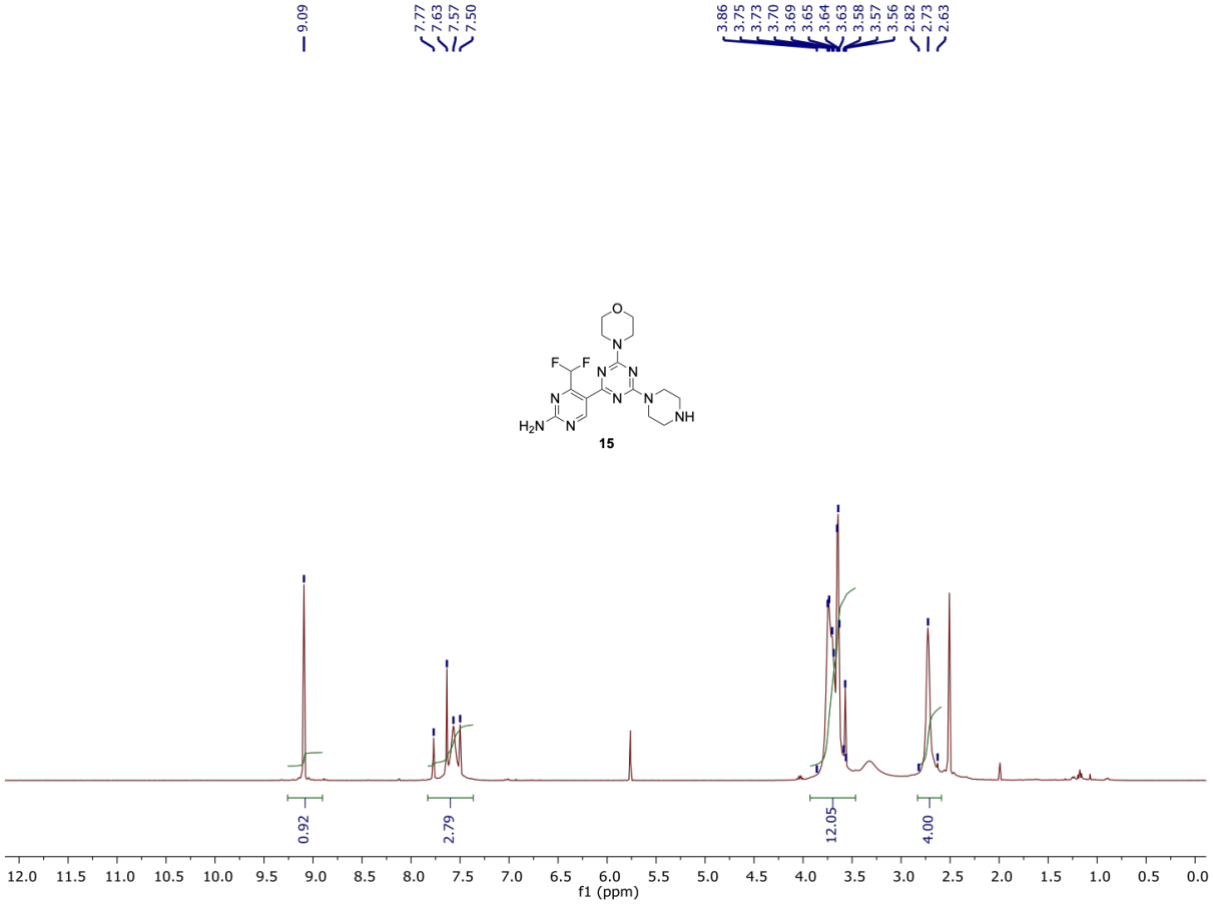

Figure S23. ^{1}H-NMR of compound **15** (400 MHz) in DMSO-d_6.

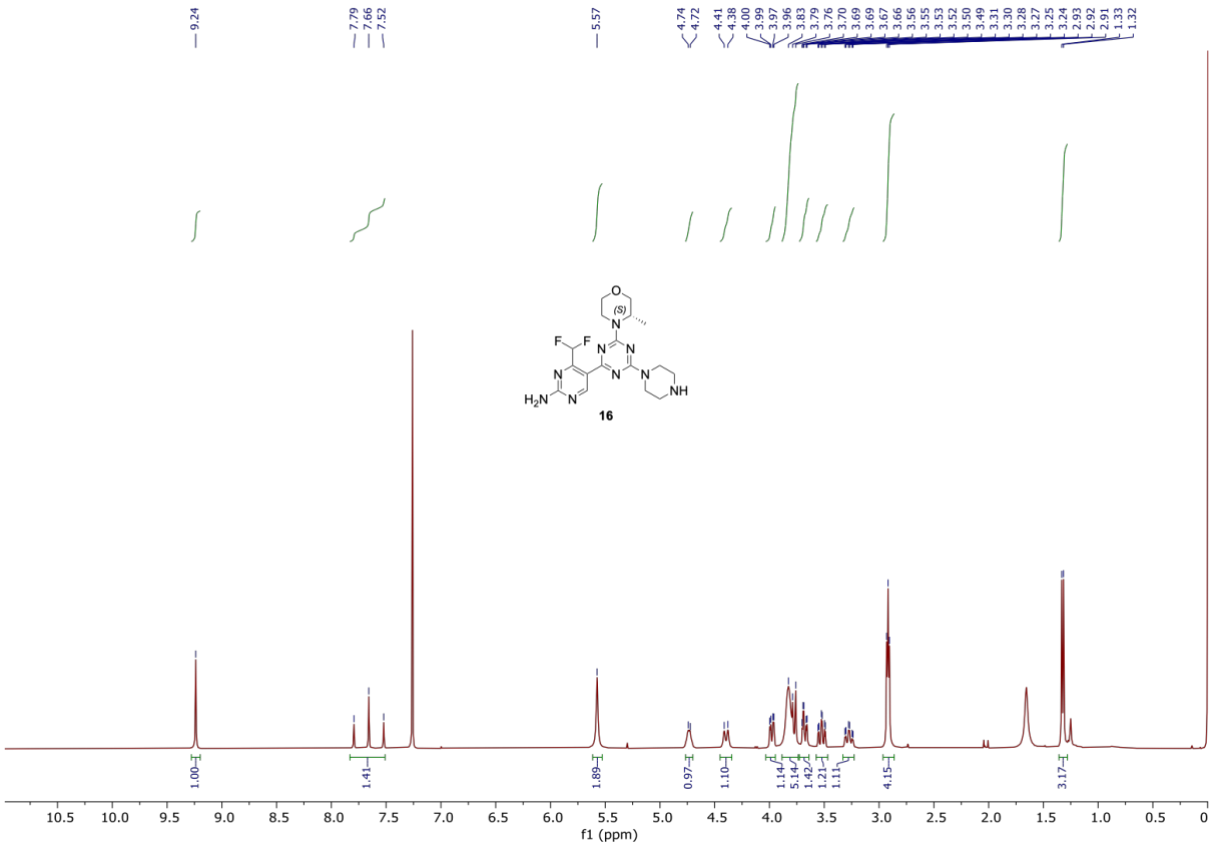

Figure S24. ^{1}H-NMR of compound **16** (400 MHz) in $CDCl_3$.

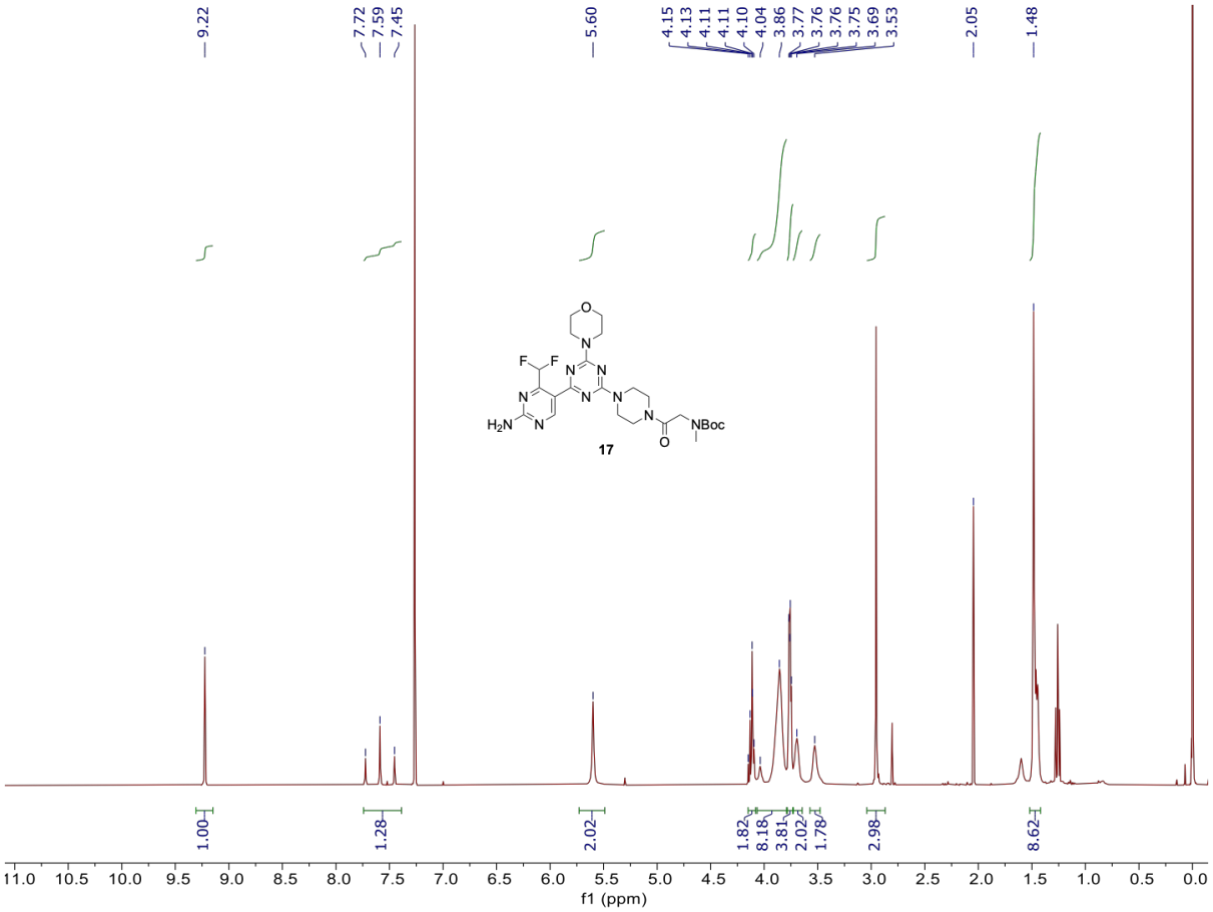

Figure S25. ^{1}H-NMR of compound **17** (400 MHz) in $CDCl_3$.

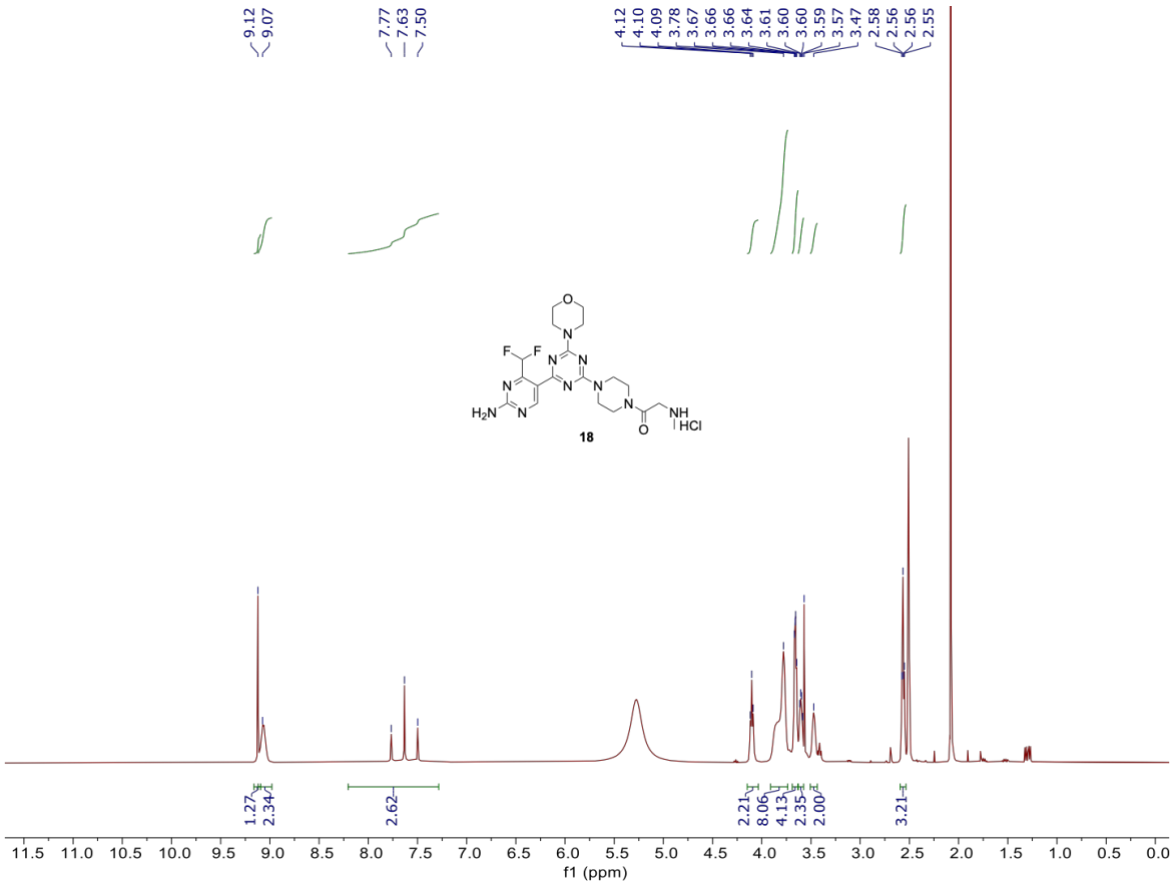

Figure S26. ^{1}H-NMR of compound **18** (400 MHz) in DMSO-d_6.

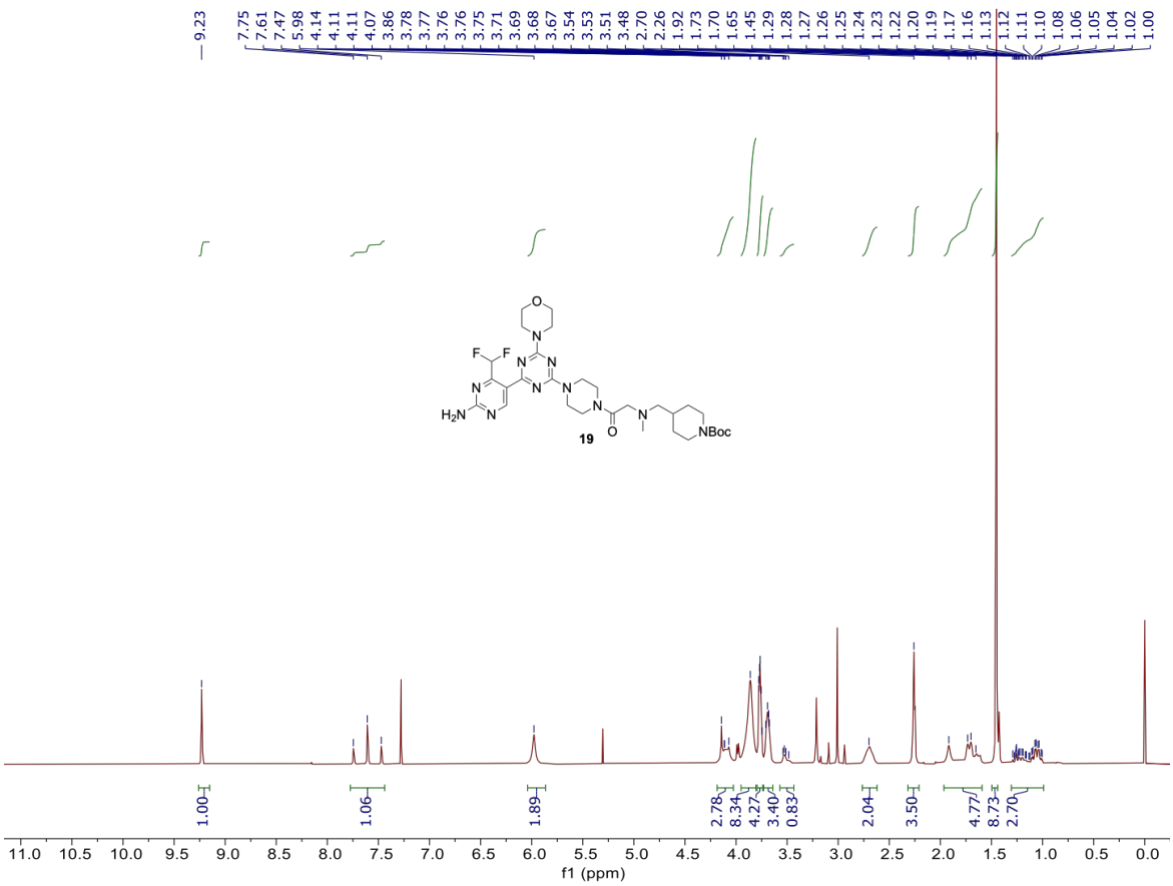

Figure S27. ^{1}H-NMR of compound **19** (400 MHz) in $CDCl_3$.

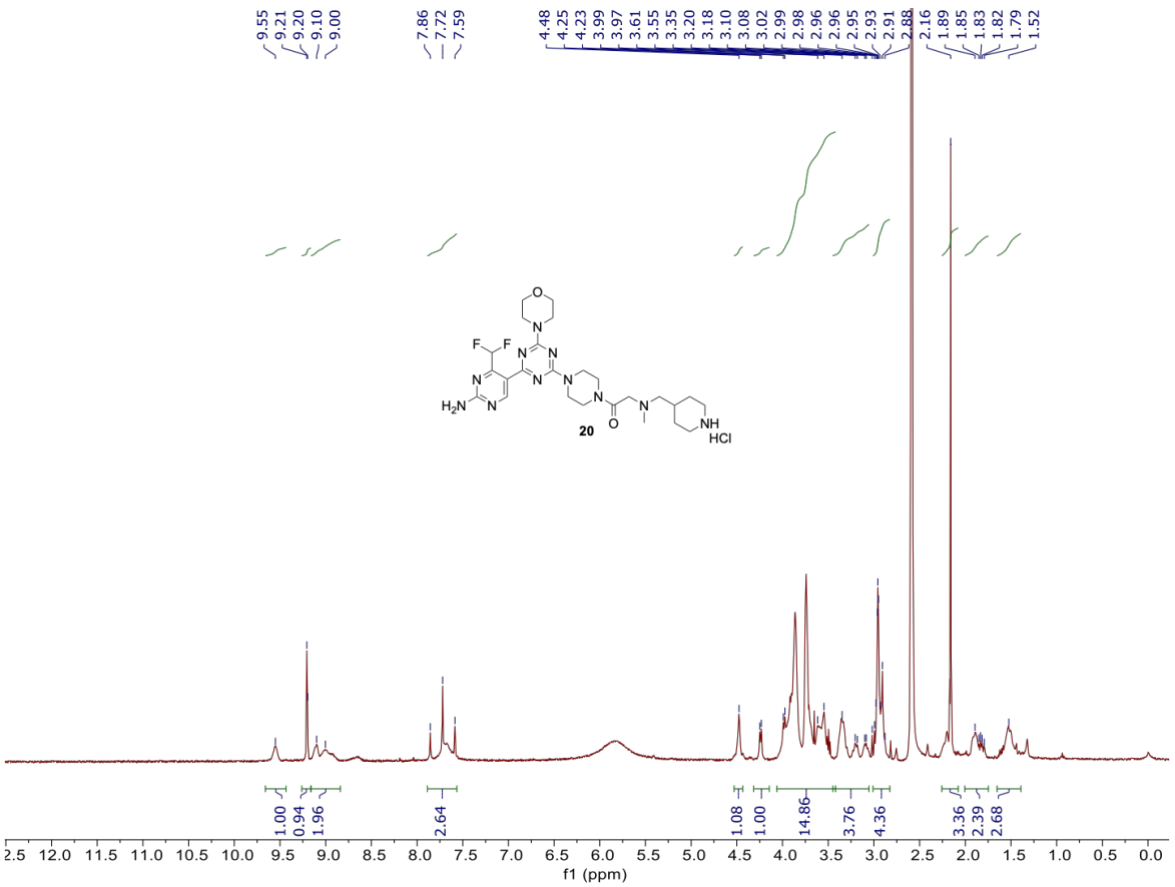

Figure S28. ^{1}H-NMR of compound **20** (400 MHz) in DMSO-d_6.

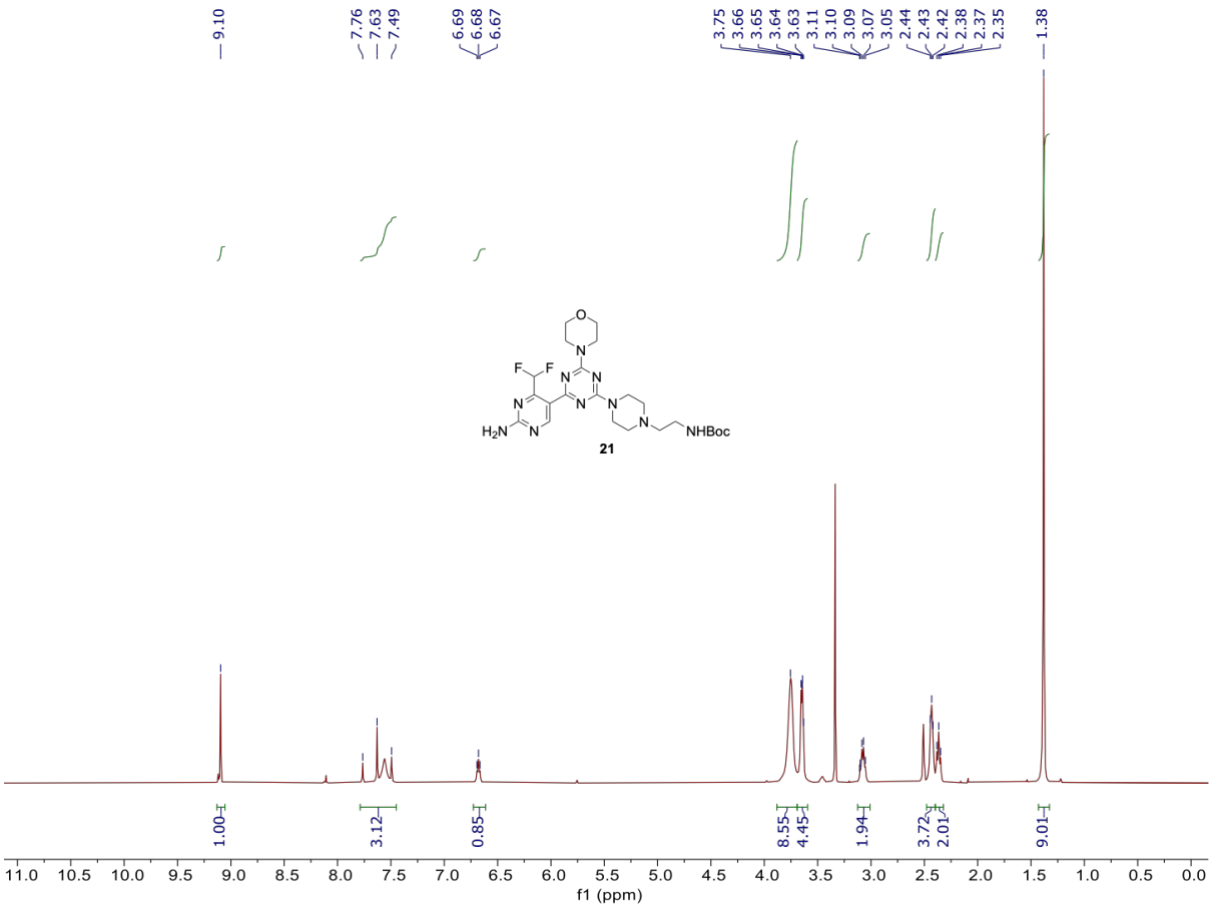

Figure S29. ^{1}H-NMR of compound **21** (400 MHz) in DMSO-d_6.

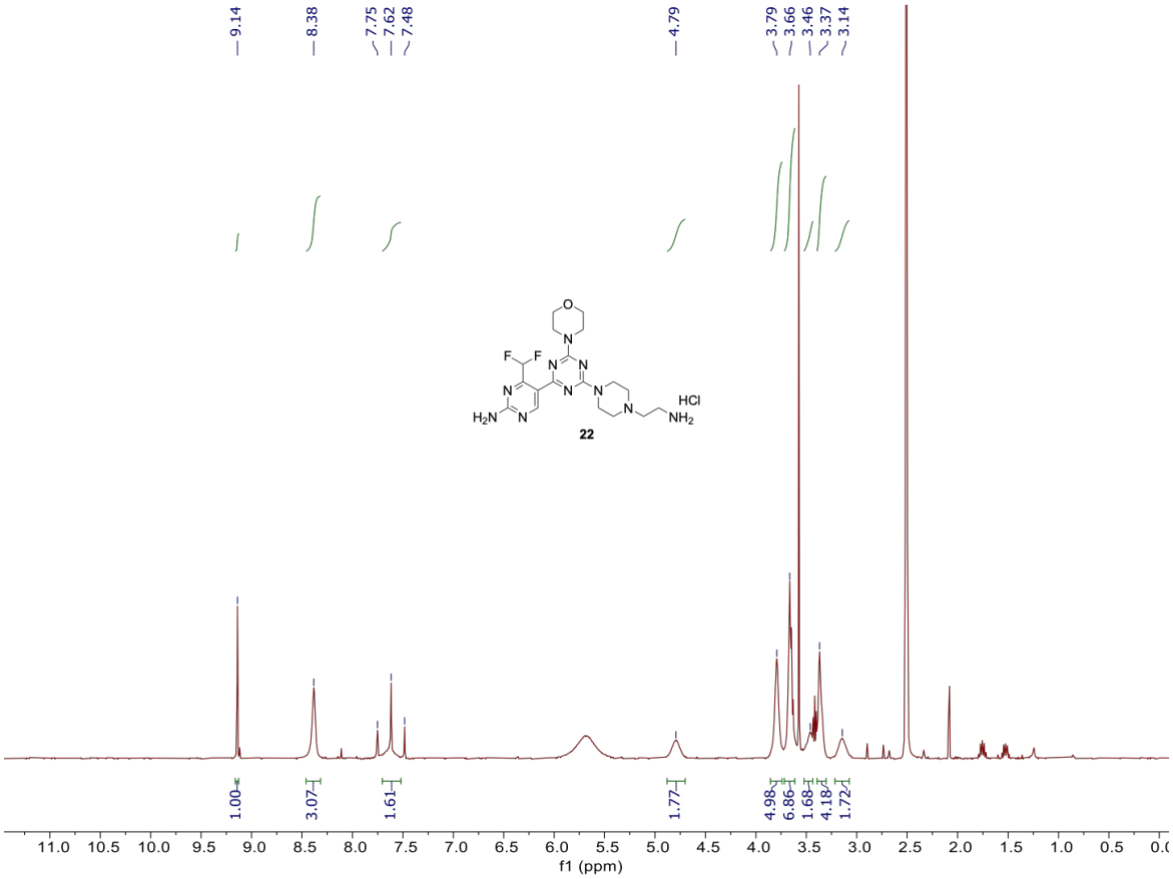

Figure S30. ^{1}H-NMR of compound **22** (400 MHz) in DMSO-d_6.

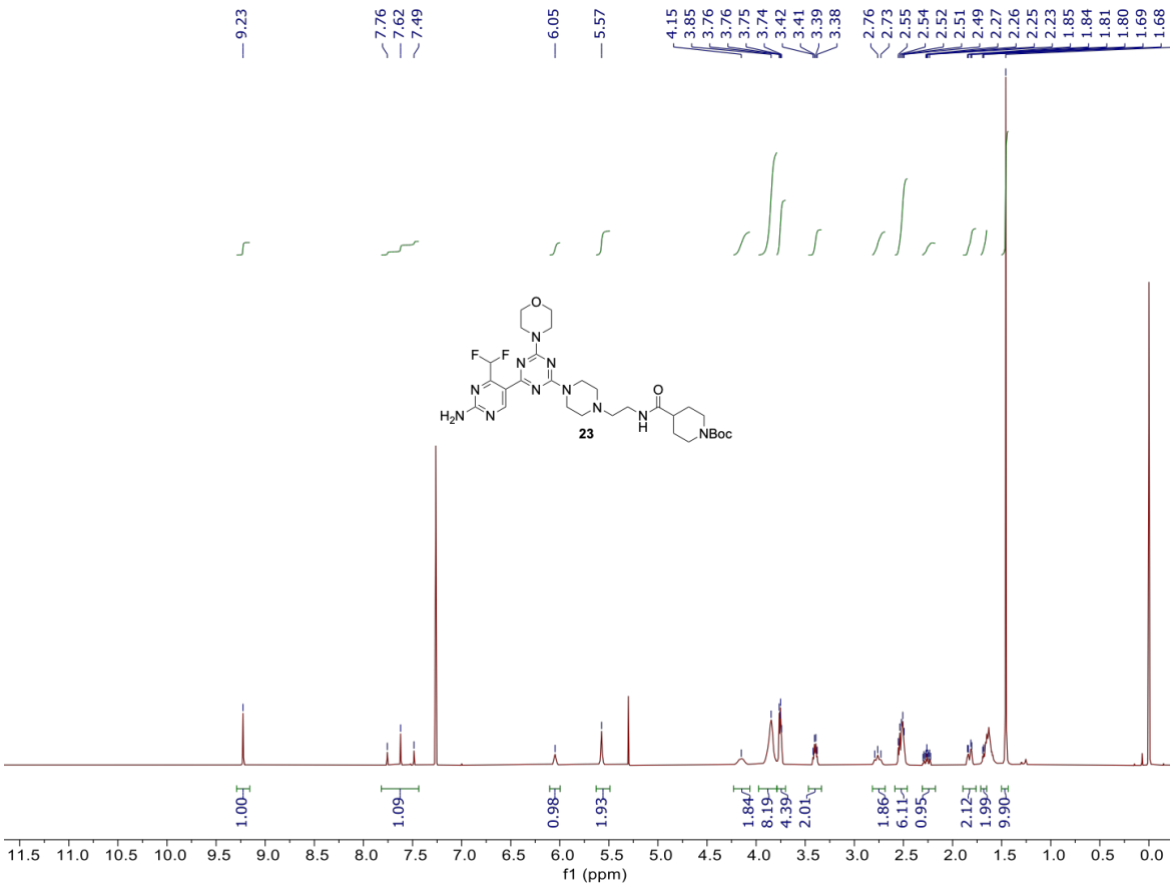

Figure S31. ^{1}H-NMR of compound **23** (400 MHz) in $CDCl_3$.

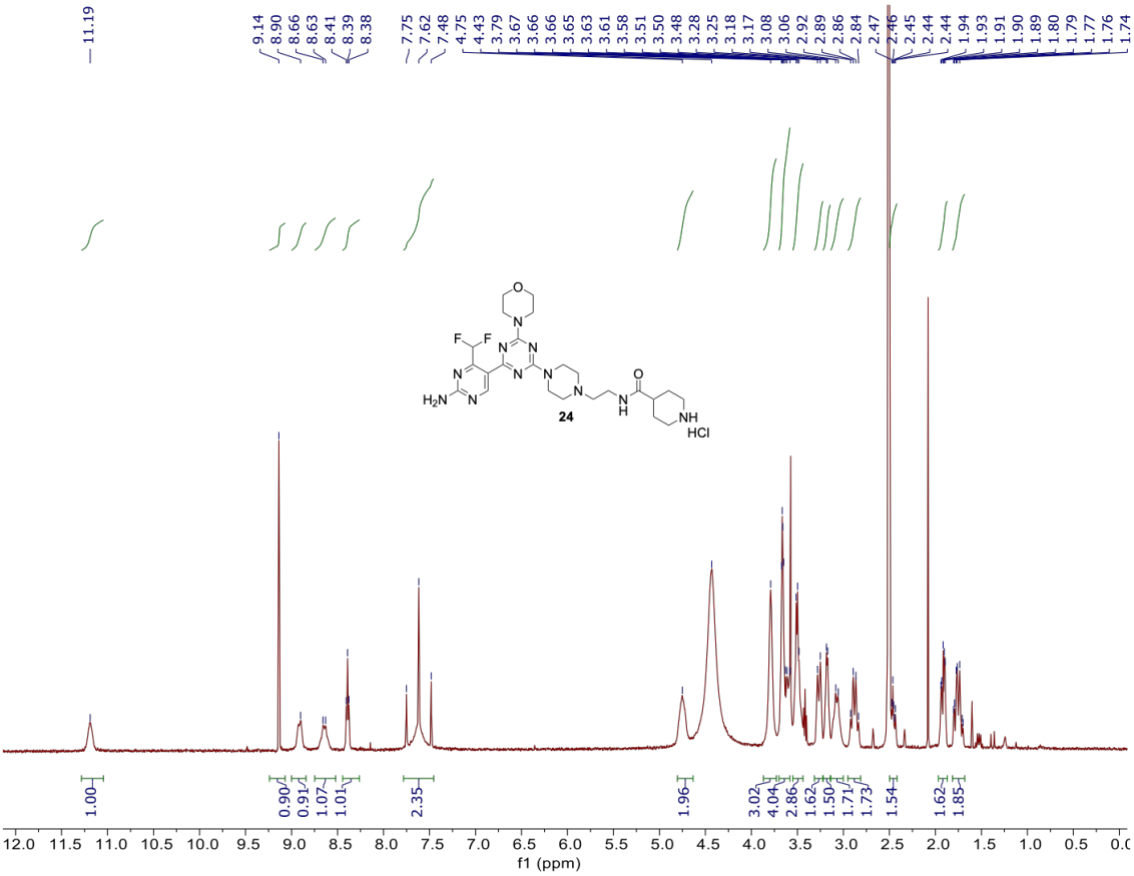

Figure S32. ^{1}H-NMR of compound **24** (400 MHz) in DMSO-d_6.

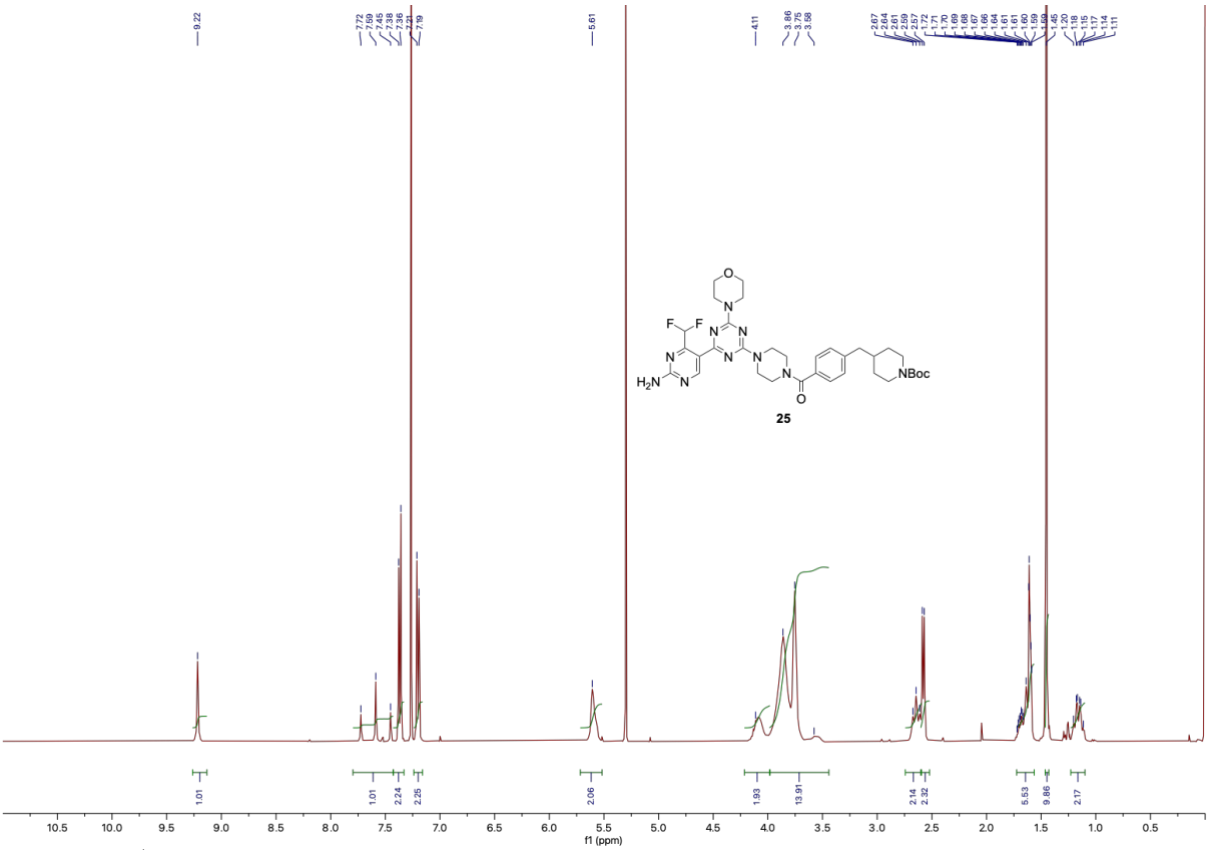

Figure S33. ^{1}H-NMR of compound **25** (400 MHz) in $CDCl_3$.

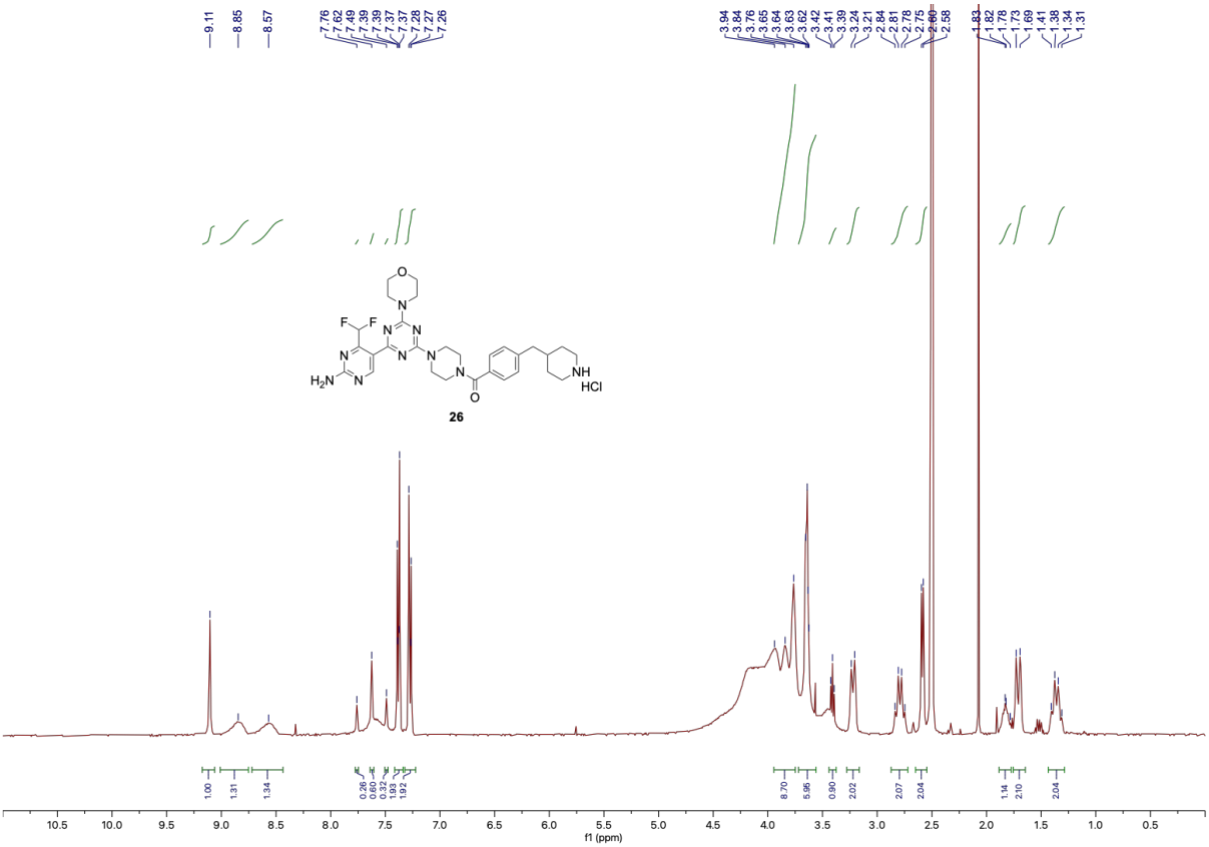

Figure S34. ^{1}H-NMR of compound **26** (400 MHz) in DMSO-d_6.

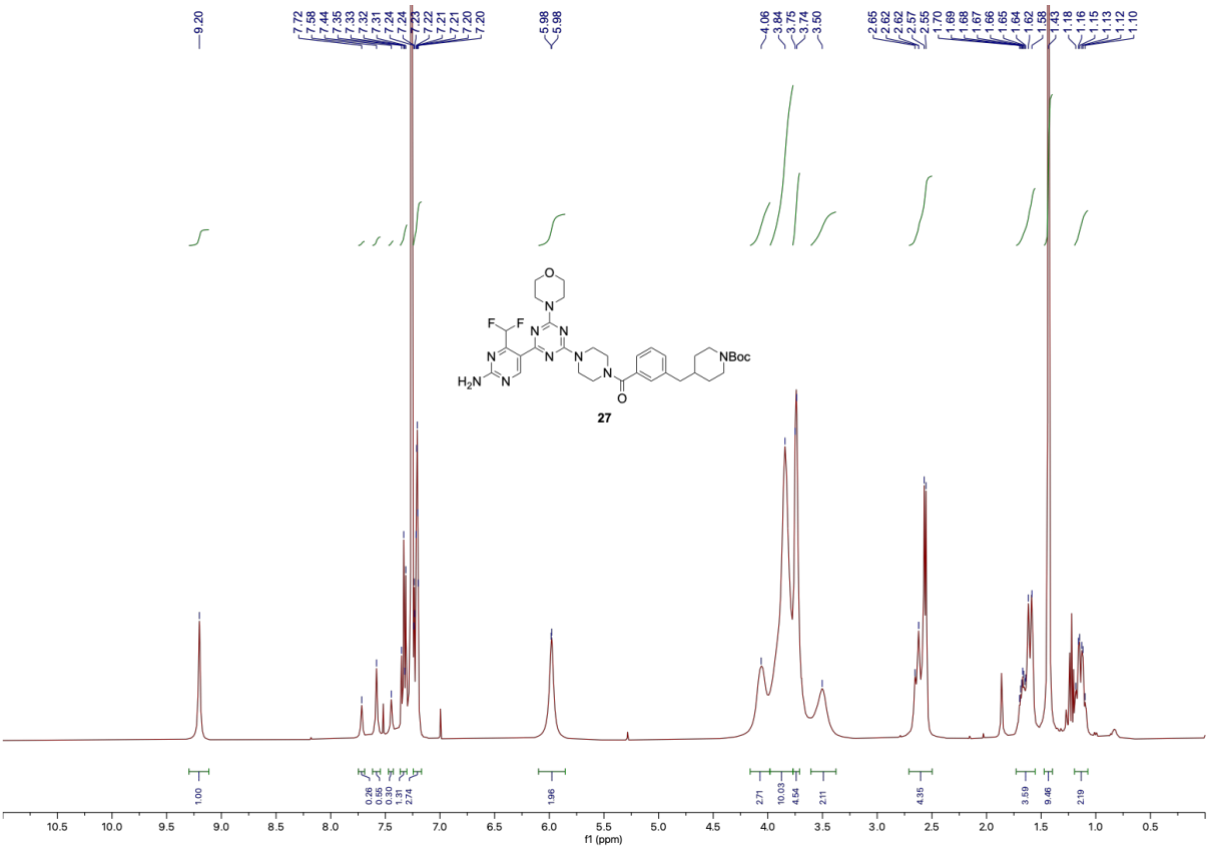

Figure S35. ^{1}H-NMR of compound **27** (400 MHz) in $CDCl_3$.

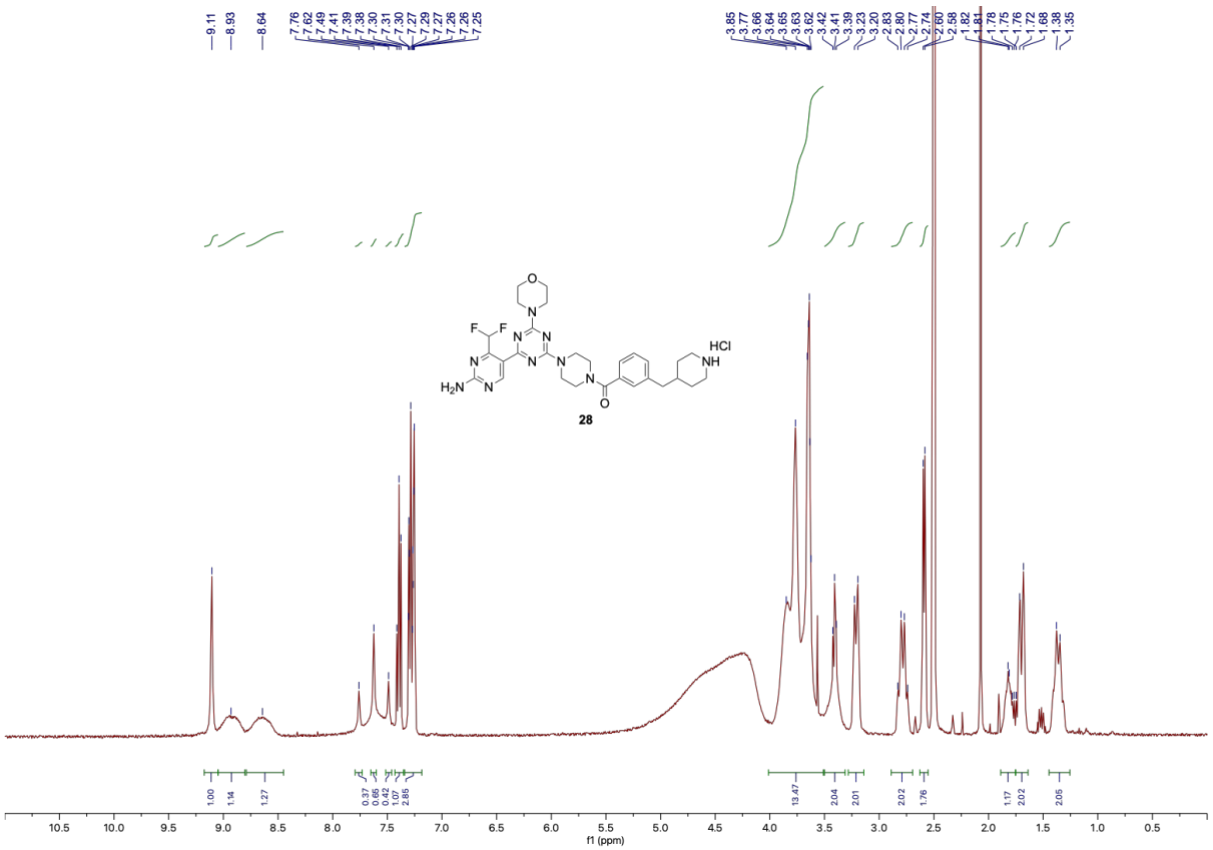

Figure S36. ^{1}H-NMR of compound **28** (400 MHz) in DMSO-d_6.

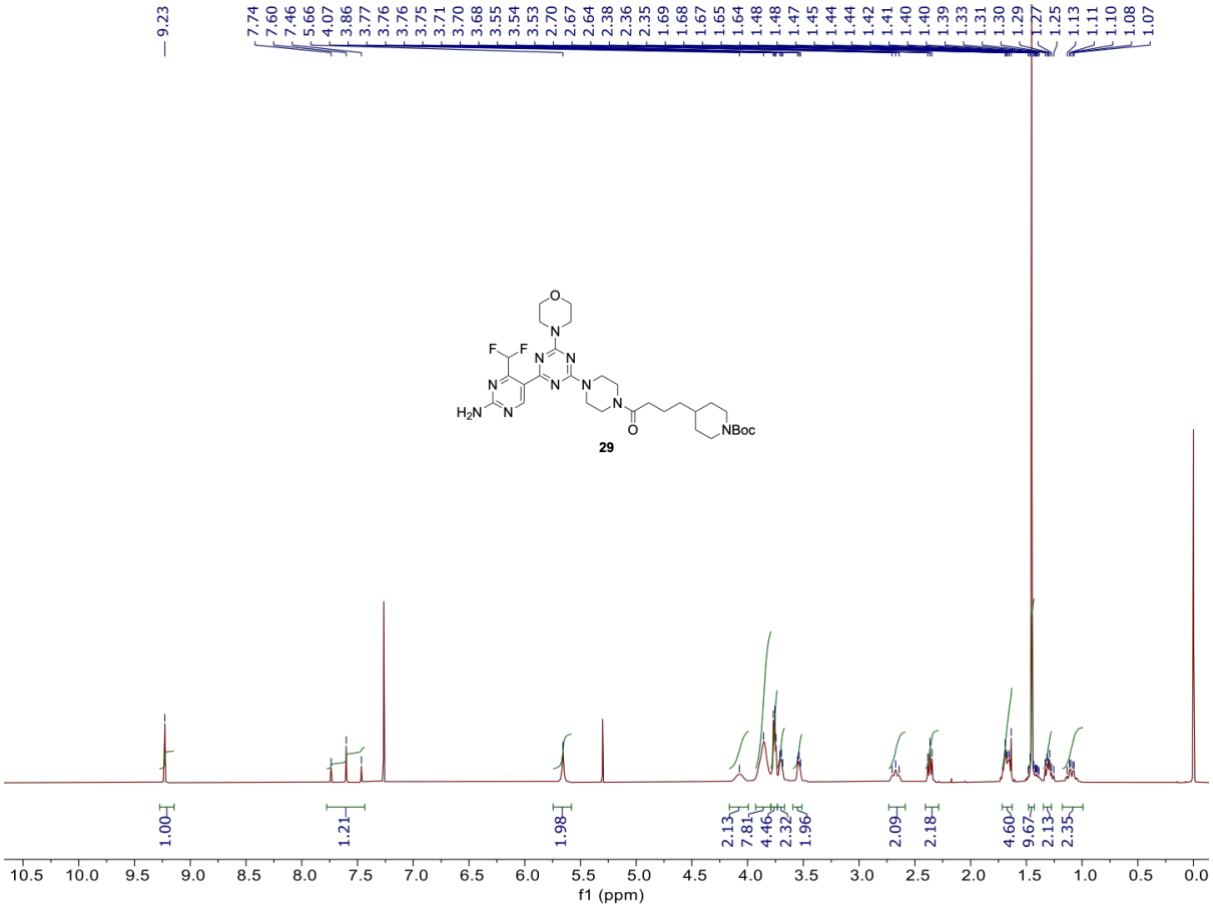

Figure S37. ^{1}H-NMR of compound **29** (400 MHz) in $CDCl_3$.

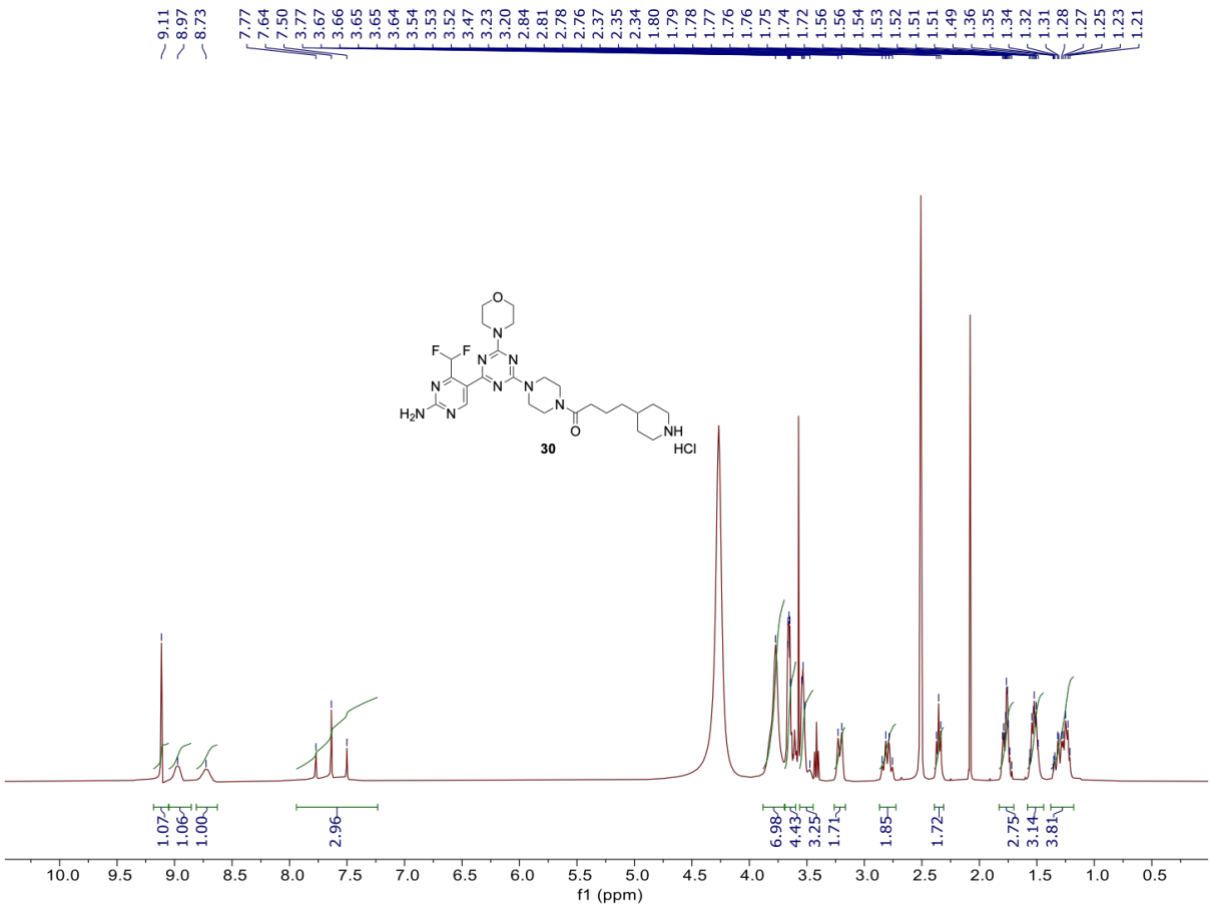

Figure S38. ^{1}H-NMR of compound **30** (400 MHz) in DMSO-d_6.

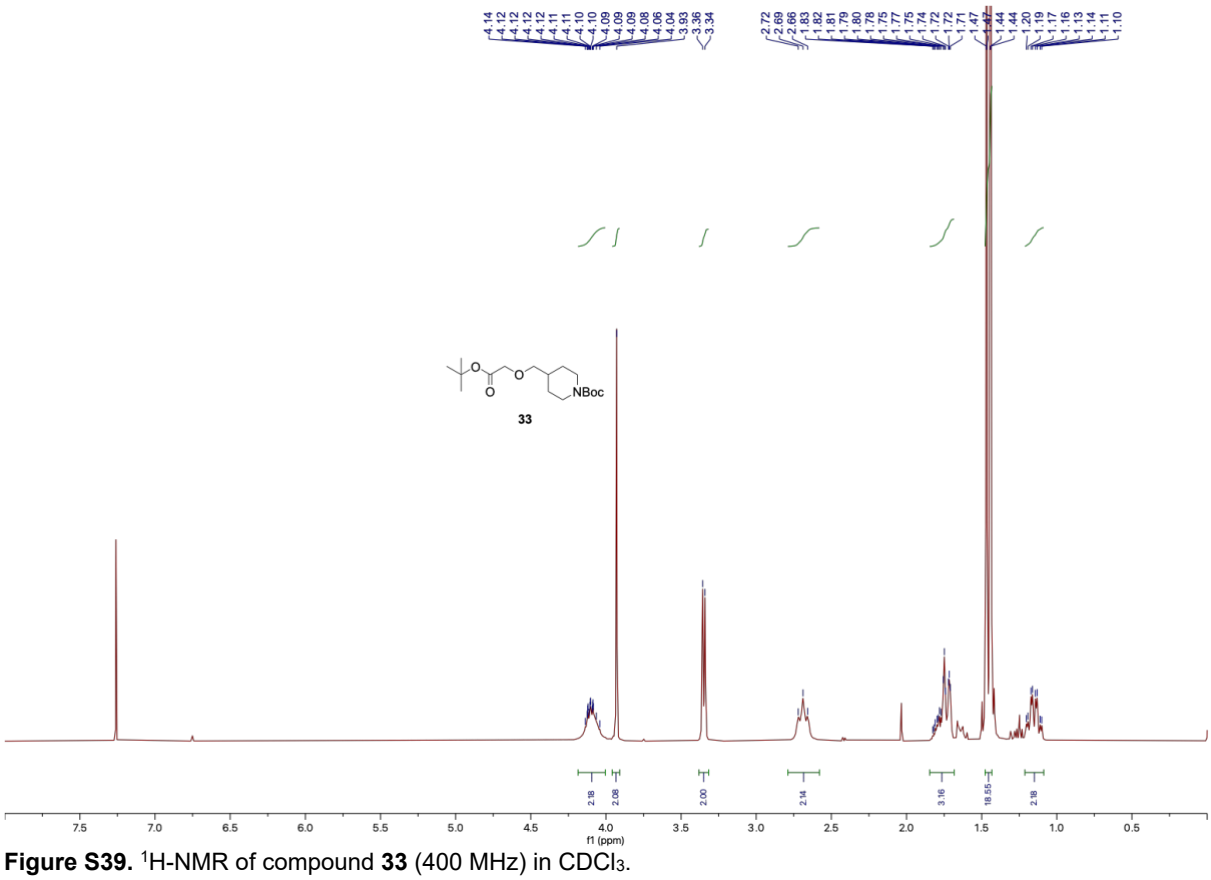

Figure S39. ^{1}H-NMR of compound **33** (400 MHz) in $CDCl_3$.

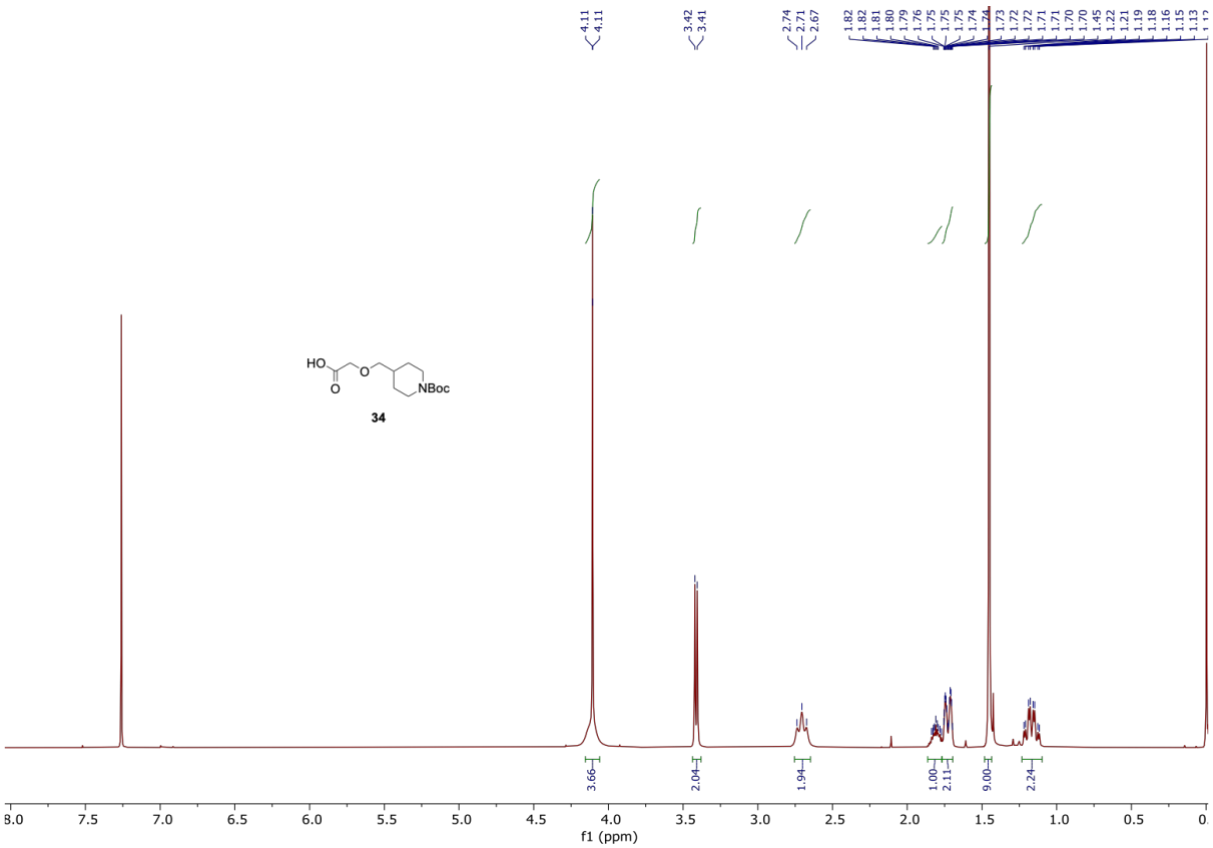

Figure S40. ^{1}H-NMR of compound **34** (400 MHz) in $CDCl_3$.

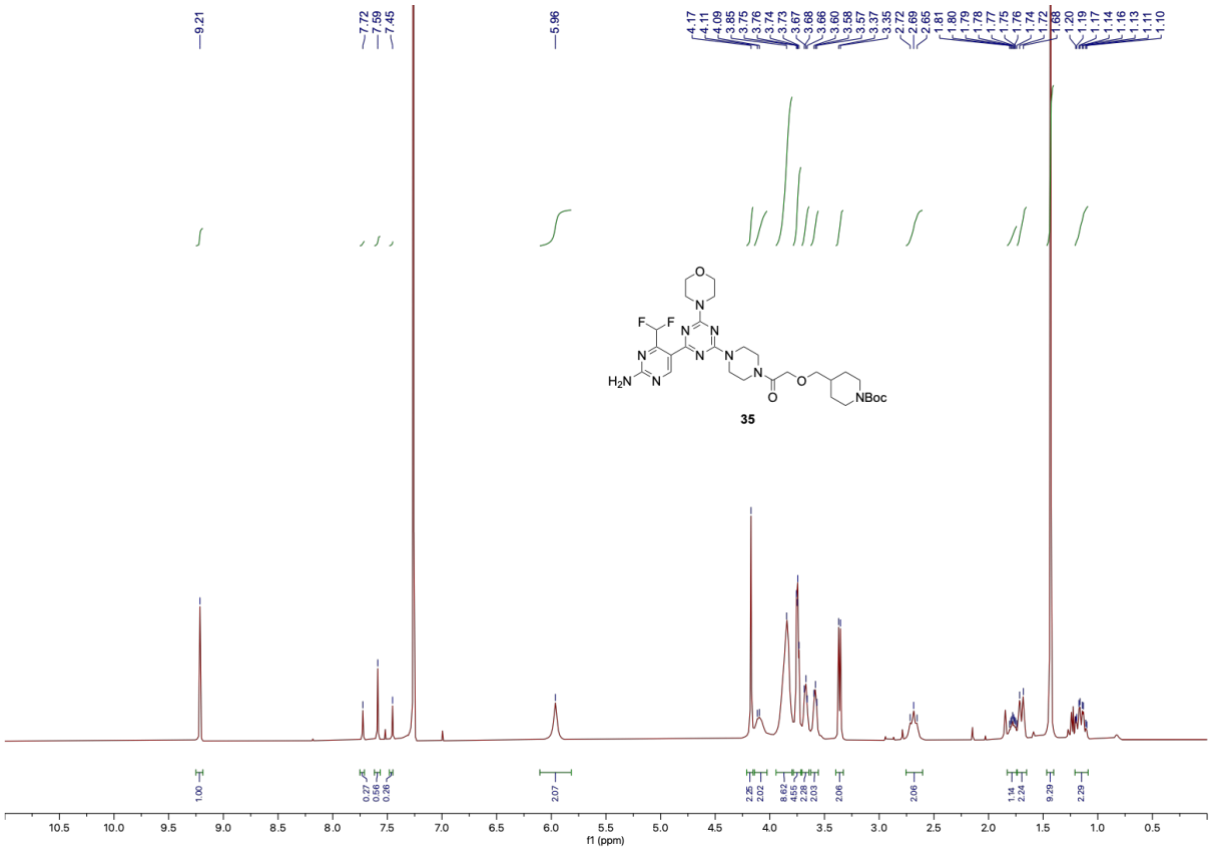

Figure S41. ^{1}H-NMR of compound **35** (400 MHz) in $CDCl_3$.

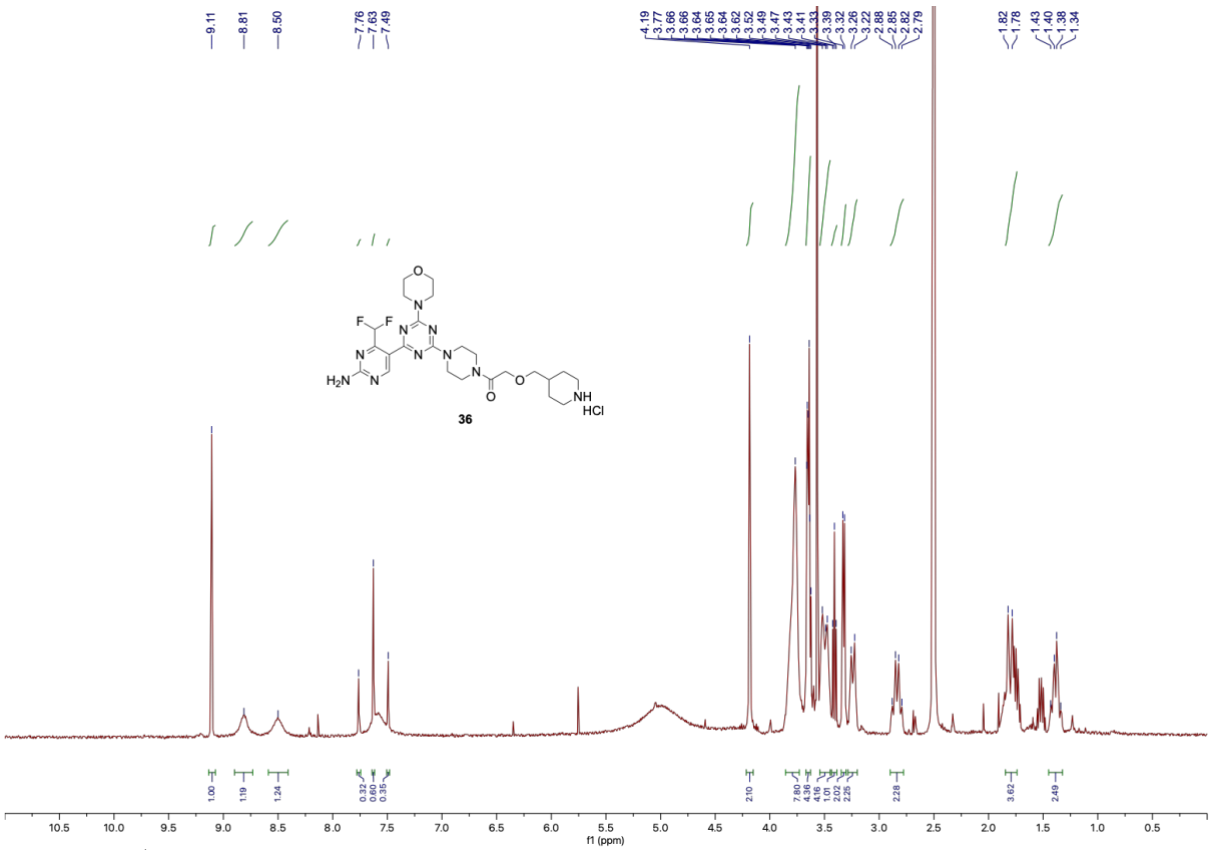

Figure S42. ^{1}H-NMR of compound **36** (400 MHz) in DMSO-d_6.

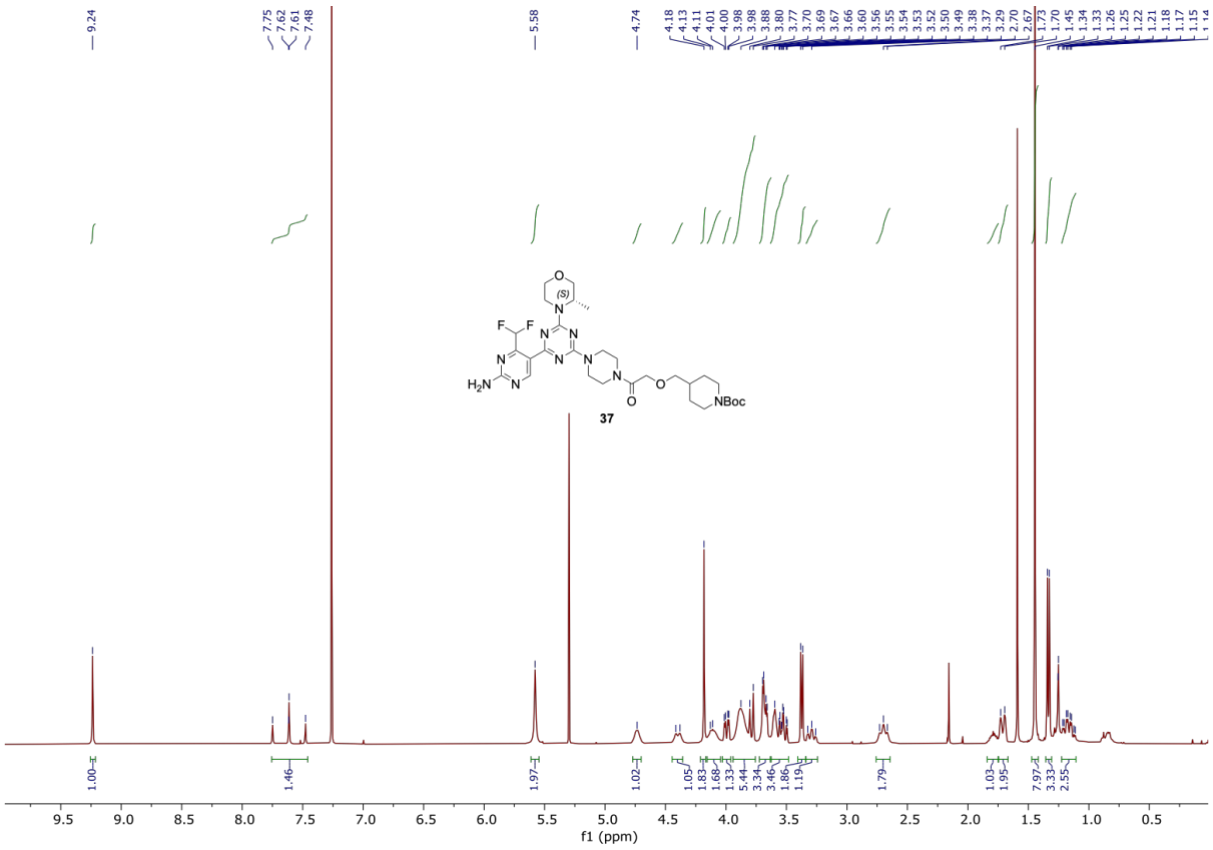

Figure S43. ^{1}H-NMR of compound **37** (400 MHz) in $CDCl_3$.

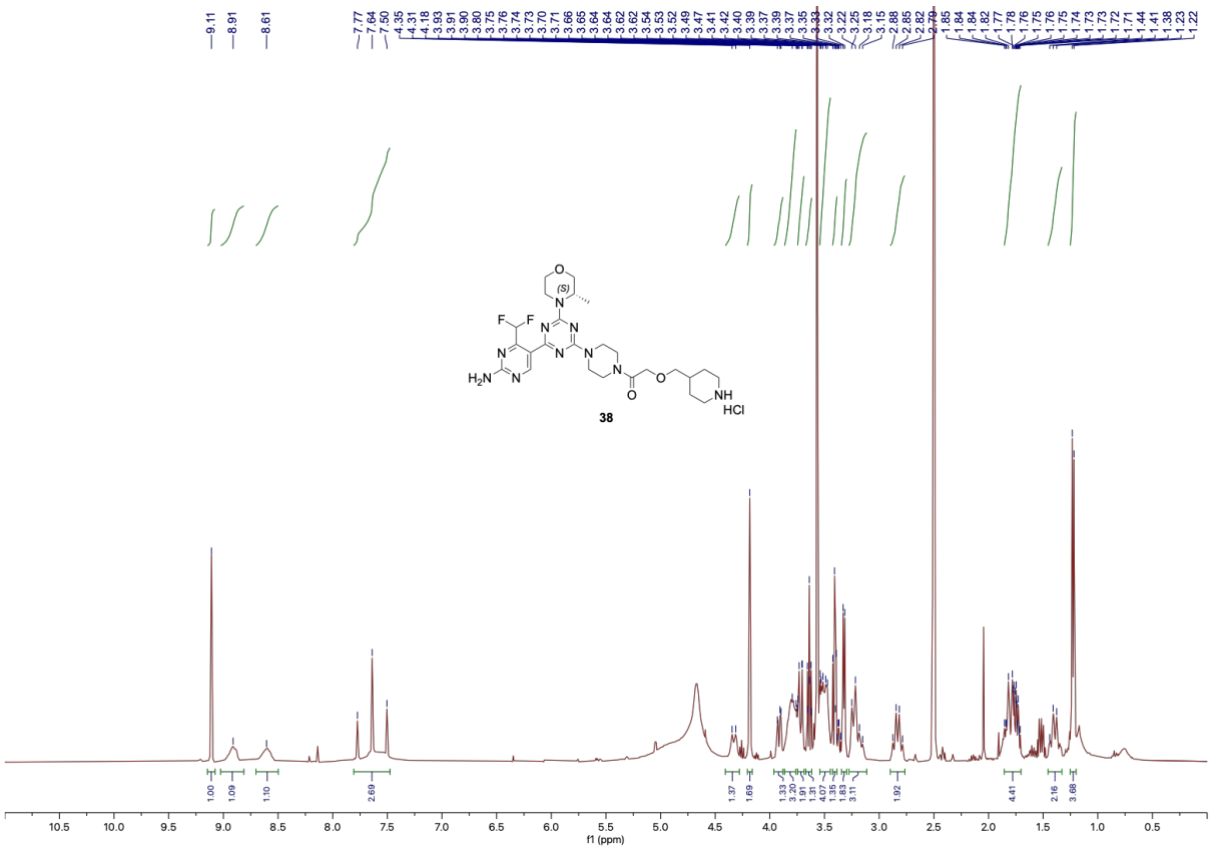

Figure S44. ^{1}H-NMR of compound **38** (400 MHz) in DMSO-d_6.

^{13}C-NMR spectra

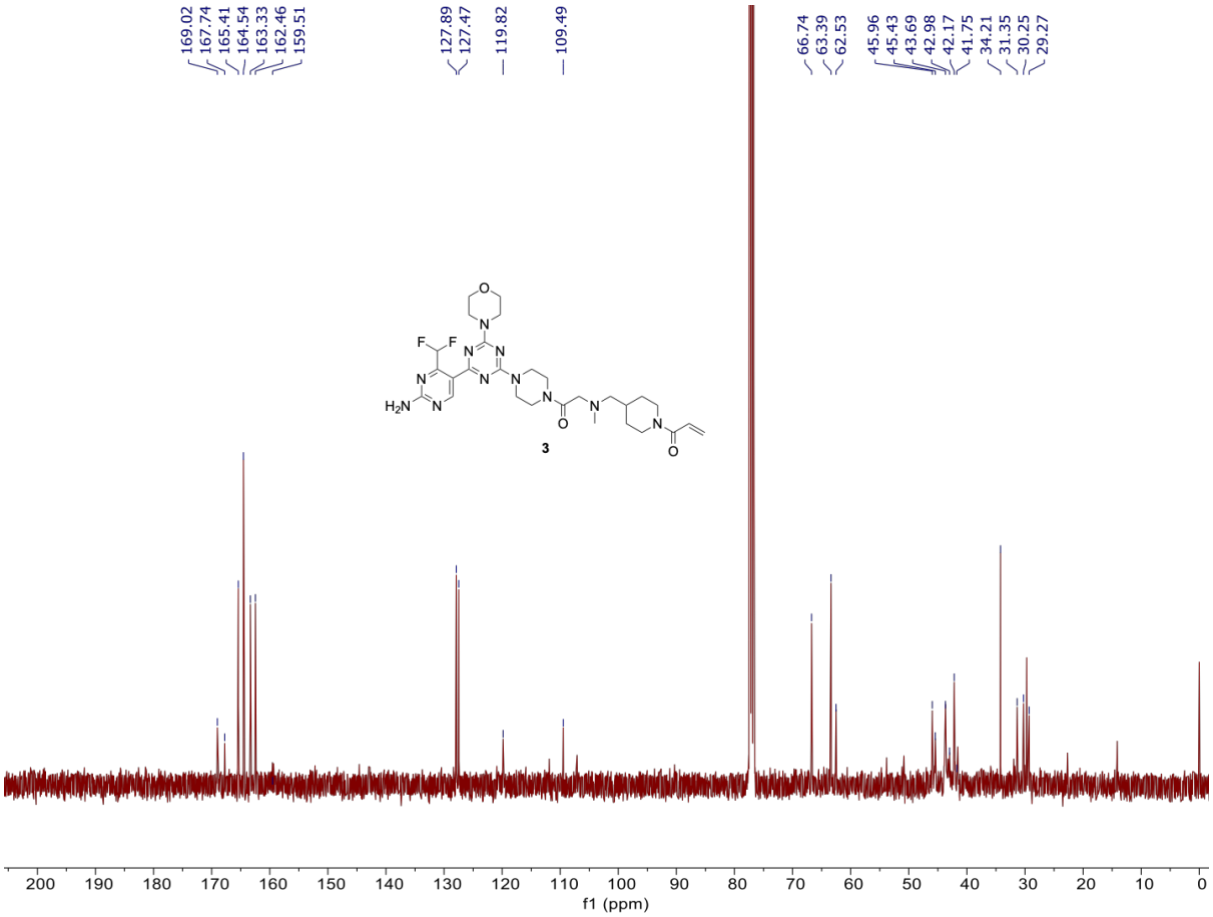

Figure S45. ^{13}C-NMR of compound **3** (101 MHz) in $CDCl_3$.

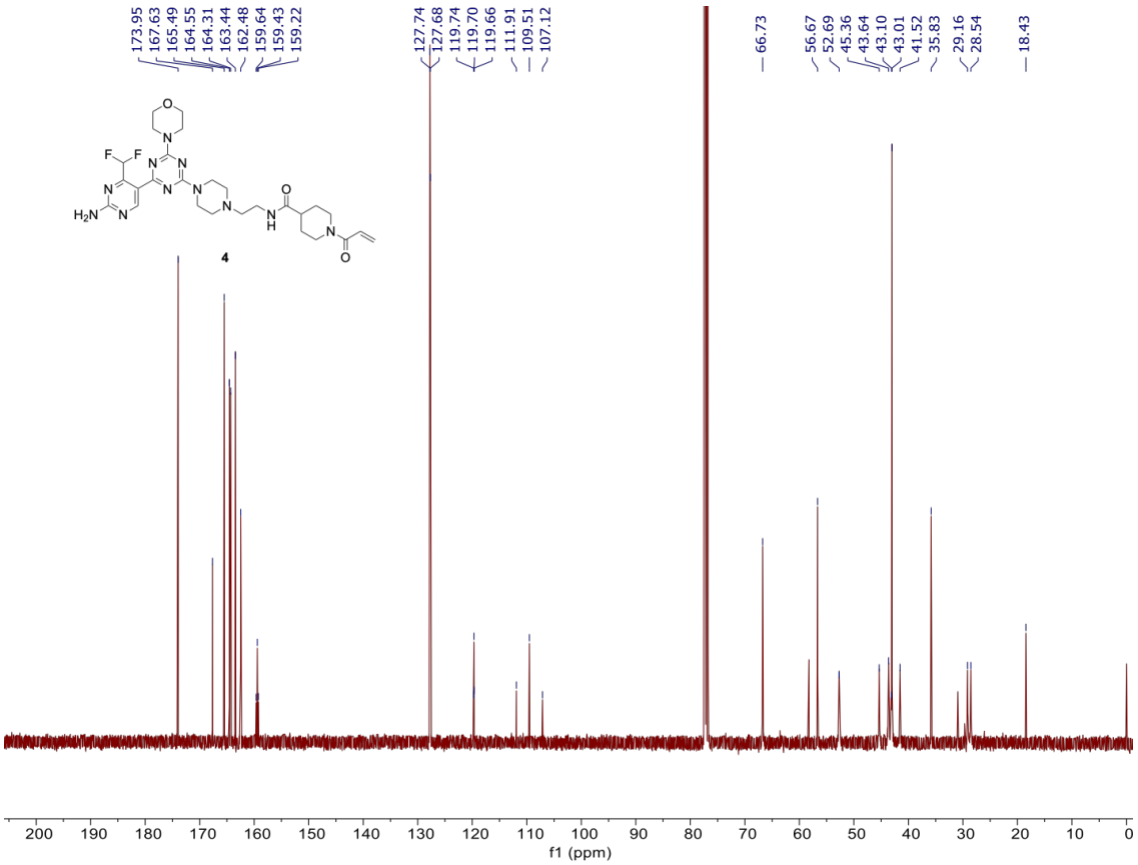

Figure S46. ^{13}C-NMR of compound **4** (101 MHz) in $CDCl_3$.

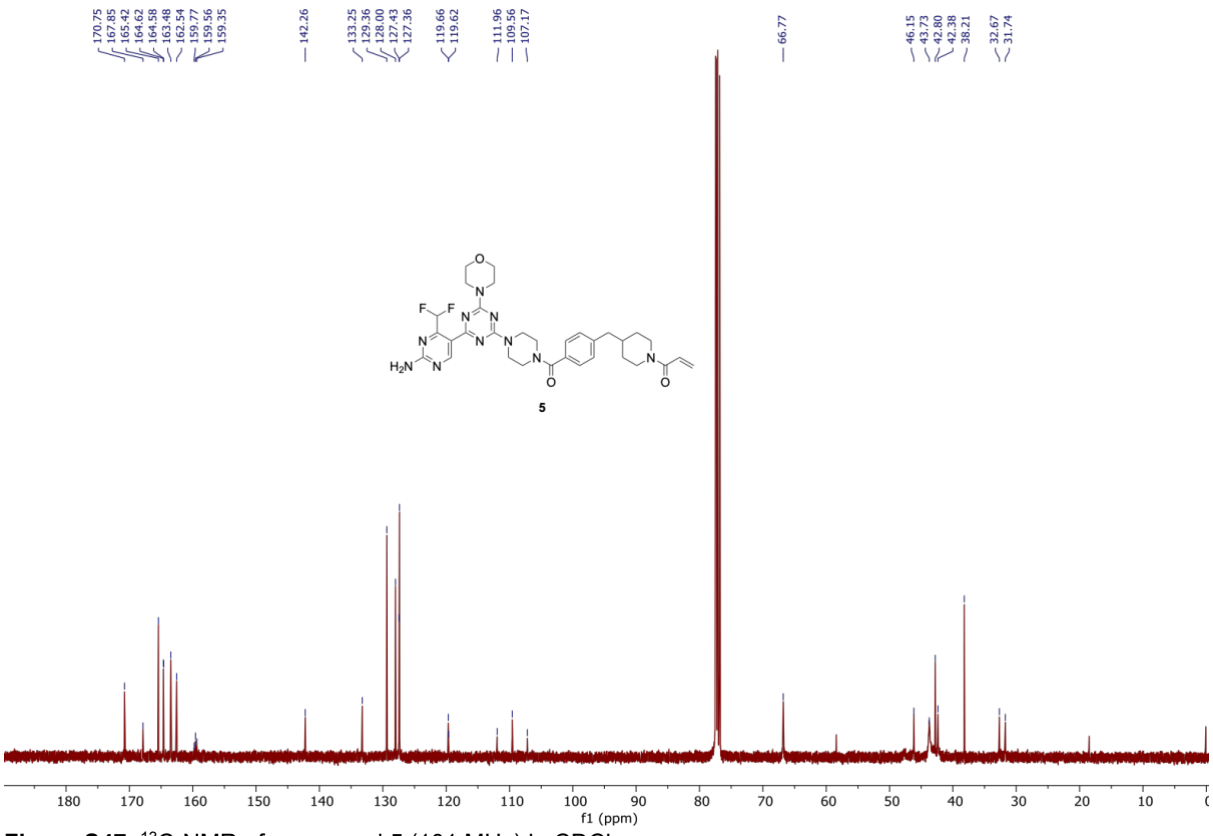

Figure S47. ^{13}C-NMR of compound **5** (101 MHz) in $CDCl_3$.

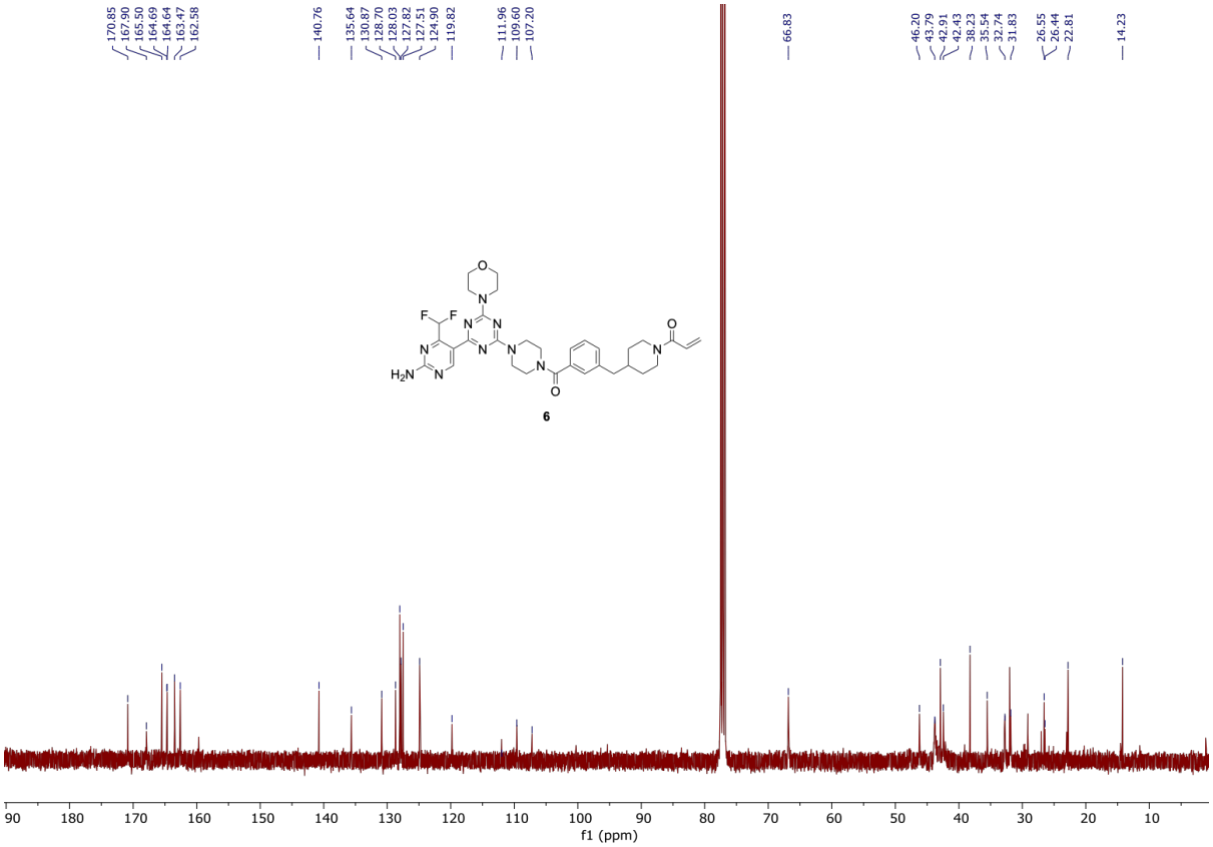

Figure S48. ^{13}C-NMR of compound **6** (101 MHz) in $CDCl_3$.

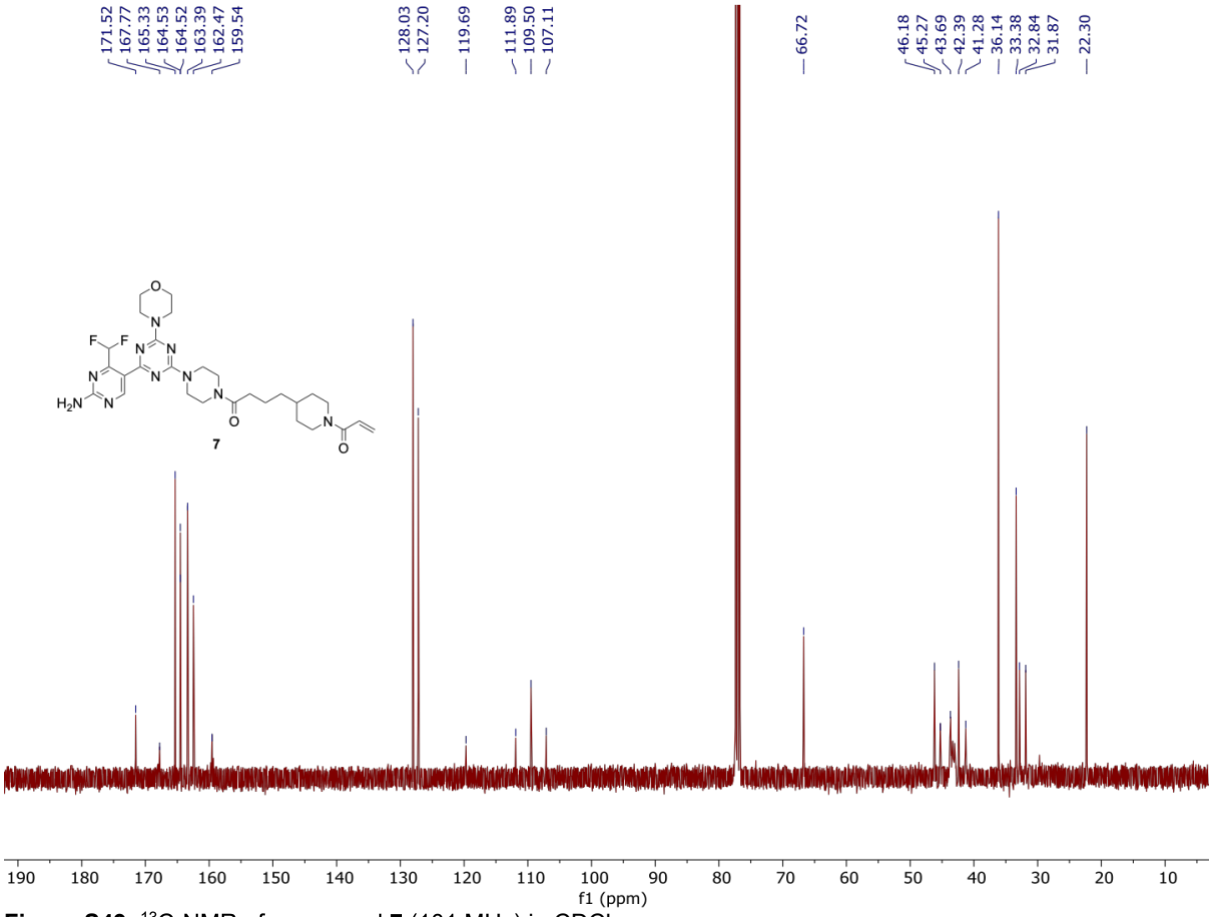

Figure S49. ^{13}C-NMR of compound **7** (101 MHz) in $CDCl_3$.

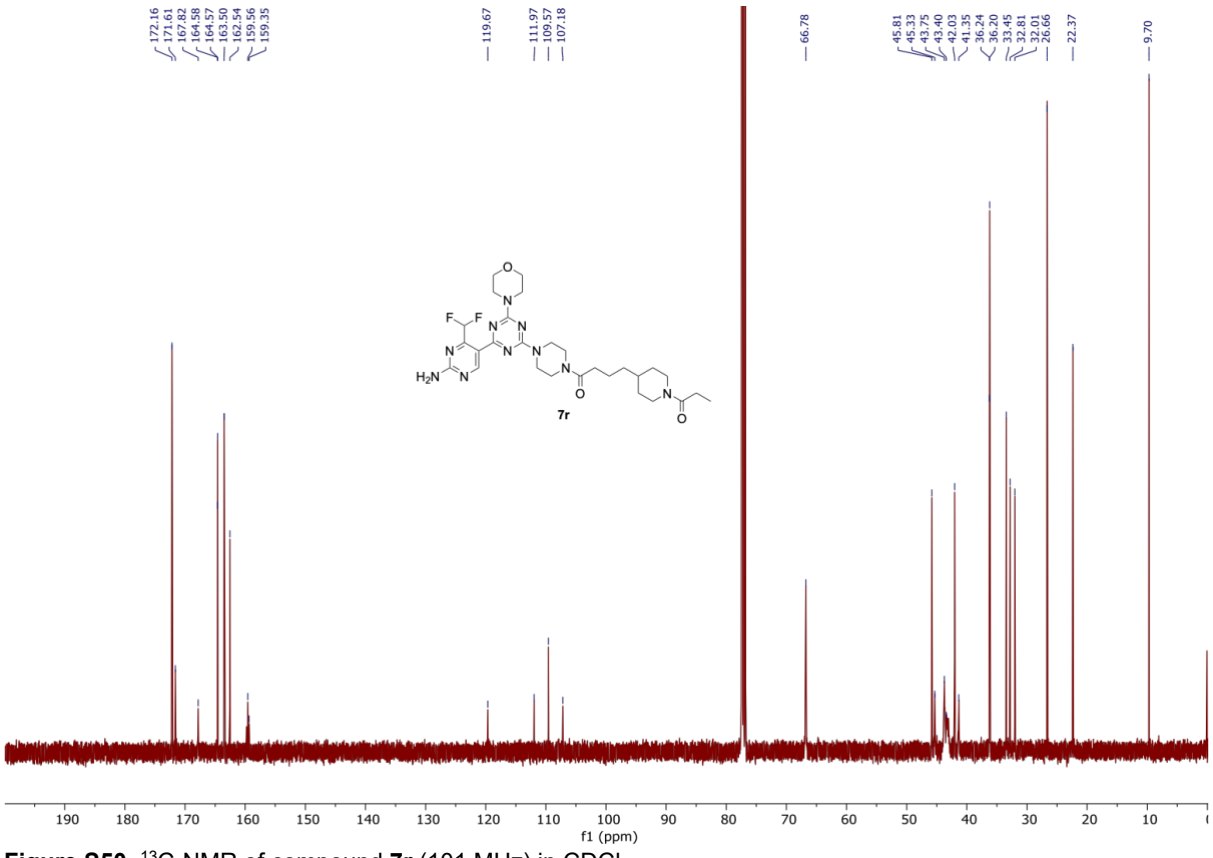

Figure S50. ^{13}C-NMR of compound **7r** (101 MHz) in $CDCl_3$.

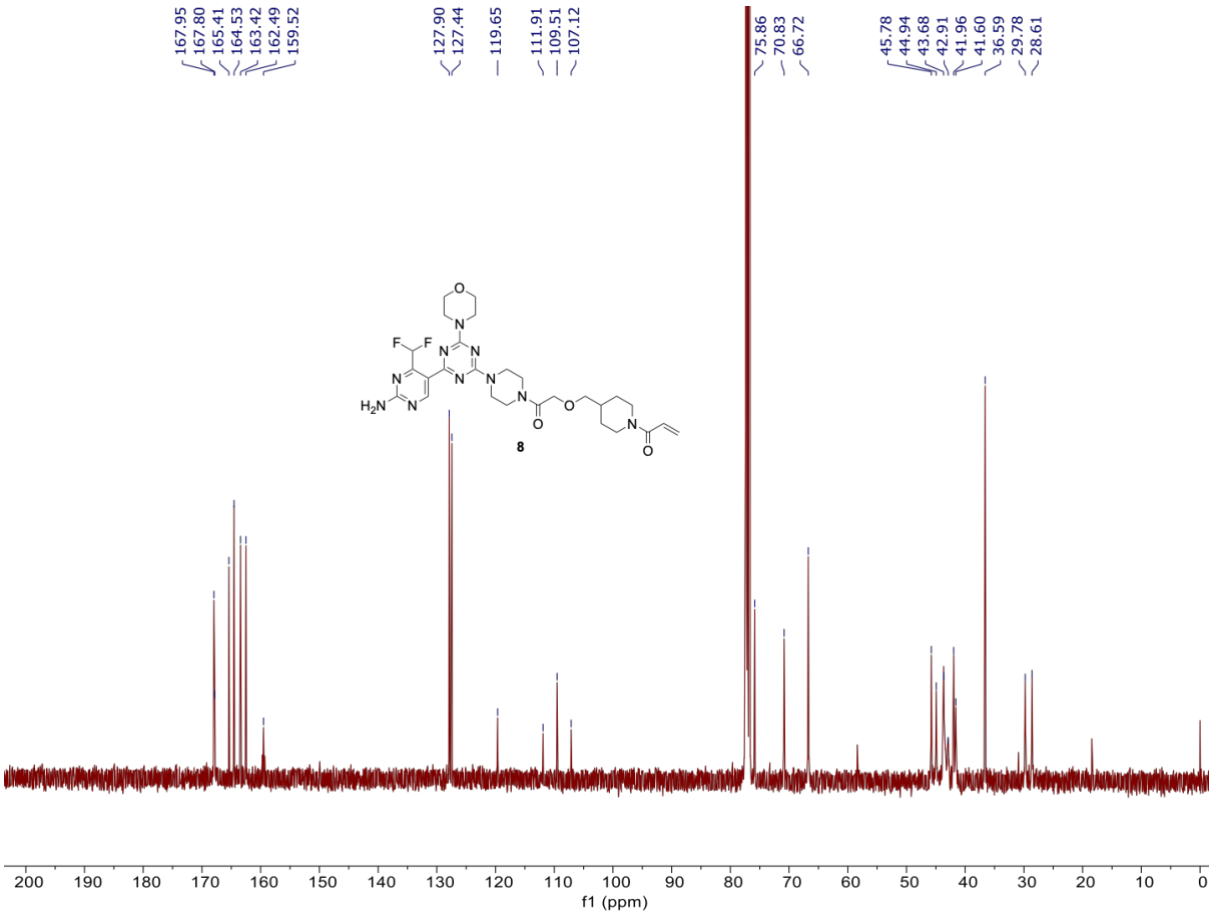

Figure S51. ^{13}C-NMR of compound **8** (101 MHz) in $CDCl_3$.

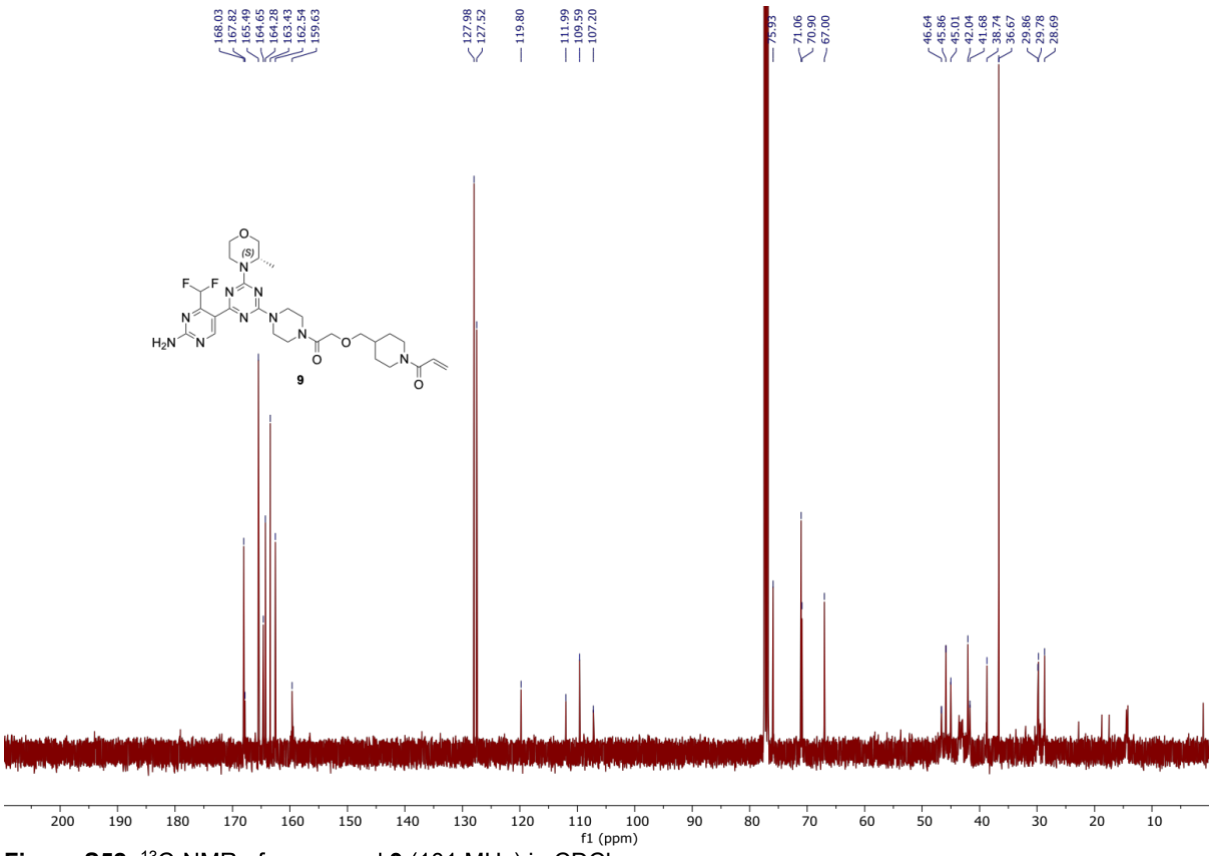

Figure S52. ^{13}C-NMR of compound **9** (101 MHz) in $CDCl_3$.

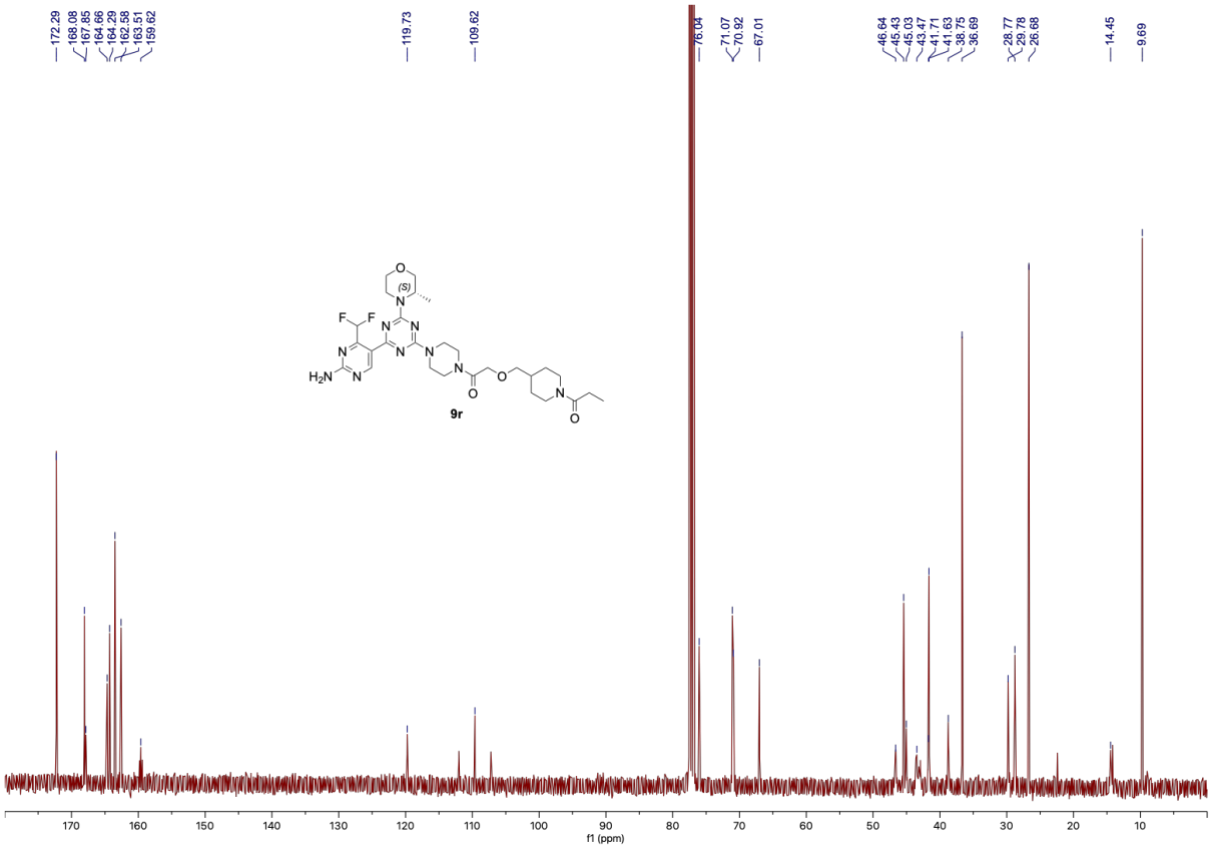

Figure S53. ^{13}C-NMR of compound **9r** (101 MHz) in $CDCl_3$.

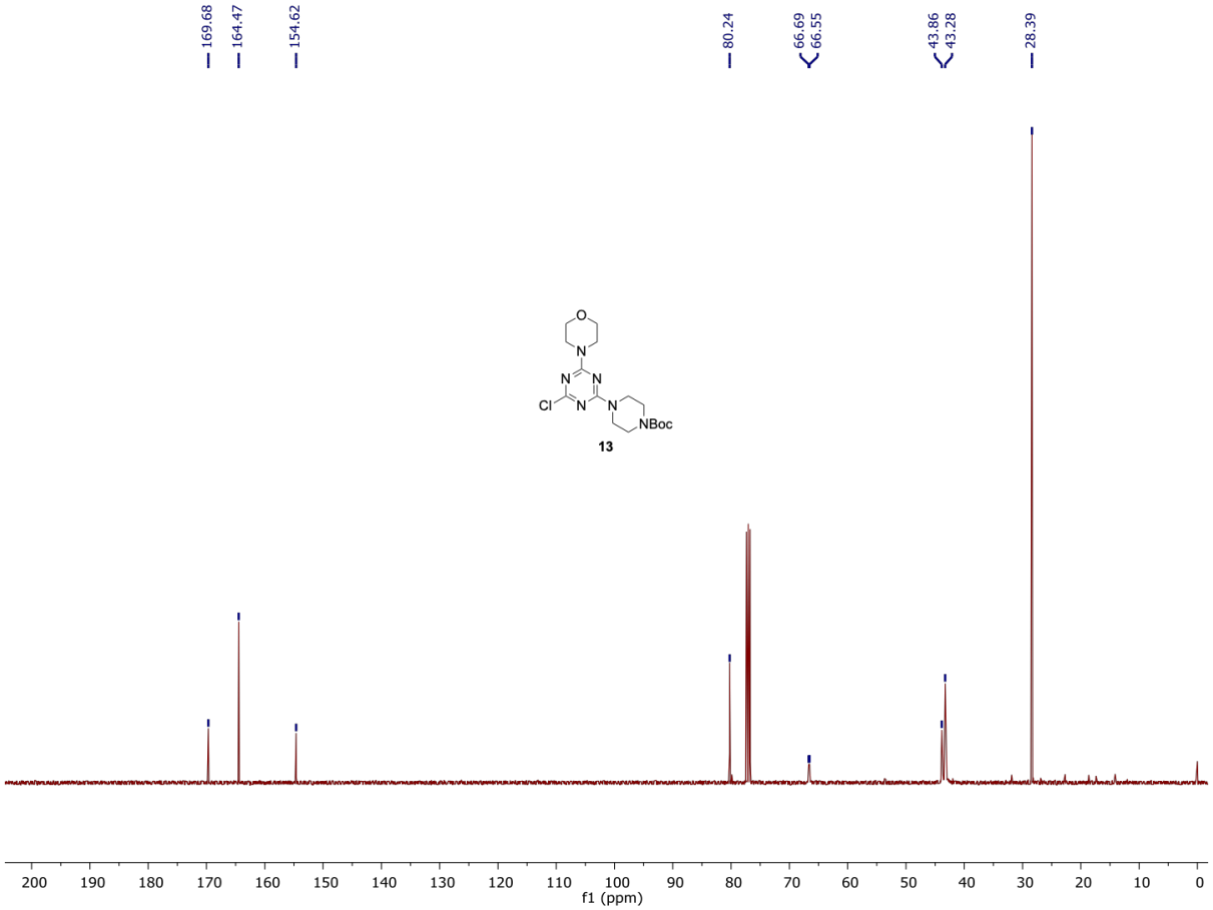

Figure S54. ^{13}C-NMR of compound **13** (101 MHz) in $CDCl_3$.

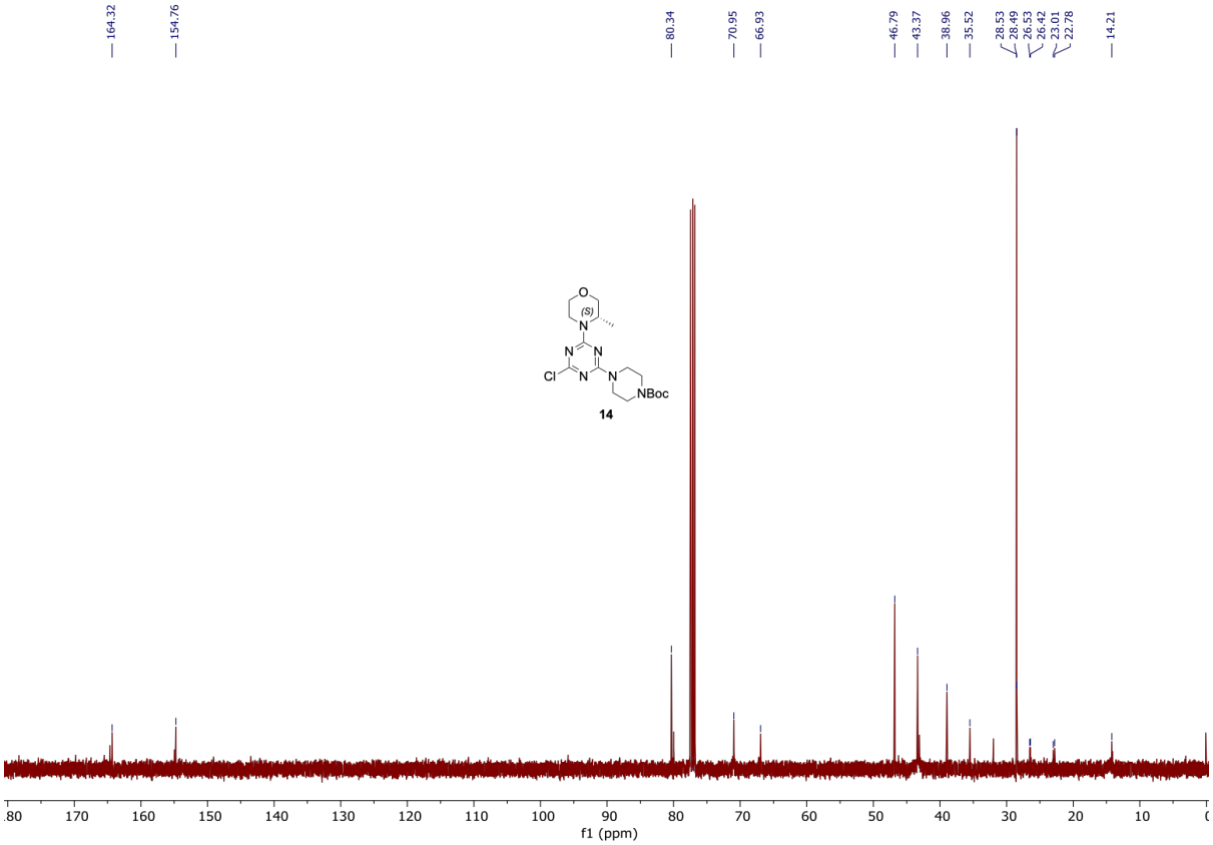

Figure S55. ^{13}C-NMR of compound **14** (101 MHz) in $CDCl_3$.

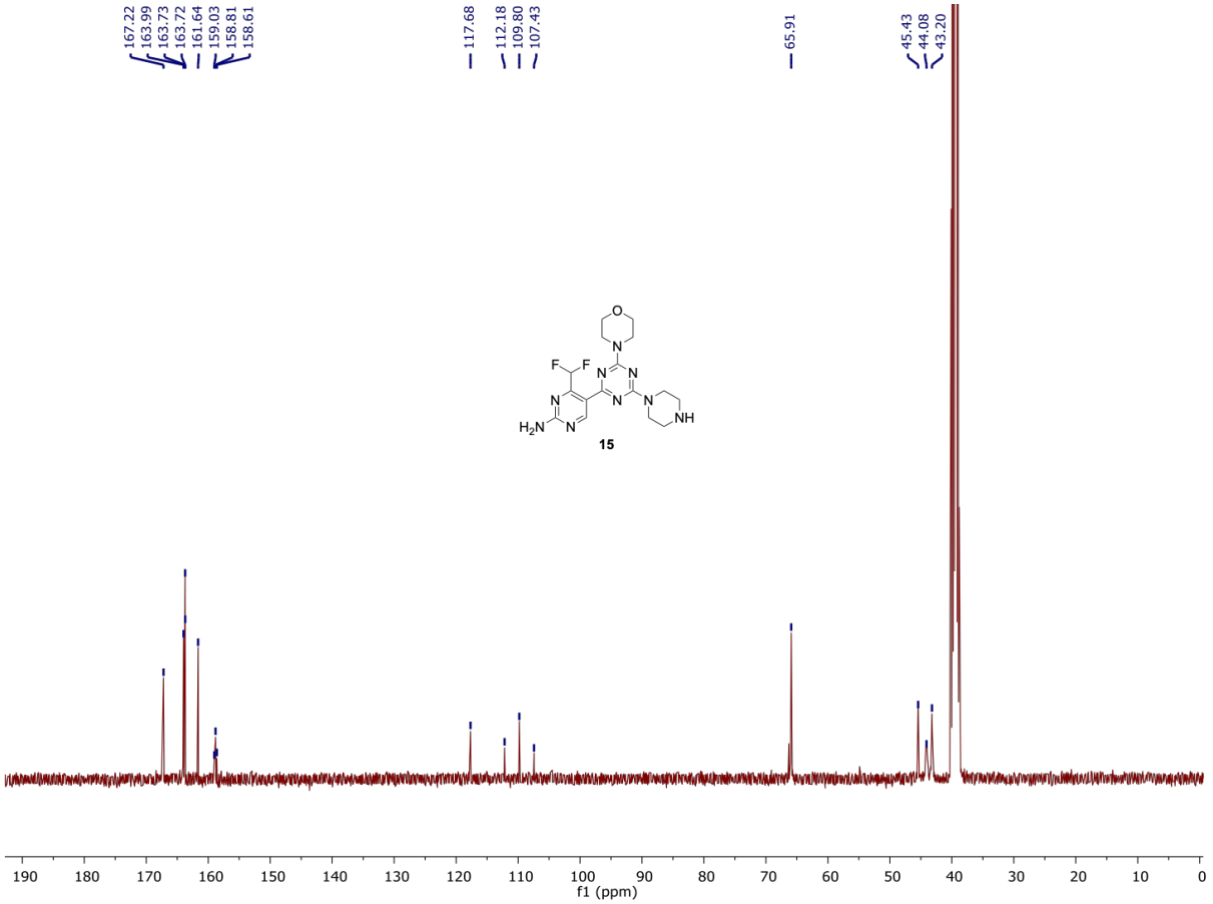

Figure S56. ^{13}C-NMR of compound **15** (101 MHz) in DMSO-d_6.

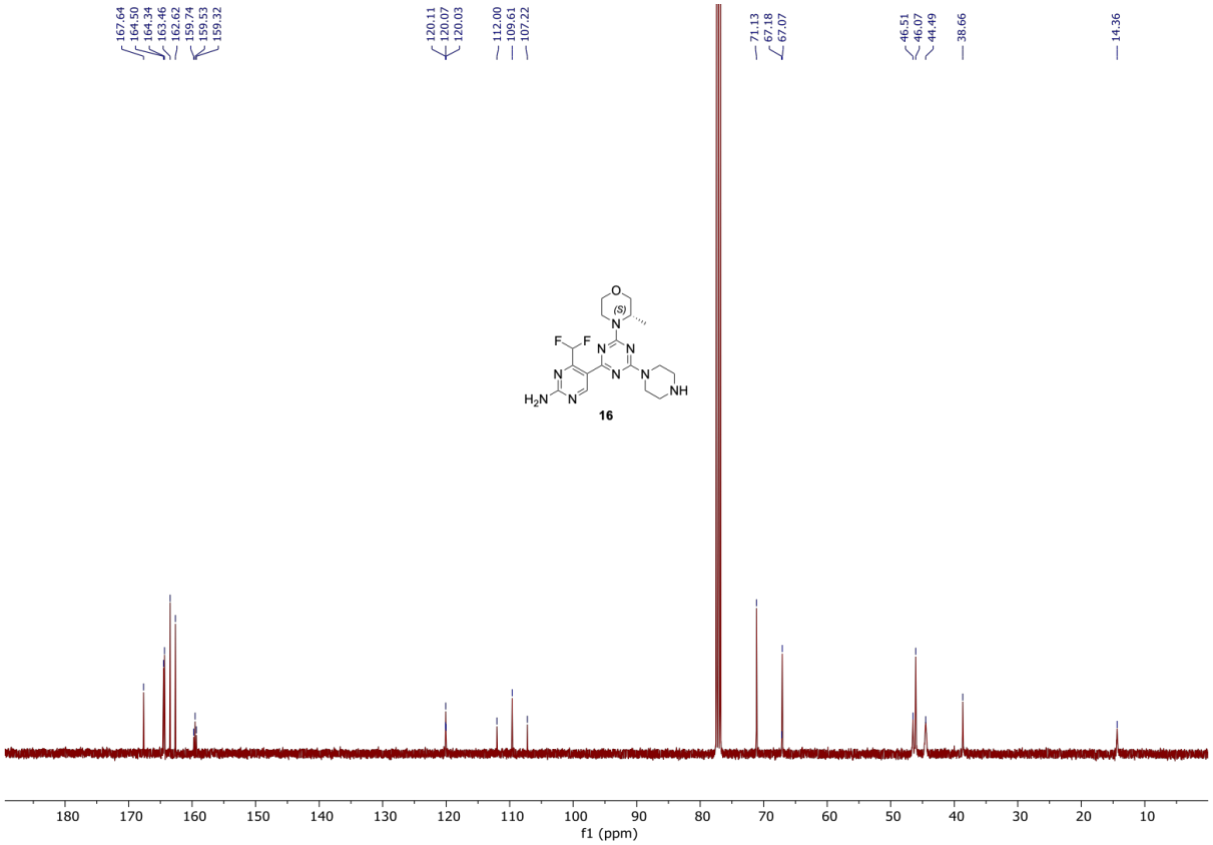

Figure S57. ^{13}C-NMR of compound **16** (101 MHz) in $CDCl_3$.

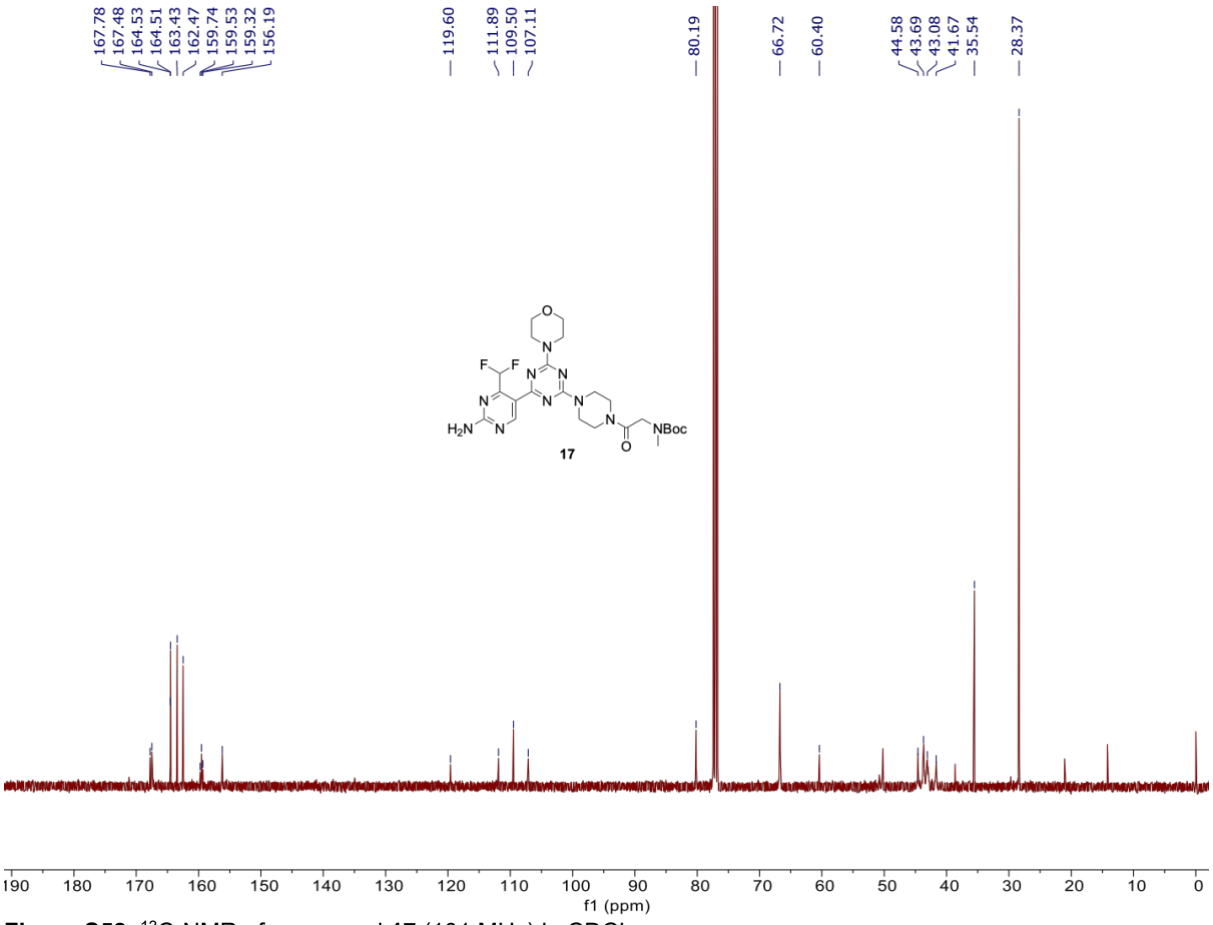

Figure S58. ^{13}C-NMR of compound **17** (101 MHz) in $CDCl_3$.

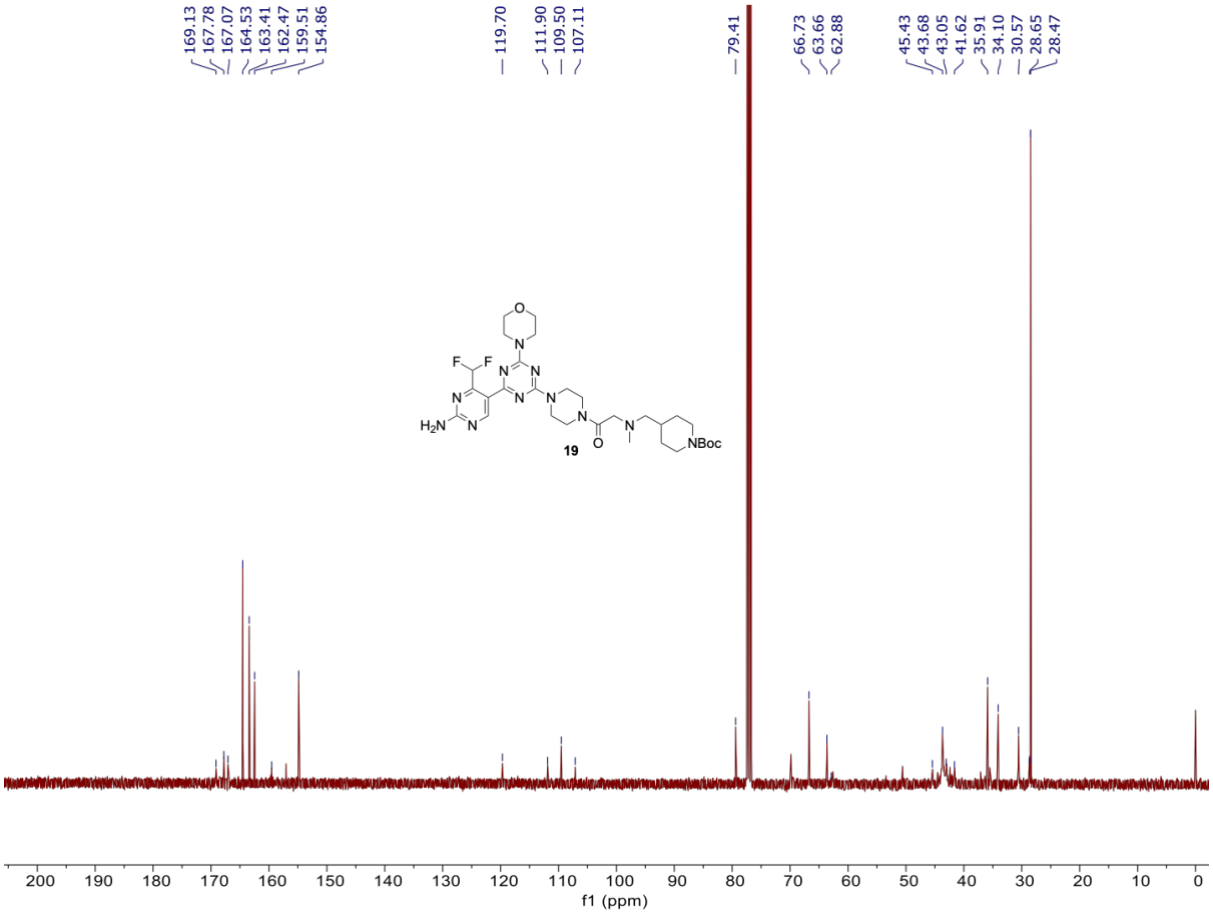

Figure S59. ^{13}C-NMR of compound **19** (101 MHz) in $CDCl_3$.

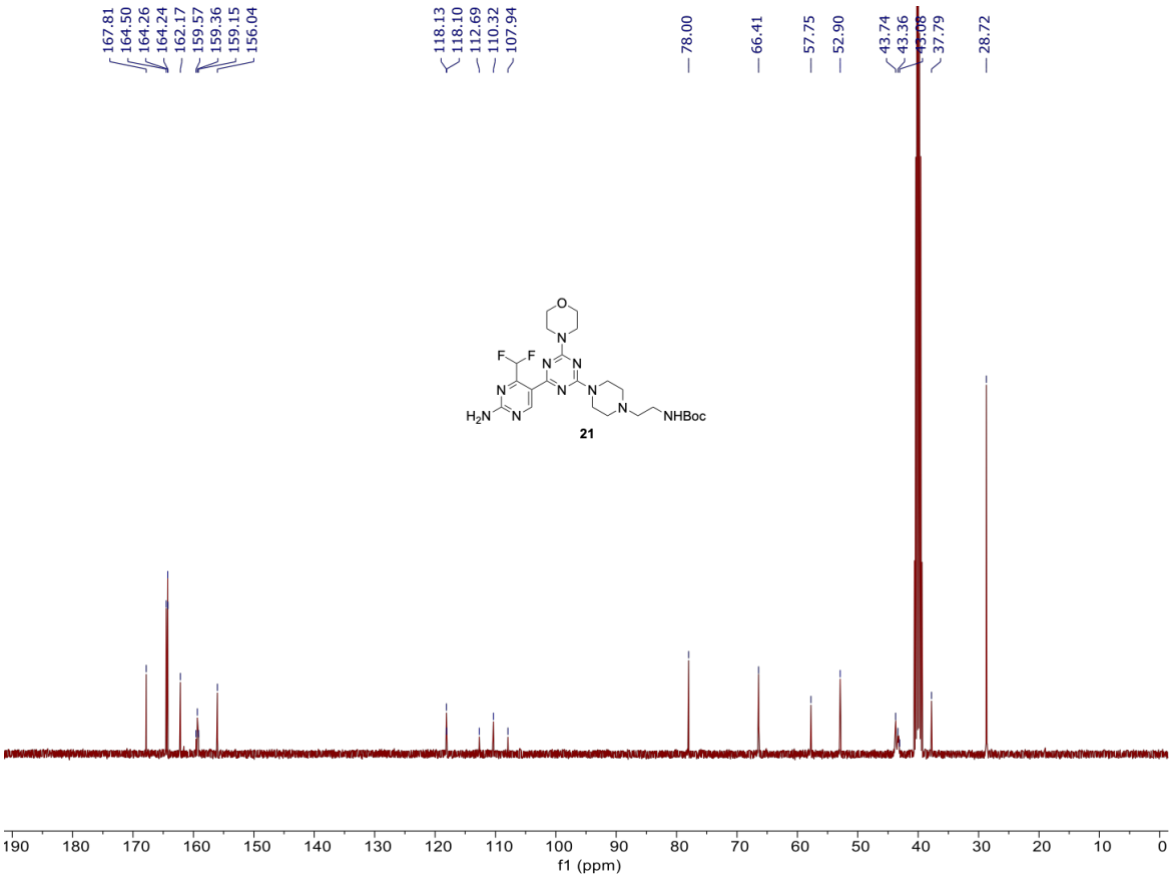

Figure S60. ^{13}C-NMR of compound **21** (101 MHz) in $CDCl_3$.

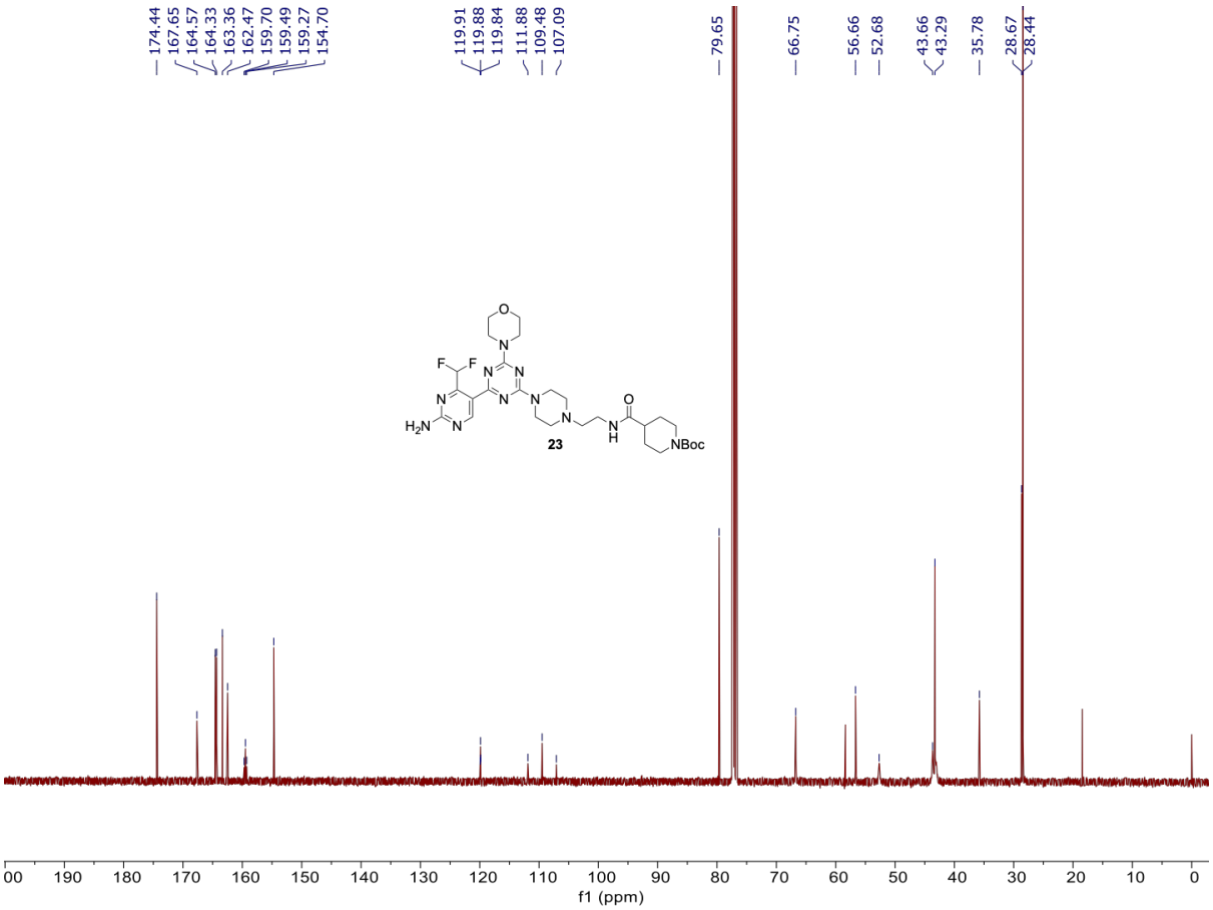

Figure S61. ^{13}C-NMR of compound **23** (101 MHz) in $CDCl_3$.

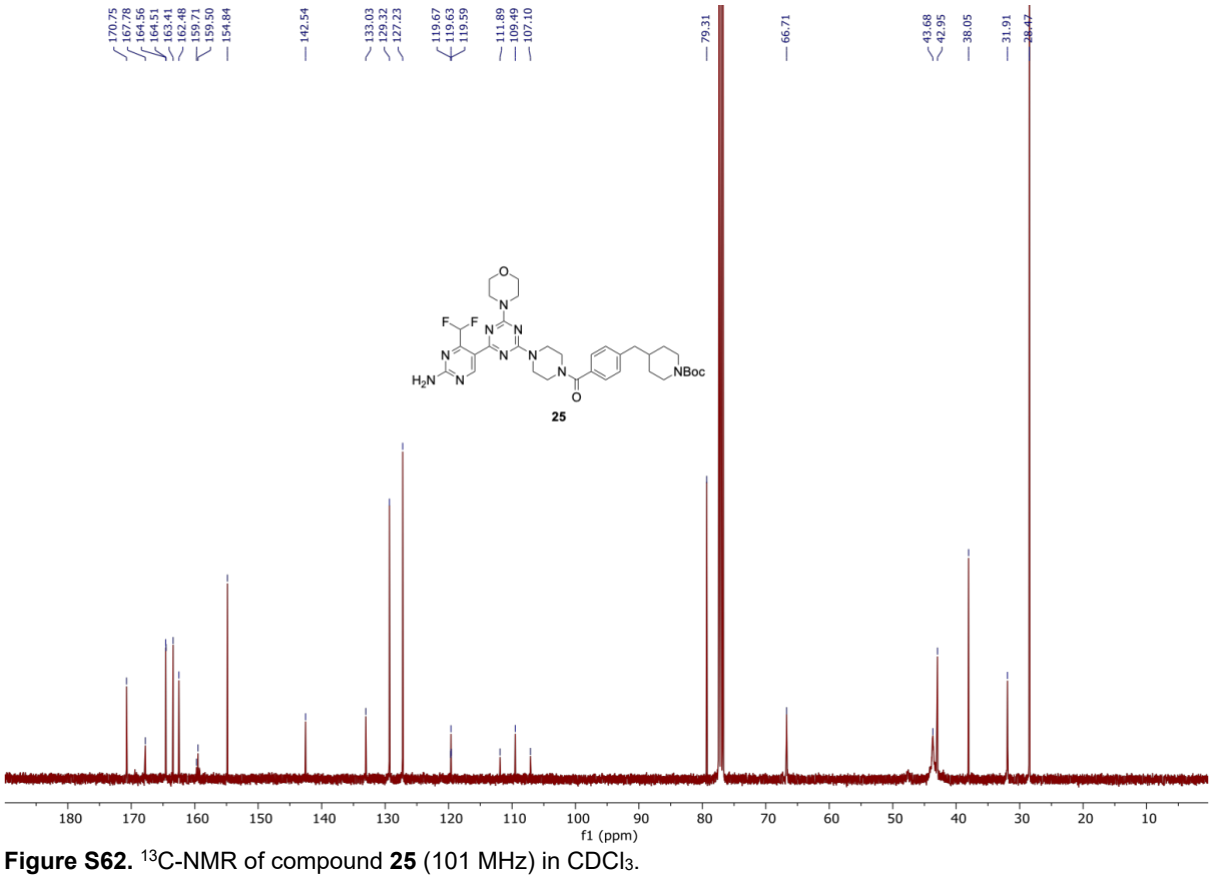

Figure S62. ^{13}C-NMR of compound **25** (101 MHz) in $CDCl_3$.

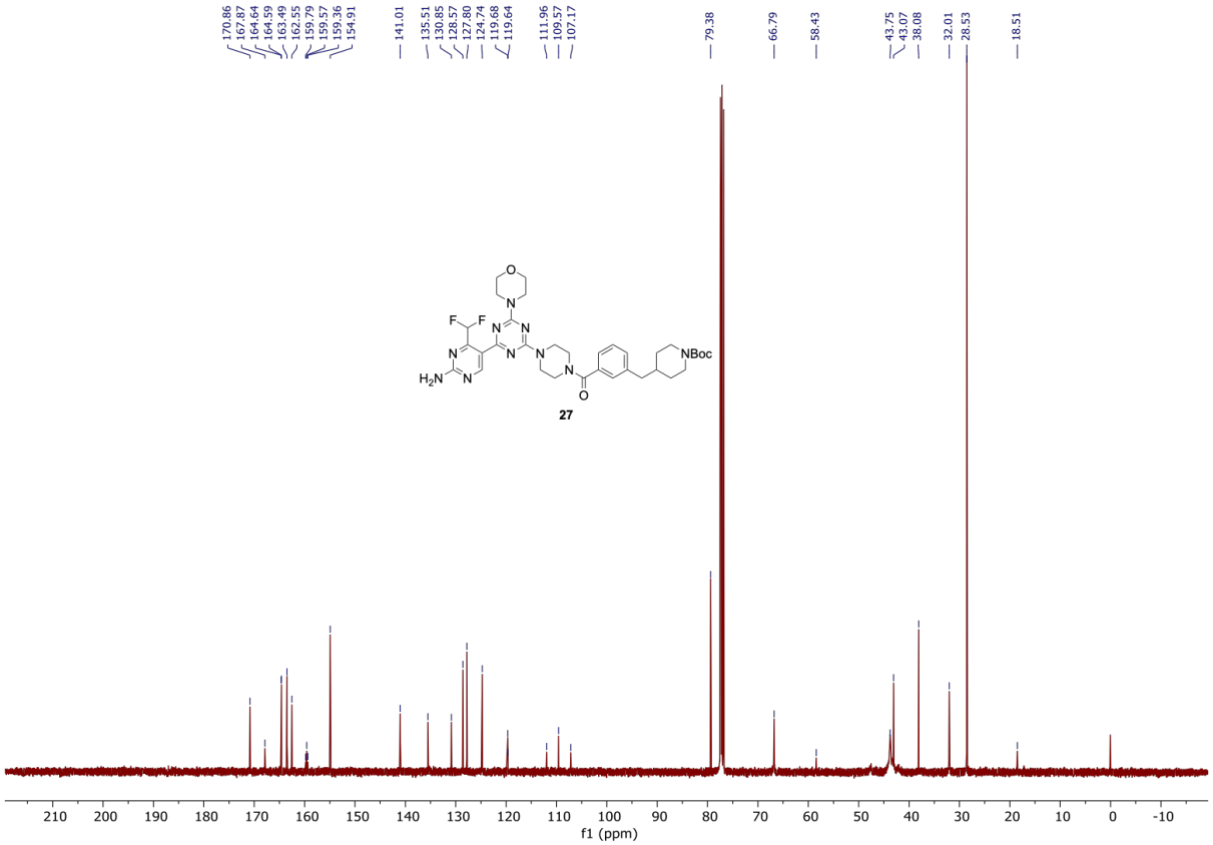

Figure S63. ^{13}C-NMR of compound **27** (101 MHz) in $CDCl_3$.

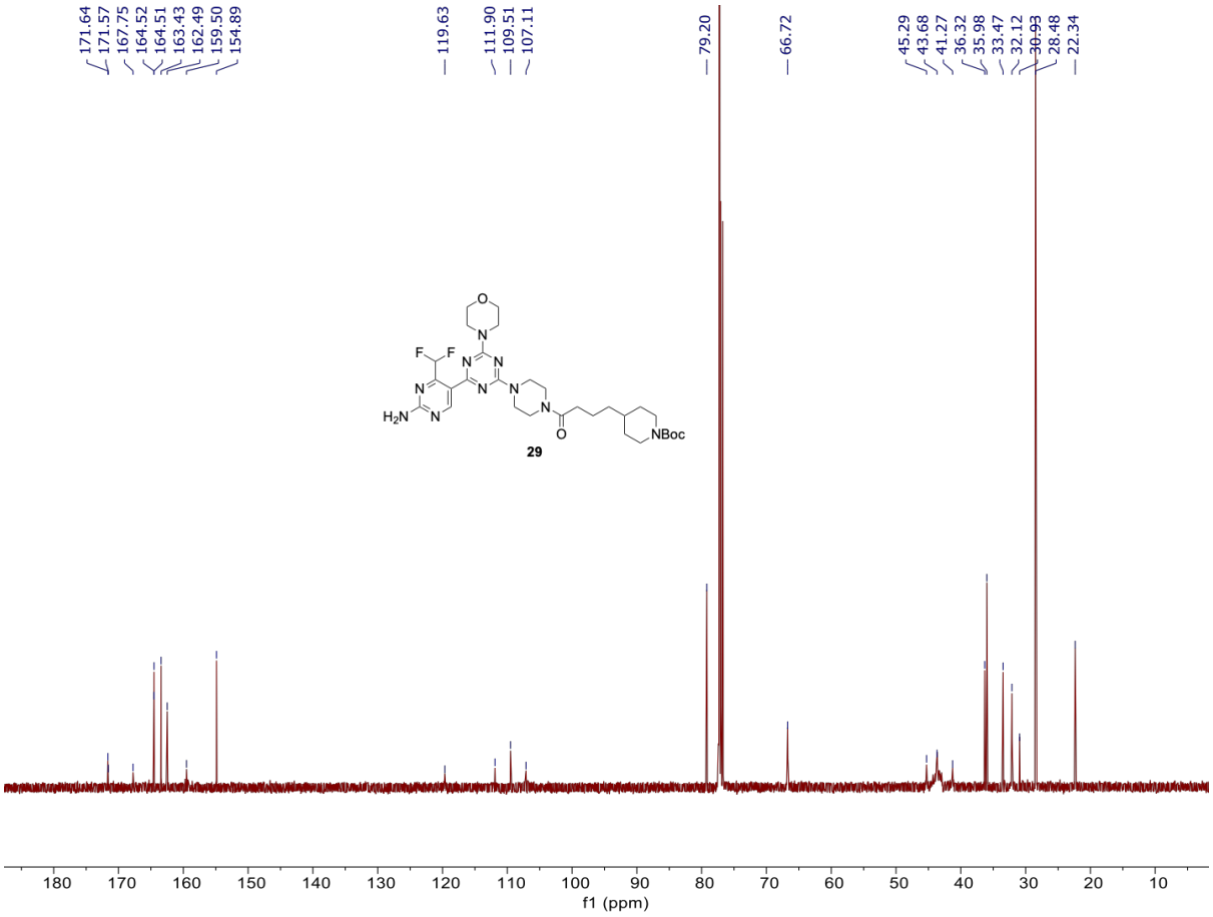

Figure S64. ^{13}C-NMR of compound **29** (101 MHz) in $CDCl_3$.

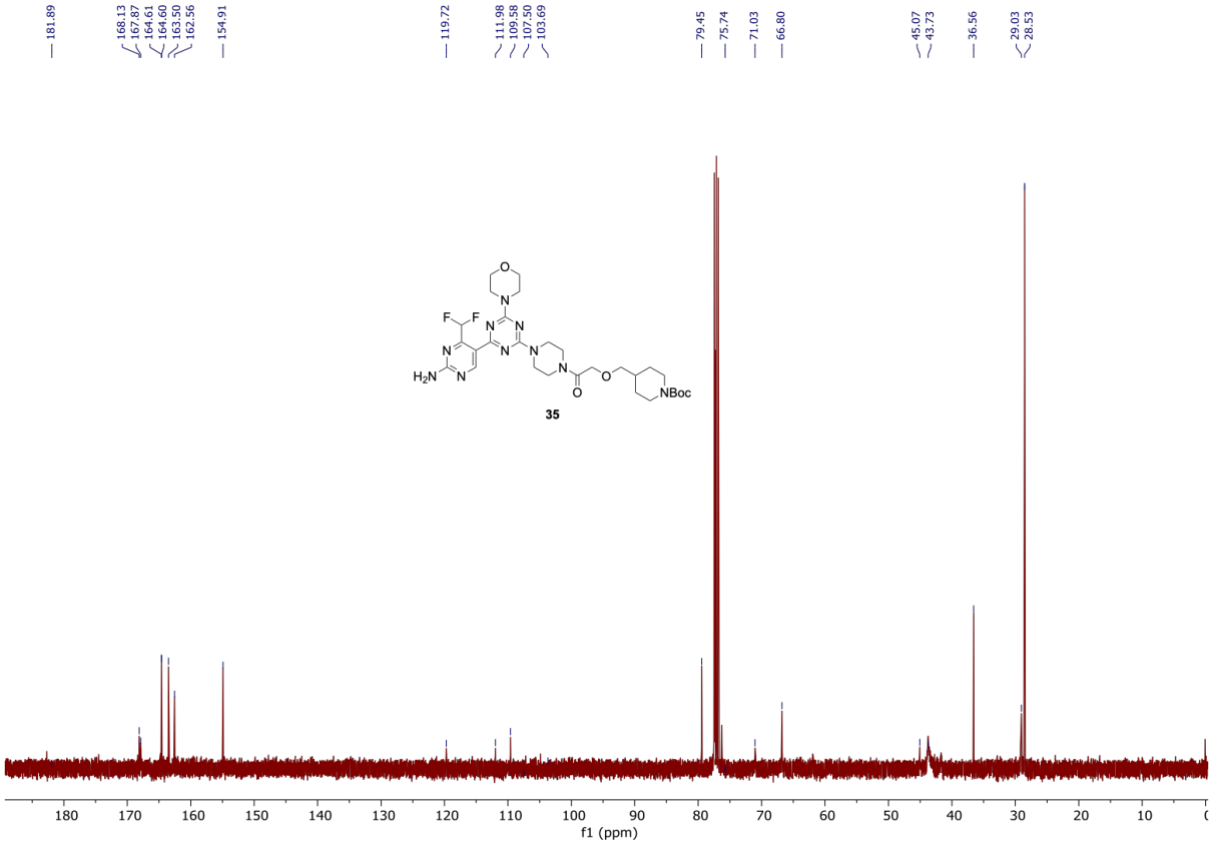

Figure S65. ^{13}C-NMR of compound **35** (101 MHz) in $CDCl_3$.

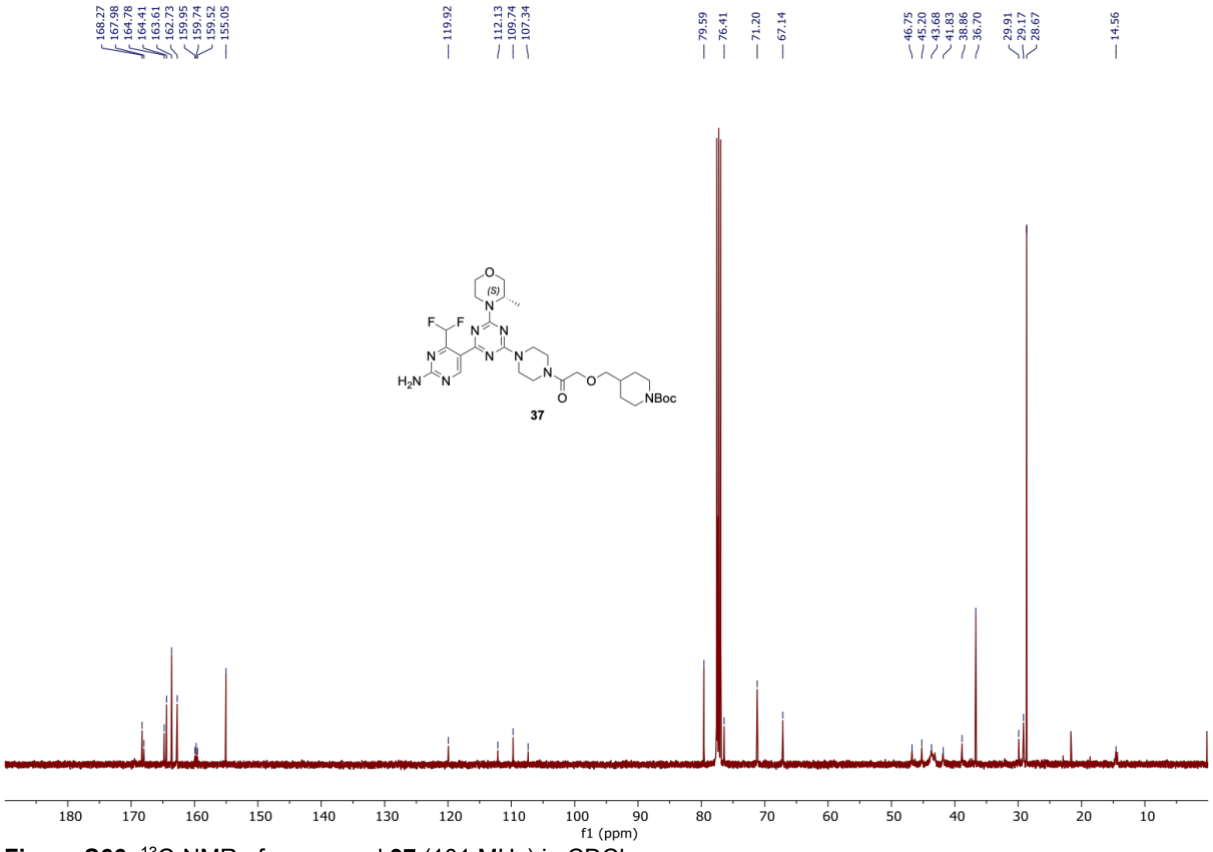

Figure S66. ^{13}C-NMR of compound **37** (101 MHz) in $CDCl_3$.

MS data

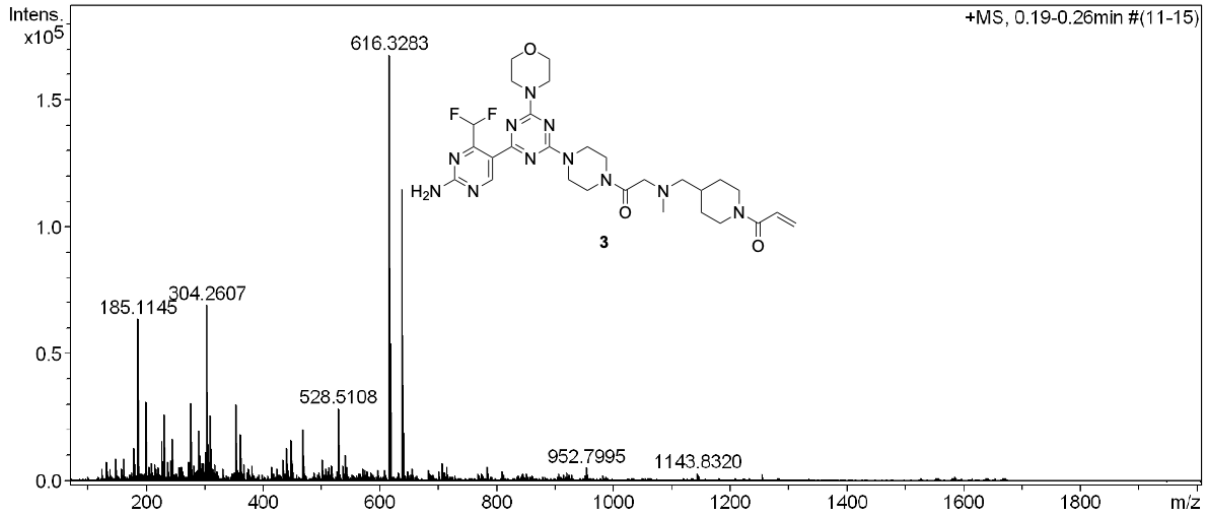

Figure S67. HRMS of compound **3**.

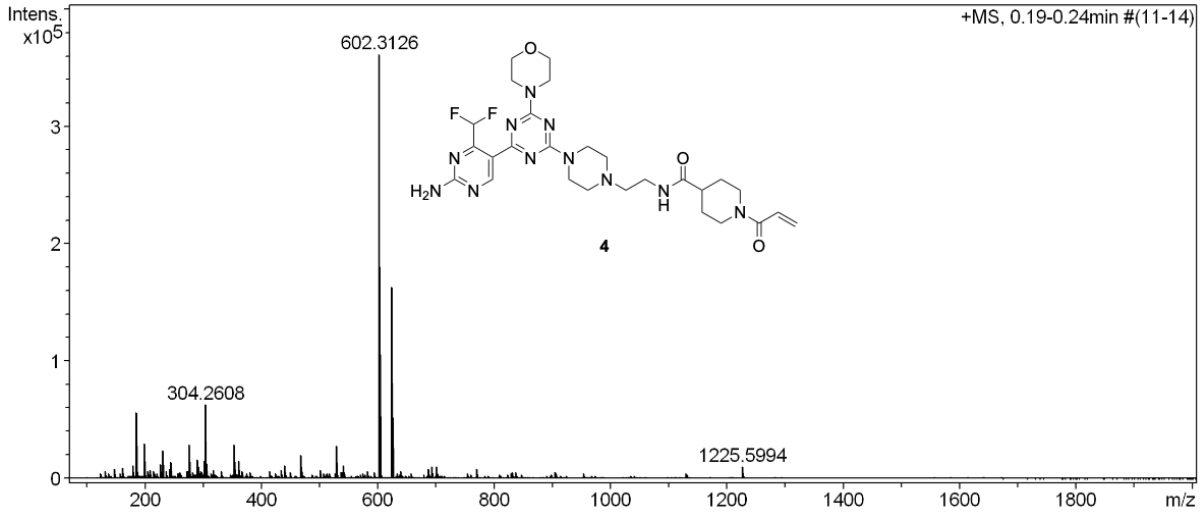

Figure S68. HRMS of compound **4**.

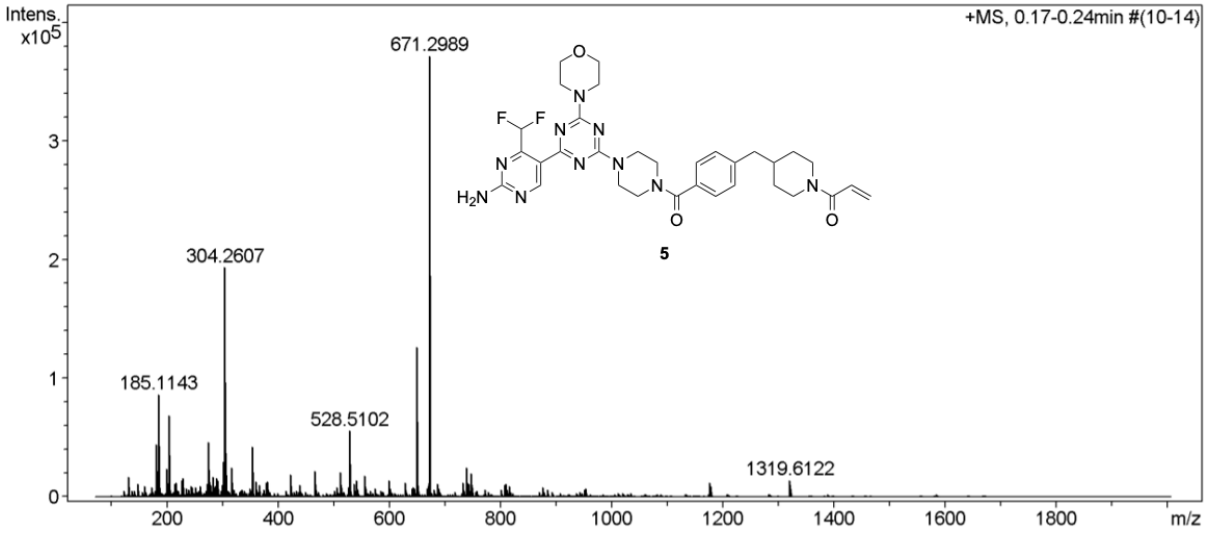

Figure S69. HRMS of compound **5**.

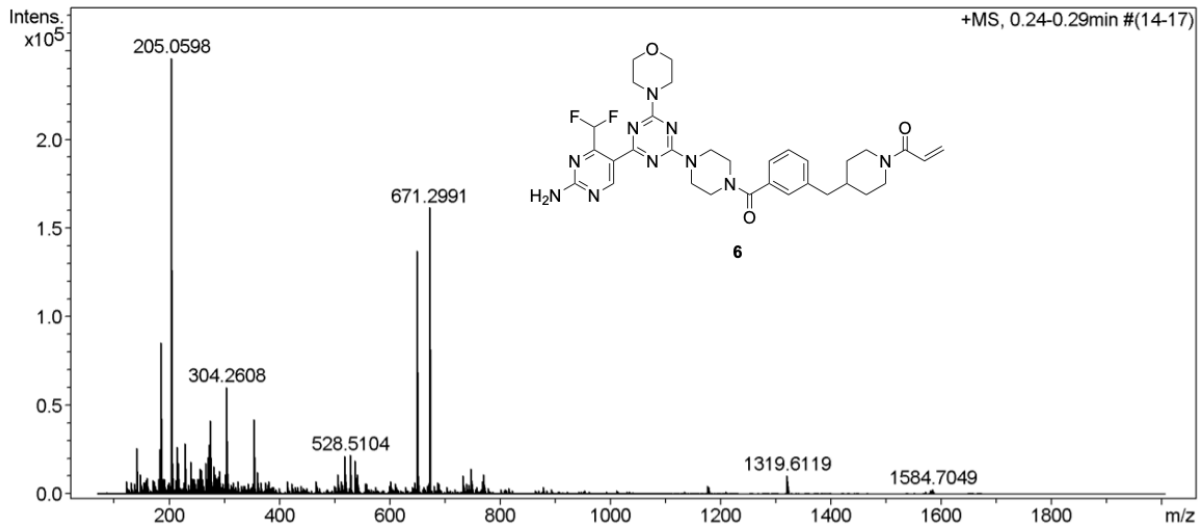

Figure S70. HRMS of compound **6**.

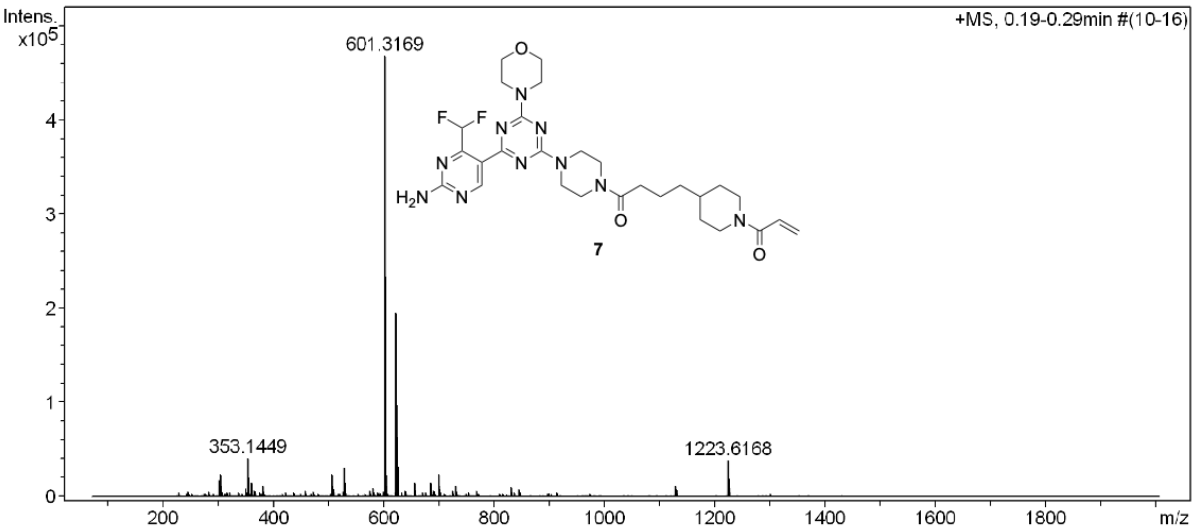

Figure S71. HRMS of compound **7**.

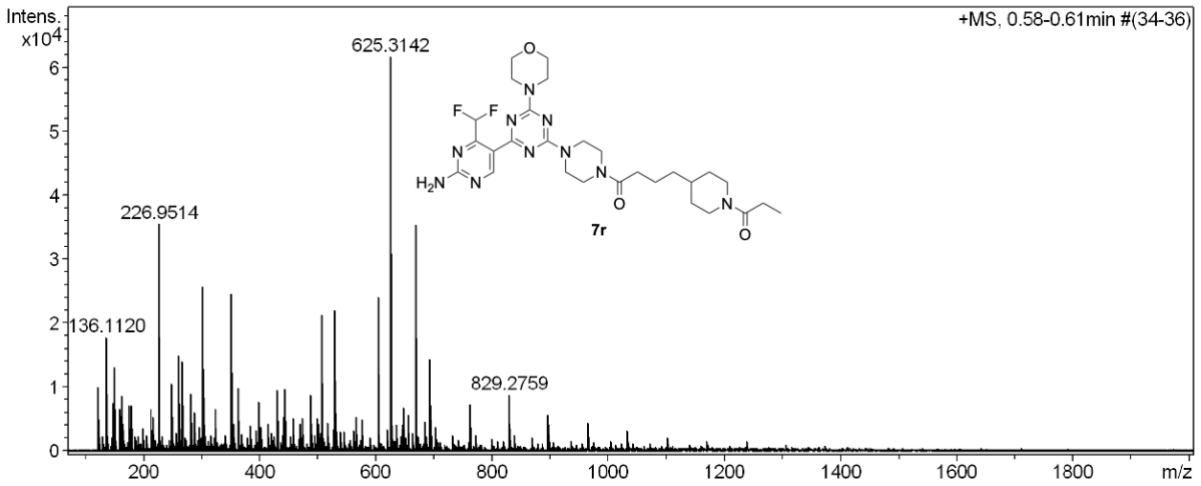

Figure S72. HRMS of compound **7r**.

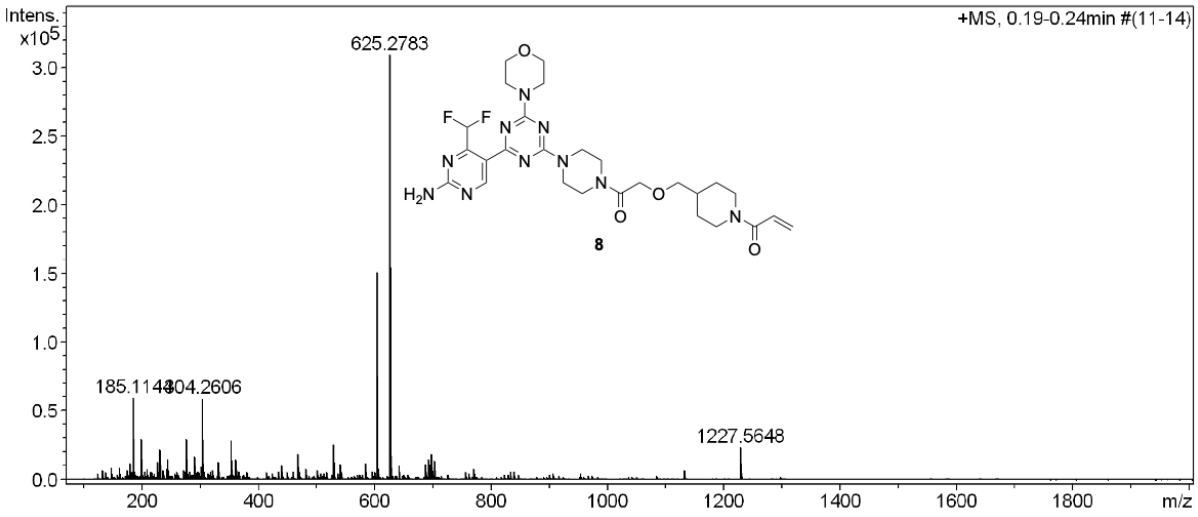

Figure S73. HRMS of compound **8**.

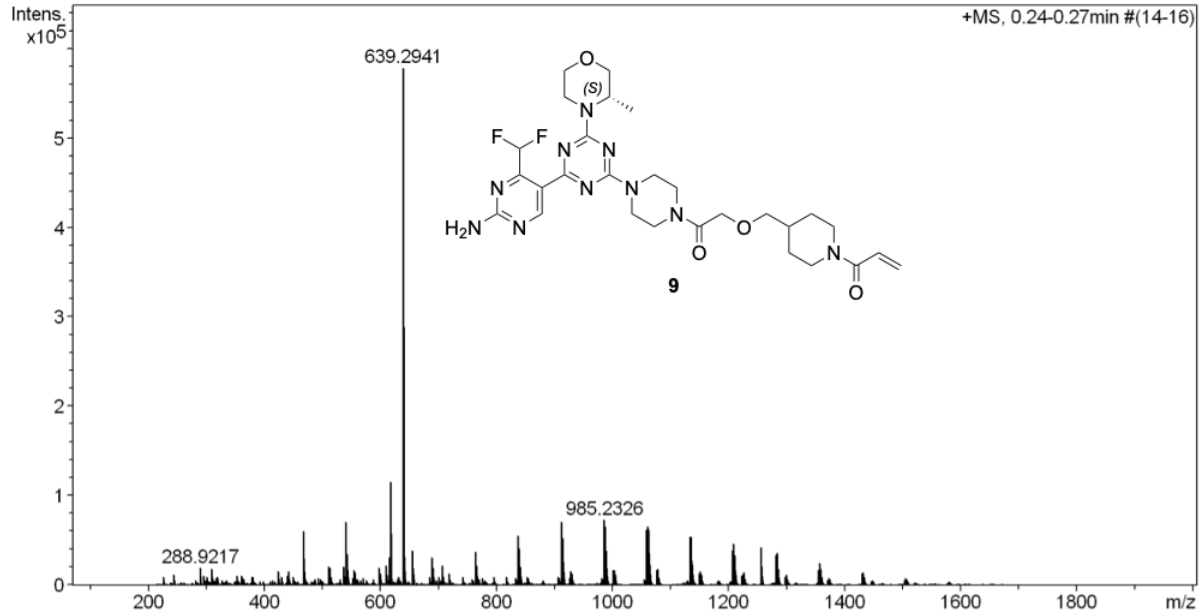

Figure S74. HRMS of compound **9**.

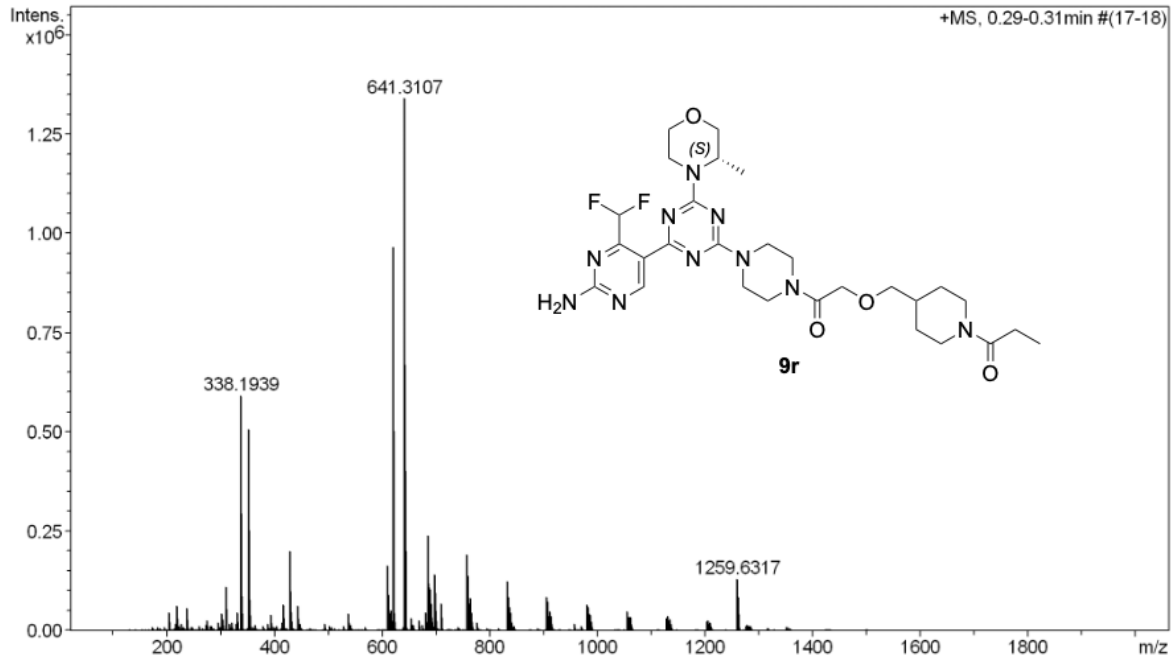

Figure S75. HRMS of compound **9r**.

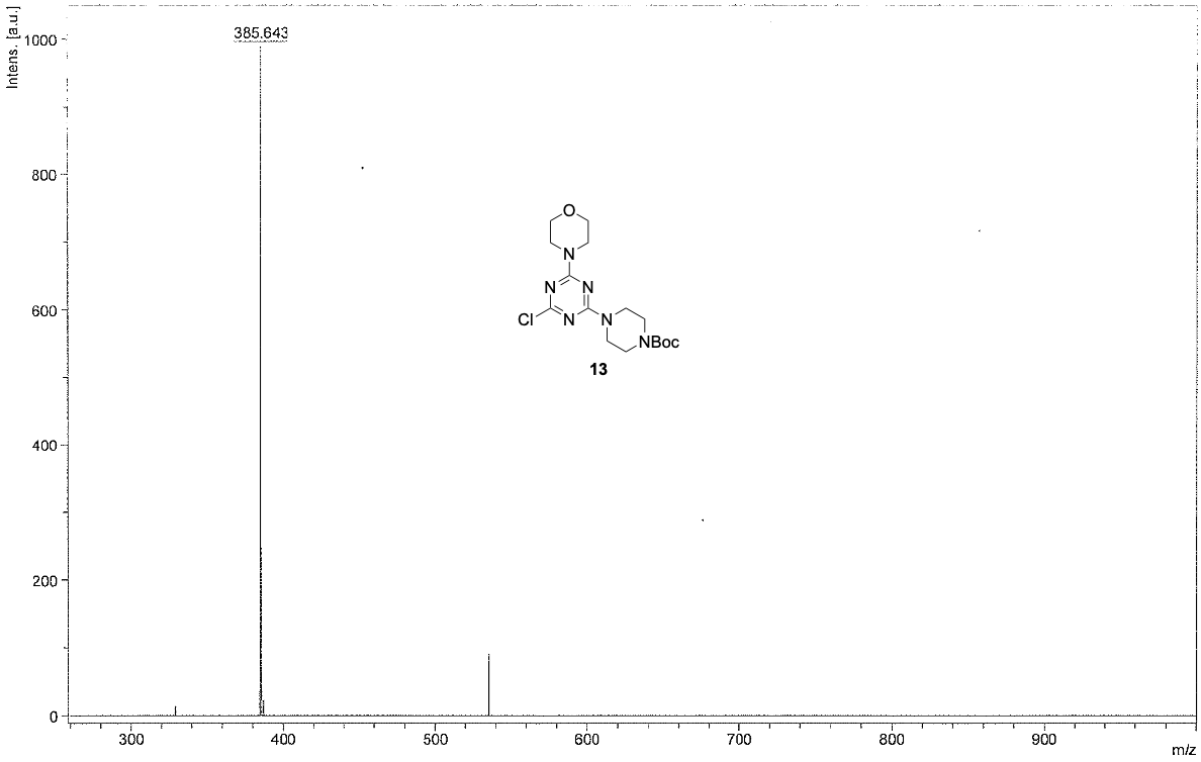

Figure S76. MALDI-MS of compound **13**.

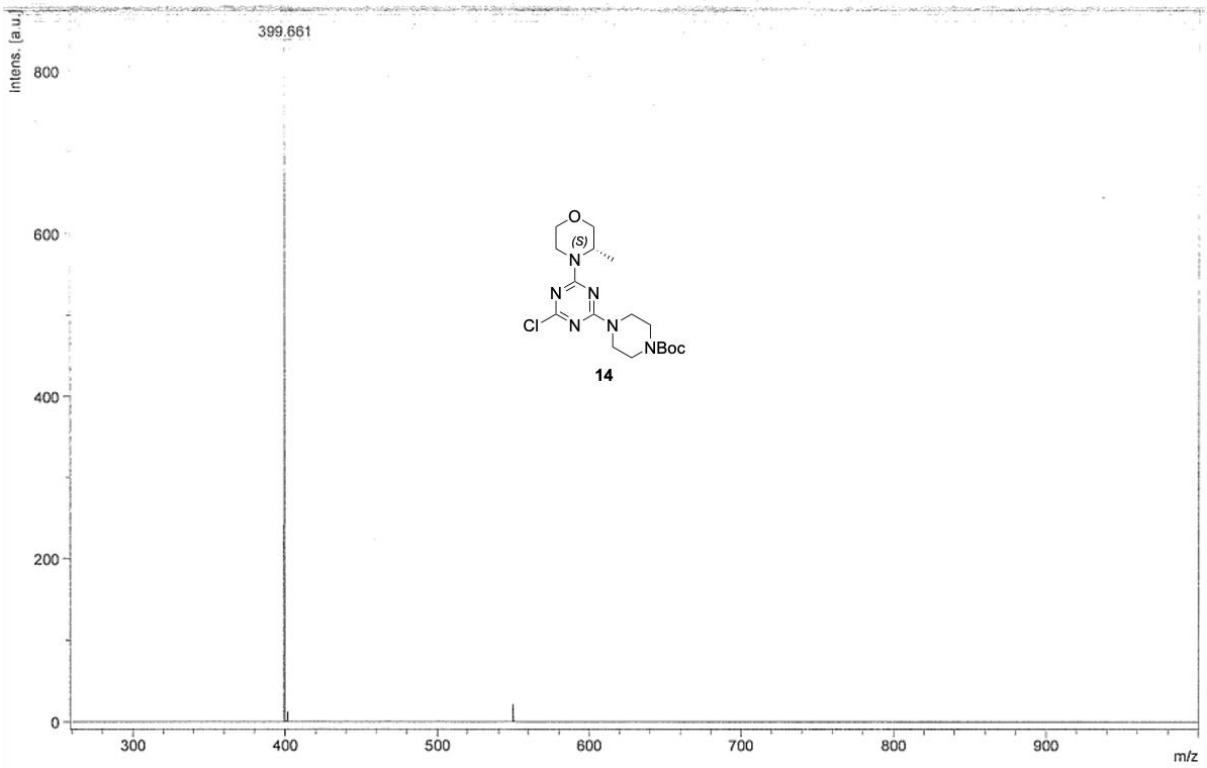

Figure S77. MALDI-MS of compound **14**.

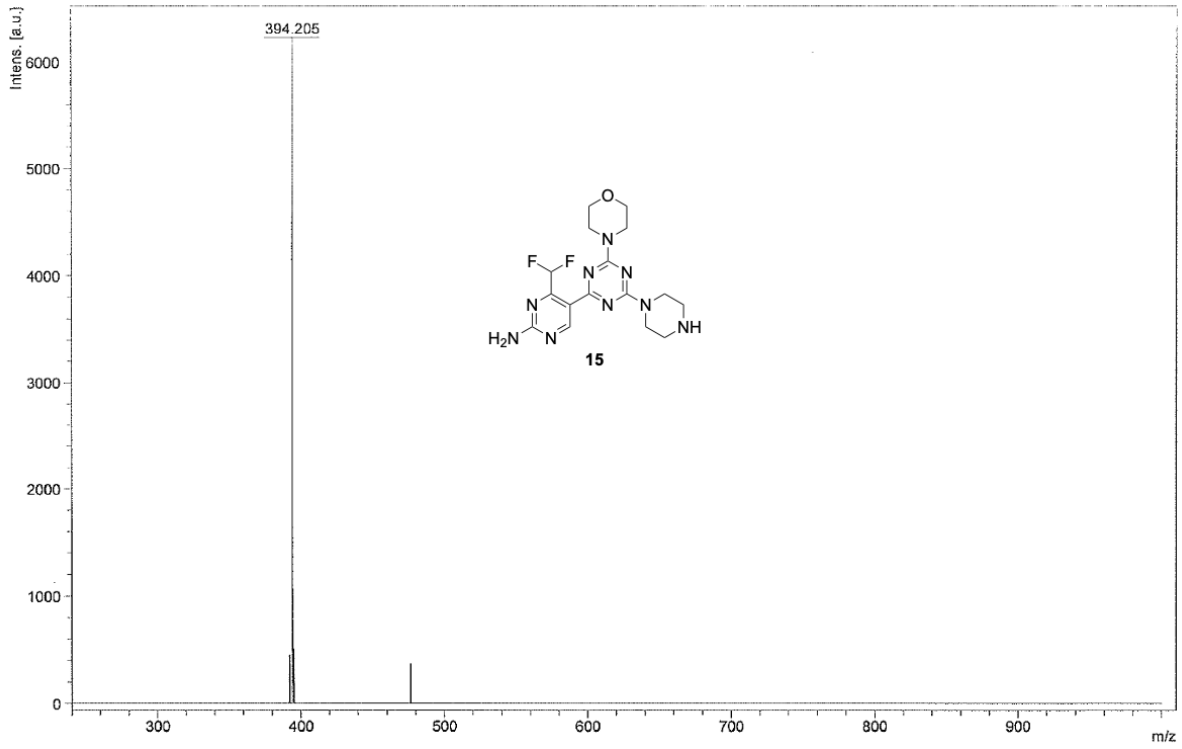

Figure S78. MALDI-MS of compound **15**.

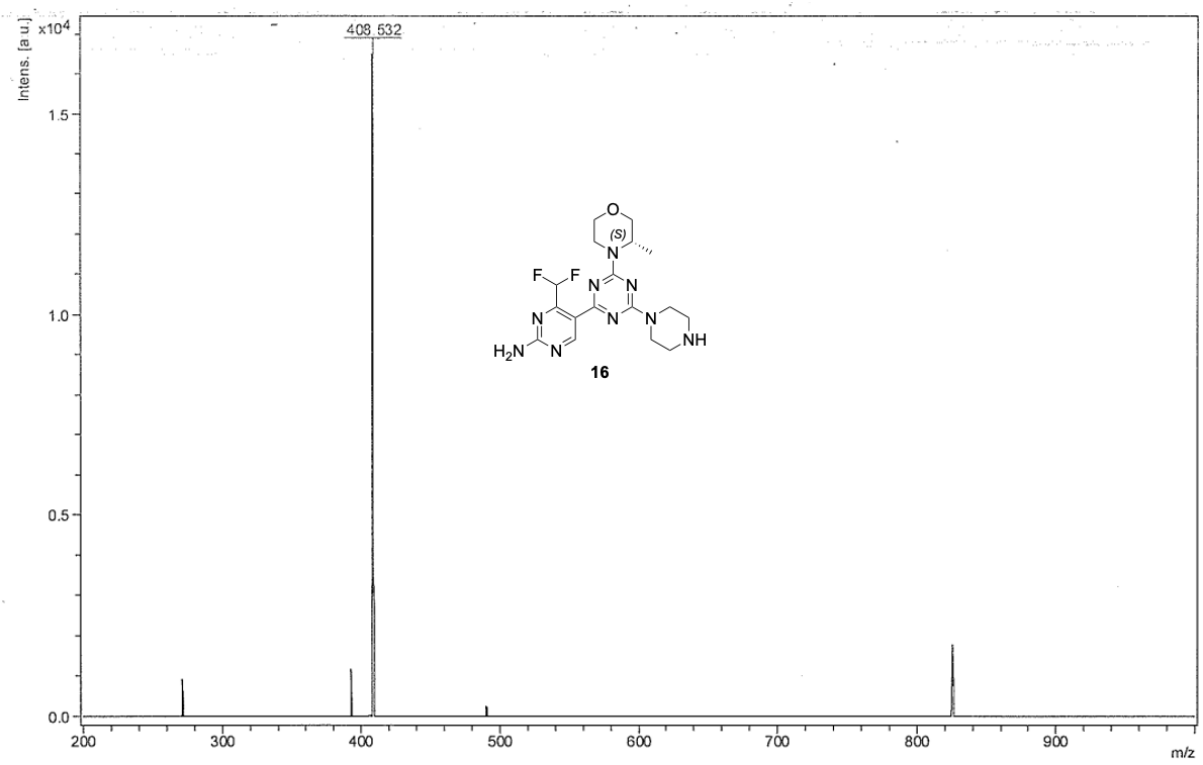

Figure S79. MALDI-MS of compound **16**.

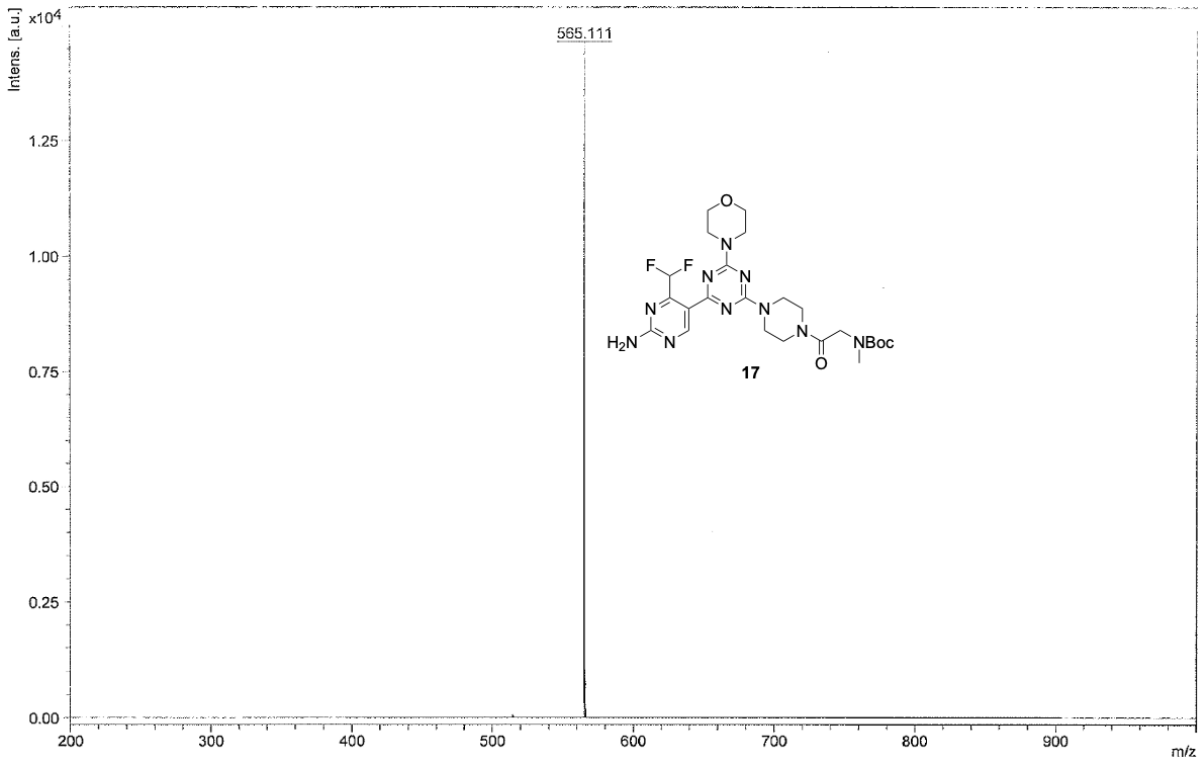

Figure S80. MALDI-MS of compound **17**.

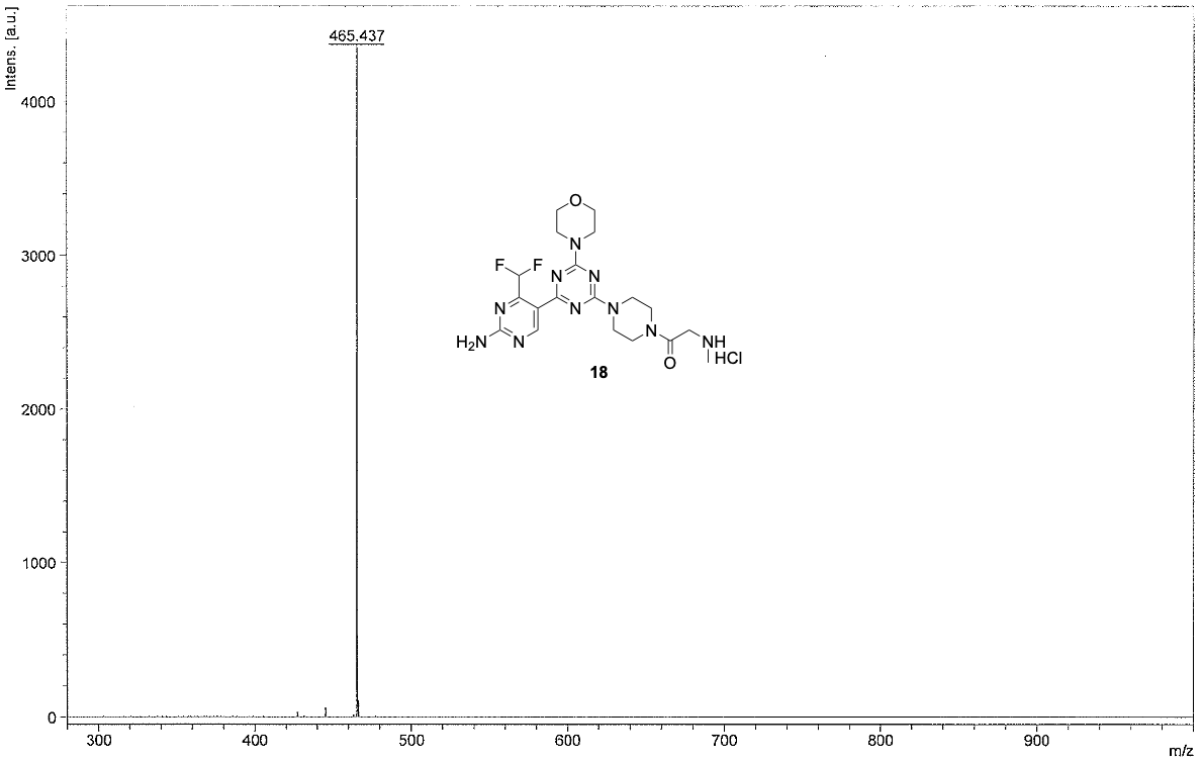

Figure S81. MALDI-MS of compound **18**.

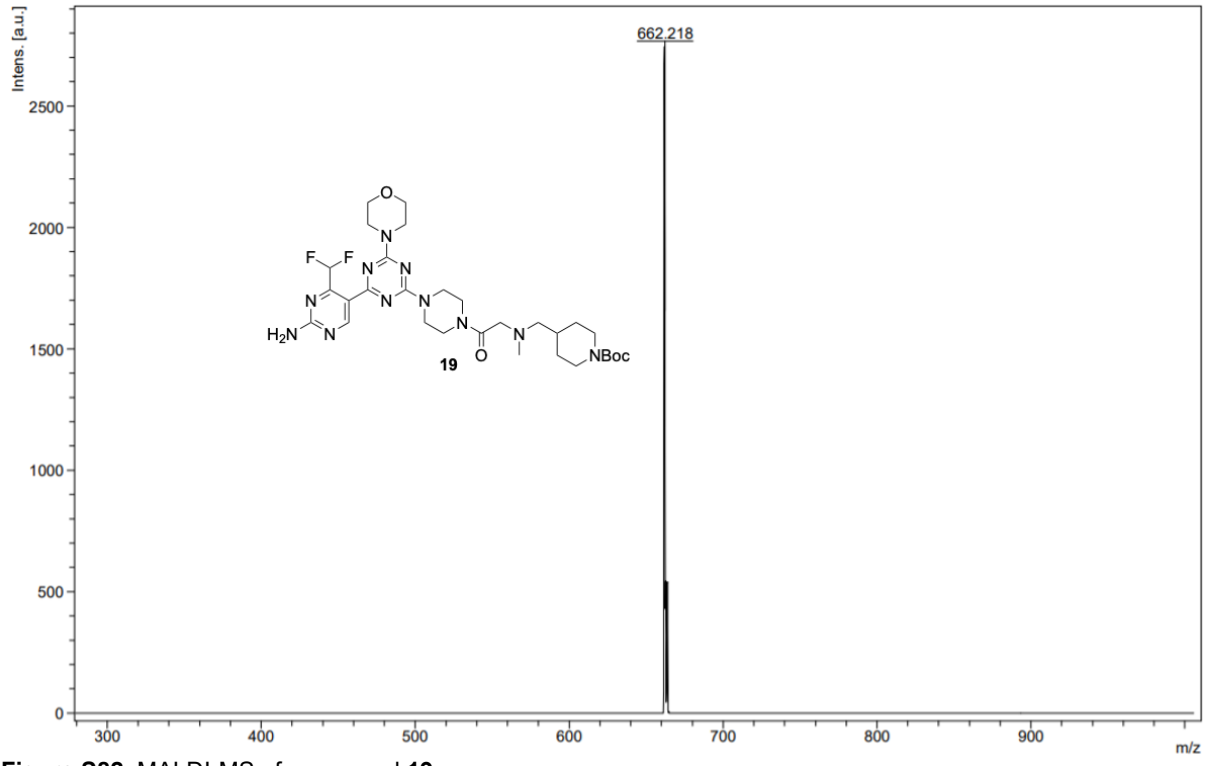

Figure S82. MALDI-MS of compound **19**.

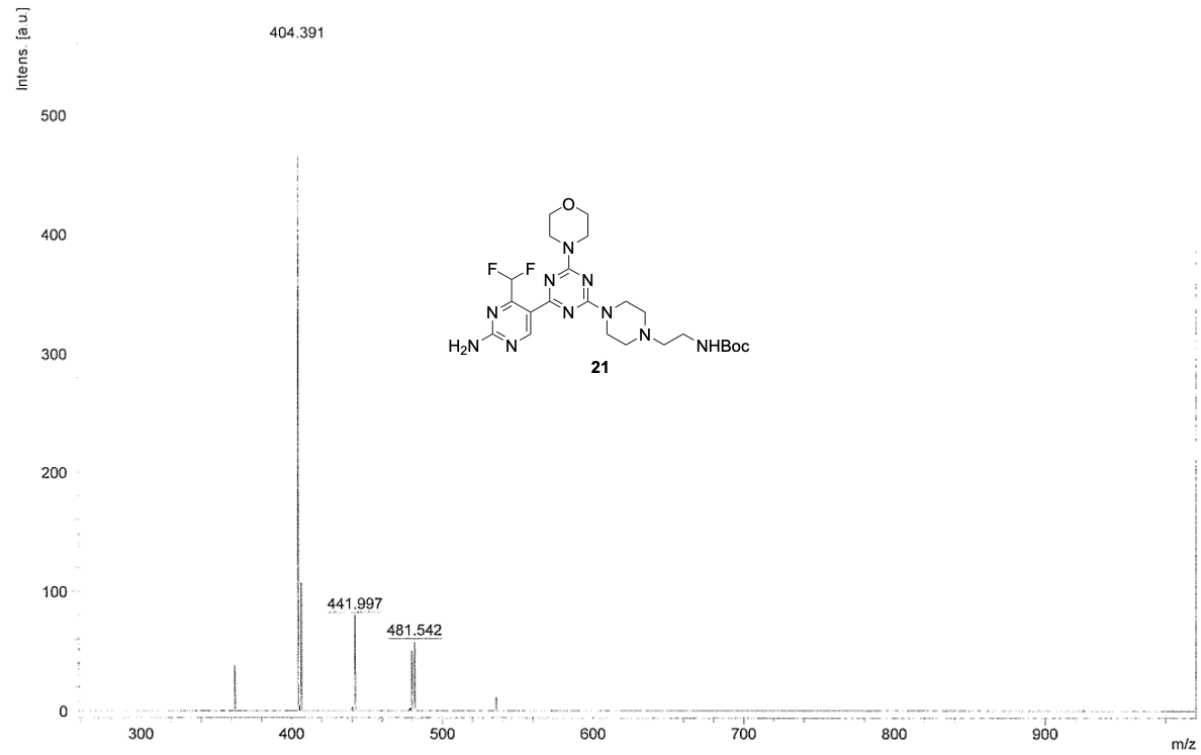

Figure S83. MALDI-MS of compound **21**.

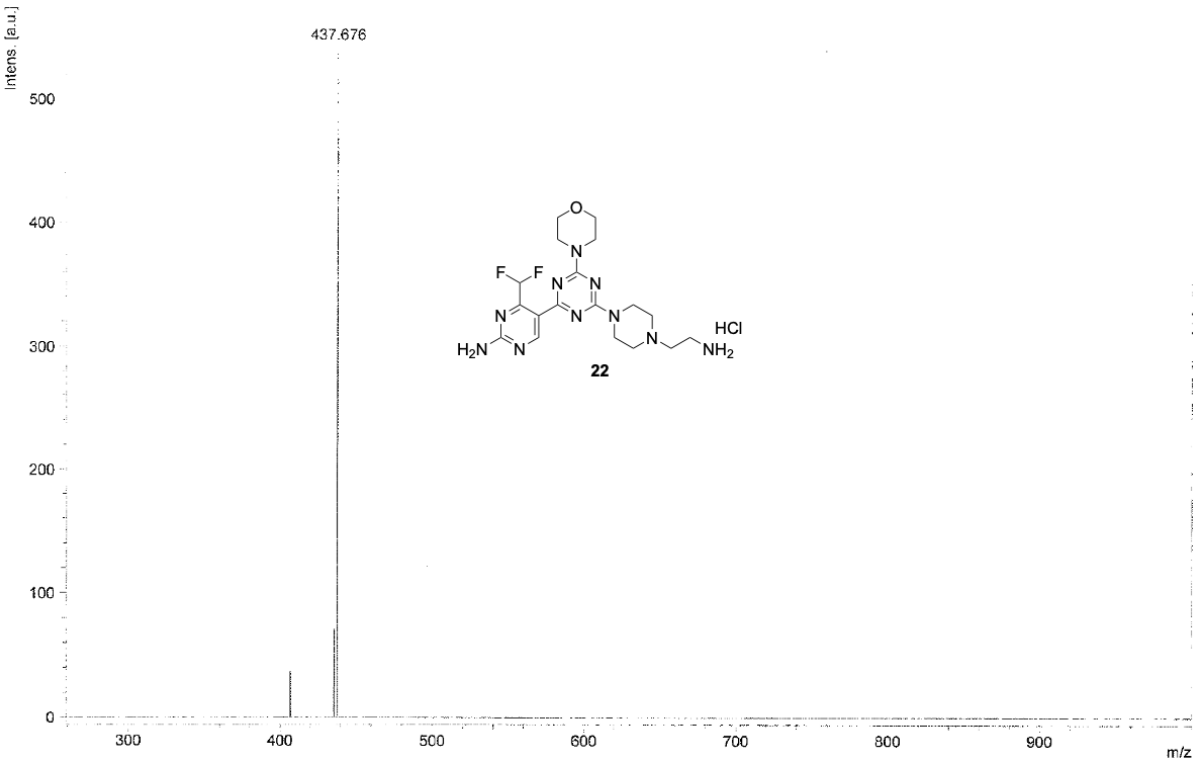

Figure S84. MALDI-MS of compound **22**.

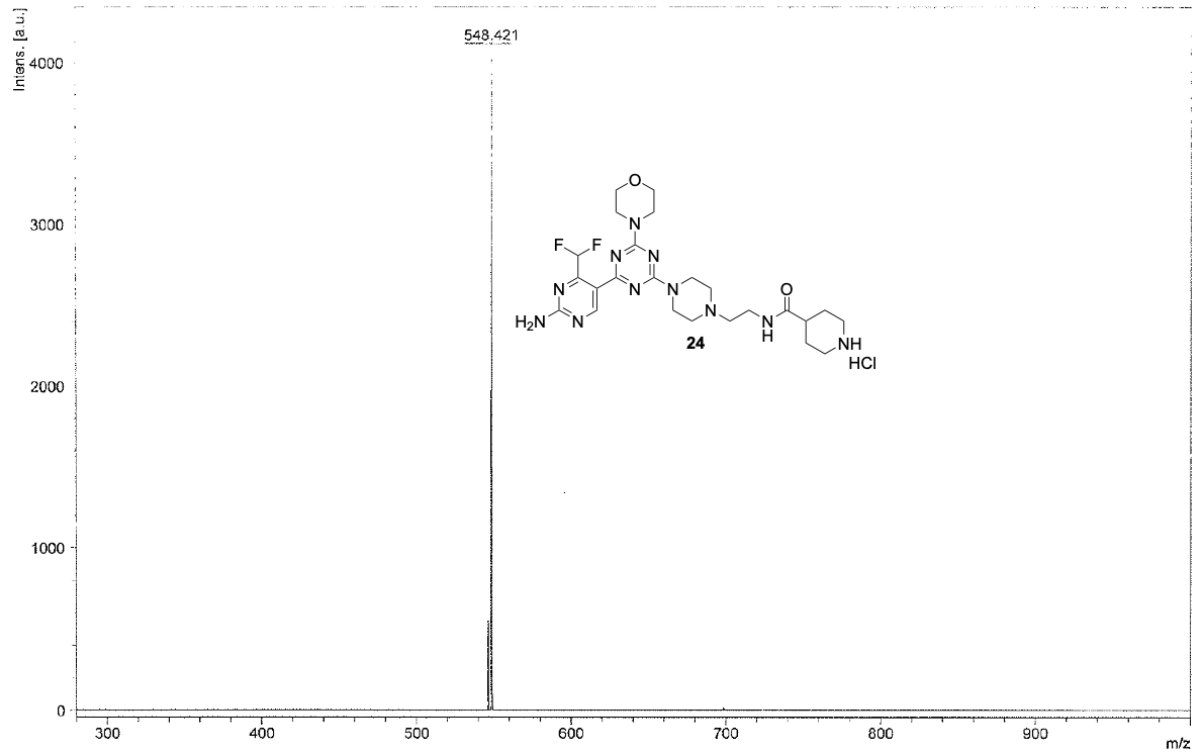

Figure S85. MALDI-MS of compound **24**.

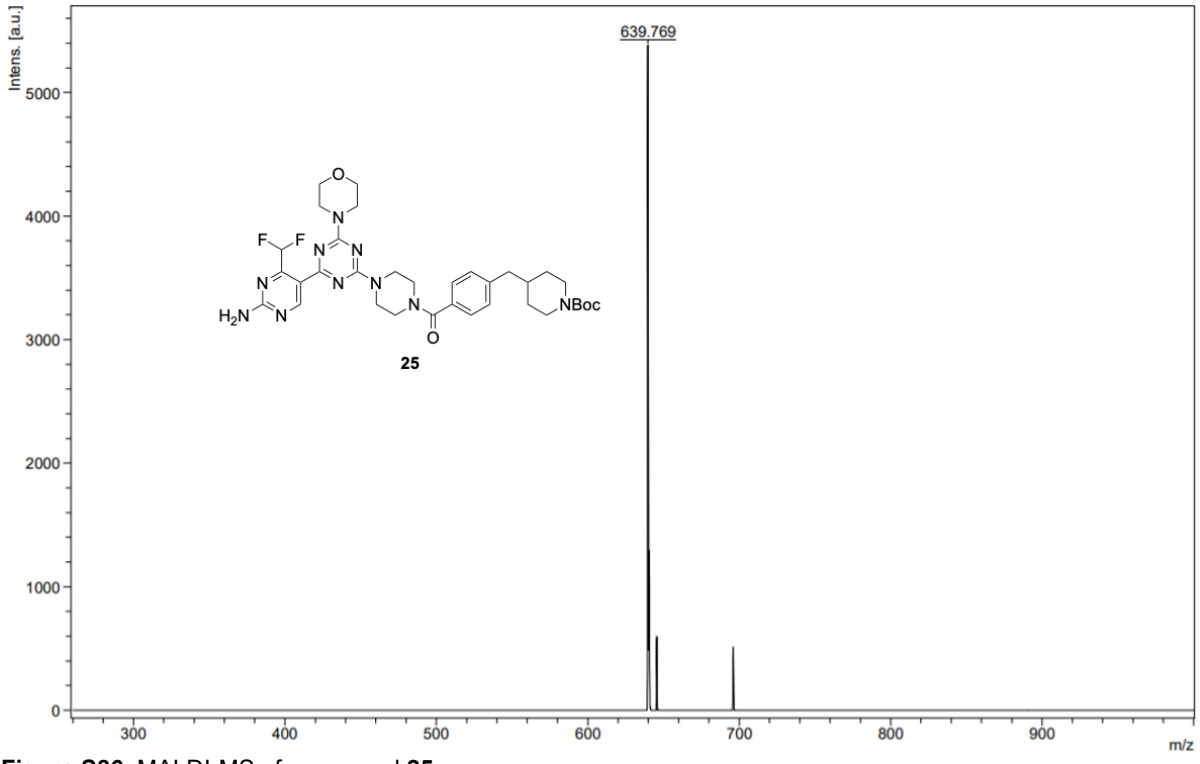

Figure S86. MALDI-MS of compound **25**.

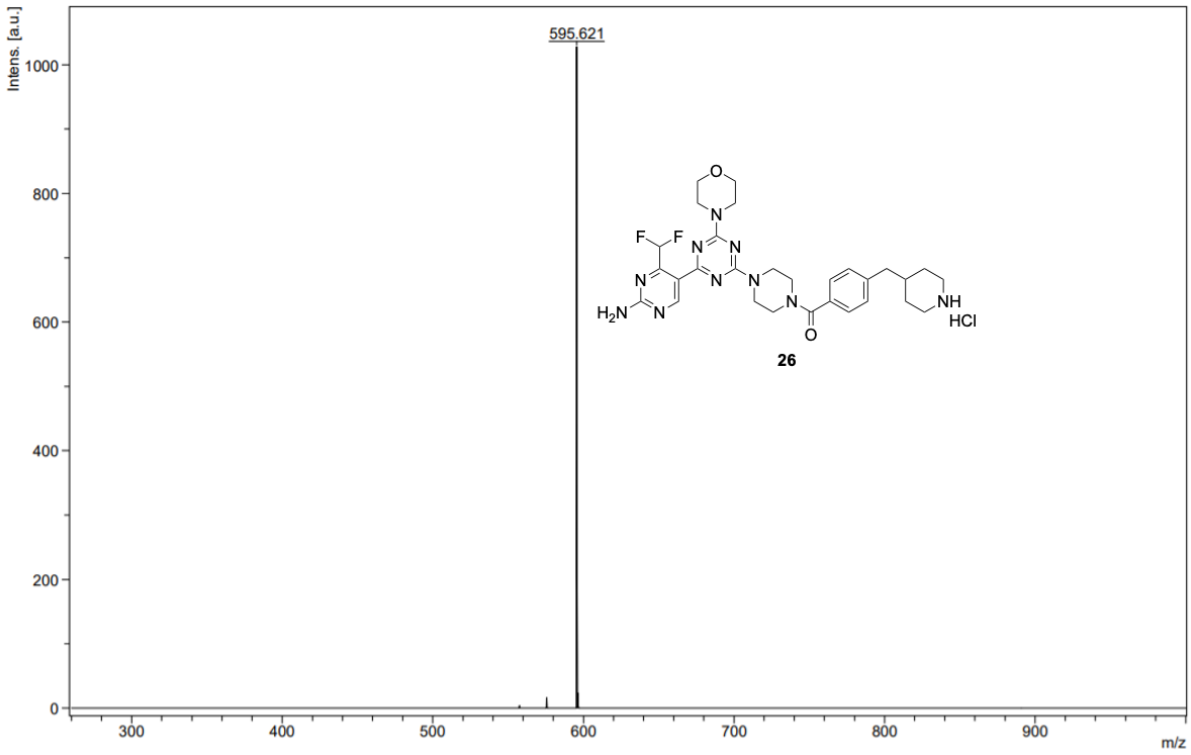

Figure S87. MALDI-MS of compound **26**.

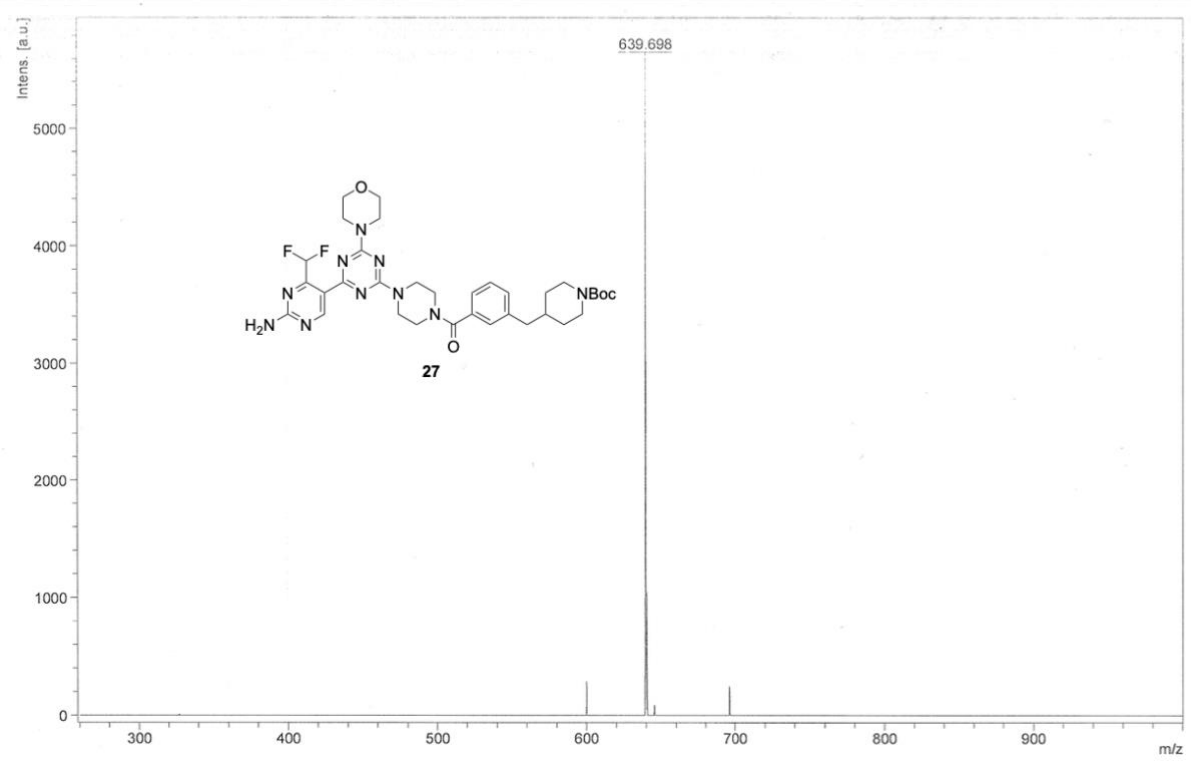

Figure S88. MALDI-MS of compound **27**.

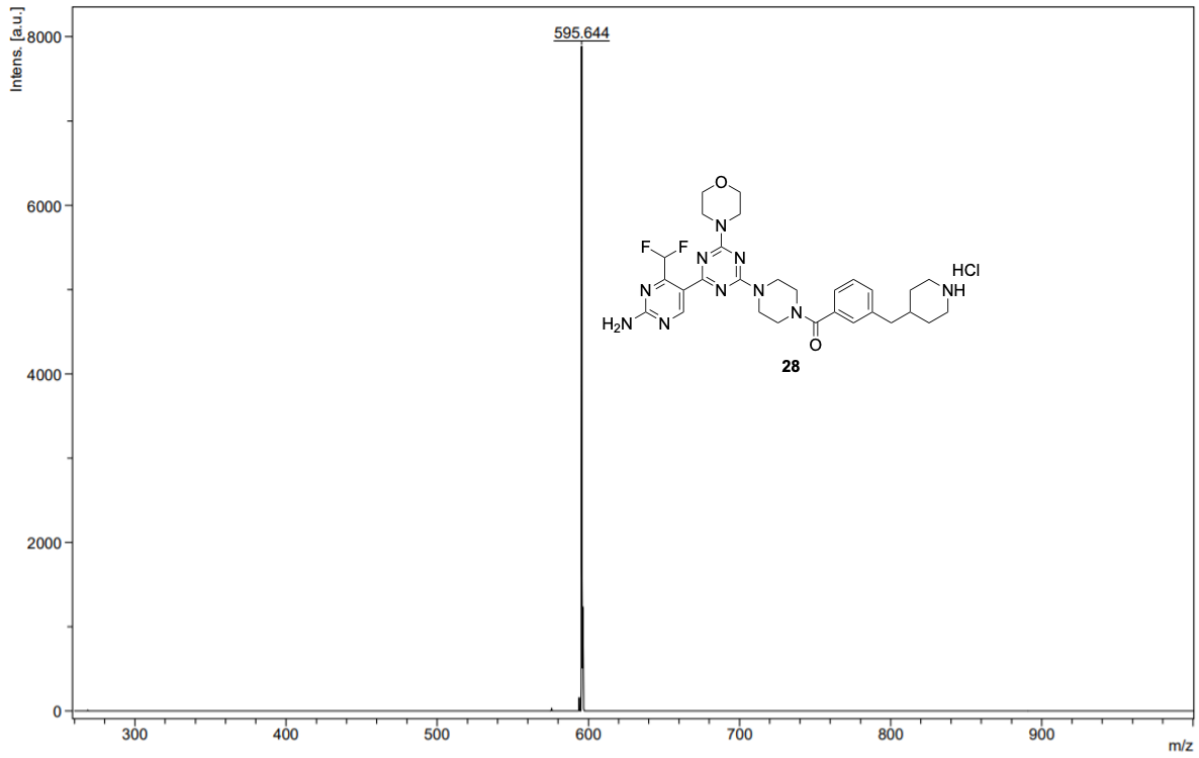

Figure S89. MALDI-MS of compound **28**.

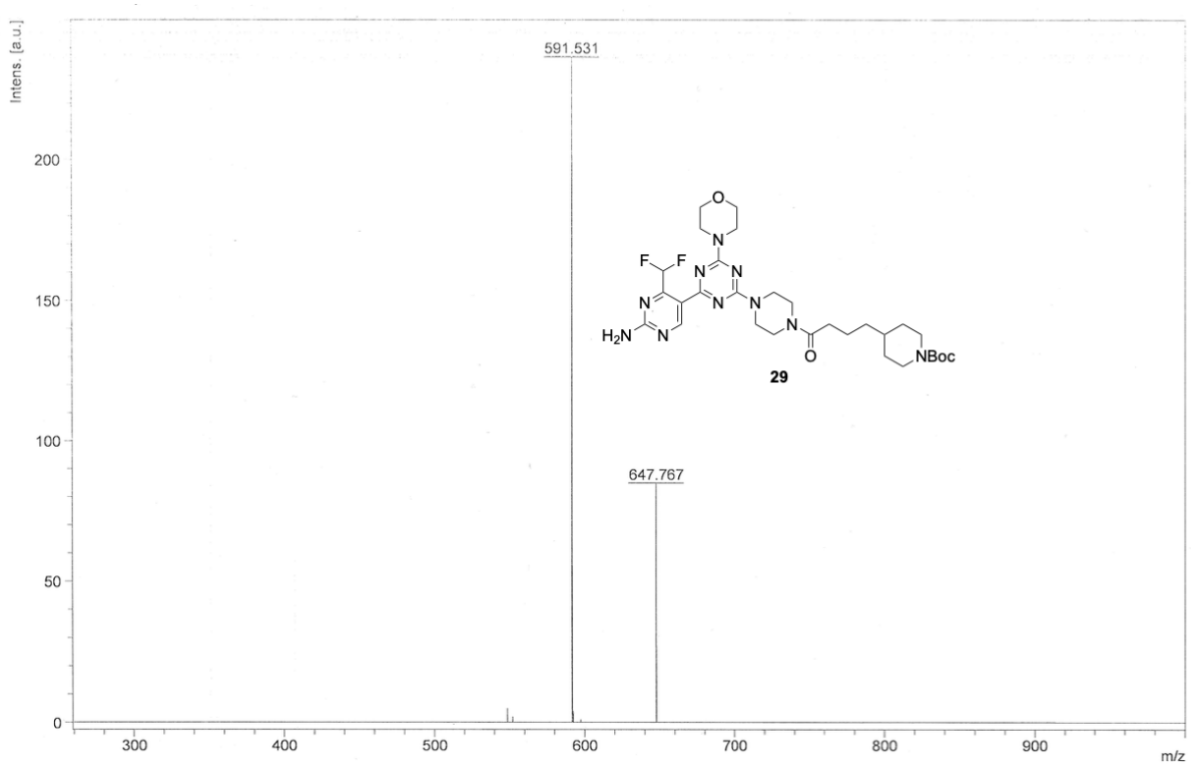

Figure S90. MALDI-MS of compound **29**.

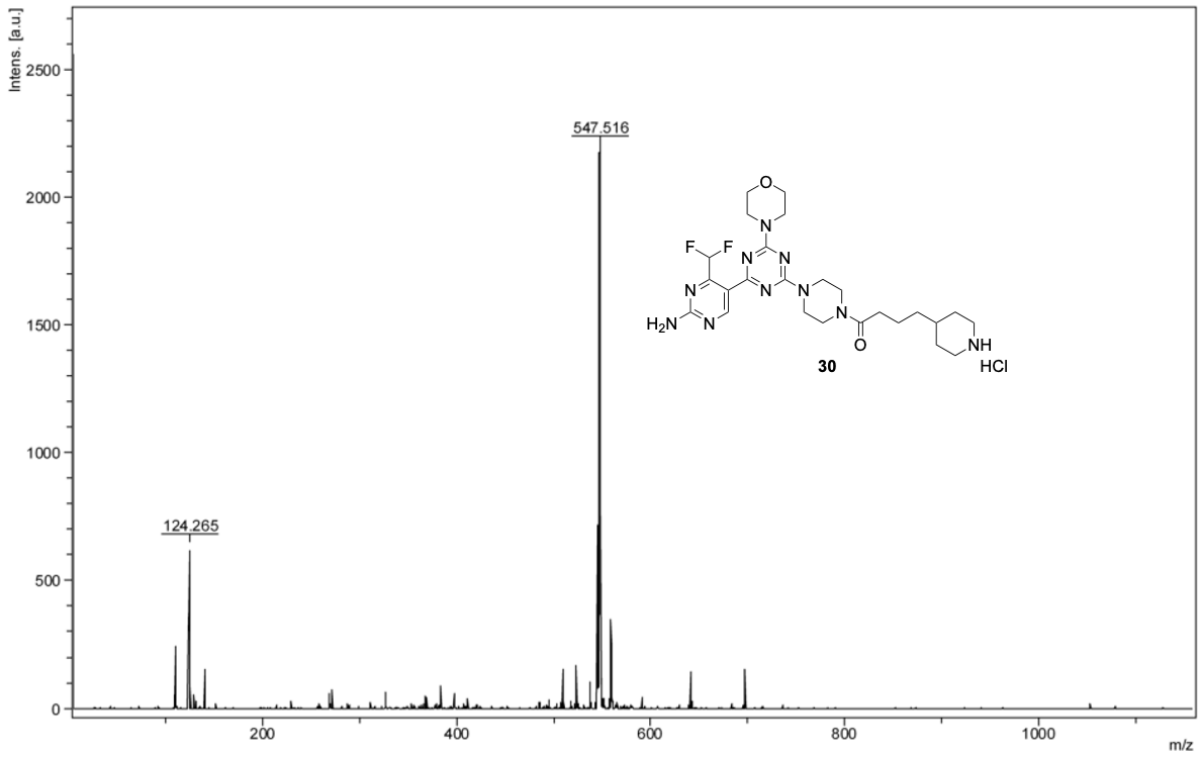

Figure S91. MALDI-MS of compound **30**.

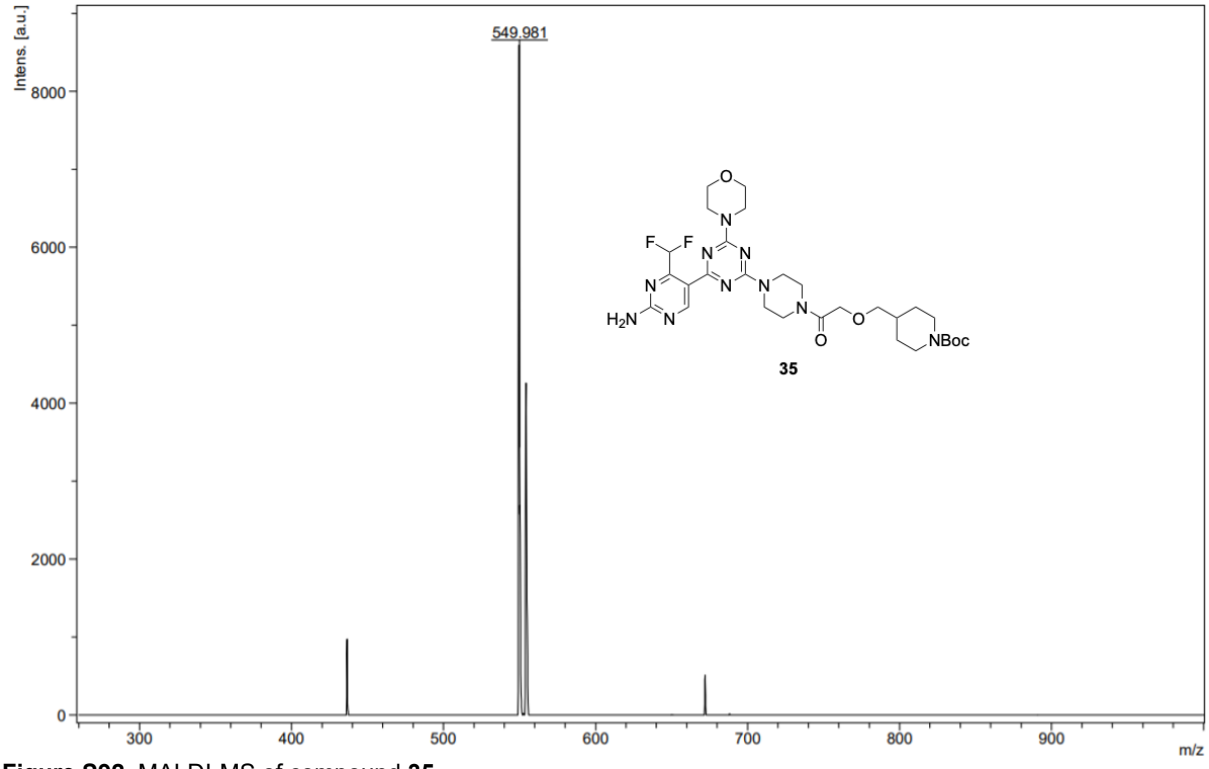

Figure S92. MALDI-MS of compound **35**.

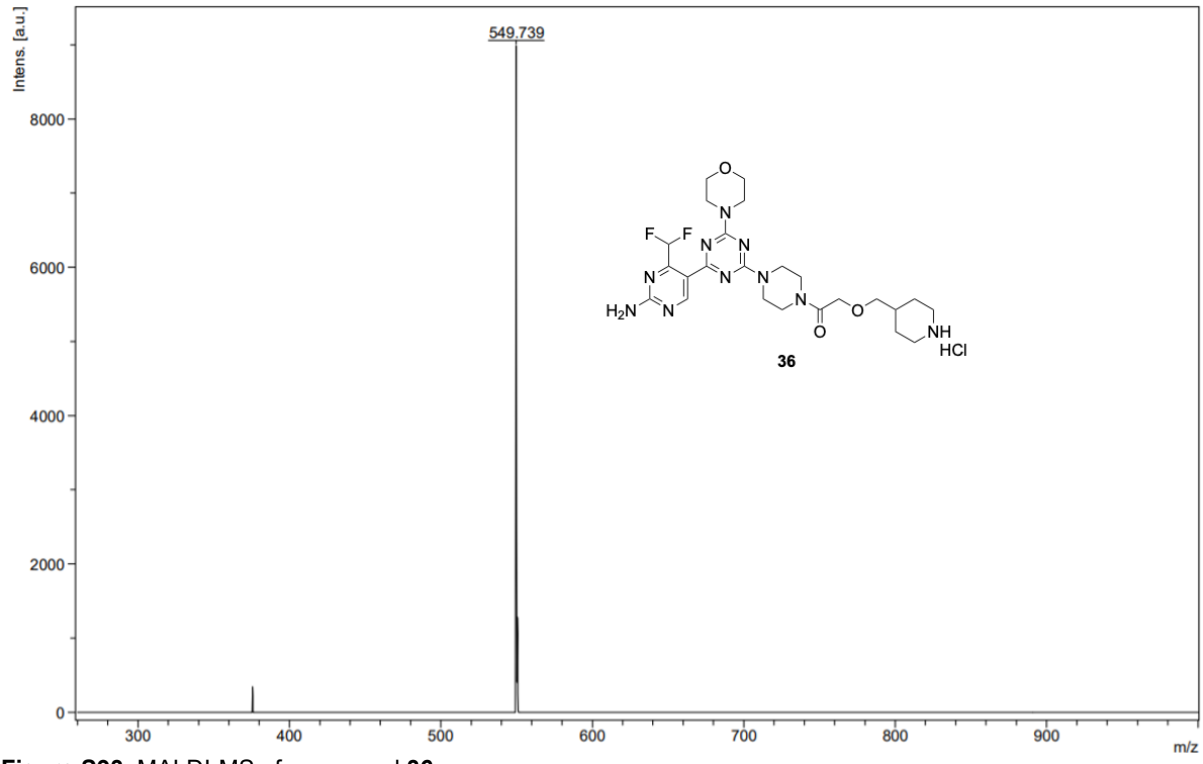

Figure S93. MALDI-MS of compound **36**.

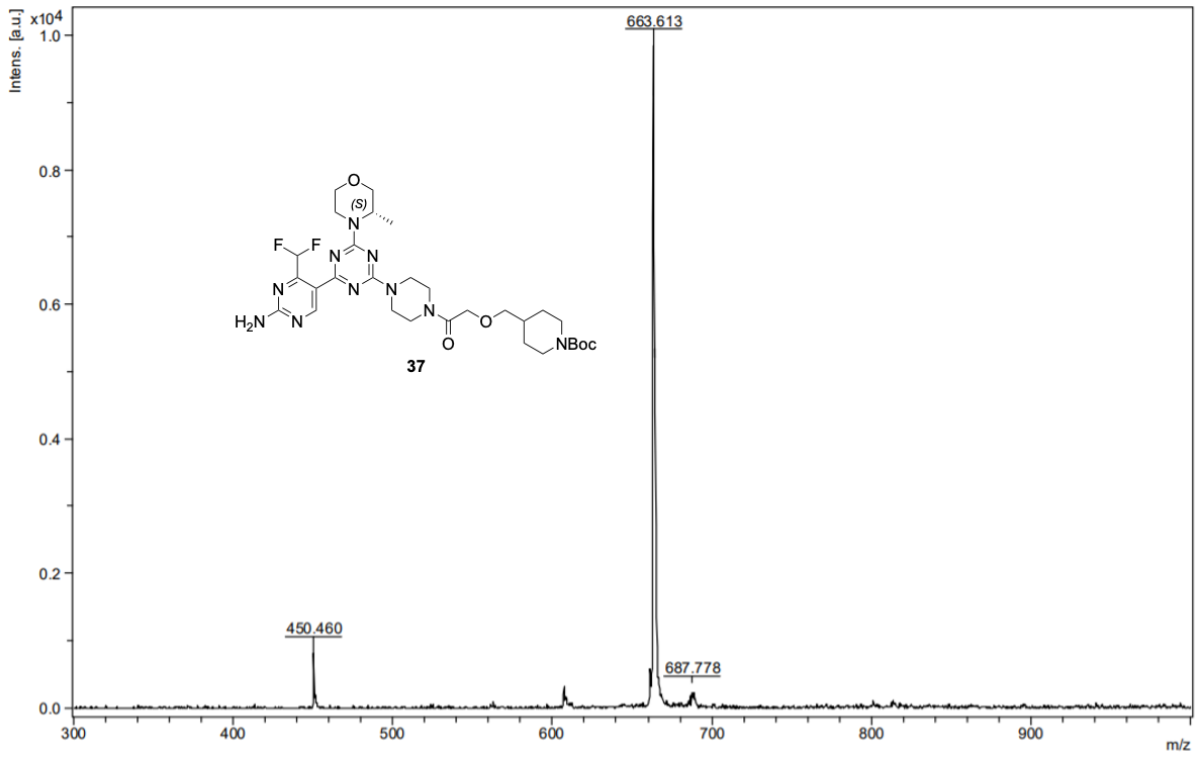

Figure S94. MALDI-MS of compound **37**.

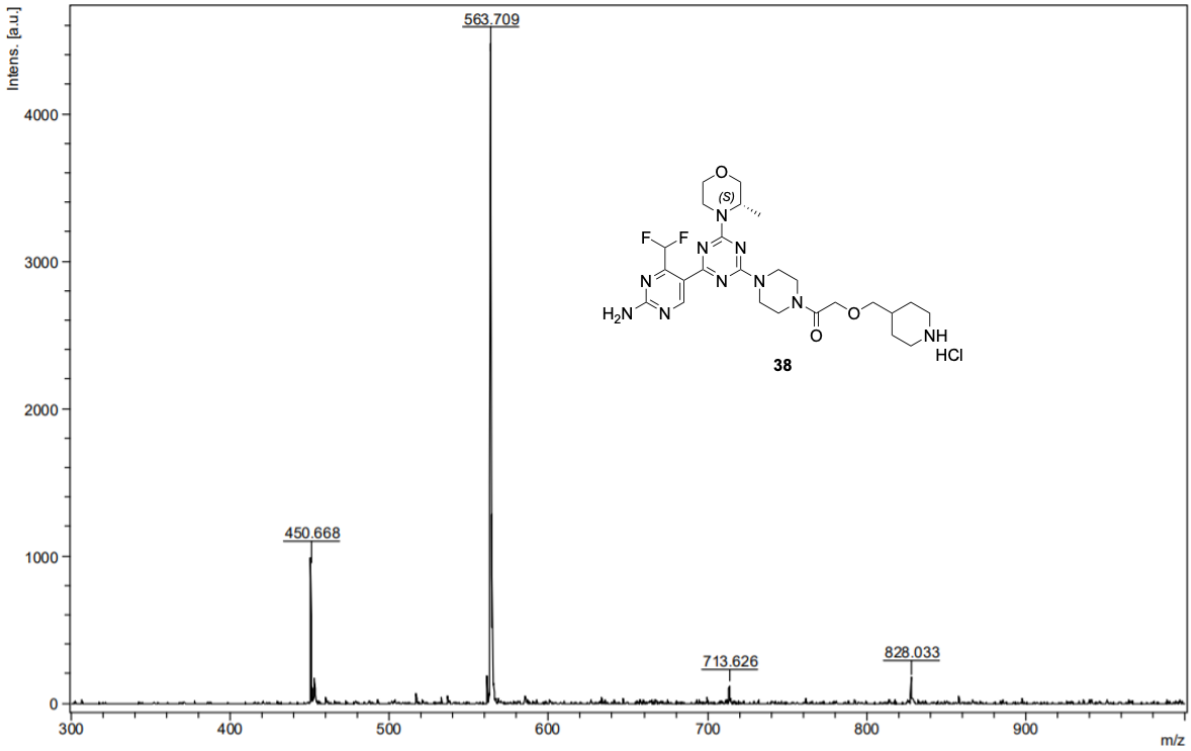

Figure S95. MALDI-MS of compound **38**.

HPLC data

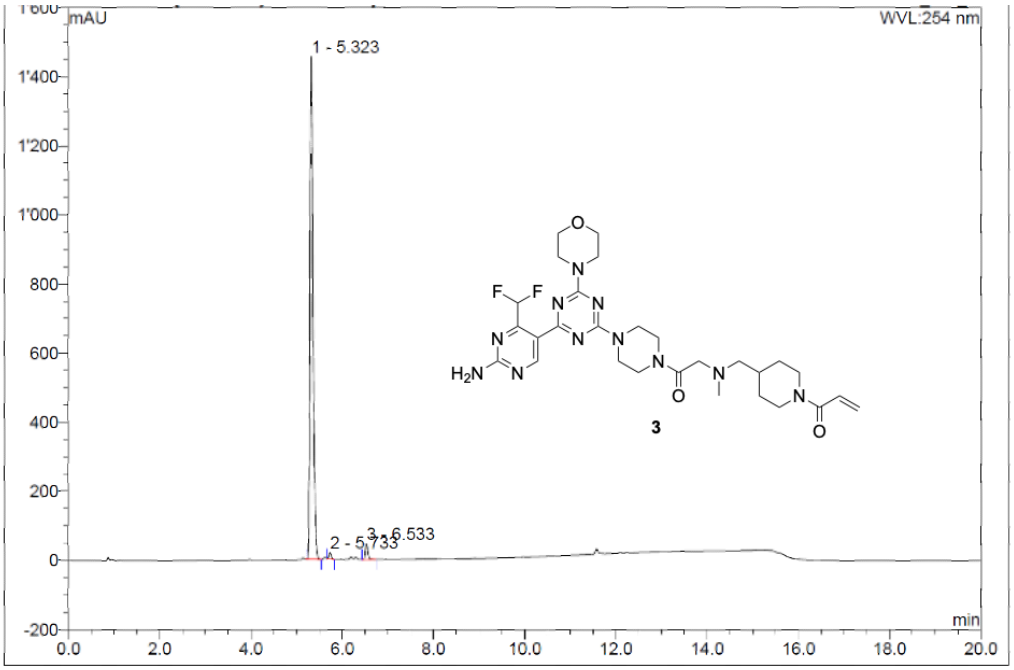

No.	Ret.Time min	Peak Name	Height mAU	Area mAU*min	Rel.Area %	Amount	Type
1	5.32	n.a.	1455.338	112.192	96.59	n.a.	BMB
2	5.73	n.a.	18.819	1.068	0.92	n.a.	BMB
3	6.53	n.a.	45.217	2.895	2.49	n.a.	BMB
Total:			1519.375	116.155	100.00	0.000	

Figure S96. HPLC chromatogram of compound **3**.

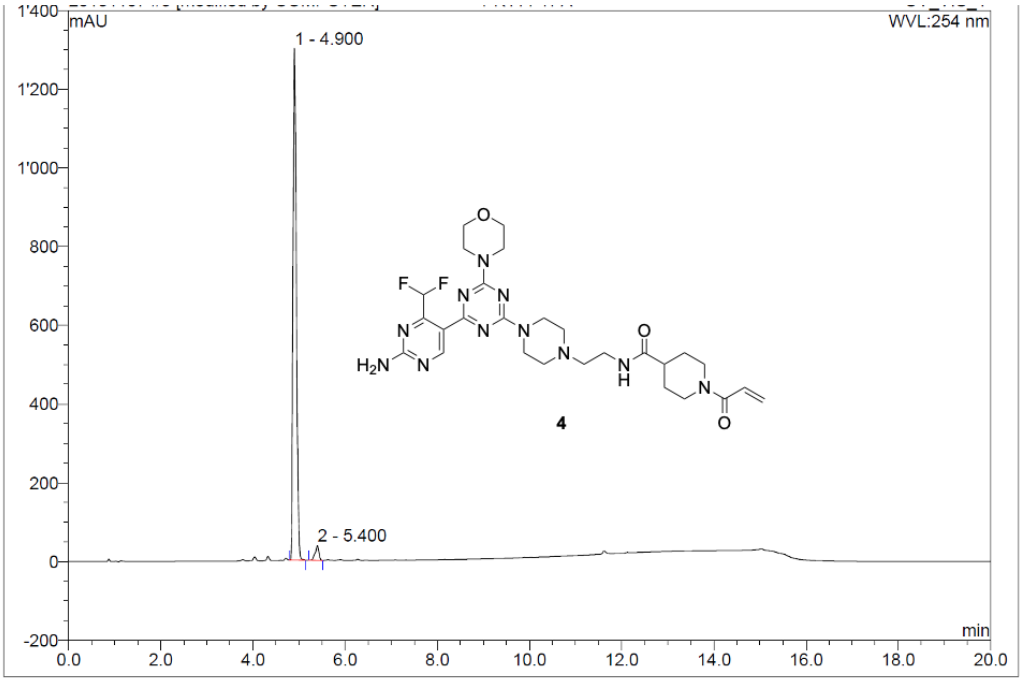

No.	Ret.Time min	Peak Name	Height mAU	Area mAU*min	Rel.Area %	Amount	Type
1	4.90	n.a.	1300.933	111.610	96.99	n.a.	BMB
2	5.40	n.a.	37.542	3.459	3.01	n.a.	BMB
Total:			1338.475	115.069	100.00	0.000	

Figure S97. HPLC chromatogram of compound **4**.

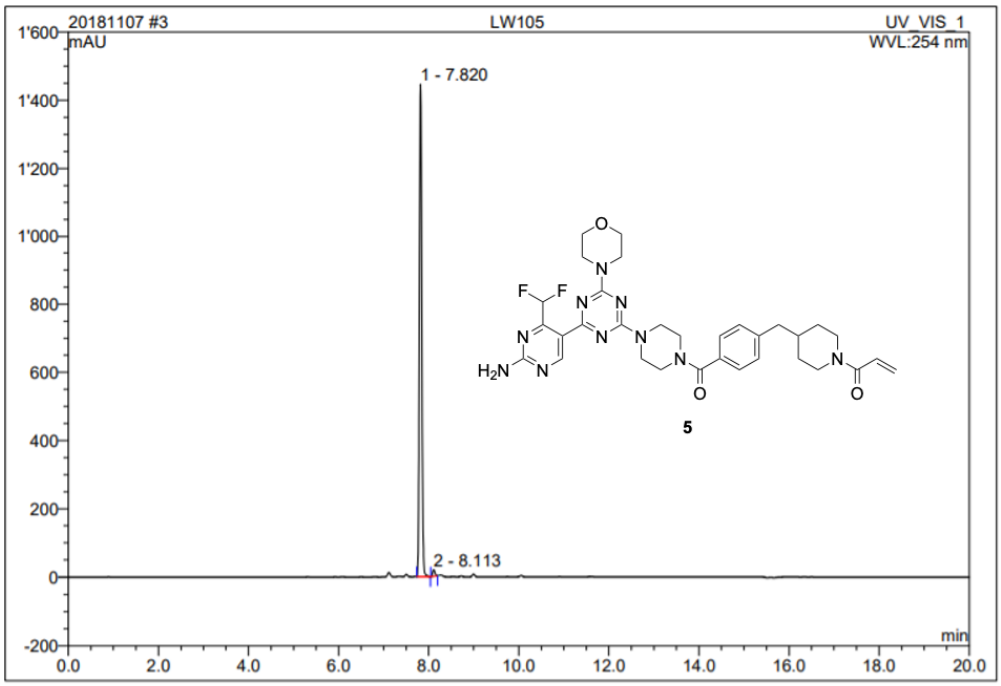

No.	Ret.Time min	Peak Name	Height mAU	Area mAU*min	Rel.Area %	Amount	Type
1	7.82	n.a.	1444.747	89.697	98.86	n.a.	BMB
2	8.11	n.a.	17.817	1.037	1.14	n.a.	BMB
Total:			1462.564	90.735	100.00	0.000	

Figure S98. HPLC chromatogram of compound **5**.

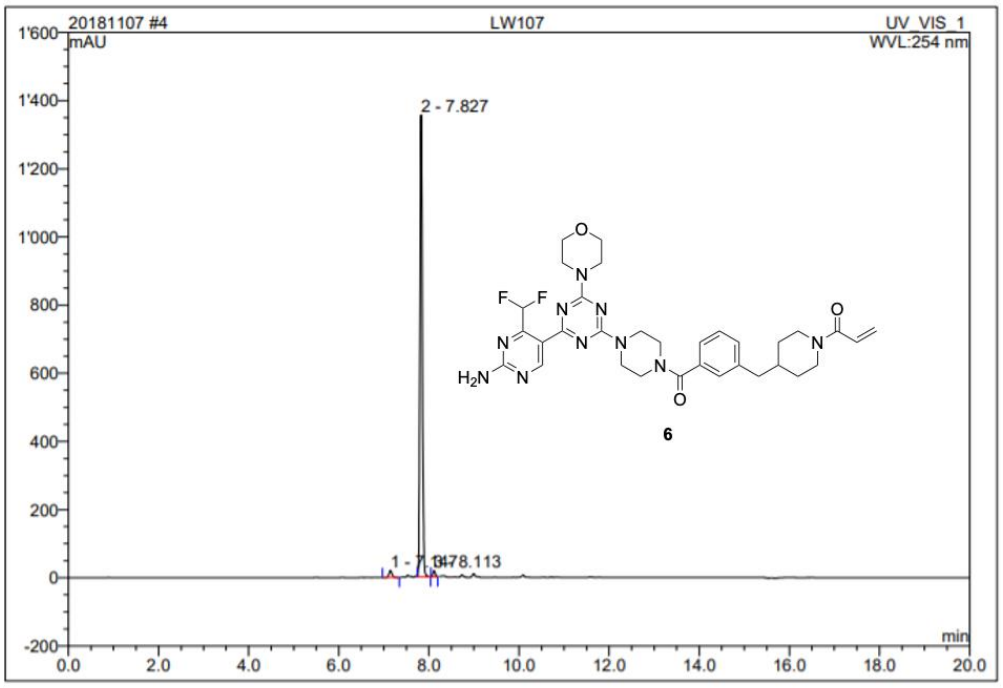

No.	Ret.Time min	Peak Name	Height mAU	Area mAU*min	Rel.Area %	Amount	Type
1	7.15	n.a.	20.929	1.632	1.87	n.a.	BMB
2	7.83	n.a.	1355.258	84.388	96.85	n.a.	BMB
3	8.11	n.a.	18.402	1.110	1.27	n.a.	BMB
Total:			1394.589	87.130	100.00	0.000	

Figure S99. HPLC chromatogram of compound **6**.

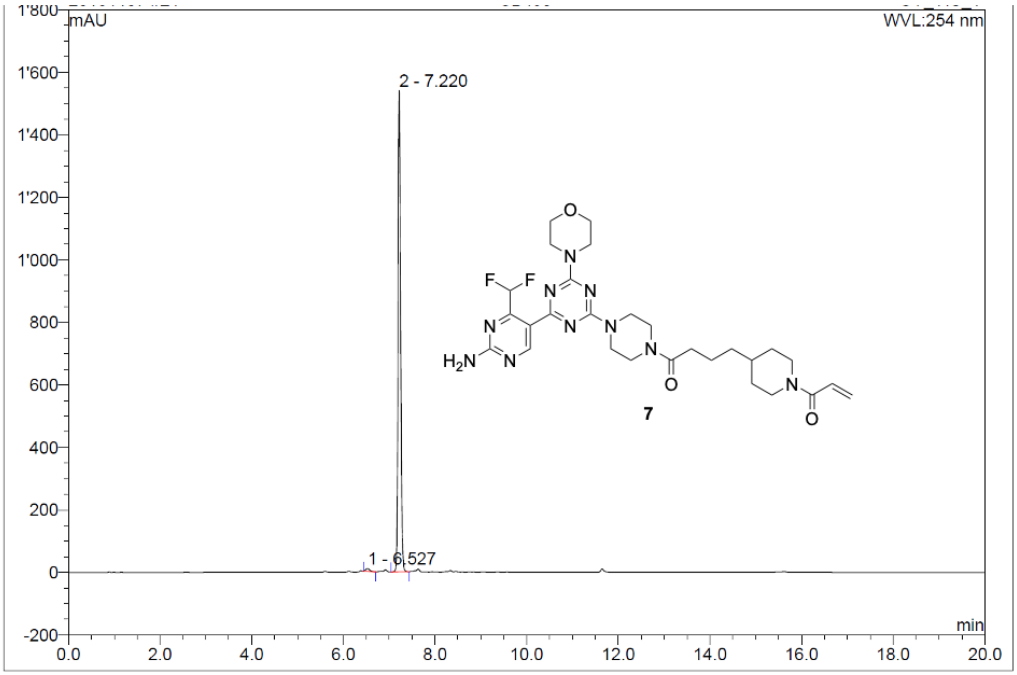

No.	Ret.Time min	Peak Name	Height mAU	Area mAU*min	Rel.Area %	Amount	Type
1	6.53	n.a.	9.940	1.057	1.05	n.a.	BMB
2	7.22	n.a.	1541.039	100.054	98.95	n.a.	BMB
Total:			1550.979	101.111	100.00	0.000	

Figure S100. HPLC chromatogram of compound **7**.

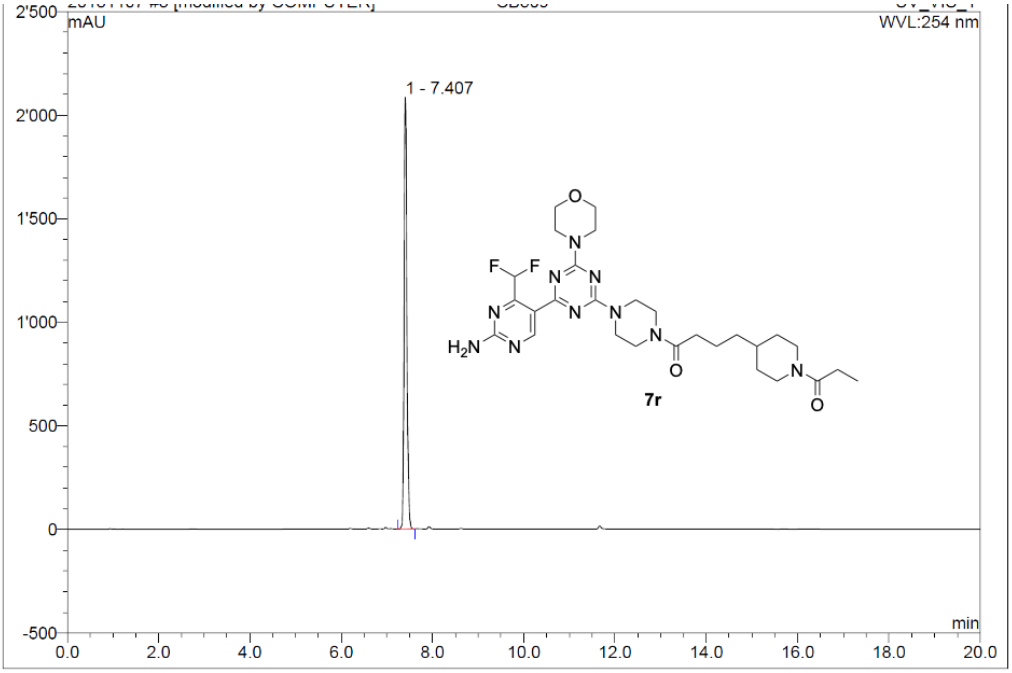

No.	Ret.Time min	Peak Name	Height mAU	Area mAU*min	Rel.Area %	Amount	Type
1	7.41	n.a.	2084.821	145.824	100.00	n.a.	BMB
Total:			2084.821	145.824	100.00	0.000	

Figure S101. HPLC chromatogram of compound **7r**.

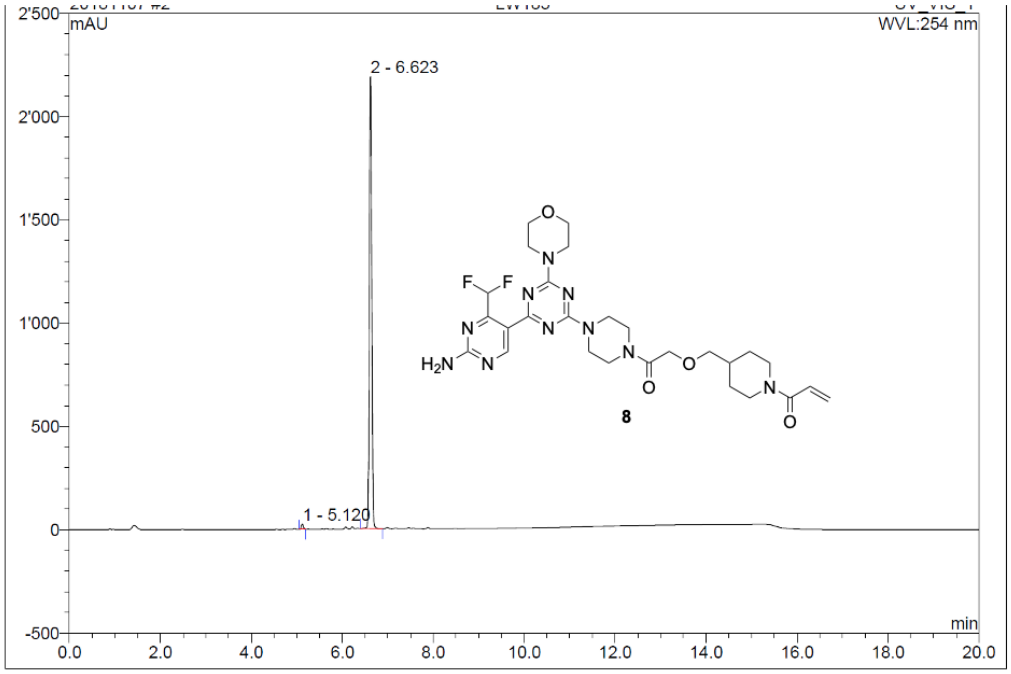

No.	Ret.Time min	Peak Name	Height mAU	Area mAU*min	Rel.Area %	Amount	Type
1	5.12	n.a.	26.542	1.423	1.05	n.a.	BMB
2	6.62	n.a.	2189.550	134.364	98.95	n.a.	BMB
Total:			2216.093	135.787	100.00	0.000	

Figure S102. HPLC chromatogram of compound **8**.

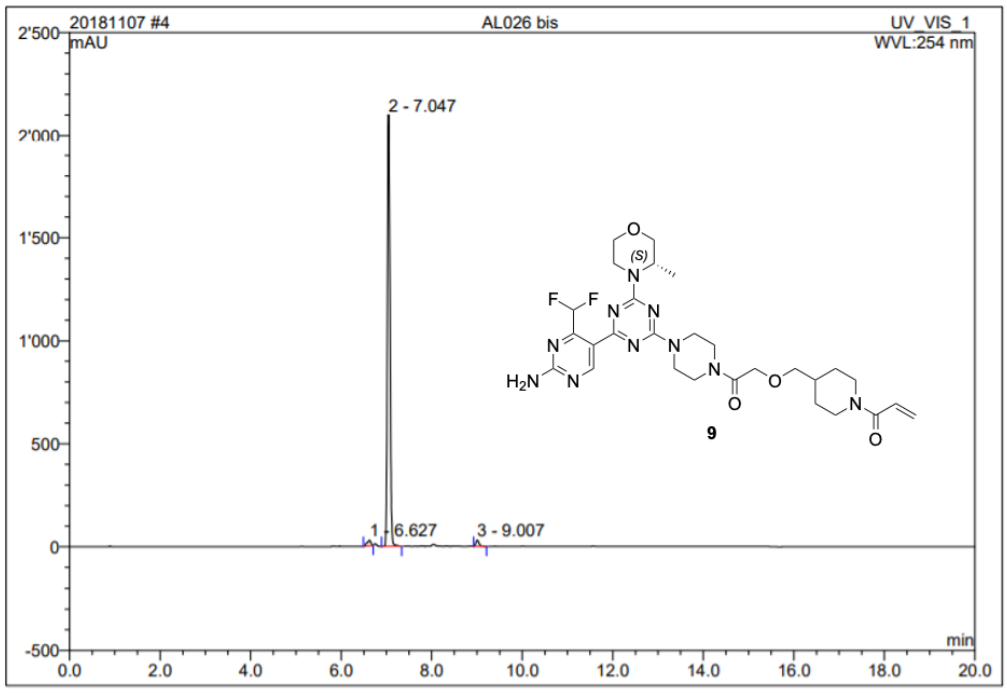

No.	Ret.Time min	Peak Name	Height mAU	Area mAU*min	Rel.Area %	Amount	Type
1	6.63	n.a.	27.318	2.629	1.77	n.a.	BMB
2	7.05	n.a.	2098.256	143.182	96.62	n.a.	BMB
3	9.01	n.a.	30.708	2.387	1.61	n.a.	BMB
Total:			2156.282	148.198	100.00	0.000	

Figure S103. HPLC chromatogram of compound **9**.

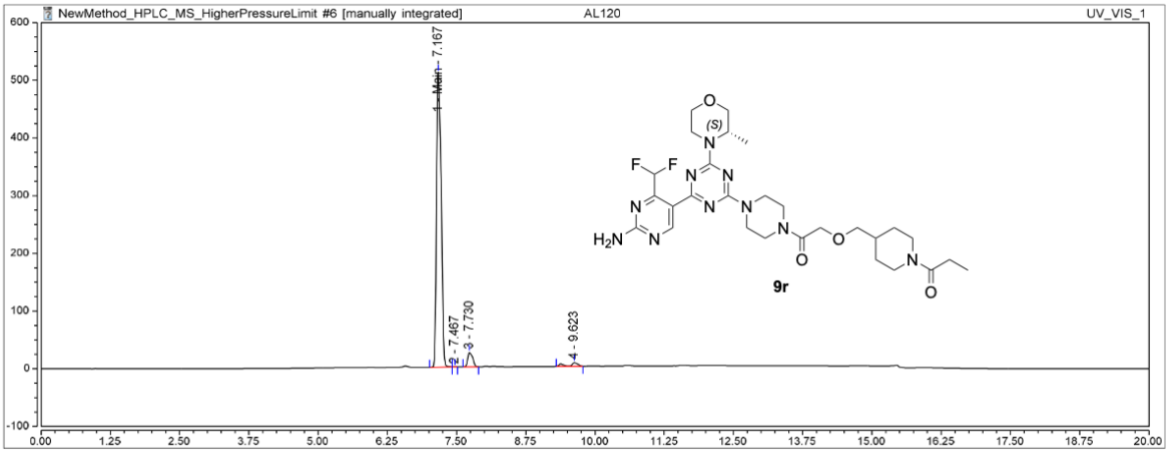

No.	Peak Name	Retention Time min	Height mAU	Area mAU*min	Relative Area %	Abs. Max. at nm	Sig.Max. mAU
1	Main	7.167	511.068	49.370	92.94	235.5	804.600
2		7.467	0.166	0.012	0.02	200.0	30.261
3		7.730	25.045	2.571	4.84	200.0	51.983
4		9.623	6.451	1.169	2.20	200.0	59.907
Total:			**542.729**	**53.123**	**100.00**	**835.55**	

Figure S104. HPLC chromatogram of compound **9r**.

MALD-MS spectra of β-mercaptoethanol (β-ME) adducts

1-(4-(((2-(4-(4-(2-amino-4-(difluoromethyl)pyrimidin-5-yl)-6-morpholino-1,3,5-triazin-2-yl)piperazin-1-yl)-2-oxoethyl)(methyl)amino)methyl)piperidin-1-yl)-3-((2-hydroxyethyl)thio)propan-1-one
(adduct with mercaptoethanol)
HPLC t_R = 5.25 min. MALDI-MS: *m/z* = 694.851 $[M + H]^+$.
Starting compound: **3**, (HPLC t_R = 5.35 min).

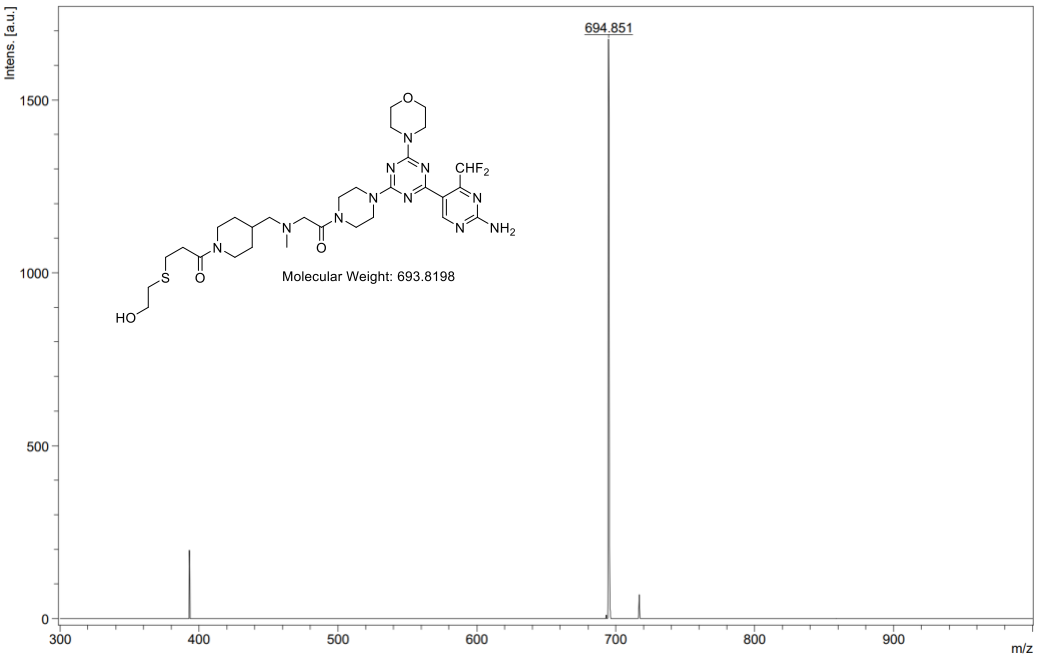

Figure S105. MALDI-MS of β-ME adduct of compound **3**.

1-(4-(4-(4-(4-(2-amino-4-(difluoromethyl)pyrimidin-5-yl)-6-morpholino-1,3,5-triazin-2-yl)piperazine-1-carbonyl)benzyl)piperidin-1-yl)-3-((2-hydroxyethyl)thio)propan-1-one
(adduct with mercaptoethanol)
HPLC t_R = 7.51 min. MALDI-MS: *m/z* = 728.118 $[M + H]^+$.
Starting compound: **5** (HPLC t_R = 7.87 min).

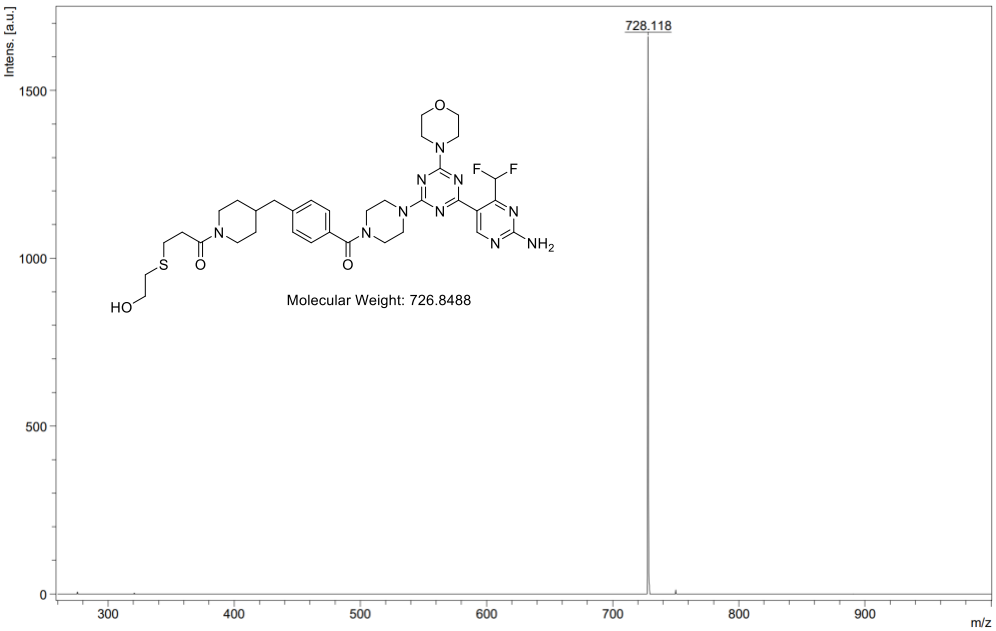

Figure S106. MALDI-MS of β-ME adduct of compound **5**.

1-(4-(3-(4-(4-(2-amino-4-(difluoromethyl)pyrimidin-5-yl)-6-morpholino-1,3,5-triazin-2-yl)piperazine-1-carbonyl)benzyl)piperidin-1-yl)-3-((2-hydroxyethyl)thio)propan-1-one (adduct with mercaptoethanol)
HPLC t_R = 7.54 min. MALDI-MS: *m/z* = 727.966 $[M + H]^+$; *m/z* = 749.909 $[M + Na]^+$.
Starting compound: **6** (HPLC t_R = 7.88 min).

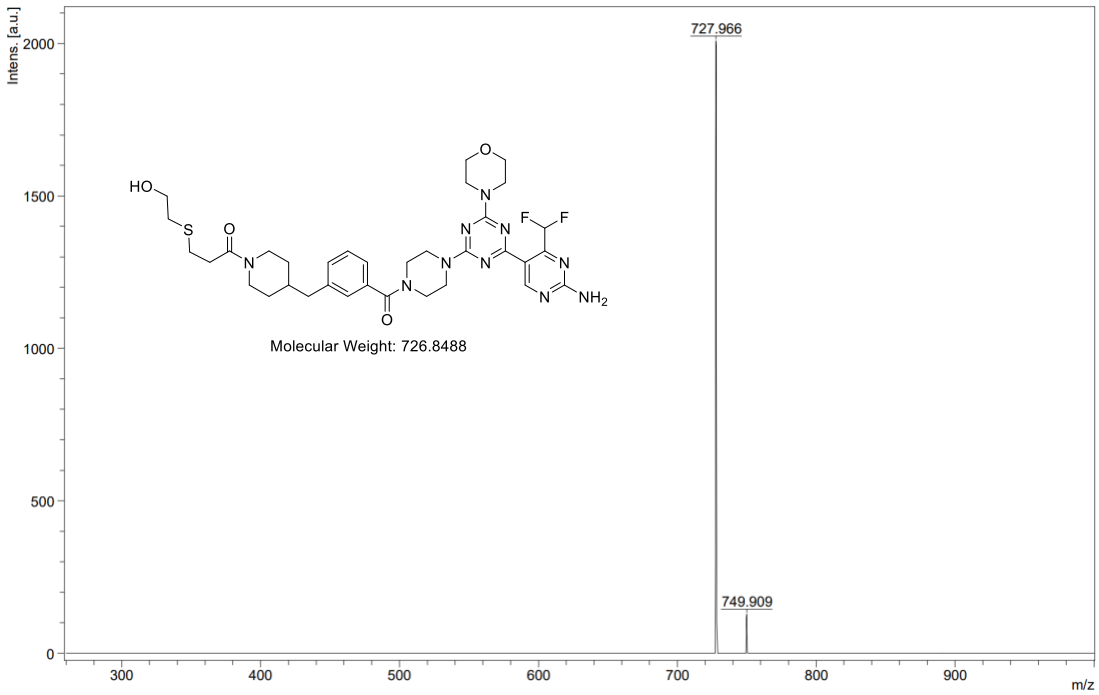

Figure S107. MALDI-MS of β-ME adduct of compound **5**.

1-(4-(4-(2-amino-4-(difluoromethyl)pyrimidin-5-yl)-6-morpholino-1,3,5-triazin-2-yl)piperazin-1-yl)-4-(1-(3-((2-hydroxyethyl)thio)propanoyl)piperidin-4-yl)butan-1-one
(adduct with mercaptoethanol)
HPLC t_R = 6.90 min. MALDI-MS: *m/z* = 679.868 $[M + H]^+$.
Starting compound: **7**, (HPLC t_R = 7.20 min).

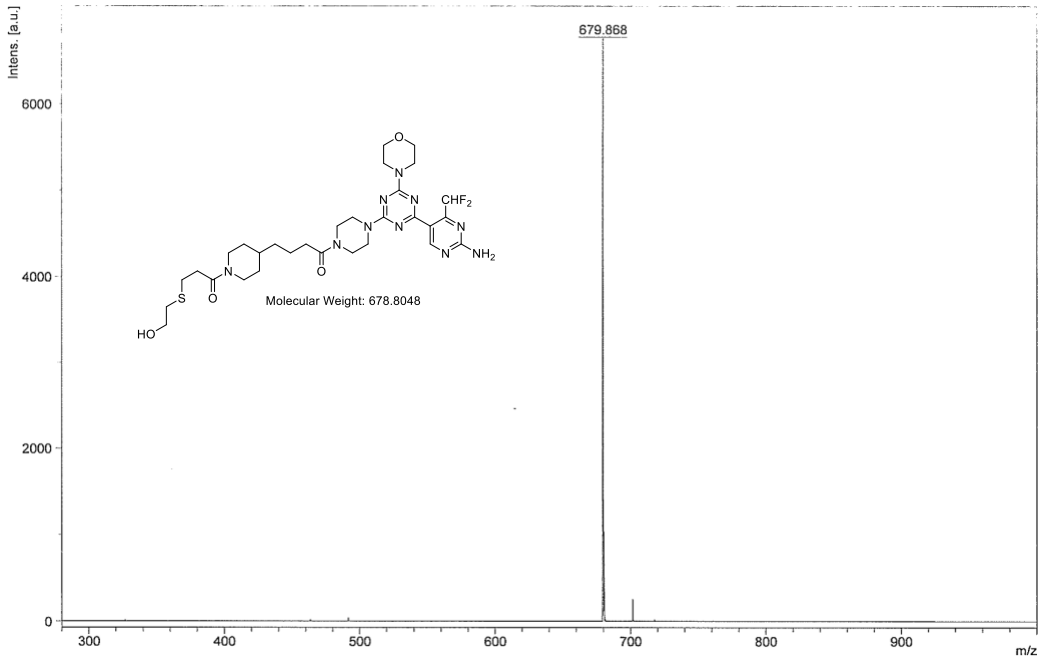

Figure S108. MALDI-MS of β-ME adduct of compound **7**.

1-(4-((2-(4-(4-(2-amino-4-(difluoromethyl)pyrimidin-5-yl)-6-morpholino-1,3,5-triazin-2-yl)piperazin-1-yl)-2-oxoethoxy)methyl)piperidin-1-yl)prop-2-en-1-one
(adduct with mercaptoethanol)
HPLC t_R = 6.42 min. MALDI-MS: *m/z* = 681.925 $[M + H]^+$; *m/z* = 703.910 $[M + Na]^+$
Starting compound: **8** (HPLC t_R = 6.66 min).

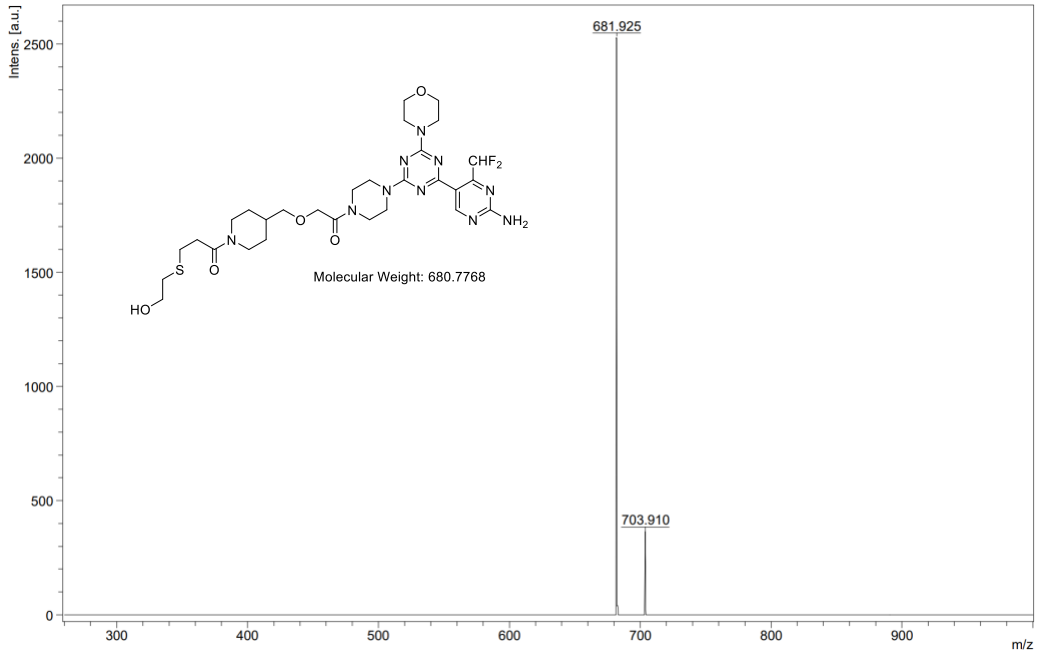

Figure S109. MALDI-MS of β-ME adduct of compound **8**.

(*S*)-1-(4-((2-(4-(4-(2-amino-4-(difluoromethyl)pyrimidin-5-yl)-6-(3-methylmorpholino)-1,3,5-triazin-2-yl)piperazin-1-yl)-2-oxoethoxy)methyl)piperidin-1-yl)-3-((2-hydroxyethyl)thio)propan-1-one
(adduct with mercaptoethanol)
HPLC t_R = 6.79 min. MALDI-MS: *m/z* = 695.3 $[M + H]^+$; *m/z* = 717.3 $[M + Na]^+$.
Starting compound: **9** (HPLC t_R = 7.05 min).

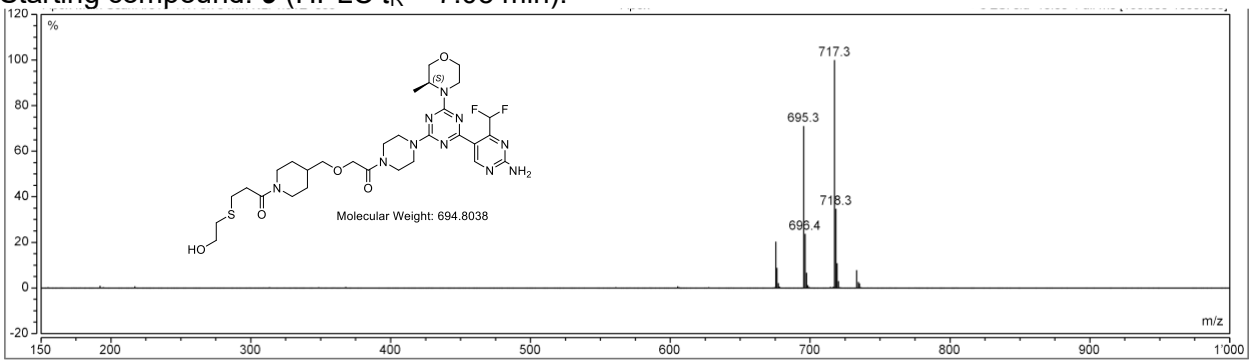

Figure S110. MALDI-MS of β-ME adduct of compound **9**.